Power Conversion System Design for Supercritical Carbon Dioxide Cooled Indirect Cycle Nuclear Reactors

by

Jonathan Paul Gibbs

B.S. Marine Engineering Systems
United States Merchant Marine Academy, 2005

SUBMITTED TO THE DEPARTMENT OF NUCLEAR SCIENCE AND ENGINEERING IN PARTIAL FULFILLMENT OF THE REQUIREMENTS FOR THE DEGREE OF

MASTER OF SCIENCE IN NUCLEAR SCIENCE AND ENGINEERING
AT THE
MASSACHUSETTS INSTITUTE OF TECHNOLOGY

June 2008

Signature of Author: _____
Department of Nuclear Science and Engineering
March 28, 2008

Certified by: _____
Dr. Pavel Hejzlar – Thesis Supervisor
Principal Research Scientist

Certified by: _____
Dr. Michael J. Driscoll – Thesis Supervisor
Professor Emeritus of Nuclear Science and Engineering

Accepted by: _____
Dr. Jacquelyn C. Yanch
Chairman, Department Committee on Graduate Students

This page intentionally left blank

To Grandpa Jack:

Thank you for giving me your engineering passion

This page intentionally left blank

Power Conversion System Design for Supercritical Carbon Dioxide Cooled Indirect Cycle Nuclear Reactors

by

Jonathan P. Gibbs

Submitted to the Department of Nuclear Science & Engineering
on March 28, 2008 in Partial Fulfillment of the
Requirements for the Degree of Master of Science in
Nuclear Science and Engineering

Abstract

The supercritical carbon dioxide (S-CO_2) cycle is a promising advanced power conversion cycle which couples nicely to many Generation IV nuclear reactors. This work investigates the power conversion system design and proposes several "Third Generation" plant layouts for power ratings ranging between 20 and 1200 MWe for the recompression cycle. A 20 MWe simple cycle layout was also developed.

The cycle designs are characterized by a dispersed component layout in which a single shaft turbomachinery train is coupled to parallel arrays of multiple printed circuit heat exchanger modules. This configuration has arrangement benefits in terms of modularity, inspectability, repairability and replaceability. Compared to the prior second generation dispersed layouts, its lower ductwork pressure drop confers approximately 2% higher thermal efficiency.

Two alternative S-CO_2 cycle designs for medium power applications were developed using an in-house optimization computer code and Solid Edge software. The first design is a recompression cycle derived from the 300 MWe design developed at MIT for Generation IV reactors. The design employs one turbine, two compressors (main and recompression) working in parallel and two recuperators (high and low temperature) and maximizes cycle efficiency while striving for a small plant footprint. The second design is a simple S-CO_2 power cycle, which has only one turbine, one compressor, and one recuperator. The main focus of the simple S-CO_2 design is cycle compactness and simplicity while achieving still attractive efficiency.

Extensive sensitivity studies were performed for both the medium power recompression and simple S-CO_2 cycles to reveal areas for performance improvement, or performance degradation. Cycle efficiency is most sensitive to turbine inlet temperature. Peak cycle pressure is also an important parameter affecting cycle efficiency, although to a smaller extent than turbine inlet temperature. Higher pressure gives higher efficiency, but this gradually saturates around 28 MPa. Other sensitivity studies included turbomachinery performance, cooling water temperature, and heat exchanger fouling and plugging.

The reference parameters chosen are a 650°C turbine inlet temperature and 20 MPa peak cycle pressure (compressor outlet) because they reach a high thermodynamic efficiency (≈47-48%) while staying within materials limitations. In order to couple the cycle to many of the Generation IV nuclear reactors a second reference case was chosen with a turbine inlet temperature of 550°C and a peak cycle pressure of 20 MPa.

Thesis Supervisor: Pavel Hejzlar
Title: Research Scientist, Nuclear Science & Engineering

Thesis Supervisor: Michael Driscoll
Title: Professor Emeritus of Nuclear Science & Engineering

Acknowledgements

First and foremost, I would like to express my deepest gratitude to my two advisors: Dr. Pavel Hejzlar and Professor Emeritus Michael Driscoll. Dr. Hejzlar's expertise in nuclear science and engineering, careful scrutiny of my technical work, and patience have been instrumental to my success at MIT. Professor Driscoll's ideas, direction, vast knowledge, and patience have guided my engineering development and I am truly fortunate to be able to call him an advisor.

I would also like to thank Dr. Nate Carstens, Dr. Yifang Gong, and Dr. Shih Ping Kao for their significant and unselfish contributions to this work. Nate provided many hours of support and guidance for problem solving and coding, Yifang provided all of the turbomachinery data, and Ping's experience has been invaluable for correctly reaching a solution, the first time! It was a pleasure to work with each of these gentlemen.

Finally, I would like to thank the exceptional people at Sandia National Laboratory and Lockheed Martin for their generous support on the supercritical carbon dioxide power cycle. The scientists and engineers at Sandia and Lockheed Martin have provided superb insight, and their financial support made this work possible.

Table of Contents

List of Figures

This page was intentionally left blank

List of Tables

1 Introduction

1.1 Motivation

Nuclear reactors have received increasing interest as a possibility for large scale energy production as green house gas emission has become more of a concern for fossil fueled power plants. Nuclear energy does not produce any green house gas as a byproduct and will not be subjected to carbon dioxide regulations. Also, ongoing interest in nuclear power motivates interest in new technologies for both the reactor side and the power conversion side of a power plant. This work is part of an ongoing research project at Massachusetts Institute of Technology with the objective of developing an optimized power conversion system for future advanced reactors. The supercritical CO_2 (S-CO_2) power conversion system (PCS) has a number of characteristics which make it an attractive candidate for Generation-IV reactor designs.

Brayton cycles operate on the principle of obtaining more work from expanding a fluid than compressing the same fluid, which is typically a gas. It is not uncommon for the compressor work to require a significant fraction of the turbine work due to the large compressibility of the working fluid as it enters the compressor(s). However, S-CO_2 has a unique advantage of having its critical point easily achievable. S-CO_2 cycles take advantage of the non-ideal properties of CO_2 near its critical point, most importantly its high density (low compressibility). This allows the compressor work fraction to be smaller than typical Brayton cycles, thus enabling achievement of higher thermodynamic efficiency at lower temperatures. For example, the compressor work requires approximately 60% of the turbine work in a LM 2500 gas turbine, but the compressor in the S-CO_2 cycle only requires about 30% of the turbine work, thus enabling higher overall efficiencies.

Interest in the S-CO_2 power conversion system can be traced back to the 1940s when the Sulzer Brothers first investigated and patented a partial condensation CO_2 Brayton cycle [Sulzer Patent, 1948]. The advantages of the non ideal gas features of CO_2 were quickly

realized, resulting in an increase in interest. Considerable attention was directed towards CO_2 in the 1960s and early 1970s. Some of the more active investigators include: Gokhstein and Verhivker in the Soviet Union [Gokhstein and Verhivker, 1969]; Angelino in Italy [Angelino, 1968]; Feher in the United States [Feher, 1967]; and Sulzer Brown-Boveri in Switzerland [Strub and Frieder, 1970]. Earnest Feher's report in 1967 was the first to propose a fully supercritical CO_2 cycle that was later called the "Feher Cycle". Feher's earlier work was a more general look at supercritical cycles [Feher, 1962].

S-CO_2 progress was slowed down by material limitations for the high temperature and high pressure applications, but a revival in the late 1990s was led by MIT and followed by others. In 1997 an investigation of the S-CO_2 cycle was conducted at the Czech Technical University in Prague, Czech Republic, and focused on the Brayton and recompression supercritical cycles [Petr, et. al., 1999]. Tokyo Institute of Technology in Japan is also actively investigating the S-CO_2 cycle and has built a test loop for further experimentation [Kato, et. al., 2001]. The MIT work is largely in collaboration with Sandia and Argonne National Laboratories and has been investigating the possibility of using S-CO_2 in an indirect cycle employing a lead-bismuth eutectic cooled reactor [Dostal, et. al., 2001], liquid sodium cooled reactor [Gibbs, et. al., 2006], the STAR-LM reactor [Moisseytsev, et. al., 2003], and with thermal spectrum gas cooled reactors [Oh, 2002]. The MIT work has covered the reactor physics and thermal hydraulic design of a 2400MWth S-CO_2 cooled fast reactor [Pope, et. al., 2004] and [Pope, et. al., 2006], respectively; reactor core design for a S-CO_2 cooled reactor [Handwerk, et. al., 2007]; shutdown cooling of a S-CO_2 reactor [Okano, et. al., 2002]; and the most recent work focused on a transient analysis of the S-CO_2 PCS with appropriate control schemes [Carstens, et. al., 2007].

1.2 Objectives and Contributions of this Work

The general contributions of this work were focused on developing a plant layout for large and medium scale power ratings and performing a number of parametric studies to identify weaknesses and areas of potential improvement. Recompression cycle layouts were developed for power ratings ranging from 20 to 1200 MWe and simple cycle layouts were developed for 20 MWe.

1.3 Supercritical CO_2 Recompression Cycle

Several variations of the S-CO_2 PCS have been considered and the recompression cycle appears to be one of the most promising renditions of the designs. Considerable work has been devoted towards the recompression cycle and a foundation for future work was completed in 2004 by Vaclav Dostal [Dostal, et. al. 2004]. The recompression cycle consists of one turbine, two compressors (recompressing and main), two recuperators (high and low temperature), and one precooler. The flow schematic is shown in Figure 1.1 and a temperature-entropy diagram in Figure 1.2.

The recompression cycle is able to achieve high thermodynamic efficiency while achieving an attractive power density as compared to other types of closed loop power conversion cycles. The recompression cycle will be primarily focused on large power applications: upwards of 300 MWe for a single loop system and 1200 MWe for multi loop systems. The recompression cycle can also be used for small and medium power applications in the same range as the simple cycle, but the focus of this work is for large power applications, however one special case at 20 MWe is also explored.

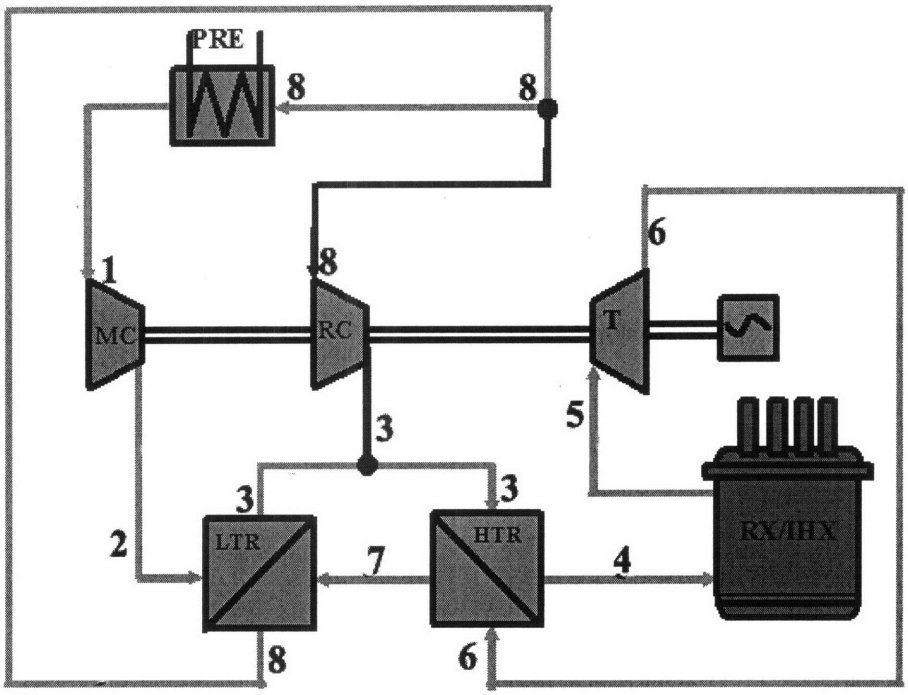

Figure 1.1 S-CO_2 recompression cycle layout [Dostal, et. al., 2004]

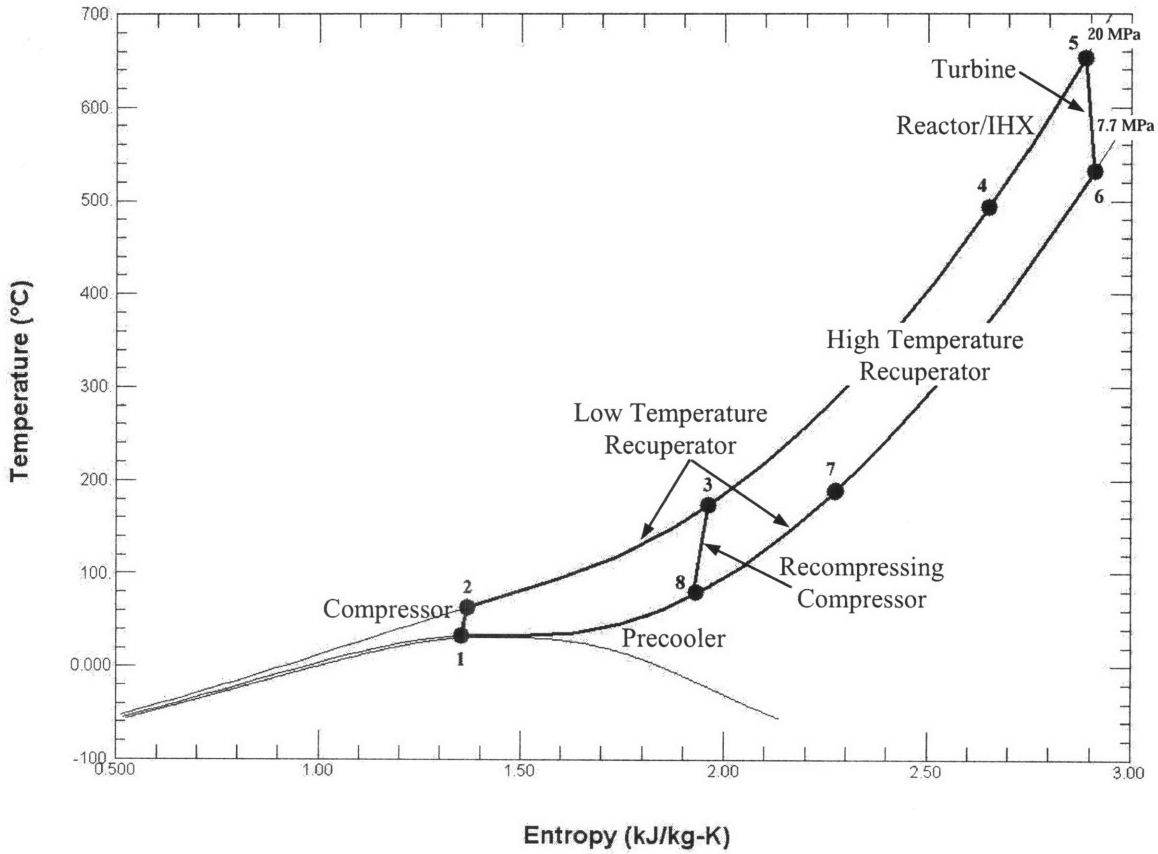

Figure 1.2 Temperature-entropy diagram of a recompression cycle with a 650°C turbine inlet temperature (numbering corresponds to Figure 1.1)

1.4 Supercritical CO_2 Simple Cycle

The simple cycle is a precursor to the recompression cycle, but trades efficiency for simplicity and compactness. The simple cycle has one less compressor and recuperator than the recompression cycle. Therefore, the cycle is much less recuperative and achieves lower net cycle efficiency. The simple cycle achieves a slightly lower thermodynamic efficiency than a Rankine cycle for the same turbine inlet temperature, but has a considerable higher power density. The simple cycle is also able to use considerably lower turbine inlet temperatures than the recompression cycle, making it a candidate to be coupled to current pressurized water reactor technologies for earlier deployment, albeit at a lower efficiency. The turbine inlet temperature is a key contributor to the overall thermodynamic efficiency; thus, a lower turbine inlet temperature will have a large efficiency penalty, and the PCS coupled to a pressurized water reactor for small and medium power applications will have a much higher power density than the currently available Rankine cycle layouts, but at lower efficiency. The main extension of the simple cycle application will be limited to small and medium power applications on the order of 50 MWe or less with slightly lower turbine inlet temperatures than the recompression cycle (~550°C). For the same design conditions the simple cycle is approximately 4-8% less efficient than the recompression cycle, depending on the particular parameters. A flow schematic for the simple cycle is shown in Figure 1.3 and a temperature-entropy diagram is shown in Figure 1.4.

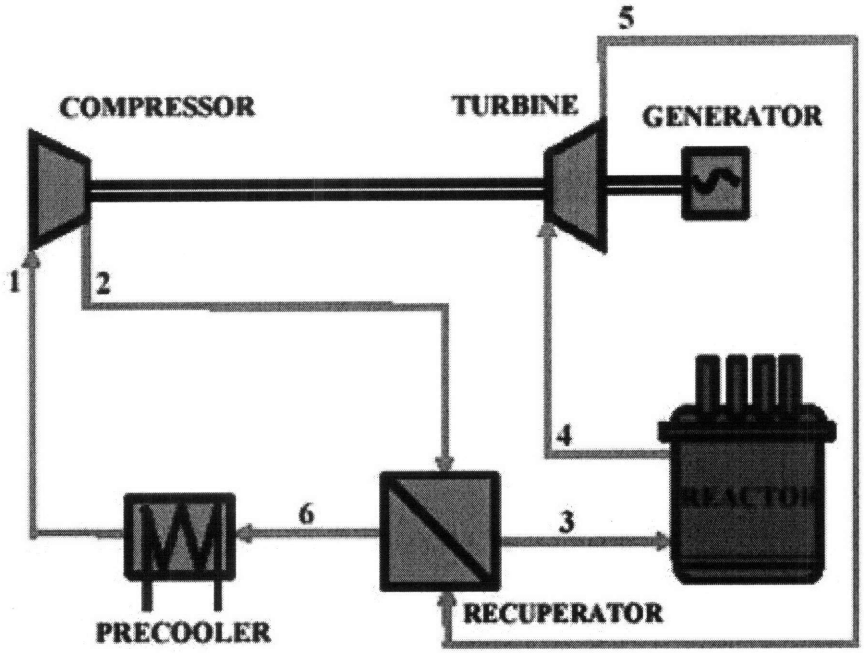

Figure 1.3 Layout of S-CO2 simple cycle [Dostal, et. al., 2004]

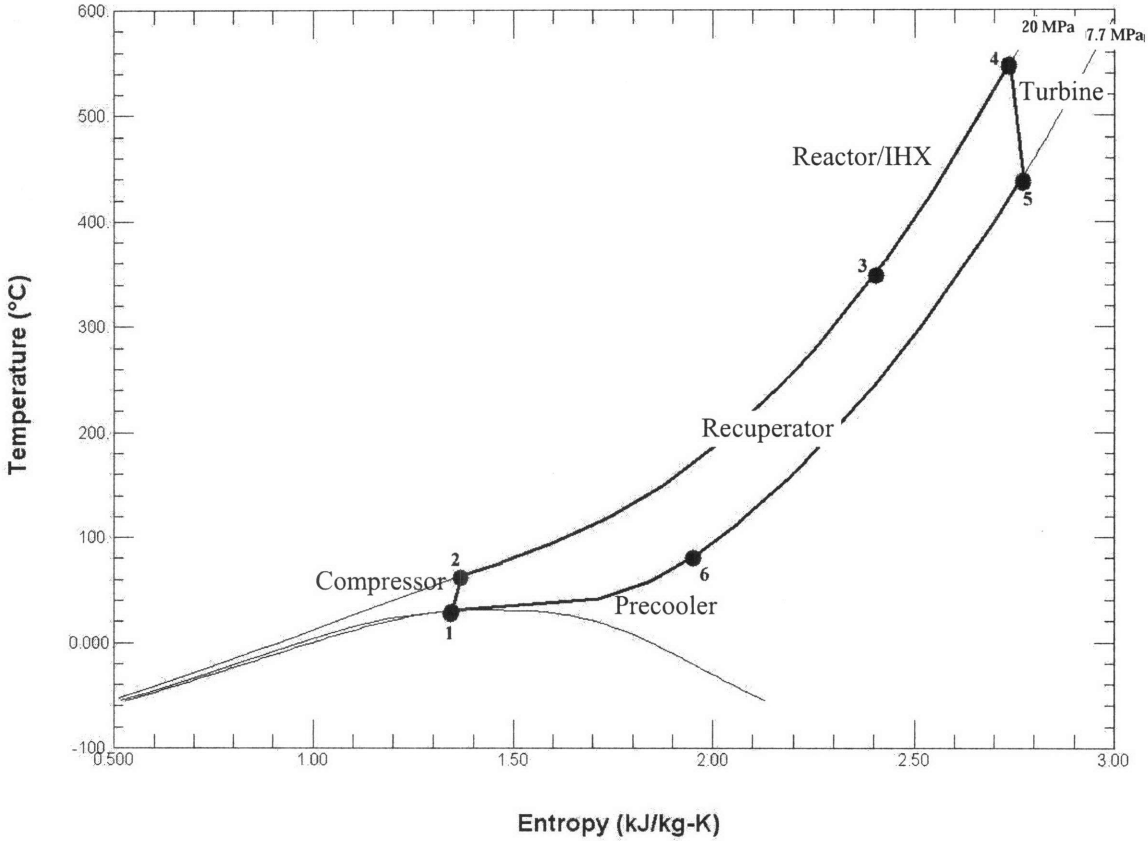

Figure 1.4 Temperature-entropy diagram of a simple cycle with a 550˚C turbine inlet temperature (numbering corresponds to Figure 1.3)

1.5 Heatric® Printed Circuit Heat Exchangers

Advances in printed circuit heat exchanger (PCHE) technology are one of the motivators for the recent increased interest in S-CO_2 cycles because they are about four to six times smaller than conventional shell-and-tube heat exchangers of equal duty [www.heatric.com]. The PCHEs employ a rugged and very compact design which is a good match for use with the S-CO_2 PCS. With the heat exchangers being the largest components in the power cycle due to the high level of recuperation (3 times more heat is recuperated than added in the reactor/IHX) it is easy to see why the development of the compact heat exchangers is so central to the success of the S-CO_2 PCS. Another alternative to the PCHEs is a simple shell and tube heat exchanger, but the volume and footprint will make the overall power cycle undesirable due to its large size. One of the goals of the S-CO_2 PCS is to achieve a high power density which is not possible with standard shell-and-tube type heat exchangers. Several compact type heat exchangers are currently available, but the PCHE appears to be the best suited match for the S-CO_2 PCS.

Printed circuit heat exchangers (PCHE) were identified as ideal heat exchange devices for the S-CO_2 PCS due to their high compactness, low pressure drop, high effectiveness, and ability to withstand large temperature and pressure differences. The PCHE is constructed by chemically etching small flow channels into plates. The plates are then stacked and diffusion bonded to form a monolithic heat exchanger core. The decision to choose the PCHE for the S-CO_2 PCS is extensively covered in References [Dostal, et. al., 2004] and [Gezelius, 2004]. The PCHEs used in the S-CO_2 PCS designs covered in this work employ 2 mm diameter semicircular flow passages, but it is possible to have a heat exchanger with other than 2 mm flow passages. Furthermore, the hot and cold plates do not have to have the same diameter flow passages, but it was found that for the S-CO_2 PCS the 2 mm flow passages on both the hot and cold plates was the ideal configuration. The other limits imposed on the S-CO_2 PCS in this work are due to the PCHE manufacturing process, which limits each unit to 1.5m long, 0.6m wide, and 0.6m tall stack height. To achieve the required thermal rating for the various power ratings, several modules can be welded on top of each other to form one large heat exchanger. It is also possible to weld the units side by side, but this work uses multiple modules on top

of each other to keep the outer plena small. The manufacturing process is shown in Figure 1.5 and the temperature-pressure operating range is shown in Figure 1.6. A pictorial comparison of PCHEs and shell-and-tube heat exchangers is given in Section 2.10.

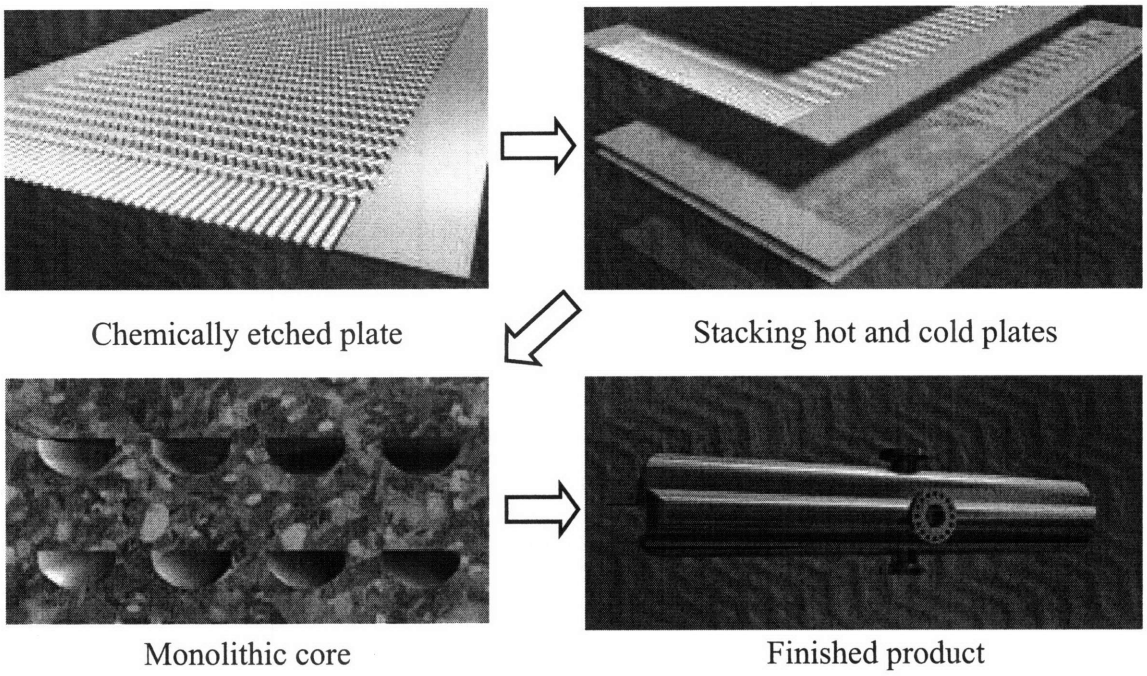

Figure 1.5 PCHE construction process [www.heatric.com]

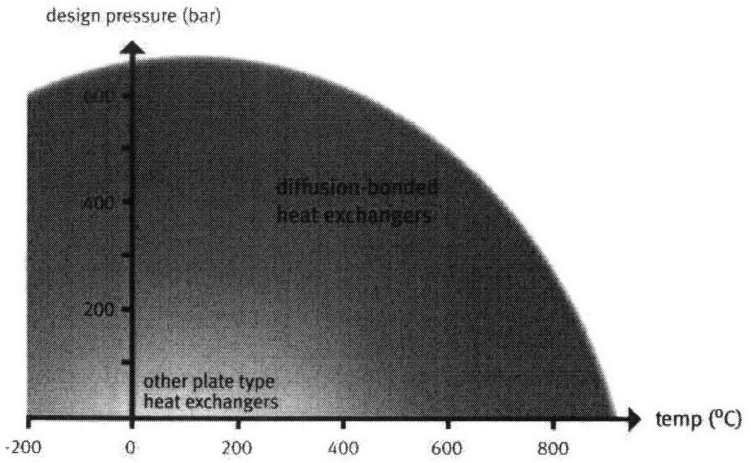

Figure 1.6 Operating temperature and pressure range of a PCHE [www.heatric.com]

Other key considerations supporting the choice to use PCHEs include the ruggedness of these heat exchangers (the manufacturer has tested PCHEs at several times higher pressures than the design pressure before a break was observed), their capability to accommodate a larger pressure difference between high and low pressure sides (20MPa against 8MPa) and extensive experience obtained with their operation in a range of applications, including those in off-shore oil rigs where ocean water is used for cooling.

1.6 Permanent Magnet Generators

Permanent magnet generators are an attractive technology to couple to the S-CO_2 PCS because of their high power density, simplicity of operation, and high rotating speed capability. Some of the main competitors to the permanent magnet generator are the traditional wound rotor generator and superconducting generators. Of these, the only generator able to currently exceed 5 MWe with a higher shaft speed (greater than 1000 RPM) is the traditional wound rotor generator. Superconducting motors are currently rated above 35 MWe, but have a low shaft speed (~120 RPM) [www.amsuper.com]. The superconducting generator has a lower power density than the permanent magnet generator and relies on cryogenic cooling, which may be undesirable due to the added complexity of the supporting equipment. Current permanent magnet technology has units available with power ratings on the order of 5-8 MWe and is expected to reach power ratings of approximately 18 MWe in 2007 and 20-30 MWe in 2008 [Shade, 2006]. Extensive work was done on the design of a permanent magnet generator in Reference [Rucker, 2005].

Another attractive feature of the permanent magnet generator is its ability to operate at high shaft speeds. This is advantageous because if the goal is to achieve a high power density, the turbomachinery size can be decreased by increasing the shaft speed. The current limit on permanent magnet generators is approximately 10,000-15,000 RPM for a 4-8 MWe machine and 4500-7000 RPM for a 20-30 MWe machine [Shade, 2006]. Many of the smaller power rating figures in this work show a permanent magnet generator to illustrate the achievable power density of the cycle, while the large power ratings (greater

than 50 MWe) show a typical wound rotor generator, which is one of the largest components in the power cycle. A picture of a permanent magnet generator is shown in Figure 1.7.

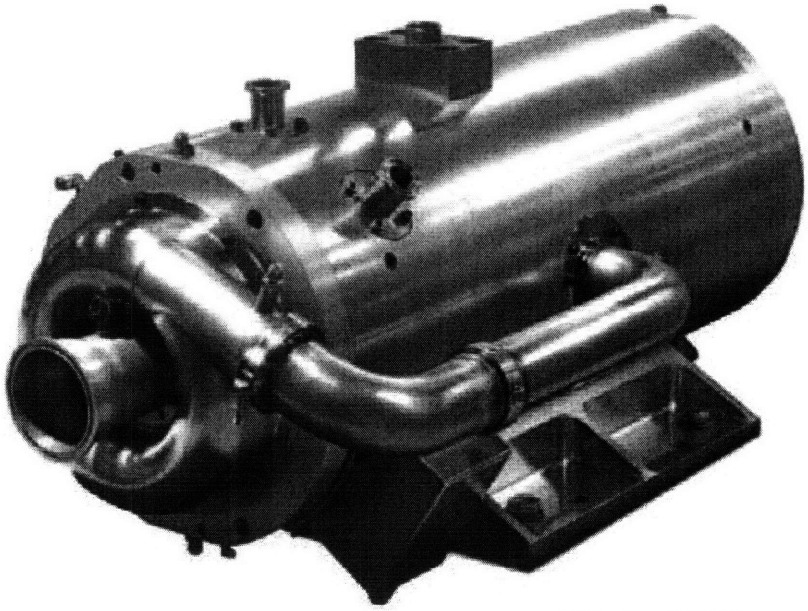

Figure 1.7 Permanent magnet generator [Shade, 2006]

1.7 S-CO_2 Steady State Analysis Code

The computational model, named CYCLES, to evaluate the S-CO_2 PCS was primarily developed by Drs. Pavel Hejzlar and Vaclav Dostal [Dostal, et. al., 2004] and was written in FORTRAN 90. CYCLES is a steady state optimization code that is primarily focused on the heat exchanger design, cycle statepoints, and pressure drops. A good description of CYCLES is given in Reference [Dostal, et. al., 2004]. General cycle parameters (reactor/IHX thermal power, turbine inlet temperature, compressor outlet pressure, compressor pressure ratio, turbomachinery efficiencies, cooling water temperature, total cycle heat exchanger volume, pipe data, etc) are provided as an input and the optimal heat exchanger length and volume allocation between the various heat exchangers is determined. Sample input files are provided in Appendices A3 and A4. Essentially, the length optimization is a means to balance the effect of the effectiveness and pressure drop for a given heat exchanger with respect to the cycle efficiency. CYCLES can also

calculate the statepoints and performance for a given design with no additional optimization.

CYCLES was later updated by Dr. Hejzlar to include the effects of using zigzag channels in the heat exchangers, effects of pressure drops in the pipes and plena, and effects due to fouling. Previously, CYCLES only used straight channels in the heat exchangers and only calculated the pressure drops in the heat exchanger cores. The updated version of CYCLES is called CYCLES-II and the improvements are described in [Hejzlar, et. al., 2006] and [Legault and Hejzlar, 2006].

The program CYCLES is broken into a number of modules to perform optimization and calculation on the various components (i.e. recuperators, precooler, turbine, etc.). General parameters are provided in an input file by the user. The program uses either tables or NIST Refprop [NIST] as the interface to obtain the required fluid properties. The tabular property lookup method is considerably quicker than calling NIST and is used for PCHE calculations, but NIST, which is also used for the turbomachinery calculations, provides more accurate results using polynomials because it does not need to interpolate between two points, which introduces error.

The phrase "fully optimized cycle" means that for a given volume the heat exchangers (recuperator(s) and precooler) are designed with the length and volume allocation that produces the highest cycle efficiency. The main use of CYCLES was to establish fully optimized designs, record the achievable performance, and then to subject each design to off design performance with the non re-optimization capability.

1.8 Materials compatibility at elevated temperature and pressure

New materials capabilities have been continually expanding the temperature and pressure operating range of power systems. Current state-of-the-art supercritical pulverized coal generation involves 565°C and 24.3 MPa while the boundaries are being further pushed to higher limits. Several ultra-supercritical cycles (above 565°C) have been constructed

in Japan and Europe with operating conditions of 32MPa and 600/610°C, and current materials research and development has a targeted pressure range of 36.5 to 38.5 MPa and temperatures of 700-720°C [Katzer J., et. al, 2007]. Thus, the operating conditions for the proposed S-CO_2 PCS are well within the limits of current and projected technologies. Corrosion characteristics of CO_2 at 650°C are known from the years of operating the British AGRs, but the effects of elevated pressure remain to be determined. Currently, tests to determine this effect are ongoing at MIT.

1.9 Applicability of S-CO_2 Indirect Cycle to Generation IV Reactors

Employed as an indirect cycle, the S-CO_2 PCS can be adapted to a wide variety of reactor types. Table 1.1 lists a representative set of GEN-IV candidates.

Table 1.1 Applicability of S-CO_2 Indirect Cycle to GEN-IV Reactors

Concept	Reactor Outlet T	S-CO_2 Turbine Inlet T	Est. S-CO_2 Cycle Thermal Efficiency
GFR	850°C (He)	800°C	53
LFR	550-800°C	530-780°C	43-52
SFR	550°C	530°C	43
MSR	700-800°C	680-780°C	49-52
SCWR	510-550°C	500°C	42
VHTR	1000°C	800°C[2]	53

Notes:

1. **Nuclear News, Nov. 2002**
2. **Limited by corrosion, and to a lesser extent by dissociation**
3. **IHX ΔT is 50°C for Gas/Gas, 20°C for Liquid/Gas**
4. **For net plant efficiency subtract approx. 4% for Gas/Gas house loads and 2% for Liquid/Gas combinations**

One principal criterion is the achievable turbine inlet temperature, which should be above about 450°C if attractive thermodynamic efficiencies are to be attained. Allowing on the order of 20°C temperature difference across an intermediate heat exchanger, this translates into a coolant core outlet temperature of 470°C or higher. The following rough approximation for S-CO_2 cycle efficiency applies:

$$\eta \approx \eta_c - 0.19 \tag{1-1}$$

Where η_c is Carnot cycle efficiency:

$$\eta_c \approx 1 - \frac{Tc}{Th}$$

in which

Tc = ambient waste heat sink temperature (~300 K)

Th = turbine inlet temperature (absolute)

However, it is important to note that the above relationship only holds for turbine inlet temperatures above 450°C. Below 450°C the pressure drops throughout the cycle become large and contribute to a more rapid efficiency decline. Furthermore, the recompression cycle has difficulty operating with a turbine inlet temperature below 400°C due to the considerably higher mass flow rates and associated pressure drops. Thus, it would be difficult to couple current PWR technology with the recompression cycle. The simple S-CO_2 cycle can operate with lower turbine inlet temperatures than the recompression cycle. Thus, if mated to a PWR with resulting Th = 300°C (573 K), and using Figure 4.12, η would only be about 22%, compared to the 32% attained by today's Rankine cycle PCS. This is too low to offset any savings provided by reduced system size. Hence, the simple and recompression S-CO_2 PCS are not attractive for GEN-III+ LWRs.

At higher temperatures the principal competition for the S-CO_2 PCS is its He Brayton PCS counterpart. Because helium is an ideal gas, it does not benefit from the low compressor work achieved in the S-CO_2 PCS by operating near the critical point of CO_2. Hence at all values of turbine inlet temperature, the He-PCS efficiency is lower.

For example, a curve fit to Dostal's CYCLES code calculations for an idealized, optimized He-PCS gives:

$$\eta = 1.33\eta_c - 0.49 \tag{1-2}$$

hence about 36% at 550°C, versus 44.6% for a S-CO_2 PCS.

Even lower values are projected if one compares a helium cycle reactor closer to practical realization such as the PBMR; fitting a curve presented in Reference [Paoletti, et. al., 2005] yields:

$$\eta = 2.23\eta_c - 1.23 \tag{1-3}$$

which predicts only 18.8% at 550°C.

The interest here is confined to indirect cycle applications. However it is worth noting that direct cycle use is feasible. For example, at MIT a CO_2 cooled GFR is under evaluation [NERI, 2005], having a core outlet/turbine inlet temperature of 650°C – building on proven British AGR experience at this temperature. Likewise attention is limited to fission reactors, but note a recent survey which concludes that most fusion reactor concepts should be compatible with use of the S-CO_2 PCS [Fernandez, et. al., 2006]. Finally, electric-generation-only is a further restriction; but again an evaluation shows potential applicability for district heating, desalination, and dry cooling tower applications [Fernandez, et. al., 2006]. The S-CO_2 cycle can also be used as a bottoming cycle for very-high-temperature reactors designed to power high temperature electrolysis hydrogen production plants [Bilge and Kazimi, 2005].

1.10 Criteria and Constraints

The plant layouts described subsequently were developed to satisfy a number of practical restrictions. Thus explicit recognition of the criteria and constraints governing key design decisions is essential at the outset, as follows:

(1) Power plant experience with pipes/ducts and valves is primarily with diameters no larger than one meter. This favors keeping S-CO_2 PCS ratings at or below about 150 MWe to avoid excessive pressure drop – especially in low pressure regions such as the turbine exhaust. This led to use of two or more parallel piping trains for larger ratings. The turbomachinery, on the other hand, is extremely compact, with single-train ratings up to 1200 MWe conceivable. However, more than two parallel circuits per turbomachine leads to excessive complexity. Rotating speed falls within generator and blade stress limits, based on a maximum rating of 600 MWe. A larger rating than 600 MWe may be employed if a counter flow turbine is used to balance thrust.

(2) Heat exchanger size limitations reinforce the above design choice. While core power densities of HEATRIC™ type printed circuit heat exchangers (PCHE) are extremely high (e.g. 30 MW/m^3), the need for large plena makes the overall pressure vessel envelope push the limits of fabricability and transportability. It is also possible to use smaller plena and place each heat exchanger module within a pressure vessel while using the contour of the vessel to guide the flow. The vessel approach was the method pursued to develop the second generation layouts and results in a lower power density than the modular approach. The vessel and modular approaches are covered more completely in Chapter 2. Considerable experience with transportation of PWR steam generators and pressure vessels insures that components or modules less than around 800 metric tons, of up to 7 meters diameter and 60 meters in length are manageable. Transportability and modularity are also essential prerequisites to the applicability of factory rather than on-site fabrication, with attendant significant cost reduction.

(3) Grid-synchronous turbomachinery favors rotational speeds of 3600 or 1800 rpm. However higher speeds are necessary for efficient design of small turbomachinery. Recent technological advances (permanent magnet generators, solid state DC-AC inverters/converters) have favored using variable speed in lieu of gearboxes and fixed speed. Applications up to 30 MWe are in the works, and 50 MWe (the breakpoint assumed here) judged attainable by manufacturers' technical representatives.

(4) Turbomachinery scaling also strongly affects the choice between radial (centrifugal) and axial configuration. Reference [Gong, et. al., 2006] addresses this complex subject in some detail, but the valid generalization can be made that small rating favors adoption of radial machinery. Radial turbines can still be used for larger ratings, but with an increased number of stages (to reduce diameter). It is assumed the switchover point for the turbine is at about 50 MWe. However, radial compressors appear to be the best suited for the S-CO_2 PCS for all power ratings presented in this work (up to 600 MWe per loop). The choice to use radial compressors is more completely covered in [Gong, et. al., 2006].

(5) Another choice which profoundly affected plant layout was the decision to employ a single-shaft turbomachinery train. A major factor was the increased rotational inertia, desirable for insuring benign response in transients. It is also noted that the PBMR design made the decision to switch from a multi-shaft to a single shaft design. Elimination of separate motors or turbines to power uncoupled compressors also leads to higher power density and lower cost. This comes at the expense of reduced flexibility in control and independent optimization of turbomachine rotational speed. Because the S-CO_2 turbomachinery is so compact, and because two compressors are required, it also made it challenging to configure the required interconnections with the much larger heat exchangers, and to accommodate valves – turbine bypass, for example – a task further complicated by the large diameter ductwork needed to avoid excessive pressure drop.

(6) Implicit in all of the above discussion is the use of a dispersed (individual components connected by ducts) rather than an integral arrangement (turbomachinery and heat exchangers bundled into a common pressure vessel). All current GFR-Brayton cycle designers, whether for He or CO_2 as the working fluid, go with dispersed, with the exception of General Atomics, whose GT-MHR is integral. (However, even General Atomics has recently expressed an increased interest in some degree of dispersion [Baxi, 2006]). A motivating factor in our view is the difficulty of accommodating valves (control, bypass, check, isolation) inside an integral vessel; and the limitation, if conventional steel pressure vessels are used, to even lower power ratings than single-train dispersed units. GA and their Russian partners have also opted for vertical turbomachinery, hence more challenging bearing designs.

(7) Worth noting is a guideline considered, but <u>not</u> adopted: namely a prejudice against single-loop PCS. With the imminent shutdown of the Zorita PWR, all contemporary and planned PWRs have 2-4 loops (BWRs, of course, are, in effect, single loop). Two or more loops are commonly credited with improved safety, startup and reduced-power operability. However, the reference unit ratings (ranging from 20 to 300 MWe) permit specification of two or more loops for all but the smallest case should this course of action be favored in the future.

The above criteria and constraints are not "hard" in the usual sense. All could be relaxed, but only with the investment of significant expenses for research, development and demonstration. It is also relevant to point out that similar considerations apply to Brayton PCS designs using working fluids other than CO_2: for example the leading choice, He, or the He/N_2 mixture of interest in France.

1.11 Thesis Organization

A brief motivation and introduction was presented in this chapter, and more will be covered on the methodology to develop the third generation cycle layouts in Chapter 2.

Chapter 3 covers the evolution from Chapter 2 to develop a recompression cycle for medium power applications. It covers the reference high performance recompression cycle, how it is adapted for various power ratings, and its sensitivity to different design conditions.

Chapter 4 covers the evolution from Chapter 3 to develop a simple cycle for medium power applications. This chapter is very similar to Chapter 3 but it is focused on a simple cycle.

Chapter 5 summarizes the most important results and discusses areas for future work

1.12 References for Chapter 1

Angelino G., "Carbon Dioxide Condensation Cycles for Power Production", ASME Paper No. 68-GT-23, 1968.

Baxi C., "Evaluation of Alternate Power Conversion Unit Designs for the GT-MHR," ICONE-14, Miami, July 2006

Carstens N., Hejzlar P., Driscoll M.J., "Dynamic Response and Safety Implications for Supercritical CO_2 Brayton Cycles Coupled to Gen-IV Reactors", MIT Canes Report, MIT-ANP-TR-114, July 2007.

Dostal V., Driscoll M.J., Hejzlar P., "A Supercritical Carbon Dioxide Cycle for Next Generation Nuclear Reactors", MIT CANES Report MIT-ANP-TR-100, March 2004

Feher E. G., "Supercritical Thermodynamic Cycles for External and Internal Combustion Engines", Astropower, Inc. Engineering Report, May 1962.

Feher E. G., "The Supercritical Thermodynamic Power Cycle", Douglas Paper No. 4348, presented to the IECEC, Miami Beach, Florida, August 13-17, 1967.

Fernandez S., et al, "Extended-Scope Applications of the Supercritical CO_2 Power Conversion System," MIT-GFR-039, August 2006

Gibbs J.P., Hejzlar P., Driscoll M.J., "Applicability of Supercritical CO_2 Power Conversion Systems to GEN IV Reactors", MIT CANES Report MIT-GFR-037, September 2006

Gokhstein D.P., Verkhivker G.P., "Future Design of Thermal Power Stations Operating on Carbon Dioxide", *Thermal Engineering*, April, pp. 36-38, 1971.

Gong Y., et al, "Analysis of Radial Compressor Options for Supercritical CO_2 Power Conversion Cycles," MIT-GFR-034, June 2006

Handwerk C.S., Driscoll M.J., Hejzlar P., "Core Design and Performance Assessment for a Supercritical CO_2-Cooled Fast Reactor, MIT CANES Report, MIT-ANP-TR-113, May 2007.

Heatric™ website www.heatric.com

Hejzlar P., Driscoll M.J., Gibbs J., Gong Y., Kao S., "Supercritical CO_2 Brayton Cycle for Medium Power Applications", MIT CANES Report MIT-ANP-PR-117, April 2006.

Kato, Y., Nitawaki T., Yoshizawa Y., "A Carbon Dioxide Partial Condensation Direct Cycle for Advanced Gas Cooled Fast and Thermal Reactors", Global 2001, Paris, September 9-13, 2001.

Katzer J., et. al., "The Future of Coal Power, Options for a Carbon-Constrained World", Massachusetts Institute of Technology, 2007

Legault D.M., Hejzlar P., "CYCLES II: A Steady State Code for Supercritical CO_2 Power Conversion System Calculations," MIT CANES Report, MIT-GFR-036, June 2006.

Moisseytsev A.V., Sienicki J.J., Wade D.C., "Turbine Design for a Supercritical Carbon Dioxide Gas Turbine Brayton Cycle", *International Congress on Advanced Nuclear Power Plants* (ICAPP 2003), Cordoba, Spain, May 4-7, 2003.

NERI Project No. 05-044, "Optimized, Competitive Supercritical-CO_2 Cycle GFR for Generation IV Service," NERI 2005 Annual Report, DOE/NE-0129

NIST Reference Fluid Thermodynamic and Transport Properties, Standard Reference Database 23, Version 7.0

Oh C., "Development of a Supercritical Carbon Dioxide Brayton Cycle: Improving PBR Efficiency and Testing Material Compatibility", Nuclear Energy Research Initiative, Proposal Number 2002-190, 2002.

Okano Y., Hejzlar P., Todreas N.E., Driscoll M.J., "Thermal Hydraulics and Shutdown Cooling of Supercritical CO_2 GT-GCFRs, MIT CANES Report, MIT-ANP-TR-088, August 2002.

Paoletti L., et al, "Interfacing the Pebble Bed Modular Reactor and the Westinghouse Sulfur Process," Trans. Am. Nucl. Soc., Vol. 92, June 2005

Petr V., Kolovratnik M., "A Study on Application of a Closed Cycle CO_2 Gas Turbine in Power Engineering (in Czech)", Czech Technical University in Prague, Department of Fluid Dynamics and Power Engineering, Division of Power Engineering, Departmental report Z-530/99, January 1999.

Pope M.A., Hejzlar P., Driscoll M.J., "Thermal Hydraulics of a 2400 MWth Supercritical CO_2-Direct Cycle GFR, MIT CANES Report, MIT-ANP-112, September 2006.

Pope M.A., Driscoll M.J., Hejzlar P., "Reactor Physics Design of Supercritical CO_2-Cooled Fast Reactors, MIT CANES Report, MIT-ANP-TR-104, September 2004.

Rucker J., "Design and Analysis of a Permanent Magnet Generator for Naval Applications", MIT Master's Thesis, Department of Electrical Engineering and Computer Science, June 2005

Shade, N., "Enormous Power In A Small Package", Compressor Tech Two, January-February 2006

Strub R. A., Frieder A.J., "High Pressure Indirect CO_2 Closed-Cycle Design Gas Turbines", *Nuclear Gas Turbines*, pp 51-61, January 1970.

Sulzer Patent Verfahren zur Erzeugung von Arbeit aus Warme, Swiss Patent 269 599, 1948.

Yildiz B., Kazimi M., "Efficiency of hydrogen production systems using alternative nuclear energy technologies", International Journal of Hydrogen Energy, Elsevier Ltd., 2005

This page intentionally left blank

2 Third Generation Plant Layouts

2.1 Introduction

The majority of the initial M.I.T. work for a power conversion system (PCS) for Generation IV nuclear reactors has been directed towards an integral layout (i.e. components enclosed in a pressure vessel), followed by a second generation effort to develop a distributed design (i.e. components connected by piping). Dostal's original design for the supercritical CO_2 (S-CO_2) employed an integral layout, similar to that of the General Atomic GT-MHR. However, recent efforts have been directed to exploring the distributed layout because of several key considerations such as maintenance and inspection ease and difficulties to accommodate bypass valves [Gibbs, et. al., 2006] [Baxi, 2006][Minatsuki, 2007]. The distributed layout also better accommodates thermal expansion because it is not enclosed tightly within a large pressure vessel. Although the ductwork pressure losses within an integral design are quite small, the distributed arrangements described in this chapter are very competitive, with less than a 1% loss due to piping.

The power conversion system (PCS) layouts were developed using SOLID EDGE™, a 3-D auto cad type software [Solid Edge™], and CYCLES, an in-house, MIT developed, recompression cycle, optimization code (see Section 1.7). The recompression cycle developed at MIT for a 300 MWe rating coupled to a Generation IV reactor was selected as the reference version for scaling the cycle to power ratings ranging from 20-300 MWe. Three power ratings have been chosen for the three reference layout designs: 20, 50, and 300 MWe. These three designs serve as possible component layouts, but any power rating in between these sizes is also possible. For larger reactor ratings multiple PCS loops are employed. Furthermore, the sodium cooled fast reactor is now the chosen Global Nuclear Energy Program (GNEP) generation IV reactor and is accordingly the reference reactor in this study [www.gnep.energy.gov]. All of the liquid cooled reactors are very similar in nature; therefore, the overall cycle layout will only be slightly affected

if lead or liquid salt is employed on the primary side of the intermediate heat exchanger (IHX).

A key aspect of the lower power ratings is their ability to use a permanent magnet generator as opposed to a wound rotor generator or some other large and bulky unit. A 20 MWe permanent magnet generator is depicted in the 20 MWe layout section. The use of variable speed turbomachinery with power electronics enables the rotational speed to increase, thus allowing the permanent magnet generator to shrink with higher speeds. Naturally, an upper limit exists, but because the generation is not limited to the standard 3600 RPM, an optimum speed for the generator and turbomachinery can be specified. Currently the upper limit of permanent magnet generators is around 30 MWe with rotational speeds typically between 4500 to 7000 RPM. Power densities for these generators are on the order of 2.4 kw/kg (3800 kW/m^3) which is approximately six times higher than conventional machines! [Shade, 2006]

Although 30 MWe is the current upper limit of the permanent magnet generators, 100 MWe was chosen as the cutoff point between variable and constant speed operation. The variable speed operation is not dictated by the desired power rating, but is an easy to implement feature and can provide a wide range of small power ratings in one unit with reasonably sized auxiliary power electronics. As the technology advances and larger permanent magnet generators become available it is ideal to use them with variable speed turbomachinery because of their impressive partial load operation; small turbomachines also optimize at higher rotational speeds. The power ratings above 100 MWe are designed for multiple loop systems using constant speed turbomachinery with the partial load being controlled by conversion loops cutting in and out. Of course, if a large power rating is designed with only one loop it is also possible to use variable speed turbomachinery for a different full power rating, but the associated power electronics will also become increasingly larger. Other methods of control include turbine and compressor inlet temperature control, bypass control, and inventory control [Carstens, et, al., 2007]. A matrix of suggested combinations to obtain desired power ratings is summarized in Table 2.1: they are intended to achieve reasonable partial load control

with minimal auxiliary equipment. Additionally, Table 2.2 lists the representative contemporary closed Brayton cycle gas turbine plant layouts.

As the power ratings increase, the overall layout shifts from a slightly nested turbomachinery train below 50 MWe to a single heat exchanger train above 50 MWe and finally to a dual heat exchanger train to achieve 300 MWe. Outside of the physical plant layout, there is a second tier tradeoff between the larger and smaller power ratings. The smaller power ratings have the option to be almost completely constructed at a remote location and transported to the reactor site and installed as one unit. The smaller ratings also are not as susceptible to the availability of large diameter high pressure pipes. In actuality, it is possible to take advantage of the piping sizes to slightly negate the lower turbomachinery efficiencies by reducing the system pressure drops to a minimum. The only limiting factor for the piping in the low rating layouts is the ability to connect large pipes to the turbomachinery casings. However, this should only be a problem for the power ratings below 30 MWe. The higher power ratings are limited to the availability of large diameter pipes. Very large diameter pipes are available from piping catalogs, but temperature and pressure requirements limit the currently available pipes to around 1 meter inner diameter for the temperature and pressure combination proposed here. Overall, the performance of the smaller power ratings is about 1% less efficient than the larger ratings. If very large diameter high pressure piping ($\geq$1.0m) is available, the large power rating can display very impressive performance, but if smaller than optimal pipes are used the piping losses will be very disadvantageous. For example, a 24 inch outer diameter pipe is readily available for use with high temperature and pressure with the wall thickness being slightly larger than two inches. If this pipe was used as the turbine inlet pipe the net cycle efficiency would be penalized approximately 1.5% due to this pipe run alone. Fortunately, this is the only large diameter pipe in the layout so the prospect of further efficiency losses due to pipe reductions is not likely. However, current pipe technology suggests that the large diameter pipes and valves will not be a problem to obtain. When the first layout was developed and the piping losses were calculated it was discovered that improperly sized pipes could easily reduce the cycle efficiency by more than 10%. As of now, all of the designs are for a distributed layout,

as opposed to an integral layout with all of the components in one pressure vessel: the configuration originally proposed by Dostal.

Table 2.1 Suggested distributed layout arrangements

Total Rating (MWe)	**Turbomachinery (comp/turbine)**	**PCS Units (loops)**	**Configuration (number of trains per PCS)**
25	radial/radial (V)	1	Single
50	radial/radial (V)	1 or 2x25	Single
100	radial/radial (V)	1 or 4x25 or 2x50	Single
125	radial/axial (C)	1	Single/Dual
150	radial or axial/axial (C)	1 3x50 (or 100+50)	Single/Dual Single
250	radial or axial/axial (C)	1 2x125	Dual Single/Dual
300	radial or axial/axial (C)	1 2x150 Or 3x100	Dual Single/Dual
500	radial or axial/axial (C)	2x250 4x125	Dual Single/Dual
750	radial or axial/axial (C)	3x250	Dual
1000	radial or axial/axial (C)	4x250	Dual
1200	radial or axial/axial (C)	4x300 2x600	Dual Dual

(V) = variable speed turbomachinery that will require power electronics to produce constant frequency AC power

(C) = constant speed turbomachinery

Dual = two recuperator trains in parallel per PCS loop; also two IHX ducts to/from PCS per loop; but one turbomachinery train per PCS loop.

Single = one recuperator train per PCS loop with one turbomachinery train.

Table 2.2 Representative contemporary closed Brayton cycle gas turbine plant layouts [Gibbs, et. al., 2006]

Concept	Arrangement / Layout
GTHTR 300 (JAERI)	• Turbine / compressor / generator encapsulated in horizontal pressure vessel • Recuperator / precooler encapsulated in separate vertical pressure vessel • Direct cycle 300 MWe
ESKOM PBMR (South Africa)	Vertical heat exchanger vessels, connected by ducts; generator outside horizontal turbomachinery train; direct cycle 175 MWe
GTMHR (US/GA, Russia)	Vertical Pressure Vessel enclosing Turbine / HP & LP compressors in central cylinder, precooler/intercooler/recuperator in surrounding annulus; generator in vessel extension (see Figure 2.1) Direct Cycle 285 MWe
MIT PBMR	Fully dispersed among a total of 21 railcar/truck-shippable modules: e.g. six recuperator modules Indirect cycle 115 MWe
MIT/INL LDRD	Single vertical PCU vessel housing all S-CO_2 components, with generator outside vessel Direct cycle, Fast Reactor 250 MWe
CEA	Study of dispersed He and S-CO_2 PCS Indirect Cycles for GFR; He primary coolant. Single shaft horizontal turbomachinery: 300 MWe
NGNP	Both integrated and non-integrated Direct Cycle versions under consideration; GTMHR used for INL Point Design studies
Framatome	Indirect Cycle, N_2 working fluid
INL	CO_2 power cycle which approaches the critical pressure (7.38 MPa) from below. Indirect Cycle 125 MWe He, N_2/He, CO_2 300 MWe
ANL	S-CO_2 power cycle very similar to the MIT version; Indirect Cycle Star LM @ 180 MWe
Tokyo Tech	Another CO_2 power cycle which approaches the critical pressure from below; Direct Cycle; more recently S-CO_2 similar to MIT 300 MWe
ORNL	Indirect cycle: liquid salt cooled core coupled to a helium PCS which employs reheat, AHTR, He, CO_2 300 MWe
(UCB)	NGNP: He, N_2/He, CO_2 300 MWe

Note: Designs are evolving and hence specifications change over time.

Below 100 MWe the turbomachinery can be chosen to be variable speed to allow for partial load operation with the proper DC/AC conversion. Above 100 MWe it may be desirable to use several loops and simply cut them in and out appropriately for lower power requirements.

2.2 Arrangements (Solid Edge)

2.2.1 Starting Point – Second Generation PCS

The first generation, as proposed by Dostal [Dostal, et. al., 2004], is shown in Figure 2.1. It is an integral design similar to that selected for the GA/Russian GT-MHR (see Figure 2.2). The major benefit is the large reduction in pressure drop achieved by elimination of ductwork. A major drawback, which led us to move to a dispersed component arrangement, is the use of a vertical turbomachinery train and generator bearings.

The first dispersed design layout is shown in Figures 2.3 through 2.5 and was developed by Peter Stahle, a Research Engineer in the MIT Nuclear Science and Engineering Department and the MIT Plasma and Fusion Center, and employs a parallel heat exchanger train layout feeding into one turbomachinery train centrally located, straddled by pressure vessels containing heat exchanger modules [Stahle, et. al., 2006]. The printed circuit heat exchangers are now housed in individual, dispersed pressure vessels connected by ductwork. Prudent vessel size restrictions also lead to use of two trains in parallel. Each heat exchanger train is capable of handling 150 MWe worth of associated thermal power. Further iterations have refined the original layout, but all of the larger power ratings have adopted the parallel heat exchanger train idea. The most recent designs are discussed in detail in their respective sections.

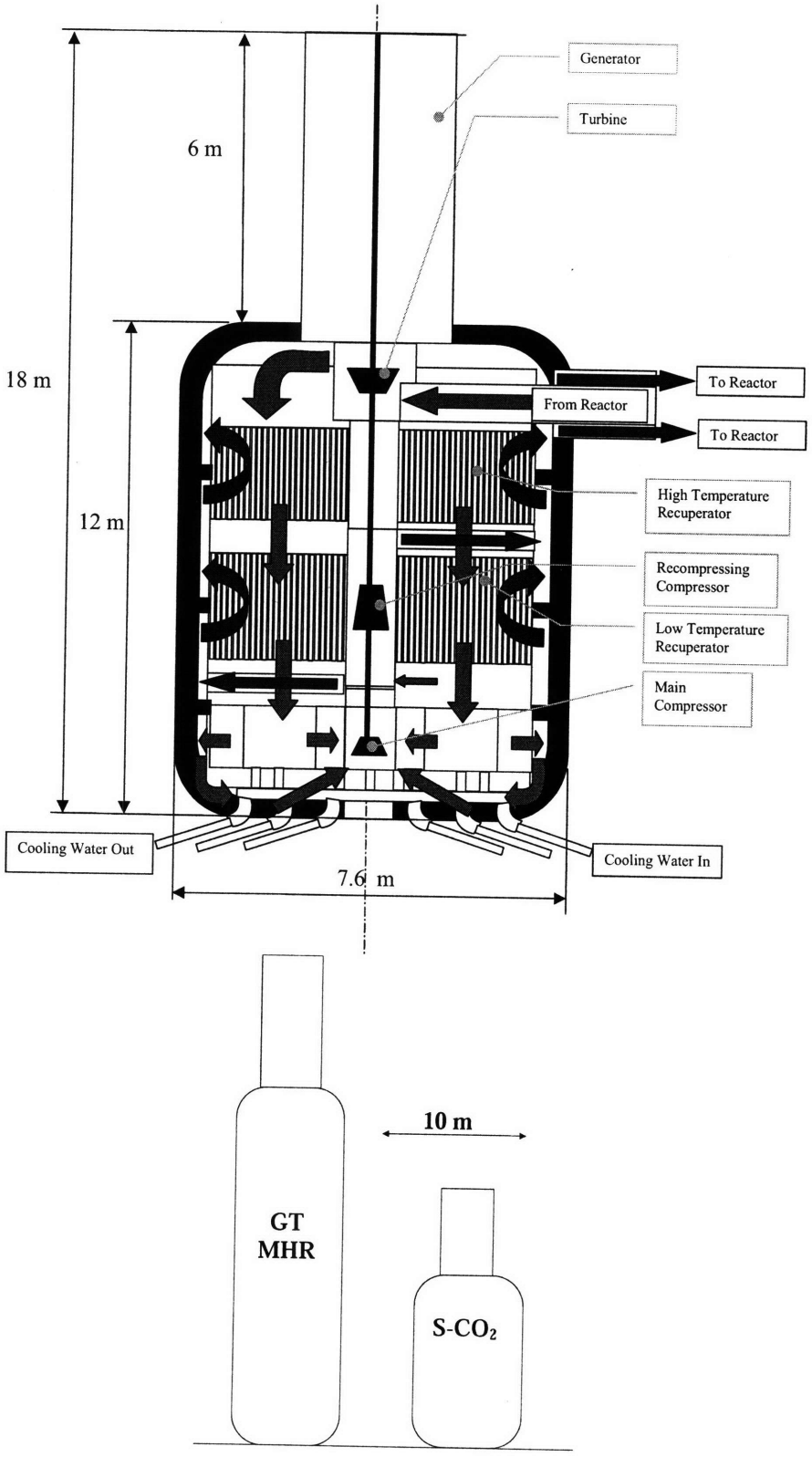

Figure 2.1 Dostal's original integral PCS arrangement [Dostal, et. al., 2004]

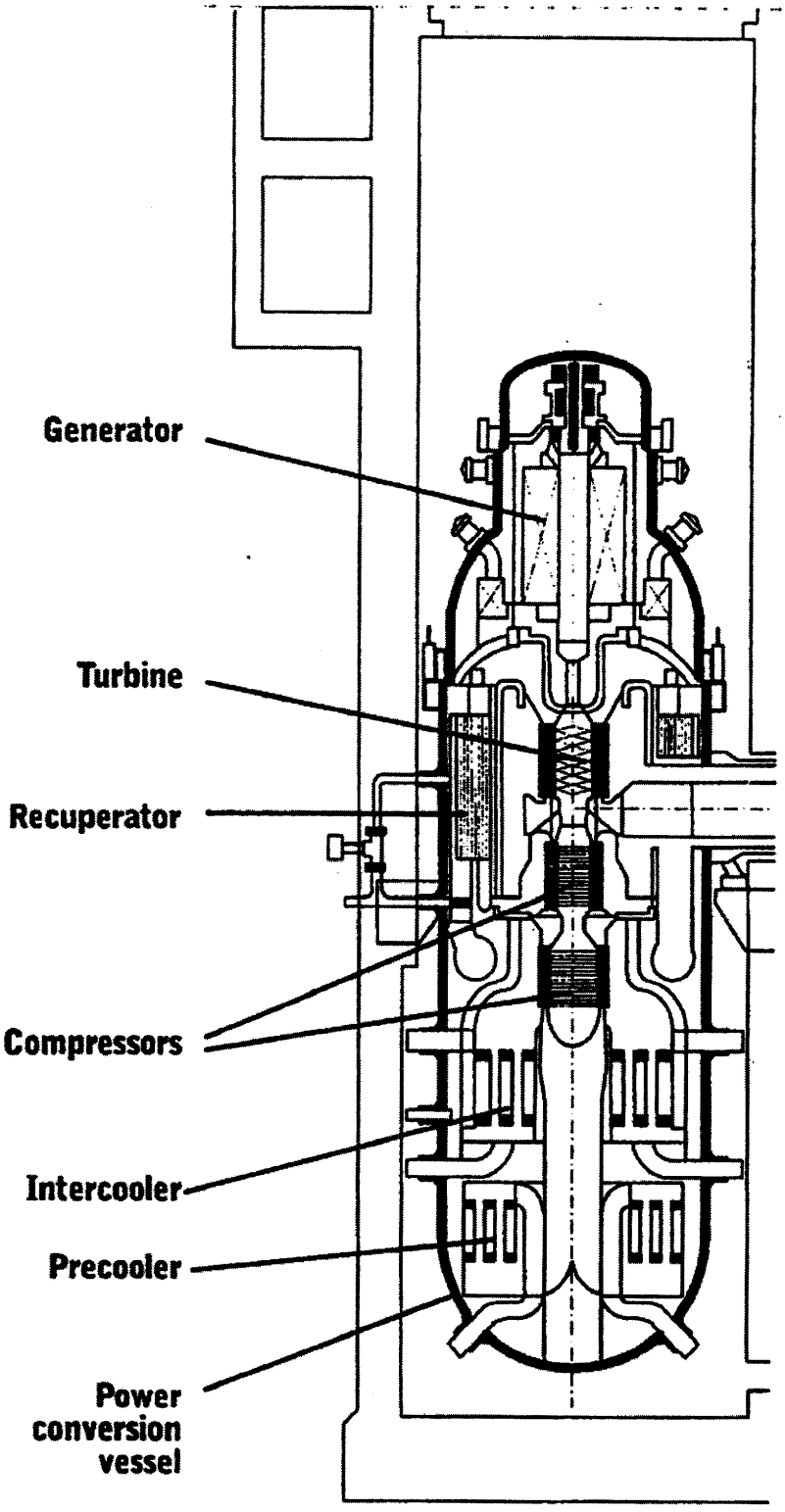

Figure 2.2 Main components of GT-MHR

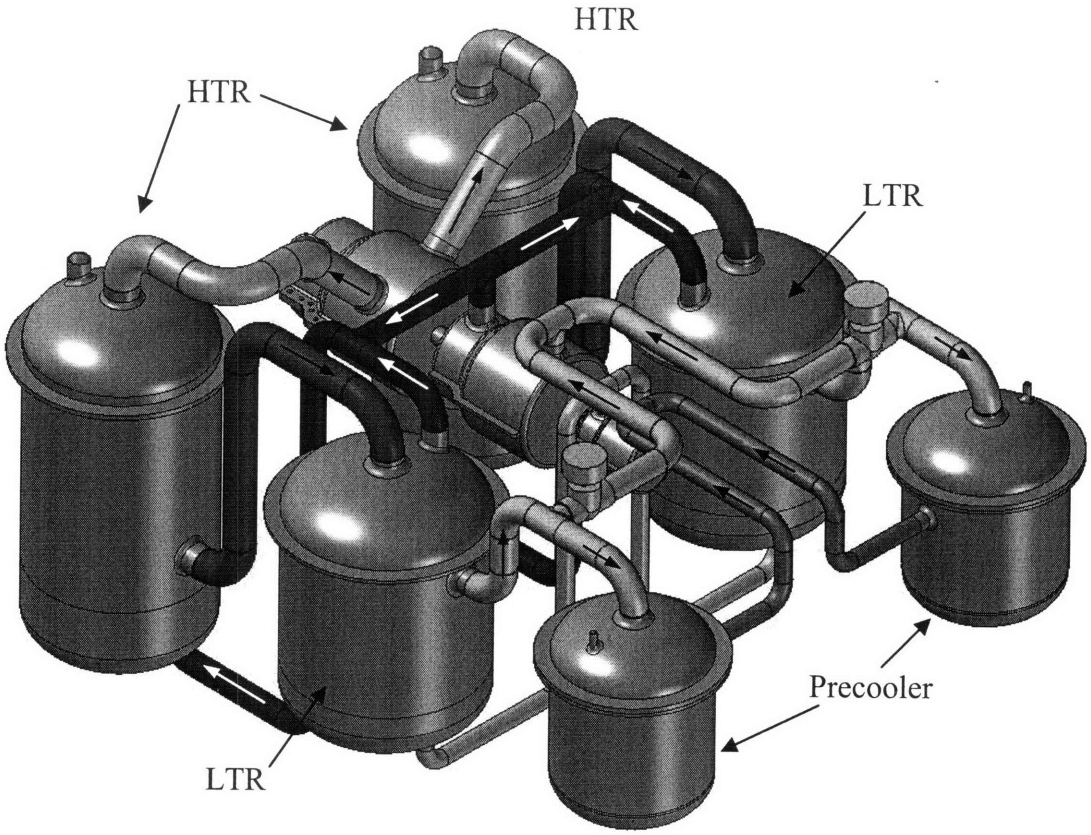

Figure 2.3 Second generation layout for 300 MWe PCS, isometric view [Stahle, et. al., 2006]

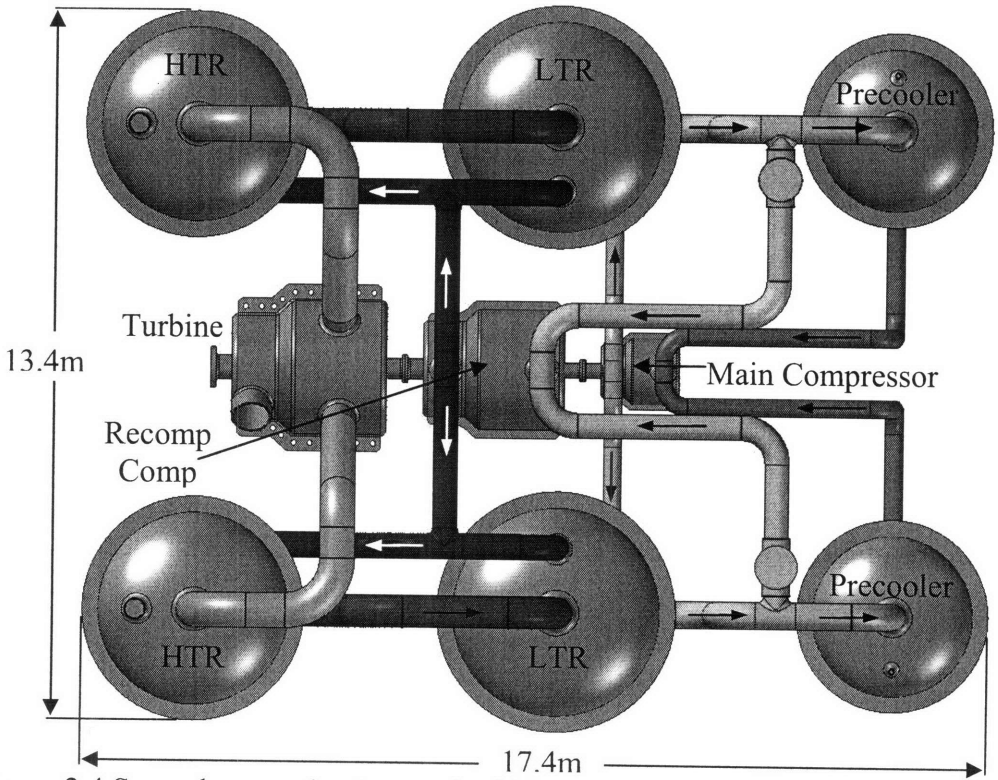

Figure 2.4 Second generation layout for 300 MWe PCS, top view [Stahle, et. al., 2006]

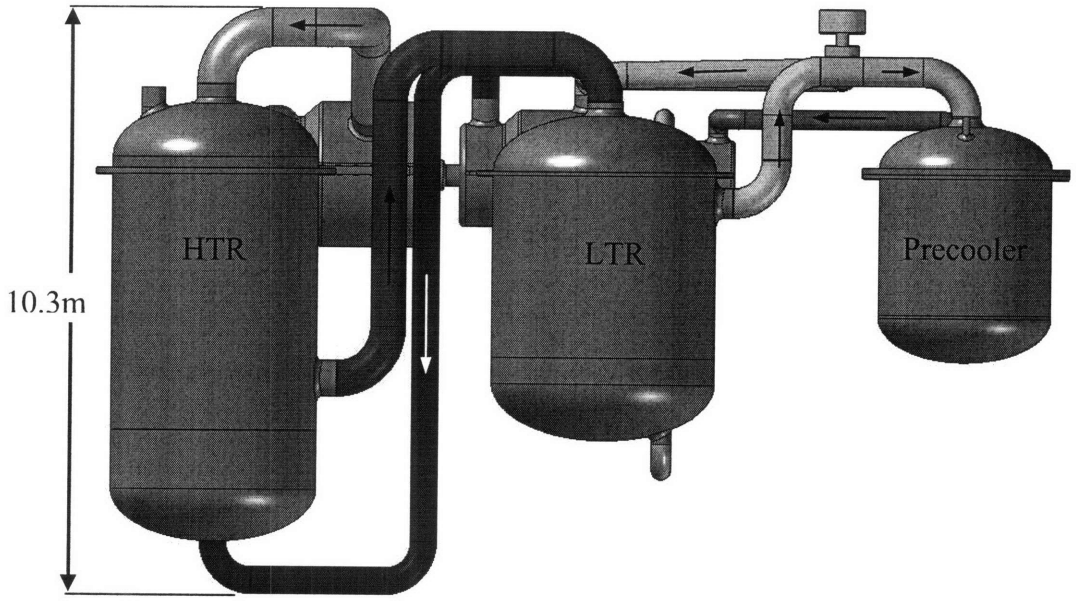

Figure 2.5 Second generation layout for 300 MWe PCS, side view [Stahle, et. al., 2006]

The depicted design employs the heat exchangers in two parallel trains with the turbomachinery in the middle. The HEATRIC™ heat exchangers are located within the six pressure vessels, with the high temperature recuperator being in the largest vessel, the low temperature recuperator being in the medium-size vessel, and the precooler in the smallest vessel. The method of feeding the fluid to the heat exchangers strongly dictates the overall layout of the piping between the heat exchanger modules and the turbomachinery. Figure 2.6 depicts how the heat exchanger modules are arranged within each pressure vessel. The HEATRIC™ heat exchangers (PCHE) in this layout employ partial counterflow heat exchangers using a "multiported" configuration with plena integrated into the diffusion bonded plates. The beginning and end of the secondary side have a partial cross flow pattern near the plena. To minimize pressure drop and its impact on efficiency, PCHEs are arranged in such a way that the hot low-pressure stream goes straight through the active core of heat exchanger and does not need special plena (plena are formed by vessel space as indicated on Figure 2.6).

The primary fluid (low pressure, high temperature) from the turbine discharge is directed down the center section of the vessel for distribution among the six modules. The fluid

flows directly through the recuperator and is collected in the outer vessel where it converges and flows to the low temperature recuperator via one pipe (primary out). The low temperature recuperator has the same flow pattern as the high temperature recuperator with the primary low pressure, high temperature fluid entering and being distributed in the middle of the vessel.

The secondary fluid (high pressure, low temperature) enters the vessel at the bottom via the inlet pipe which discharges the fluid to a small distribution plenum. Within the plenum is a baffle which directs the fluid to three of the six triangular shaped paths, as seen in Figure 2.4. Three of the triangular paths are used for distribution and three are used for collection of the secondary fluid. Once the fluid enters the secondary distribution channel it flows in opposite directions across the two bordering recuperator modules. Each plate on the secondary side contains small end plena, where flow from individual channels is collected and directed through small side openings. The fluid is then collected in the remaining three triangular paths and is directed to the plenum at the top of the vessel where it leaves via one pipe (secondary out).

After the CO_2 leaves the low temperature recuperator it is split between the recompressing compressor and the precooler. The flow from the low temperature recuperator to the precooler is directed into the "primary in" channel, with the cooling water using the secondary side.

This design has several strengths and weaknesses. The strengths include the piping layout being a feasible design, as it allows for thermal expansion in the piping runs to accommodate stress, and the pipes are readily available pipe sizes. Although detailed stress calculations have not yet been performed on the layout, the design appears to be tolerant of expansion and also able to easily adjust if necessary to accommodate higher stresses. However, the disadvantages are the increased probability of mixing water and CO_2 in the precooler, low power density of the heat exchanger vessels, and long single pipe runs, which cause a significant efficiency penalty. Although the probability of contaminating the CO_2 side of the system with water is still low due to the differential

pressure being in favor of the CO_2, the vessel layouts include more welded seams and the presence of non-heat-exchanger structures. The risk of leakage within each heat exchanger module's core is low because of the diffusion bonding, but handling the fluid within each vessel adds an extra risk. Also, the design of triangular plena that contain high pressure while allowing for thermal expansion is challenging.

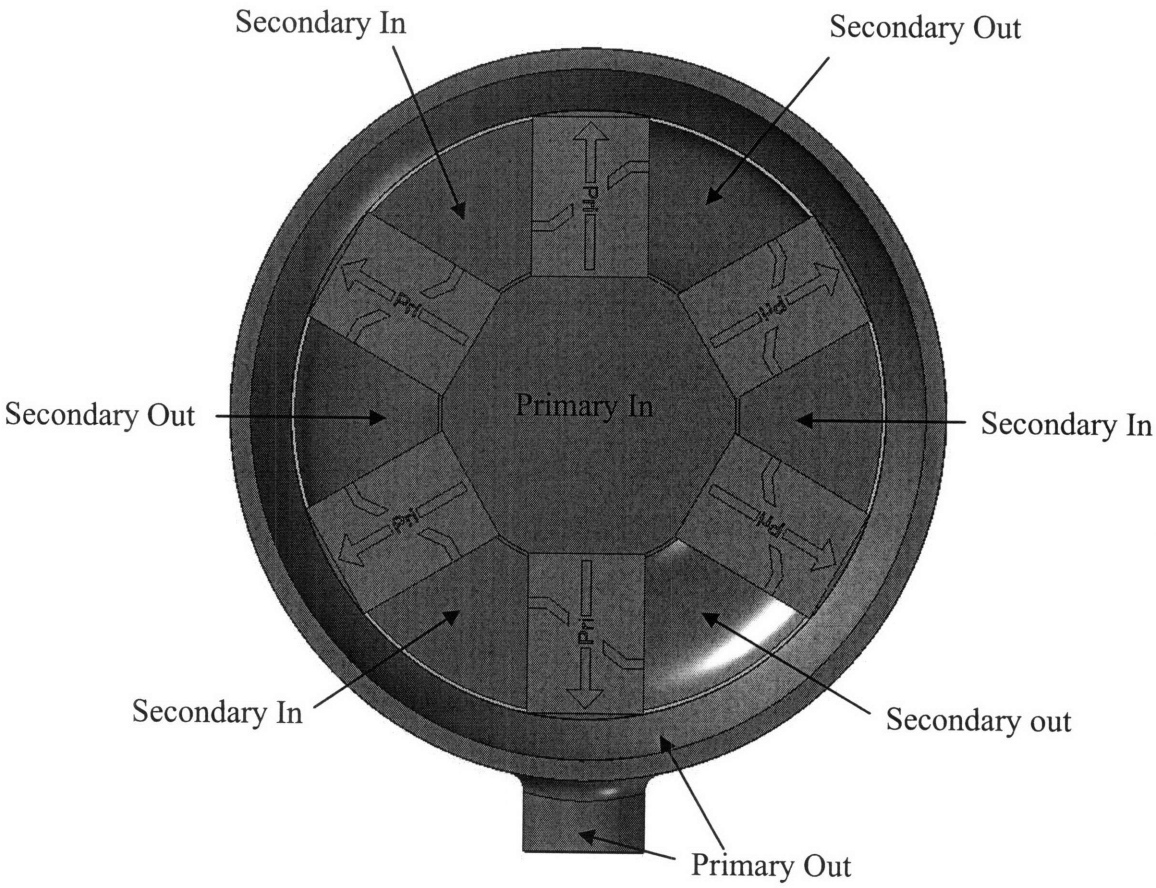

Figure 2.6 Cross section depiction of heat exchanger vessel
for second generation layout [Stahle, et. al., 2006]

Arranging the heat exchanger modules in the vessels reduces their power density, which carries over to give a lower power density to the overall layout. The power density of a HEATRIC™ heat exchanger core is around 25-30 MWt/m^3, but if they are arranged within a vessel as shown in Figure 2.7 the power density is reduced to around 7.6 $MWth/m^3$ (for the HTR). This lower power density partially negates the advantage of

using this type of compact heat exchanger. The size of conveniently manipulated pressure vessels also limits the total rating of a heat exchanger train. Also, using a pressure vessel for arranging the heat exchanger modules increases the overall length of piping runs and limits the use of several parallel pipes to reduce the associated pressure losses. With the pipe sizes depicted in the above layout the pressure drops would lead to 10% reduction in overall cycle efficiency. Clearly this is unacceptable and can be improved upon. The pipes between heat exchanger modules were later increased to reduce the very high pressure losses, but the best the design could achieve still exhibited 4% efficiency reduction. The power density for the arrangement in the third generation layout for the HTR is approximately 29.7 MWth/m^3 exclusively for the core, and is reduced to about 11.4 MWth/m^3 for a complete module (plena included). Although this is not a huge power density improvement upon the heat exchangers arranged within a vessel, it does allow for a better piping arrangement and increased modularity.

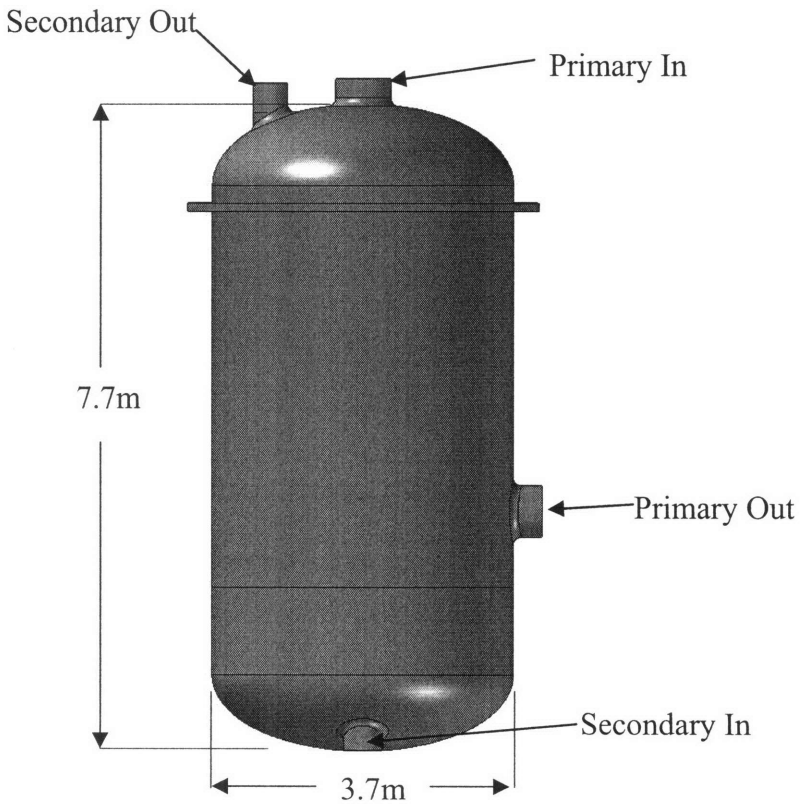

Figure 2.7 Heat exchanger vessel for second generation layout
(dimensions shown for a 150 MWe HTR vessel) [Stahle, et. al., 2006]

2.2.2 Third Generation Cycle Layouts

The advanced multiported HEATRIC™ heat exchangers with a full counterflow pattern and zig-zag channels have very high core power density and make it possible to reduce the overall volume of the PCS. The heat exchangers are the largest components in the power conversion cycle; therefore, their layout generally dictates the overall layout. The heat exchangers could still be arranged with several modules arranged in a pressure vessel, but they can be more efficiently arranged to have a very high power density and enable the use of many parallel pipe runs to make the piping losses more moderate. The most recent version of the cycle layout, as described in this report, exploits this very high heat exchanger power density and has the modules arranged in a parallel fashion. This approach was originally introduced to reduce the pressure losses on the high pressure side of the recuperators, but it also has an added advantage in the transportability of the modules. These modules are essentially separate heat exchangers which will then be welded into a frame, possibly on location, but preferably at the manufacturer's plant to make the full heat exchanger unit. Once again, a detailed stress analysis has not been performed, but the cycle can easily be adjusted to add expansion loops if this proves necessary.

Each heat exchanger module is comprised of numerous diffusion bonded plates making up the core with welded plena. The optimum design has the module restricted in two directions; length and width. The length is fixed because each unit (HTR, LTR, and PRE) are optimized for a specific length of heat transfer and the width is fixed due to HEATRIC™ manufacturing limits of 60cm due to the maximum width of the photosensitive film necessary for the etching process currently available. Therefore, the only way to expand the volume is in the vertical direction. It is desirable to limit the height of each module to around 5m to keep the distance the fluid must travel to a minimum. Each module has an inlet and outlet for both the low pressure and high pressure side. This can be an added bonus for replacement, if necessary; since a single module can be removed and replaced. Also, this arrangement makes it possible for the turbine to have a very large diffuser. This increases the turbine total to static efficiency while only minimally adding to the overall footprint of the layout. Using the same

number of modules for both the high and low temperature recuperators, the CO_2 can be directly discharged from one module to the next via a very short pipe run (approximately ½ meter) which circumvents the necessity of many large diameter pipes and reduces the large pressure losses associated with large piping runs in the 2nd generation design. Essentially, the recuperators (HTR and LTR) are arranged as parallel modules which are fastened together to form the full recuperator unit. The number of parallel modules is based on the required recuperator volume and the desired height. Initially, the height was based on keeping the overall height to around or below 5m, but this can be relaxed at the expense of a minor increase in piping pressure loss if designing for a minimum footprint is the prime concern. Fewer heat exchanger modules will make the layout taller and less wide.

The issue of stress analysis also has to be considered. Because of the large ΔT in the cycle between full operational and ambient temperatures the thermal expansion needs to be addressed. The heat exchanger units could in principle be welded together to essentially make one large block, but the end modules will move more than the center modules. This issue can be addressed by not directly welding the modules together, but placing a softer alloy spacer between each module and strapping the modules together. Each module would have to be secured to the foundation separately. This allows each separate module to expand individually, which allows the end module to only move as much as the center module, thus greatly reducing the transverse motion of the pipes and putting equal strain on each pipe. In addition, such arrangement makes the modules easily replaceable. Clearly, the high temperature recuperator has a larger ΔT than the low temperature recuperator or the precooler. Therefore, the high temperature recuperator will expand more vertically than both the low temperature recuperator and precooler. The overall effect of this on the piping has not been closely analyzed yet, but if the unequal differential expansions are indeed a problem this can be remedied by simply moving the total heat exchanger units farther away from each other and extending the length of the input/output connectors, and adding an expansion bend if necessary. This will slightly increase the overall footprint of the cycle and reduce efficiency, but it will better tolerate the vertical motion caused by expansion.

To summarize:

Advantages of the third generation design are:

- Smaller footprint
- Very low ΔP throughout cycle, thus, higher cycle efficiency
- Better transportability, inspectability, and repairability/replacement due to modularity
- Standard HEATRIC™ configuration

Disadvantages of third generation design:

- More welded connections
- Large collection/distribution manifolds with closely spaced connector elbows

2.3 Heat Exchanger Arrangement

Because cycle efficiency is proportional to fractional pressure losses, i.e, pressure loss in each section divided by pressure in this section, pressure losses on the low pressure side are the key pressure losses that need to be reduced. Therefore, the arrangement of PCHEs is dictated by the requirement of minimum pressure loss on the hot side.

When the first power conversion layout was completed and the piping losses analyzed, the turbine was arranged to discharge to the outside plenum of the high temperature recuperator. Experimenting to find the most highly compact design for the very low power ratings, one layout directed the low pressure fluid to the inside plenum. When the piping losses were calculated for this design it was discovered that the losses were extremely large. The inside plenum is limited to receiving the fluid from either the top or the bottom, while the outside plenum can receive the fluid from any height along the side, or from the top or bottom. This is important for two reasons: fluid pressure losses and stress considerations. The inside plenum requires some of the fluid to travel the entire height of the heat exchanger before entering the active core through a more narrow flow

path. If the low pressure fluid is in the inside plenum it will have a much higher fractional pressure loss and larger effect on cycle performance than if the high pressure fluid is so located. It is also desirable to have the low pressure fluid in the outside plenum because the external fluid boundary will not need to be as strong. In the manufacturing process of these heat exchangers the inside plenum is part of the plate stack which is joined by diffusion bonding. This allows the heat exchanger to withstand extremely high stress, and is already well suited, with no extra reinforcement, for the high pressure fluid. Therefore, because of the lower fractional pressure drop and stronger heat exchange characteristics, it is important to use the inner plenum for the high pressure fluid. Although this is not required, the lower fractional pressure losses significantly reduce the pressure loss penalty in the cycle. A cutaway of a HEATRIC™ heat exchanger as used in the power conversion cycle has been drawn in SOLID EDGE and can be used to easily view the flow distribution and path through the unit. This can be seen in Figure 2.8.

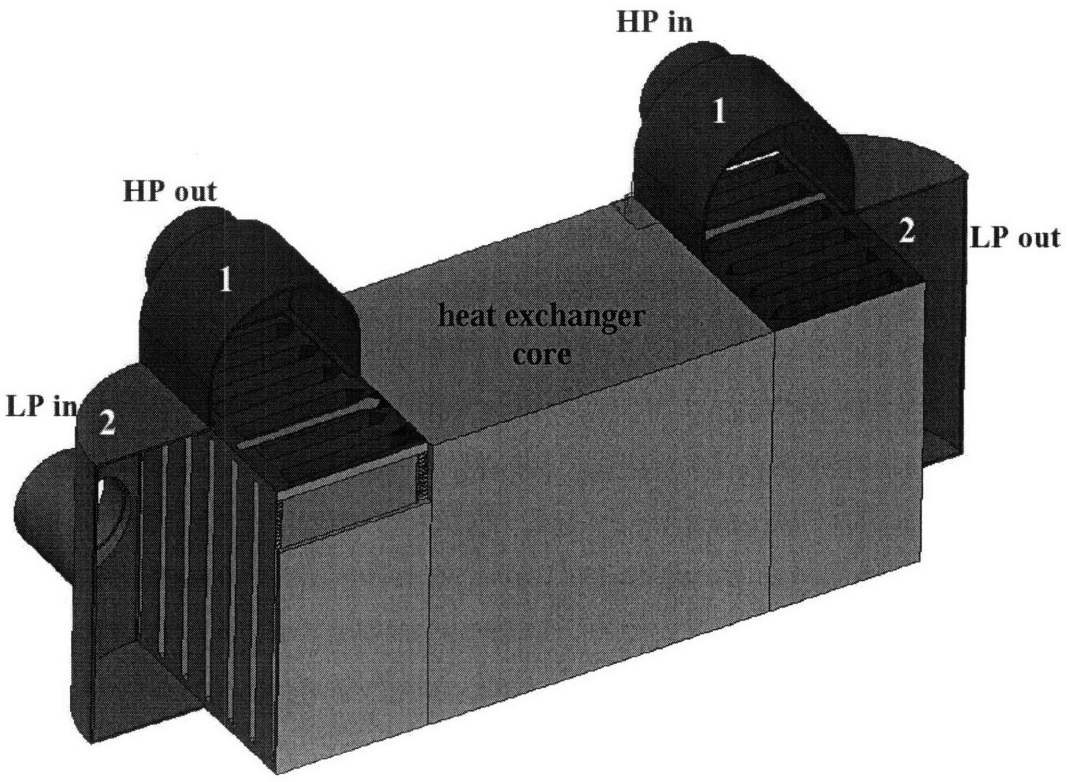

Figure 2.8 Cutaway view of PCHE

This arrangement of PCHE modules is the same as developed in the MIT report CANES-ANP-PR-117 "Supercritical CO_2 Brayton Cycle for Medium Power Applications" [Hejzlar, et. al., 2006]. The high and low pressure sides of the heat exchanger are shown in red and green (component 1 and 2), respectively. When the fluid enters the high pressure side it is distributed into the blue channels which run the entire height of the unit. From the blue channels the fluid is distributed into the core and is collected on the opposite side in the blue channels. The low pressure fluid enters the heat exchanger via the green inlet and is distributed to the orange channels. The low pressure fluid enters the heat exchanger on the end opposite to the high pressure fluid to obtain a counterflow configuration. The orange distribution channels are positioned between the high pressure blue channels and also extend the full height of the heat exchanger. The low pressure fluid enters the distribution channels from the side plenum cover through numerous drilled passages. Although the low pressure inlet and outlet pipes are shown entering from the side, it is possible to connect them to the plenum at any point along the outside, thus enabling more freedom in the associated piping. Also, easily seen in Figure 2.8 is the distance the fluid must travel once it enters the plenum before it is distributed through the active core. The average distance for the high pressure plenum is one half the overall height and that of the low pressure plenum can be slightly less than one quarter of the overall height.

Once the inside plenum was designated to handle the high pressure fluid, it was also discovered that the net cycle efficiency could be raised even further by increasing the cross sectional flow area of the high pressure plenum. The initial size of the high pressure plenum caused a large penalty due to its small flow area. Noteworthy efficiency gains were made until the initial plenum was increased to 5x its original cross sectional area, where it reached a plateau. In Figure 2.9 on the right is a picture of the initial size of the HEATRIC™ heat exchanger plate. The drawing on the left is an AutoCAD depiction of what the new shape of the high pressure plenum will look like. Increasing the high pressure plenum flow area 5x increases the length less than 3x while making a noticeable performance increase.

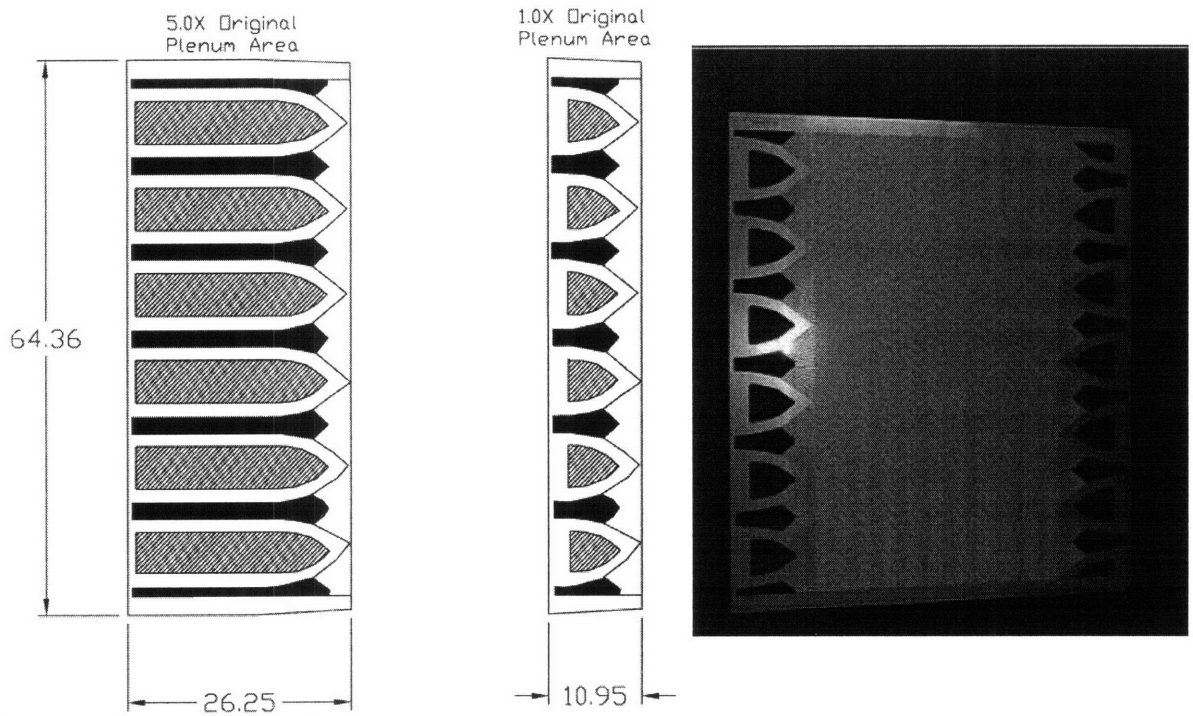

Figure 2.9 Increasing the HP plena volume of the PCHE

It is also evident in the above figures how the addition of the large plena increases the length of the heat exchanger. The active core length is less than 1m for most of the heat exchangers, but the overall length is now approximately 2m due to the plena. The plena can be increased or decreased depending on the pipe size, but if the pipes are attached on the end (as opposed to the side) the maximum usable diameter is about 0.5m (20in). Regardless, the heat exchanger is very compact compared to other types of heat exchangers.

Once the high and low pressure flow through a heat exchanger module was established, the piping considerations for connecting the various components were primarily to keep the major losses to a minimum. It is more important for the low pressure fluid to have more short and straight runs than the high pressure fluid. Also, using the same number of high temperature recuperator modules as low temperature recuperator modules, it is possible to discharge directly from one module to the next, essentially making numerous parallel recuperation modules bundled together to form one large unit.

2.4 Third Generation Layout – 300 MWe

For the 300 MWe power conversion unit (Figures 2.11-2.13), the CO_2 is delivered from the intermediate heat exchanger (IHX) or nuclear reactor via two 1m diameter pipes to feed into one turbine inlet pipe. After the CO_2 is expanded in the turbine it enters two large diffusers which double as distribution manifolds, to deliver the fluid to the low pressure side of the high temperature recuperators. The CO_2 is fed to the outside plenum of the HTR from the turbine diffuser and exits the opposite outside plenum. The CO_2 flows from the outside plenum of the HTR to the outside plenum of the LTR via one 20 inch inner diameter pipe for each module. The CO_2 is collected at the exit of the LTR in a large diameter collection manifold where the flow is split between the precooler and recompressing compressor.

Because the precooler modules are much smaller than the two recuperators it is not effective to try to evenly pair the precooler modules with the LTR modules. Also, an effective flow split mechanism is required between the LTR and precooler. Therefore, the LTR cannot directly discharge the CO_2 to the precooler the way that the HTR delivers the fluid to the LTR. The flow from the LTR to the precooler is handled by using a large collection manifold between the two heat exchangers. The LTR discharges to the collection manifold and the precooler receives the fluid from the opposite side, thus allowing a variation in the number of modules. This method increases the minor losses by adding one additional fluid entrance and exit loss, but at this point in the cycle the fluid density is already high enough to not have these additional losses contribute noticeably. The large collection manifold also allows the fluid to directly flow to the recompressing compressor via a large diameter pipe. The collection manifold is large enough to allow the recompression feed pipe diameter to be limited by the size of the compressor casing and not the available pipe sizes, making the pressure drop between the collection manifold and the recompressing compressor negligible.

The precooler is arranged in four modules to receive the fluid from the collection manifold and discharge directly to a smaller collection manifold which directs the fluid to the main compressor. From the main compressor the fluid is sent at 20 MPa to another

large collection manifold which distributes the flow to the high pressure side of the LTR. Control valves are located on both compressor outlets to manage the correct recompression flow split. The fluid flows counterflow to the low pressure fluid through each heat exchanger module and is discharged to another collection manifold to allow for the collection of the additional mass flow from the recompressed fraction. The collection manifold discharges to the high pressure plena of the high temperature recuperator. Although the fluid temperature is slightly higher at this stage of the cycle the additional entrance and exit losses and are significant due to the fluid being at high pressure which, lowers the fractional pressure loss.

An issue arose considering the numerous pipe penetrations in the collectors. When the ASME pressure vessel code (NB 3338.2) was checked it was found that

> "the arc distance measured between the center lines of the adjacent nozzles along the inside surface of the shell is not less than three times the sum of their inside radii for openings in a head or along the longitudinal axis of a shell and is not less than two times the sum of their radii for openings along the circumference of a cylindrical shell."

The above layout pertains to the "three times the sum of their inside radii" arc. Originally, the pipes modeled as 22" outside diameter and 1" thick (20" inside diameter) were the sections:

- Turbine to high temperature recuperator
- High temperature recuperator to low temperature recuperator
- Low temperature recuperator to split T
- Split T to precooler
- Low temperature recuperator to merge T

To satisfy the ASME pressure vessel requirements for this particular layout there are two options: reduce the pipe diameters for the above listed pipes or to put a spacer between

each heat exchanger module to accommodate the necessary distance. With no spacers the pipes are 0.6m apart, on center. Therefore, the pipes will have to be reduced to 15.74" inner diameter. When this option is further explored in terms of pressure loss calculations it is found that it is not very detrimental to overall system performance. Reducing the pipes to satisfy the pressure vessel code lowered the cycle efficiency by 0.06%. However, if the modules are moved slightly apart to allow for thermal expansion (which is a preferred option) the initial 20 inch inner diameter pipes may be used.

The maximum size pipe able to be attached to the heat exchanger modules is limited by the allowable width. As of now, HEATRIC™ is unable to make the modules wider than 0.6m. For this reason, the pipes were modeled as 20 inch outer diameter pipes to allow for the necessary welding/connection method. This may be slightly conservative, but it allows for additional required space if the pipe walls need to be increased, or to possibly increase the inside diameter later on. However, increasing the pipes to 20 inch inner diameter will only result in an efficiency increase of 0.08%; plus, the spacer method will likely be employed. Because HEATRIC™ has relatively small field experience with this type of application the required maintenance protocol is somewhat unknown. Using the spacers allows for much easier inspection and removal of the heat exchanger modules. The spacers could easily be cut, facilitating the removal of the modules, more so than if the modules were welded together. This is not a focal point of this report, but it is important enough to mention for further consideration at a later stage when a stress analysis is performed.

One more possibility not depicted by the above layouts is to take two heat exchanger modules and weld them together before attaching the plena, to essentially make the unit twice as wide as the manufacturing limit. Once this is done attach a plenum that will cover the wider heat exchanger. This will allow a much larger diameter pipe to be connected to the heat exchanger, which will increase the overall flow area and improve efficiency. For example, if the 20" outer diameter pipes with 1" thick walls were used the total flow area for two pipes is $0.328m^2$ compared to $0.785m^2$ for a 1m inner diameter pipe. This is a 2.4 times increase in flow area. However, with this method the spacers

will also have to be used to satisfy the ASME requirements on vessel penetrations. The dual module/one large plenum pipe method will further complicate the layout, make it more vulnerable to leaks, and require both single modules to be removed for maintenance. Therefore, it is suggested that this option not be explored at this time. Finally, it is noted that the 0.6m limit of the module width is dictated by the size of photosensitive film for the etching process. In discussions with HEATRIC^{TM} engineers it was learned that this is not necessarily a hard limit, and if there is a strong interest in larger module size accompanied by the order of a significant number of PCHEs, larger film size could be developed.

The cycle code calculated efficiency is 48.0%, which is only about 0.7% lower than the efficiency obtained for the PCS assuming zero pressure drops in pipes and PCHE plena (but including pressure drops in the active cores of PCHE). This is significant improvement of cycle performance in comparison with the 2nd generation layout where cycle efficiency was 44%. If the 15.7 inch inner diameter ASME requirement reduced pipes were not required, the efficiency can be raised only approximately 0.05% for 20 inch inner diameter pipes. Once the stress analysis is performed and the correctly sized spacers for the heat exchangers are determined, the pipes may be able to be increased slightly, but no further significant piping gains can be made to improve the cycle performance. The pertinent data for the performance estimates can be found in Table 2.3. All of the piping sizes in the layout depictions do not necessarily correspond to standard pipe sizes. The pipes are merely represented as generically sized (i.e. a specified inner diameter) and it is assumed that once the actual pipe sizes are chosen a standard pipe very similar in size can be used. However, the pipe sizes were checked with respect to very preliminary stress calculations to ensure that at least the ASME code for hoop stresses at operating temperature and pressure were satisfied.

Table 2.3 Pertinent data for cycle performance calculations

Electrical power ($MW_{electric}$)	150.3
Thermal Power ($MW_{thermal}$)	313.0
Maximum operating pressure (MPa)	20.0
Turbine Inlet Temp (°C)	650.0
Pressure Ratio	2.60
*Reactor/IHX pressure drop (kPa)	500.0
*Turbine Efficiency (%)	95.0
*Main Compressor Efficiency (%)	85.07
*Recompressing Compressor Efficiency (%)	89.8
*Mechanical Efficiency (couplings) (%)	99.0
*Generator Efficiency (%)	98.0
*Frequency Converter/Switchyard Efficiency (%)	98.0
Main Comp Inlet Temp (°C)	32.0
Cooling water temp (°C)	20.0

*Assumed values

The turbomachinery was sized based on the work by Dr. Yifang Gong [Gong, et. al., 2006]. The turbine is modeled as a four stage axial turbine, the recompressing compressor is modeled as a three stage radial compressor, and the main compressor is modeled as a one stage radial compressor. The actual length of each turbomachine can vary with the length of the diffuser/inlet/outlet chambers. Also, the casings can be increased or decreased in diameter to accommodate attachment of larger pipes. This is not an issue for the 300 MWe power rating, but the smaller power ratings may require an oversized turbine casing or accept larger pressure losses throughout the cycle.

The control valve placement for all the designs is based on previous work at one of the initial stages of layout design, but has not been further verified. Currently, the control valves are placed on the high pressure side of each compressor. The valves are only meant to control the flow split between the two compressors. Further considerations may reveal the need for control valves at another location along with anti-surge valves. The partial load control also remains to be established and will have to be added in the future. Depending on the required control scheme the PCS layout may have to be adapted to allow for the additional control components. Also not depicted in any of the PCS layouts are the reactor isolation valves. Control valves for partial load control are not shown because the most efficient and effective method has not yet been established. The

method of control is not a focal point of this report and the PCS layout will have to be adjusted once the control method is resolved. The recent report by Carstens (2007) is a significant step in this direction.

Other issues not addressed in the layout are the treatment of the foundation and the component insulation. It is assumed that the foundation can be developed at a later time when the layout has undergone all the stress calculations and modifications (if necessary) for thermal expansion. The actual foundation should not be very difficult to design. The biggest concern will be securing the turbomachinery. The heat exchangers can be placed on the floor or an individual foundation secured to the floor. The insulation is also not covered because that one is of the last considerations, and probably the easiest. Currently, there should be no constraints limiting the placement of external insulation in the necessary locations. Also, the amount of insulation required is dependent on the final layout design. One issue not yet resolved is whether internal insulation will be required in the hottest (e.g. 650°C) ductwork.

For PCS layouts one has the option of placing the generator next to the turbine or the main compressor. If it is placed next to the turbine, the shaft between the turbine and the two compressors will need to sustain a smaller torque than if it is placed next to the main compressor. Also, the shaft between the turbine and the generator will only have to be designed for the induced torque between the two components. Up to this point the actual shaft design has not been performed. The shafts depicted in the PCS layouts are only for illustrative purposes. Figures 2.11 through 2.13 show the PCS layout in isometric, plan (horizontal), and elevation (top) views, respectively. In these and many of the following figures, the abbreviations listed in Table 2.4 are used as labels to identify principal components, with several components depicted in Figure 2.10.

Table 2.4 Key to figures

Indicator		Component
TUR		Turbine
RC		Recompressing compressor
MC		Main compressor
IHX		Intermediate heat exchanger
HTR		High temperature recuperator
LTR		Low temperature recuperator
PRE		Precooler
GEN		Generator
FSV		Flow split valve
CV		Control valve
BV		Bypass valve

*figure key is good for all following PCS layouts

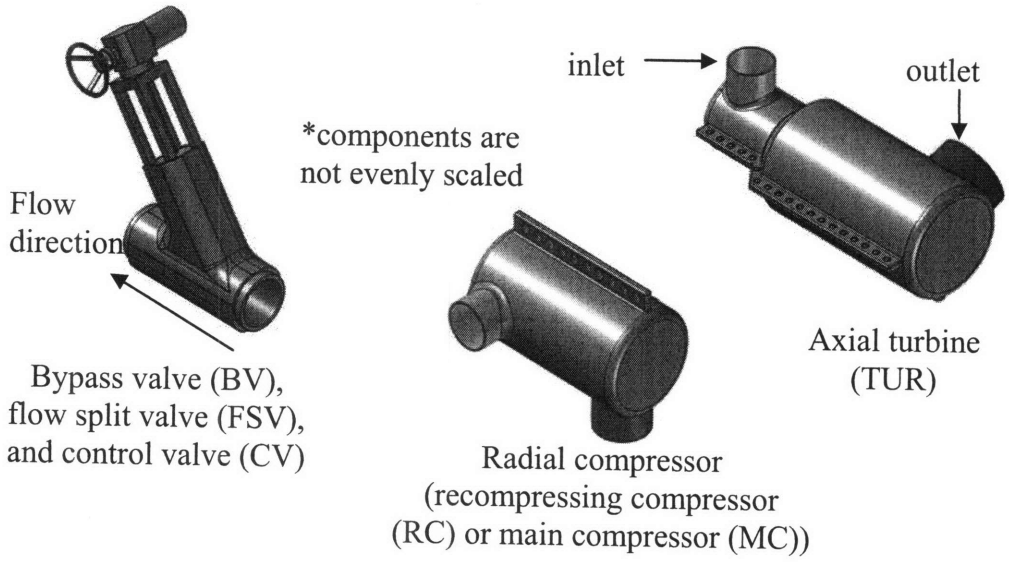

Figure 2.8 – Typical cycle components

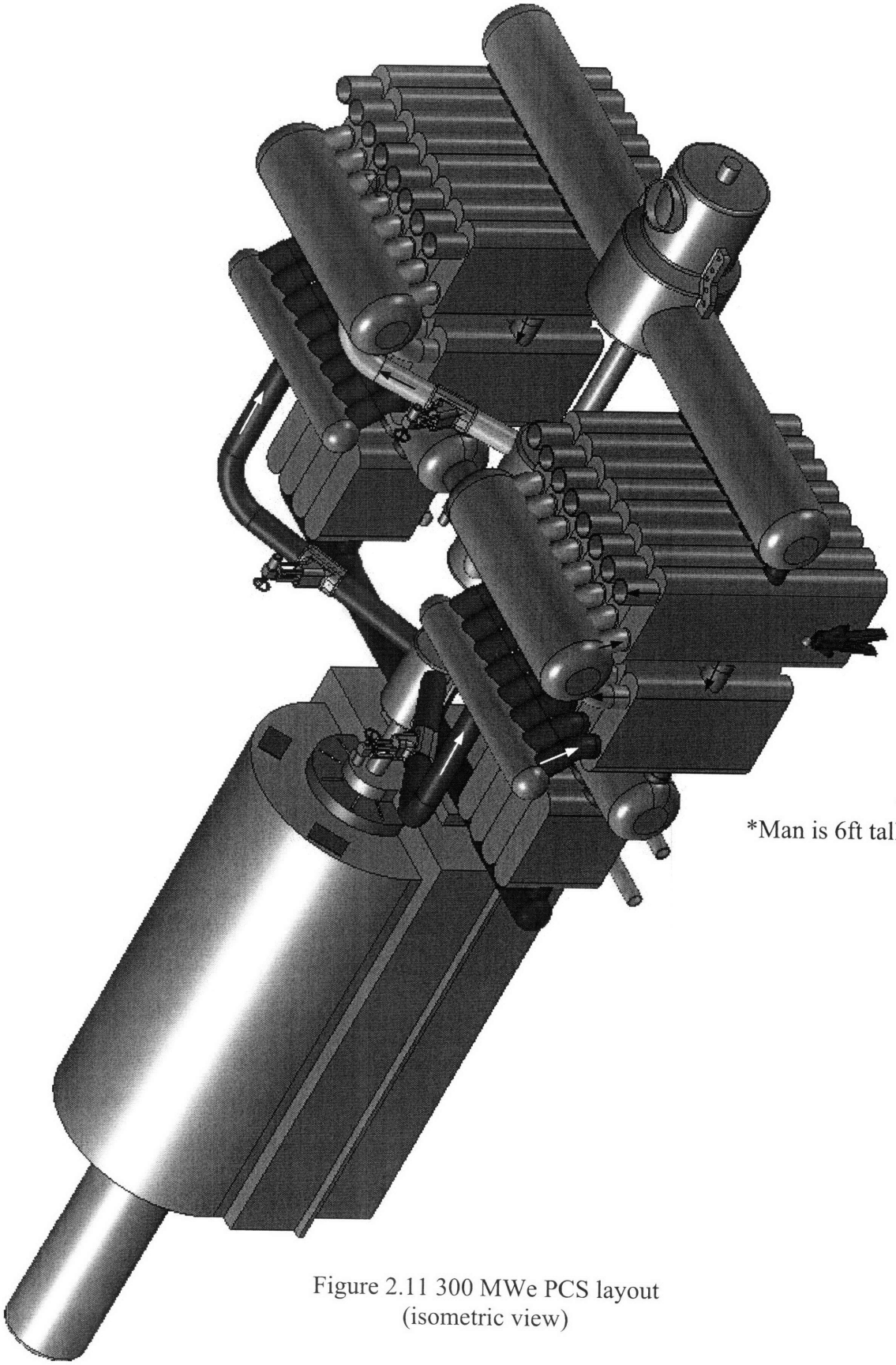

*Man is 6ft tall

Figure 2.11 300 MWe PCS layout
(isometric view)

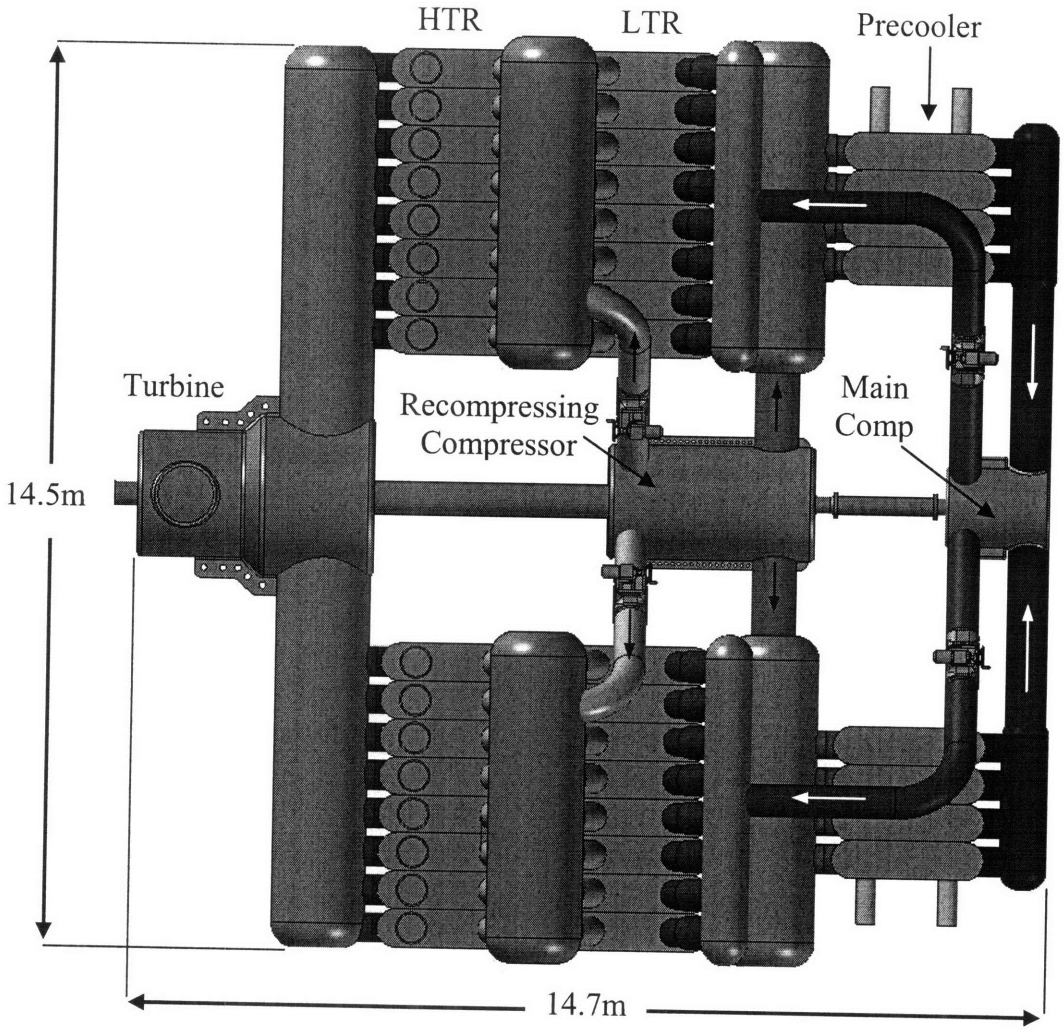

Figure 2.12 300 MWe PCS layout (top view)

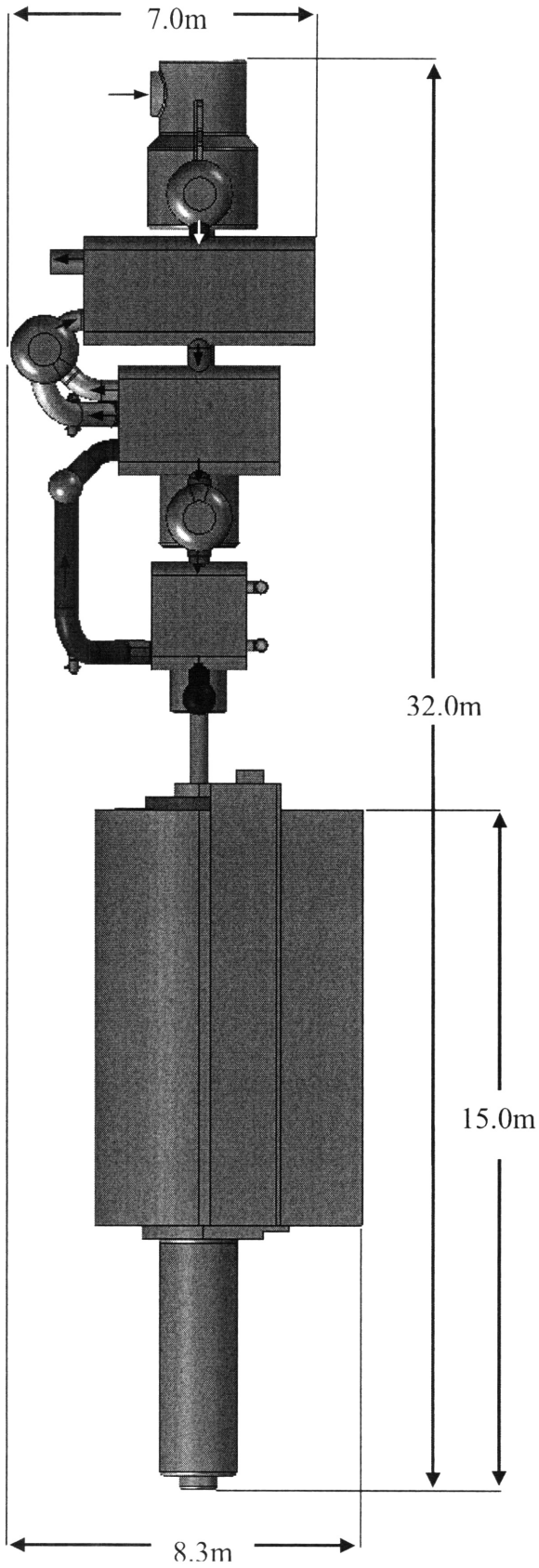

Figure 2.13 300 MWe S-CO_2 power conversion system, side view

The mass estimate for each power rating was broken down according to each component. All of the material in each system was assumed to be stainless steel except for the precooler which was assumed to be made of titanium to allow for salt water exposure. The masses of the valves were obtained from an Atwood and Morrill valve catalog [Atwood and Morrill, Co.], and all are 20 inch valves unless noted otherwise. These estimates do not include the heat exchanger spacers, cooling water piping to the precooler, cooling water pump, generator, insulation, or support structures. Component mass estimates are given in the set of Tables 2.5.

Table 2.5a Heat exchangers (PCS) mass estimate for 300 MWe PCS

Element	Material	Number	Height (m)	Total Mass (M.T.)
HTR				
LP plenum	S.S.	32	5.30	15.70
HP plenum	S.S.	32	5.30	147.0
Core	S.S.	16	5.30	200.0
Total				362.4
LTR				
LP plenum	S.S.	32	3.75	11.10
HP plenum	S.S.	32	3.75	104.0
Core	S.S.	16	3.75	148.0
Total				263.1
PRE				
LP plenum	titanium	16	2.20	1.86
HP plenum	titanium	16	2.20	17.4
Core	titanium	8	2.20	23.0
Total				42.3
Grand Total				**668.0 M.T.**

Table 2.5b Intermediate heat exchanger mass estimate for 300 MWe PCS

Element	Material	Number	Height (m)	Total Mass (M.T.)
IHX				
LP plenum	S.S.	32	1.35	7.80
HP plenum	S.S.	32	1.35	37.40
Core	S.S.	16	1.35	117.0
Grand Total				**162.0 M.T.**

Table 2.5c Turbomachinery mass estimate for 300 MWe PCS

Element	Material	Number	Total Mass (M.T.)
Turbine	S.S.	1	19.5
Recompressing Compressor	S.S.	1	15.0
Main Compressor	S.S.	1	3.50
Grand Total			**38.0 M.T.**

*Shaft masses are included in the turbomachine's mass

Table 2.5d Pipe and valve mass estimate for 300 MWe PCS

Element	Material	Number	Length (m)	Total Mass (kg)
IHX to TUR				
Pipe from collector to junction	S.S.	2	6.0	13750
Pipe from junction to turbine	S.S.	1	7.0	6400
TUR to HTR				
Diffuser	S.S.	2	6.0	11200
Pipes to HTR	S.S.	16	0.35	900
HTR to LTR				
Pipes to LTR	S.S.	16	0.60	1500
LTR to PRE				
Collector	S.S.	2	5.10	10200
Pipes to collector	S.S.	16	0.30	800
Pipes to PRE	S.S.	8	0.40	450
LTR to RC				
Pipes from collector to RC	S.S.	2	1.0	440
PRE to MC				
Pipes to collector from PRE	S.S.	2	0.40	500
Collector	S.S.	2	2.50	2550
Pipe from collector to MC	S.S.	2	2.90	1150
MC to LTR				
Pipe from MC to collector	S.S.	2	7.60	2400
20 inch valve	S.S.	2		7400
Collector	S.S.	2	5.10	10200
Pipes to LTR from collector	S.S.	16	1.10	2750
RC to HTR				
Pipe from RC to collector	S.S.	2	4.70	1450
Valve	S.S.	2		7400
Collector	S.S.	2	5.10	10200
Pipes to HTR from collector	S.S.	16	0.50	1150
LTR to HTR				
Pipes from LTR to collector	S.S.	16	1.30	3300
HTR to IHX				
Pipes to IHX	S.S.	16	6.60	35500
Piping Grand Total				**132.0 M.T.**

*Mass values represent the total mass for the pipe sections, not individual pieces

*The densities for all the mass calculations were 7900 kg/m^3 for stainless steel and 4506 kg/m^3 for titanium

Total indirect power conversion cycle mass estimate: 963 metric tons

The heat exchangers (including the IHX) are approximately 86.2% of the total weight

The turbomachines are approximately 3.9% of the total weight

The pipes and valves are approximately 9.9% of the total weight

2.5 Third Generation Layout – 50 MWe

The 50 MWe power conversion layout is very similar to the 20-25 MWe layout except that it needs two parallel high and low temperature recuperators connected by a manifold. This was necessary to keep the overall height of the conversion unit to a minimum and limit the distance the fluid travels within each recuperator. At this power rating, the precooler is still small enough to keep it as one module. The turbomachinery is currently shown beneath the heat exchangers, but the PCS can be rotated to have the turbomachinery on top if an adequate foundation/frame is developed. The 50 MWe PCS can be seen in Figures 2.14 through 2.16 and the component mass estimates are in Table set 2.6.

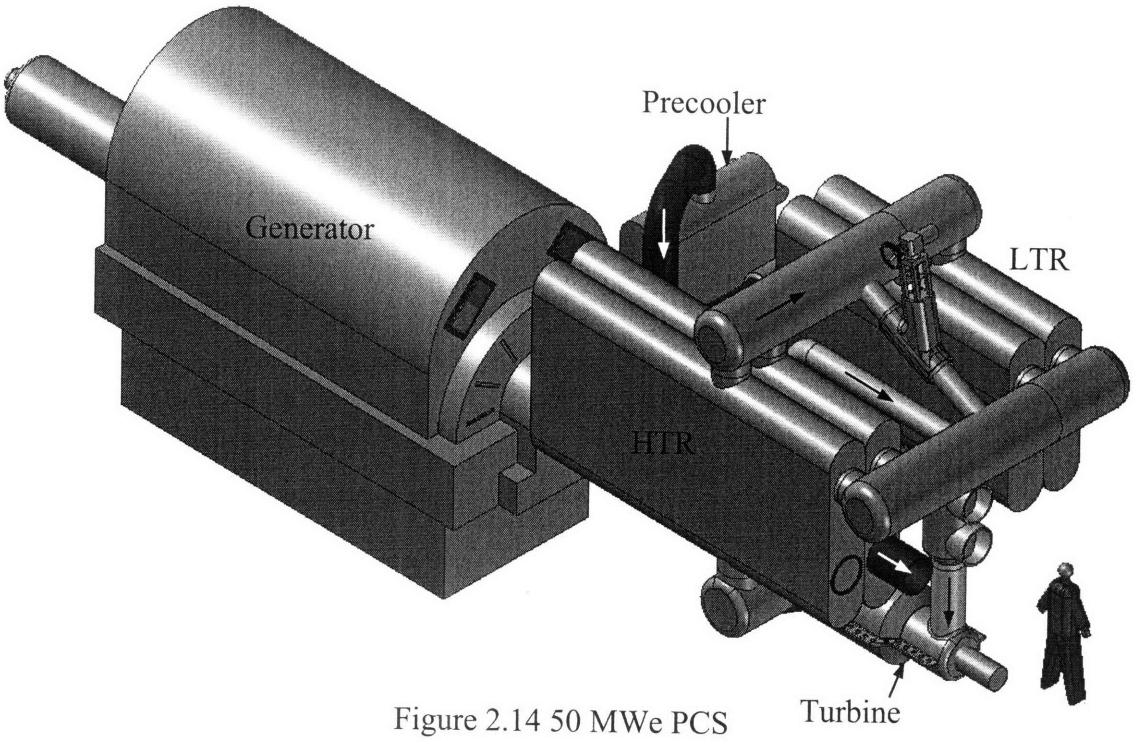

Figure 2.14 50 MWe PCS isometric view

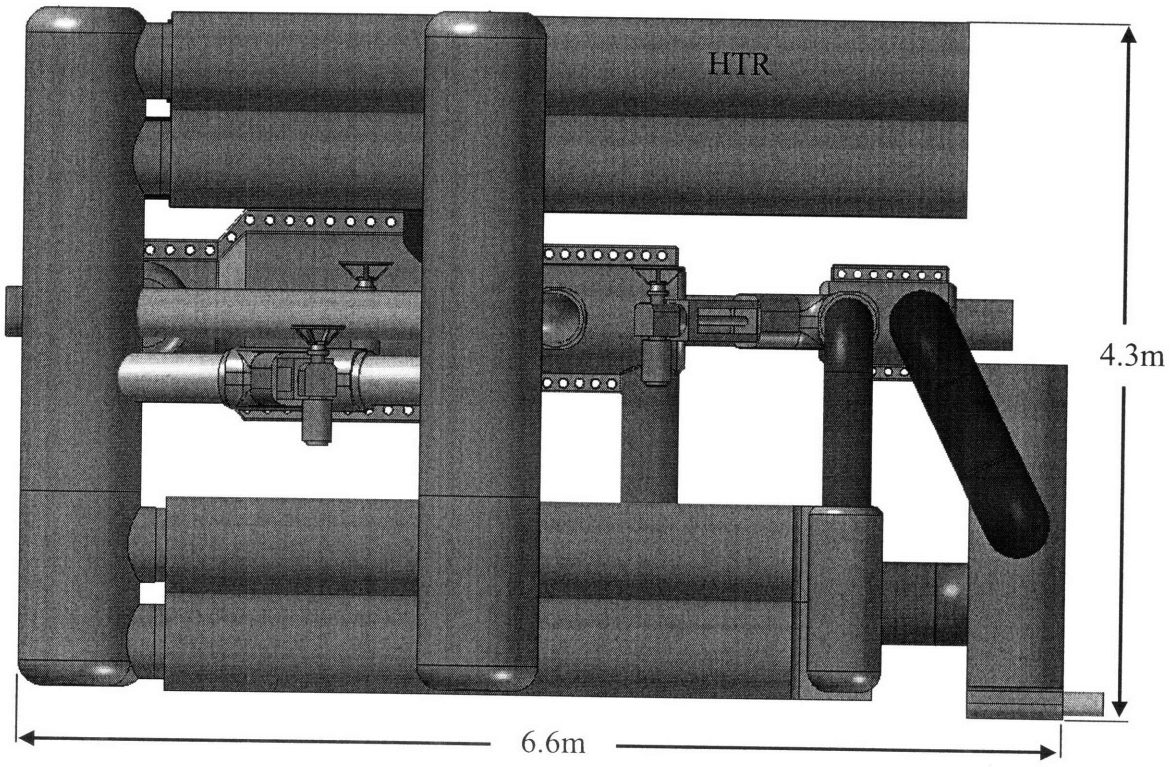

Figure 2.15 50 MWe PCS top view

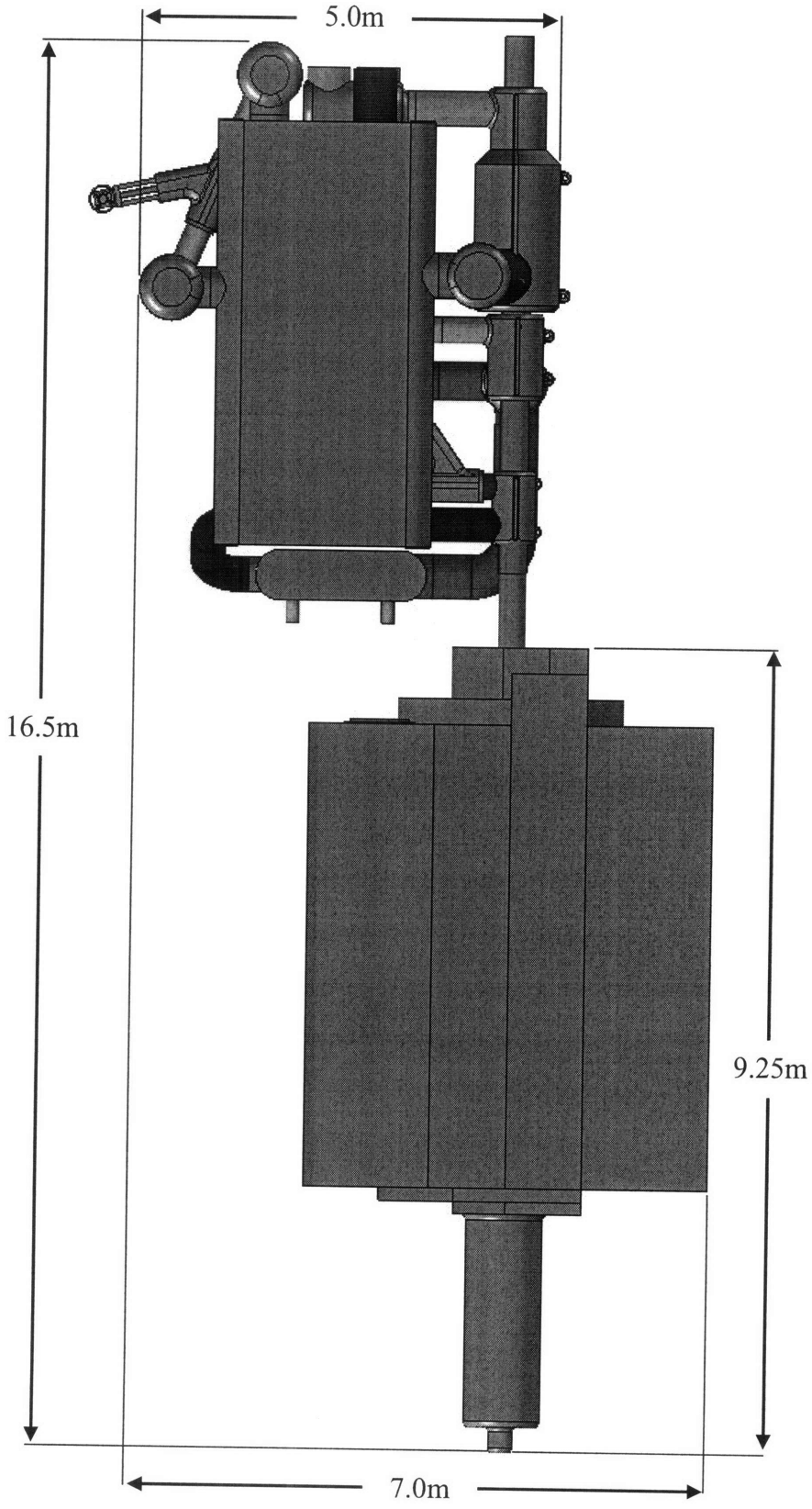

Figure 2.16 50 MWe PCS side view

Table 2.6a Heat exchanger mass estimate for 50 MWe PCS train

Element	Material	Number	Height (m)	Total Mass (M.T.)
HTR				
LP plenum	S.S.	4	6.0	2.20
HP plenum	S.S.	4	6.0	20.8
Core	S.S.	2	6.0	40.0
Total				63.0
LTR				
LP plenum	S.S.	4	4.72	1.75
HP plenum	S.S.	4	4.72	16.40
Core	S.S.	2	4.72	29.60
Total				47.75
PRE				
LP plenum	titanium	2	1.25	0.20
HP plenum	titanium	2	1.25	2.00
Core	titanium	1	1.25	4.75
Total				6.95
Grand Total				**118 M.T.**

Table 2.6b IHX mass estimate for 50 MWe PCS train

Element	Material	Number	Height (m)	Total Mass (M.T.)
IHX				
LP plenum	S.S.	4	0.90	1.0
HP plenum	S.S.	4	0.90	4.75
Core	S.S.	2	0.90	9.75
Grand Total				**15.5 M.T.**

Table 2.6c Turbomachinery mass estimate for 50 MWe PCS train

Element	Material	Number	Total Mass (M.T.)
Turbine	S.S.	1	4.0
Recompressing Compressor	S.S.	1	3.0
Main Compressor	S.S.	1	1.2
Grand Total			**8.2 M.T.**

*Shaft masses are included in the turbomachine's mass

Table 2.6d Pipe and valve mass estimate for 50 MWe PCS train

Element	Material	Number	Length (m)	Total Mass (kg)
IHX to TUR				
Pipes to collector	S.S.	2	0.30	200
Pipe from collector to turbine	S.S.	1	6.50	1975
Collector	S.S.	2	1.20	925
TUR to HTR				
Pipe to collector	S.S.	1	0.25	100
Collector	S.S.	1	1.20	550
Pipes to HTR	S.S.	2	0.25	75
HTR to LTR				
Pipes to collector from HTR	S.S.	2	0.25	75
Collector	S.S.	1	4.20	1350
Pipes from collector to LTR	S.S.	2	0.25	75
LTR to PRE				
Pipes to collector from LTR	S.S.	1	5.10	400
Collector	S.S.	1	1.20	925
Pipes from collector to PRE	S.S.	1	2.60	400
LTR to RC				
Pipes from collector to RC	S.S.	1	1.10	100
PRE to MC				
Pipes from PRE to MC	S.S.	1	4.80	600
MC to LTR				
Pipe from MC to collector	S.S.	1	2.90	265
12 inch valve	S.S.	1		1620
Collector	S.S.	1	1.10	175
Pipes to LTR from collector	S.S.	2	0.25	75
RC to HTR				
Pipe from RC to collector	S.S.	1	2.90	265
12 inch valve	S.S.	1		1620
Collector	S.S.	1	5.10	2300
Pipes to HTR from collector	S.S.	2	0.25	75
LTR to HTR				
Pipes from LTR to collector	S.S.	2	0.25	75
HTR to IHX				
Pipes to IHX	S.S.	2	3.90	2375
Piping Grand Total				**16.50 M.T.**

*Mass values represent the total mass for the pipe sections, not individual pieces
*The densities for all the mass calculations were 7900 kg/m^3 for stainless steel and 4506 kg/m^3 for titanium

Total power conversion mass estimate: 158 M.T.

The heat exchangers (including the IHX) are approximately 84.5% of the total weight
The turbomachines are approximately 5.0% of the total weight
The pipes and valves are approximately 10.5% of the total weight

2.6 Third Generation Layout - 20-25 MWe

The 20 MWe layout was the first power conversion unit to be designed using SOLID EDGE in conjunction with CYCLES and is considerably different than the large power rating layouts in that it is able to use only one standard HEATRIC™ heat exchanger module. This enables the complete conversion unit to be very compact and have the turbomachinery closely nested in between the high and low temperature recuperators. The flow paths between and inside the heat exchangers is the same as in the larger rating PCS, with the low pressure fluid using the outside plenum and the high pressure fluid flowing through the inside plenum. However, there are several minor differences that deserve mention. The 20 MWe layout is the simplest layout in that it has no collection manifolds or distribution chambers, and because it is able to use one heat exchanger module there is no concern over evenly distributing the flow between modules. The turbine is modeled with a very long diffuser to increase the total-to-static efficiency. Also, in the figures which follow, a 20 MWe permanent magnet generator is included to show the relative size of the generator as compared to a 6ft tall man and to the rest of the power conversion components. Depending on the method of partial load control, the cycle has further room for efficiency improvement. If a method other than a high-to-low pressure bypass between the HTR and LTR is used, it is possible to add one or more additional pipes between the recuperators to cut down on the pressure losses on the low pressure side of the system.

An interesting aspect of the smaller power ratings (below about 50 MWe) is the potential for future use of a vertical arrangement for the turbomachinery train. Depending on the overall thrust and weight of the turbomachinery, the entire power conversion layout may be able to stand upright, resulting in a tiny footprint. The bearing design/selection is outside the scope of this report, but is a feature that should be explored at a later point.

The 25 MWe layout may be considered as a straightforward expansion of the 20 MWe system. The optimum heat exchanger core lengths do not change, only the height will expand linearly to accommodate the extra volume.

The 20-25 MWe PCS layouts are shown in Figures 2.17 through 2.20 and the masses are listed in Table set 2.7. Also, a comparison between a 20 MWe permanent magnet generator and a 20 MWe wound rotor generator is shown in Figure 2.21.

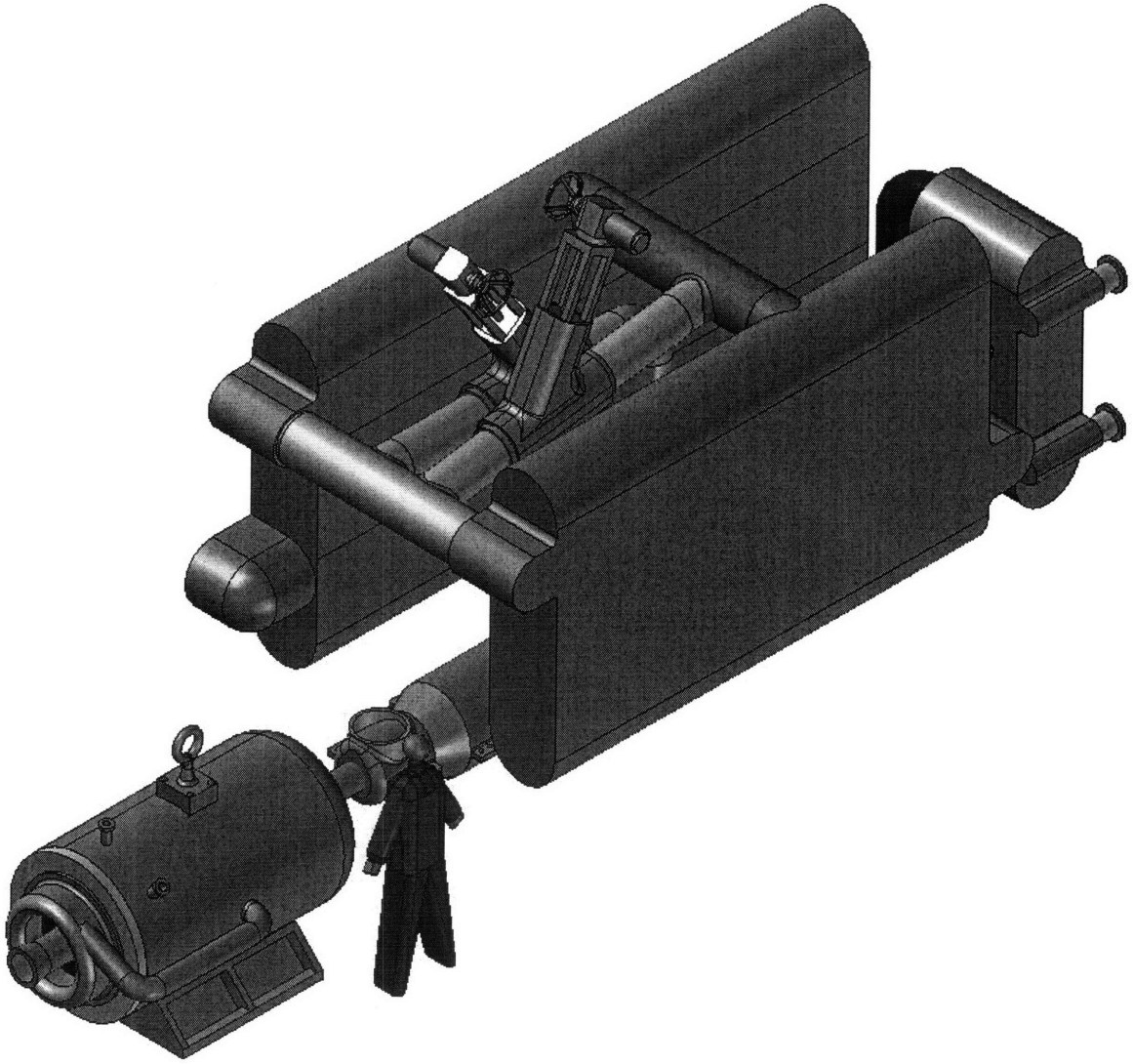

Figure 2.17 20 MWe PCS with PM generator (isometric view)

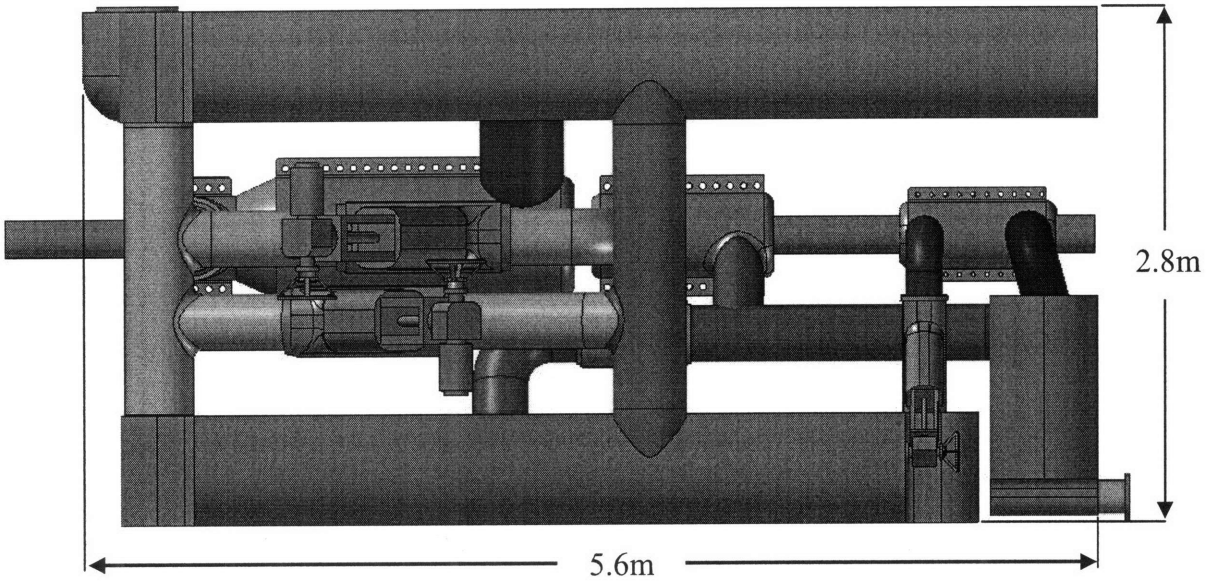

Figure 2.18 20 MWe PCS (top view)

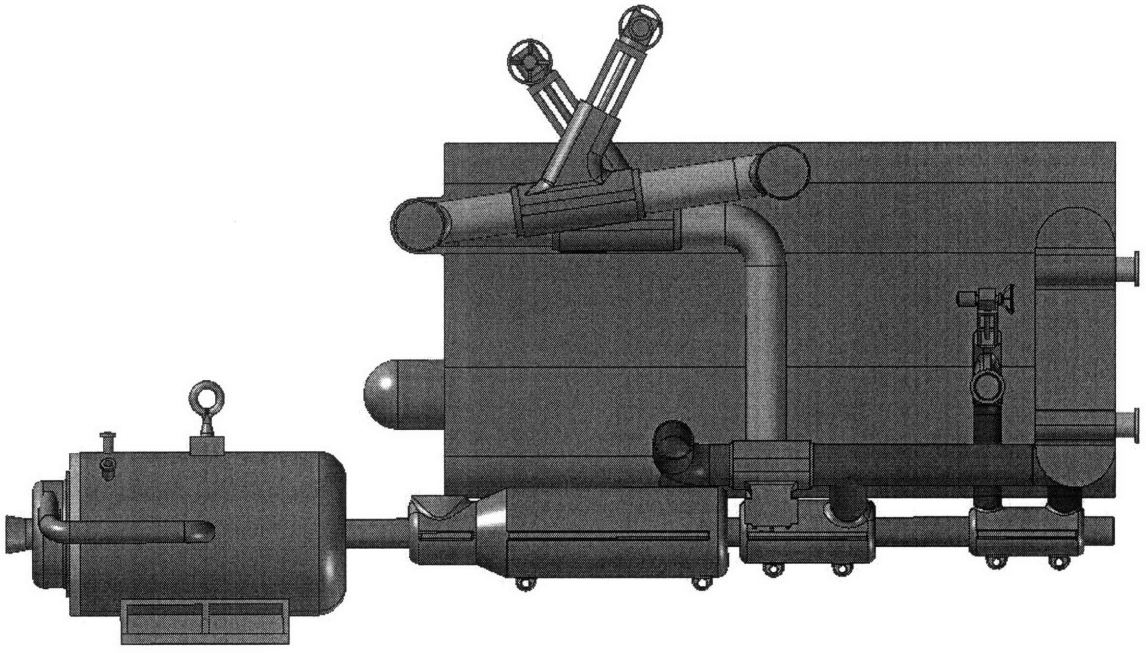

Figure 2.19 20 MWe PCS with PM generator, side view
LTR removed to allow nested components to be visible

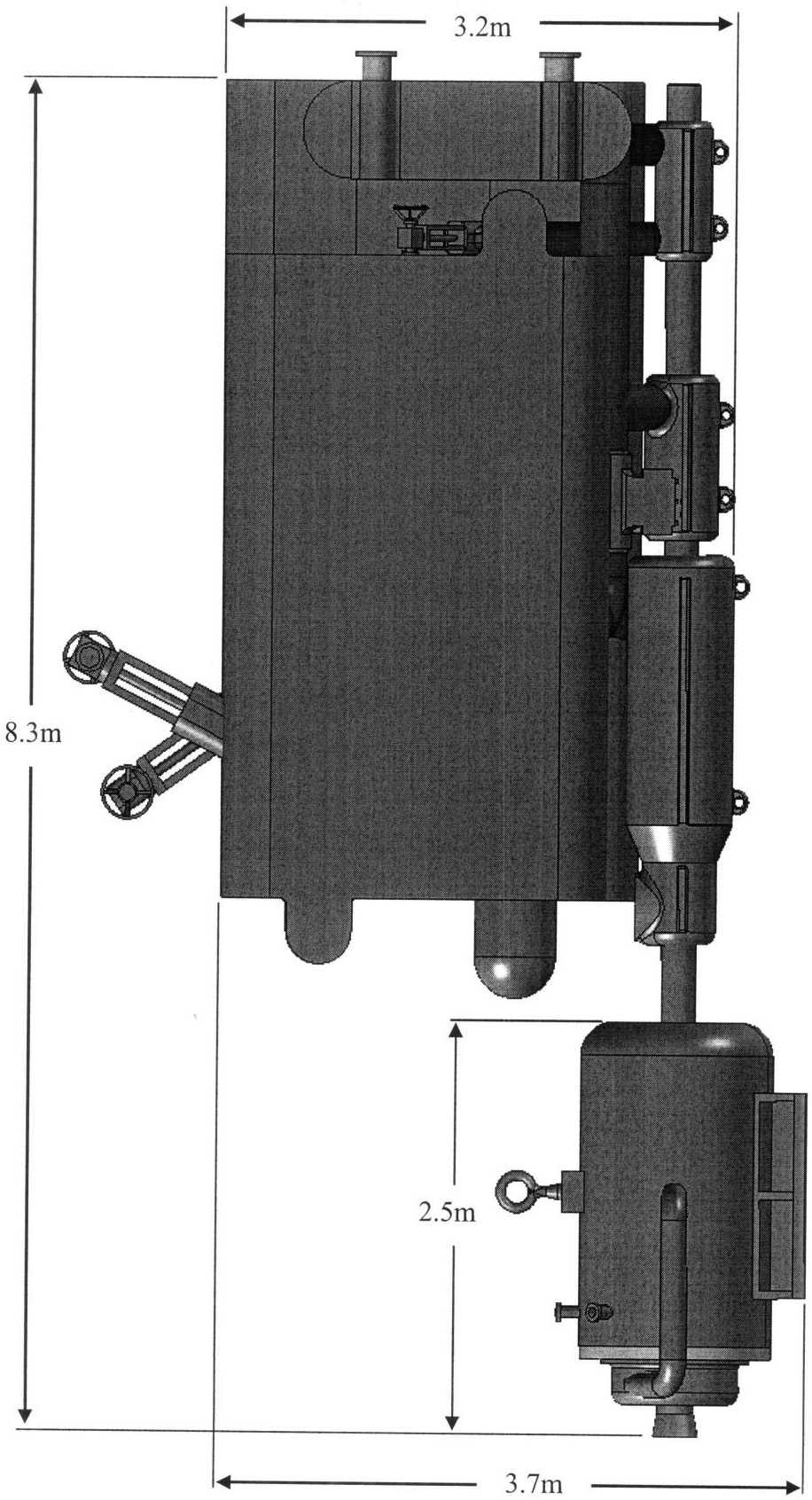

Figure 2.20 20 MWe PCS with permanent magnet generator (side view)

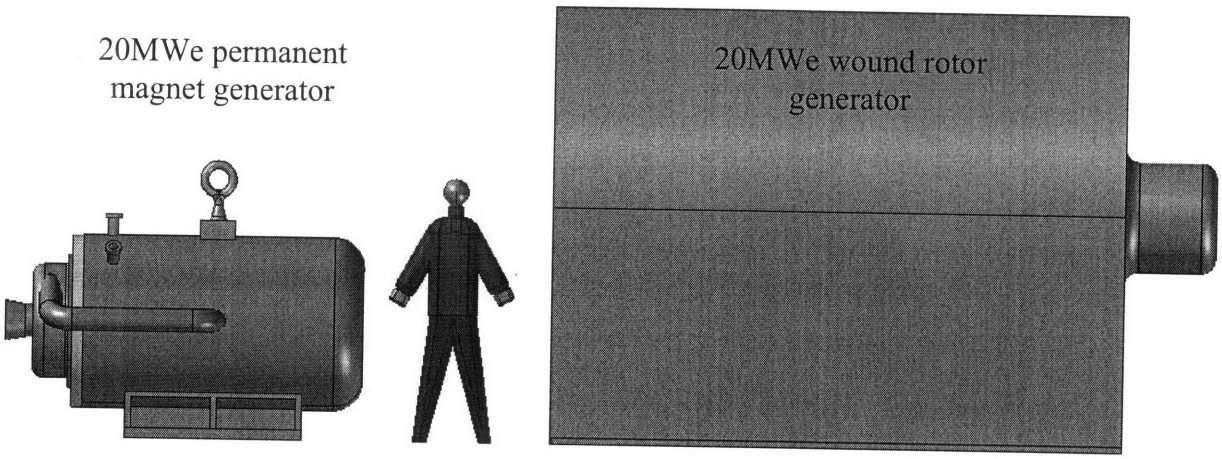

Figure 2.21 Permanent magnet vs. conventional generator comparison

Table 2.7a Heat exchanger (PCS) mass estimate for 20 MWe PCS train

Element	Material	Number	Height (m)	Total Mass (M.T.)
HTR				
LP plenum	S.S.	2	6.0	0.90
HP plenum	S.S.	2	6.0	8.70
Core	S.S.	1	6.0	16.0
Total				25.60
LTR				
LP plenum	S.S.	2	4.72	0.75
HP plenum	S.S.	2	4.72	6.85
Core	S.S.	1	4.72	11.85
Total				19.50
PRE				
LP plenum	titanium	2	1.25	0.05
HP plenum	titanium	2	1.25	0.50
Core	titanium	1	1.25	1.90
Total				2.45
Grand Total				**47.50 M.T.**

Table 2.7b IHX mass estimate for 20 MWe PCS train

Element	Material	Number	Height (m)	Total Mass (M.T.)
IHX				
LP plenum	S.S.	2	0.90	0.45
HP plenum	S.S.	2	0.90	2.20
Core	S.S.	1	0.90	7.60
Grand Total				**10.25 M.T.**

Table 2.7c Turbomachinery mass estimate for 20 MWe PCS train

Element	Material	Number	Total Mass (M.T.)
Turbine	S.S.	1	1.50
Recompressing Compressor	S.S.	1	0.50
Main Compressor	S.S.	1	0.30
Grand Total			**2.3 M.T.**

*Shaft masses are included in the turbomachine's mass

Table 2.7d Pipe and valve mass estimate for 20 MWe PCS train

Element	Material	Number	Length (m)	Total Mass (kg)
IHX to TUR				
Pipe to turbine	S.S.	1	3.0	2530
TUR to HTR				
Pipe to HTR	S.S.	1	0.35	110
HTR to LTR				
Pipe to LTR	S.S.	1	0.60	225
LTR to PRE				
Pipe to PRE	S.S.	1	0.40	175
LTR to RC				
Pipe from collector to RC	S.S.	1	1.10	25
PRE to MC				
Pipe from PRE to MC	S.S.	1	2.90	150
MC to LTR				
Pipe from MC to LTR	S.S.	1	7.60	75
8 inch valve	S.S.	1		525
RC to HTR				
Pipe from RC to merge T	S.S.	1	4.70	200
12 inch valve	S.S.	1		1620
LTR to HTR				
Pipe from LTR to HTR	S.S.	1	1.30	190
HTR to IHX				
Pipe to IHX	S.S.	1	5.0	440
Piping Grand Total				**6.30 M.T.**

*Mass values represent the total mass for the pipes, not individual pieces

Total indirect power conversion cycle mass estimate: 67 M.T.

The heat exchangers (including the IHX) are approximately 87.2% of the total weight

The turbomachines are approximately 3.4% of the total weight

The pipes and valves are approximately 9.4% of the total weight

2.7 Comparing the high and low power ratings

The low power ratings have the advantage of using one or two of each heat exchanger module per power conversion unit and not having the pipe sizes being a limiting factor in the design. However, the downside to the lower power ratings is the slightly lower turbomachinery efficiencies. If a power rating smaller than 20 MWe is desired, the layout will be the same as for the indicated 20 MWe layout, but the overall length will shrink linearly with power. The transition between the high and low power rating layouts begins around 50 MWe. The small layouts, below 50 MWe, resemble more of a nested configuration with the pipes running between the middle of the heat exchanger bundles. For the very small ratings ($\leq$20 MWe) the turbomachinery train can also be positioned between the heat exchangers. Above 20 MWe it is suggested that the single heat exchanger (single HTR, LTR, and PRE module) be replaced by multiple modules when the overall height is greater than 6m. The multiple modules can be placed next to each other and the flow can be distributed and collected via a header system. Unless the heat exchangers are subdivided into very small units and packaged into one large vessel there are few ways to distribute the flow without a header. The layout of a single unit above 50 MWe should be shifted away from the nested turbomachinery design to the parallel heat exchanger design, with a single or dual train. This shift is to add a degree of simplicity to the layout to allow for easy removal of the increasingly larger turbomachines. To achieve power ratings above 50 MWe with the small rating layout it is desirable to use more than one loop.

As the power ratings approach 150 MWe the overall length of the conversion unit will remain the same, but the width will increase as more heat exchanger modules are added. When the power ratings exceed 150 MWe it is possible to maintain the single train heat exchanger approach, but it is suggested to break the unit into two parallel trains feeding into one set of turbomachinery. The reason for this is simple: to more efficiently handle the pressure losses with fewer long piping runs. However, this will also cause the conversion unit to be slightly more expensive with respect to the initial capital investment due to the additional piping.

2.8 Attaching the intermediate heat exchanger

Attaching the intermediate heat exchanger is very important because if done improperly it can result in a several percent loss on overall efficiency. Attaching the IHX to the 150 MWe power rating proved to be quite trivial, with only one large feed pipe connected to the turbine inlet. However, connecting the IHX to the 300 MWe unit can be more complicated because of the need to accommodate the two large turbine inlet pipes.

The IHX connecting the reactor to the power conversion cycle is modeled for liquid metal/gas heat transfer with a 550°C turbine inlet temperature and the primary coolant being 20°C above the secondary coolant outlet temperature. Sodium was used as a liquid metal since current GNEP efforts are focused on sodium cooled reactors. Because sodium has high conductivity, and it is desirable that its passage through small 2 mm channels is smooth to prevent potential blockage, straight channels were used. Although 550°C is not an exact match with the depicted 650°C turbine inlet PCS layouts, the only change in PCS appearance would be in the height and length of the IHX. The increase in heat exchanger size with lower turbine inlet temperature is approximately 10% or less, depending on a cost benefit analysis. For small power ratings (<50 MWe) it is possible to lower the turbine inlet temperature from 650°C to 550°C without a noticeable efficiency reduction attributed to the undersized heat exchangers (Figure 3.7). Thus, any appearance changes in the layouts as a result of lowering the turbine inlet temperature to 550°C will be small. If a gas cooled reactor was used the IHX would be a gas/gas heat transfer and zigzag channels would be used instead of straight channels. The overall volume would only slightly increase because the power density for a CO_2/CO_2 exchanger is approximately 27 MW/m^3, and the Na/CO_2 unit is approximately 28 MW/m^3. Using the Na/CO_2 unit as the reference design, the CO_2/CO_2 exchanger would change in appearance due to reduced overall length because of the zigzag channel arrangement, but increase in overall height. Regardless, the depicted arrangement of the IHX should not affect the rest of the power conversion component layout, but will slightly reduce the overall footprint.

The high power density in the sodium/CO_2 IHX makes it quite compact. To keep the overall height of the IHX to 5m or less the unit could be broken into three modules. However, the issue of connecting the eight HTR modules to three IHX modules then has to be addressed. By using eight IHX modules the overall footprint is only marginally increased, and the CO_2 distribution between the IHX and HTR is easily handled. Also, the repairability of this arrangement is significantly better in terms of accessibility, and easier than if distribution and collection manifolds were employed. Hence, the IHX is arranged for both the 150 and 300 MWe layouts by creating the same number of modules as the high temperature recuperator. This method allows a parallel configuration to be used, thus enabling the use of many parallel pipes connecting the two heat exchangers. The other option to connect the HTR to the IHX would be to feed the CO_2 into a large collector manifold from the HTR with fewer and larger pipes leading from the collector to the IHX. Currently, the IHX is connected to the HTR via multiple 20 inch inner diameter pipes. The many pipe options facilitate later adjustments for thermal expansion and stresses which would be quite difficult with one or two very large diameter pipes. It is also noted that IHX pressure drop on the CO_2 side is only one half of the pressure drop assumed in the cycle calculations (250 kPa versus 500 kPa), hence cycle efficiency can be increased from 48% to 48.5%.

The configuration explored in this work has the IHX located outside of the reactor vessel, but it is also possible to have the IHX within the reactor vessel. If the IHX is located outside of the reactor, the CO_2 from the HTR is fed into the outside plenum of the IHX. Previously, the outside plenum was used for the low pressure fluid to limit the fractional pressure loss, but for the IHX the outside plenum is more favorable for efficiently handling the flow. Also, the heat transport and transfer efficiency of liquid sodium is much higher than CO_2; therefore, it is intuitive to route it to the inside distribution channel which is usually has a higher associated pressure drop. If the IHX is located inside of the reactor vessel it is desirable to have the CO_2 flow into the high pressure plena and have the sodium use the low pressure plena. If the CO_2 was directed through the low pressure plena a rupture would be a more serious accident than if the CO_2 were to flow in high pressure plena due to the higher rate of CO_2 discharge into the reactor.

For the IHX located outside of the reactor vessel, the HTR pipes to the IHX feed into the near side of the IHX in order to limit the distance traveled to reach the heat exchanger and to extend the overall length of the required turbine feed pipe. The turbine feed pipe is the largest and longest pipe in the cycle and needs to have the largest expansion loop. For the 150 and 300 MWe layouts the overall length of travel from the IHX to the turbine is approximately 13m, but the total pressure loss through the collector and multiple pipe bends is approximately 50 kPa (≈0.2% fractional pressure loss) and reduces the overall cycle efficiency less than 0.1% compared to that of an ideal (infinite diameter) feed pipe. The CO_2 flows through the IHX via straight channels in a counterflow pattern and is collected in a large collection manifold before being sent to the turbine via a 1m inner diameter pipe for the 150 MWe rating. The core of the IHX is approximately 1.7m long, which is a result of adopting straight channels rather than zigzag channels.

Attaching the IHX to the turbine for the dual heat exchanger train layout is difficult with two individual turbine feed pipes. One solution is to have both IHX assemblies feed the CO_2 into one turbine feed plenum. Also, moving the header outlet to the top of the collection manifold allows the feed to be removed vertically, enabling a stress-friendly expansion bend. The two IHX outlet pipes are connected together with one common turbine feed projected along the centerline to the turbine. The overall effect of choosing one turbine feed line is a negligible efficiency reduction as compared to twin feed pipes, but it allows for a simpler turbine casing design. Also, at a later stage when a detailed stress analysis is performed, the turbine feed expansion loop can easily be adjusted to make it larger or smaller to alleviate the induced stresses without affecting the overall layout and footprint of the plant.

Attaching the IHX to the smaller power ratings is slightly different than for the dual heat exchanger train layout. For the very small power ratings there is no need to break the IHX into several modules. However, as soon as the HTR is broken into more than one module it is desirable to also break the IHX into the same number of modules to allow direct discharge between modules. This allows a parallel arrangement without the need

of collection manifolds. For an IHX consisting of more than one module, the turbine inlet piping can be handled several ways: create one large IHX discharge plenum for the CO_2 with one large pipe running to the turbine inlet; use a collection manifold on the outlet of the IHX plenum with one large pipe running to the turbine inlet; or have two parallel pipes running from the IHX (one pipe from each module plenum) and join the two pipes into one turbine inlet pipe shortly before the casing penetration. At this point, the best option is to use the two parallel pipes joined together. Currently, the feasibility of creating one large discharge plenum instead of two normal plena is unexamined. The IHX outlet will be the hottest high pressure point in the cycle at 550°C and approximately 19.5 MPa (assuming a 500kPa pressure drop thru the IHX) and should be designed on the conservative side until all of the PCHE capacities are known. It is also possible to have a 650°C IHX outlet temperature if a higher temperature reactor is employed. The option of using a collection manifold at the IHX exit connected to one large pipe is also a feasible option. However, this needs further investigation regarding the area of the maximum size pipe capable of being attached to the turbine casing and the current maximum size of high temperature and pressure pipe available. The parallel pipe option makes the single feed pipe run distance a minimum, hence having the potentially smallest pressure drop.

The sodium is fed into the inside plenum of the heat exchanger via a similar pipe and distribution manifold as used in the PCS. The sodium pipes and distribution/collection manifolds are merely shown to depict a possible arrangement, and have not been sized for optimum performance. Handling the sodium will not be very difficult because of the lower operating pressure, and the modest ΔT between the two fluids keeps the operating temperature within a reasonable range. However, prevention of sodium freezing in start up and shutdown scenarios will be a complication.

The IHX is shown isolated in Figures 2.22 and 2.23 and attached to several PCS layouts in Figures 2.24 through 2.28.

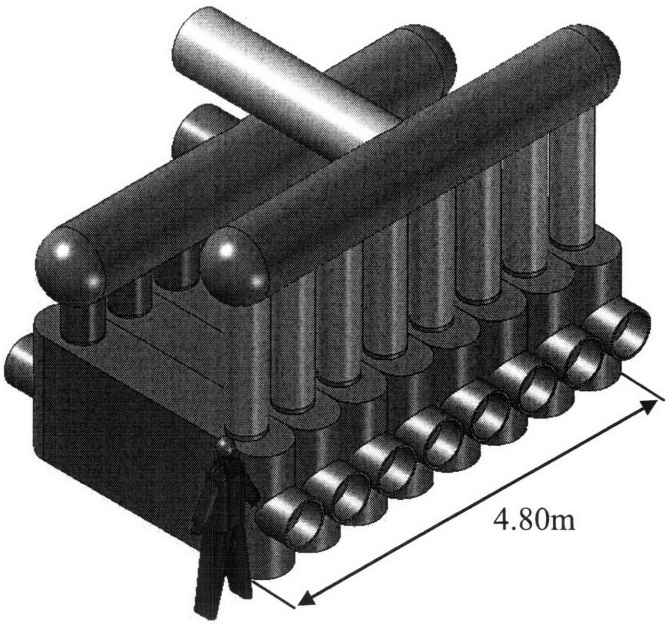

Figure 2.22 150 MWe IHX (isometric view)

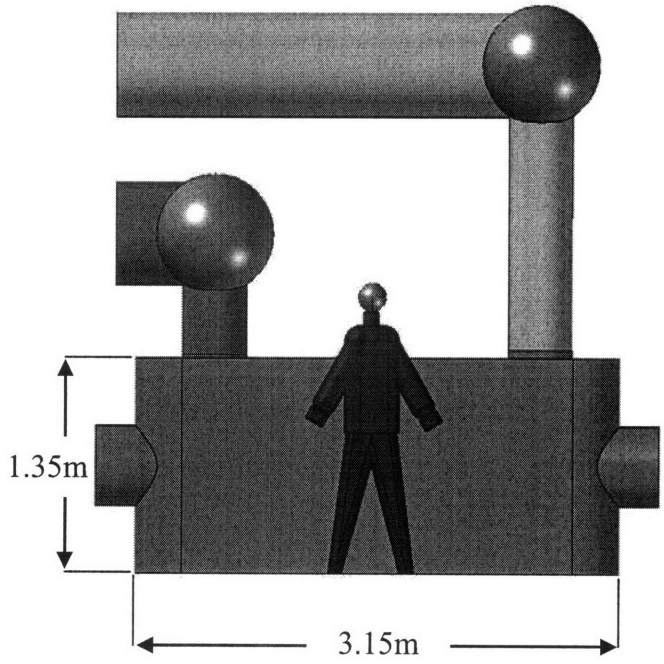

Figure 2.23 150 MWe IHX (side view)

Weight (does not include connecting pipes and manifolds) ≈ 81 M.T.

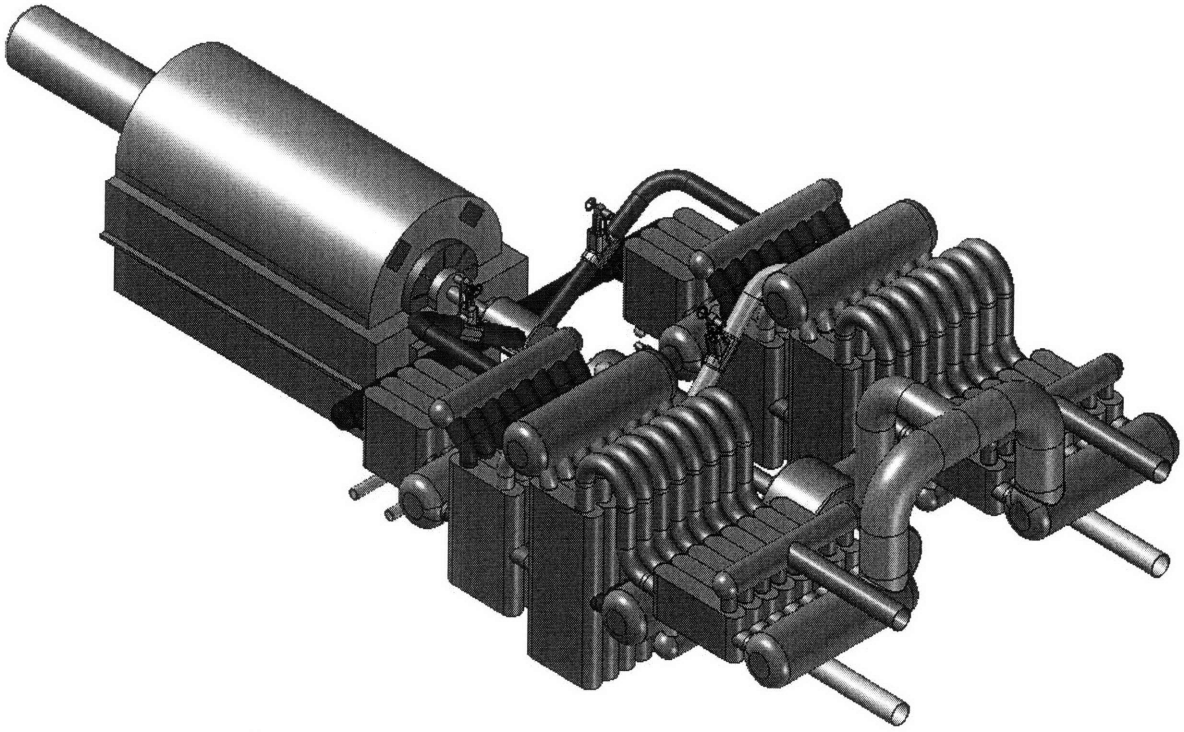

Figure 2.24 300 MWe PCS with IHX and generator
with two 150 MWe IHX assemblies

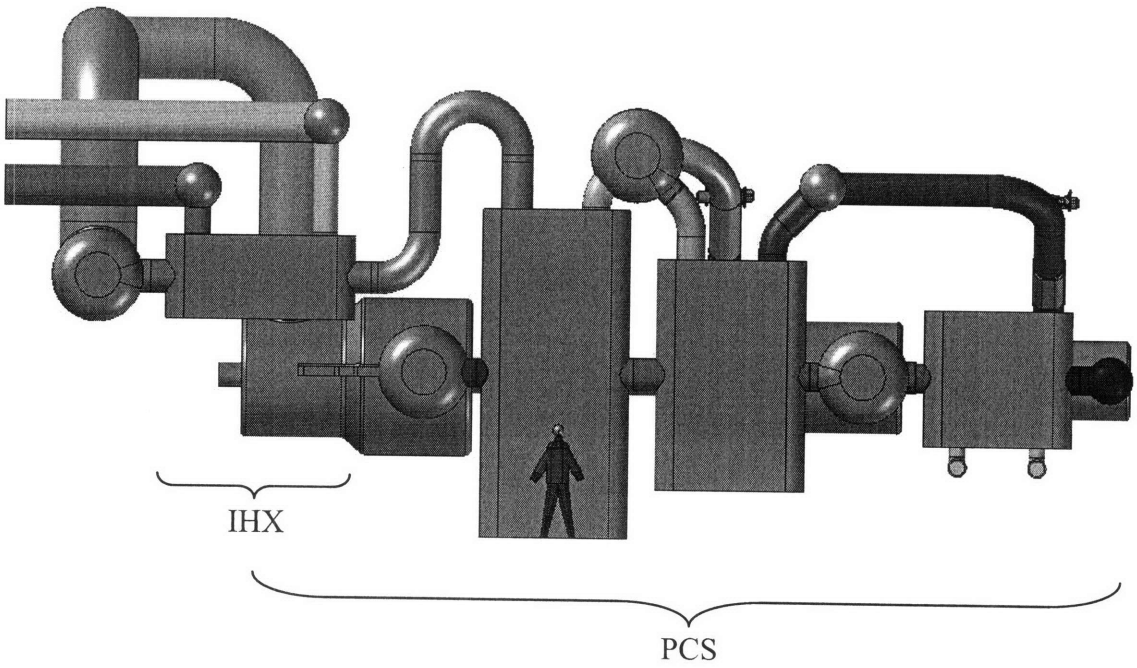

Figure 2.25 300 MWe PCS with IHX (side view)

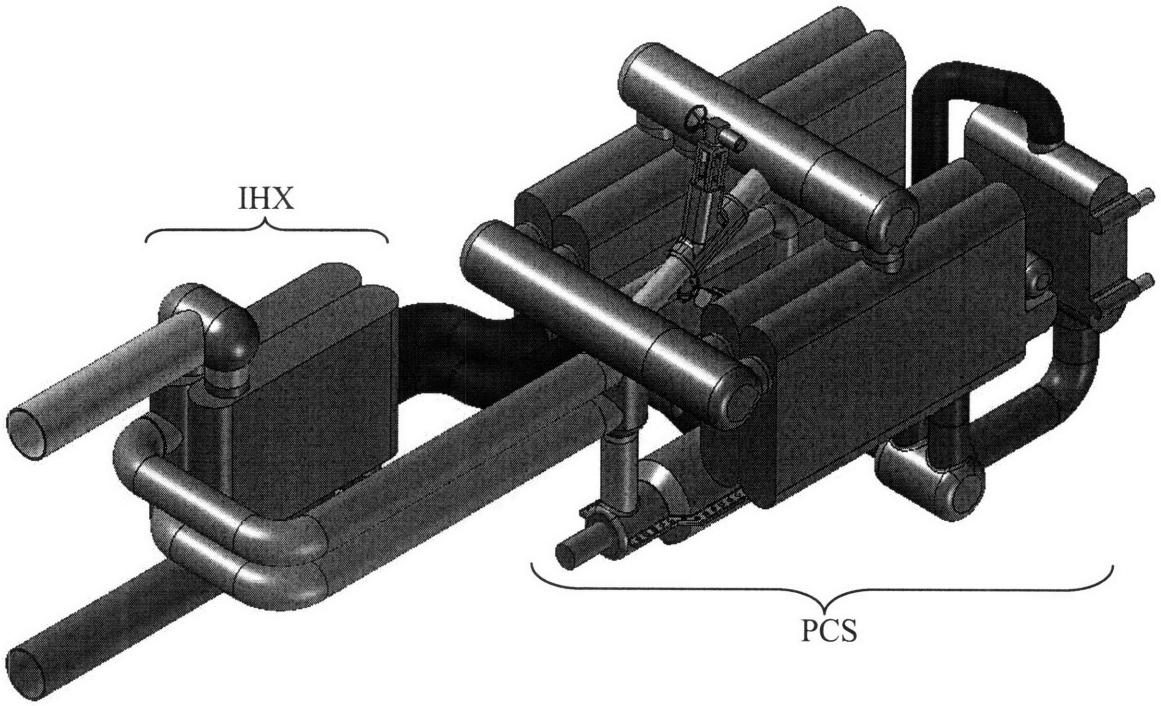

Figure 2.26 50 MWe PCS with IHX (isometric view)

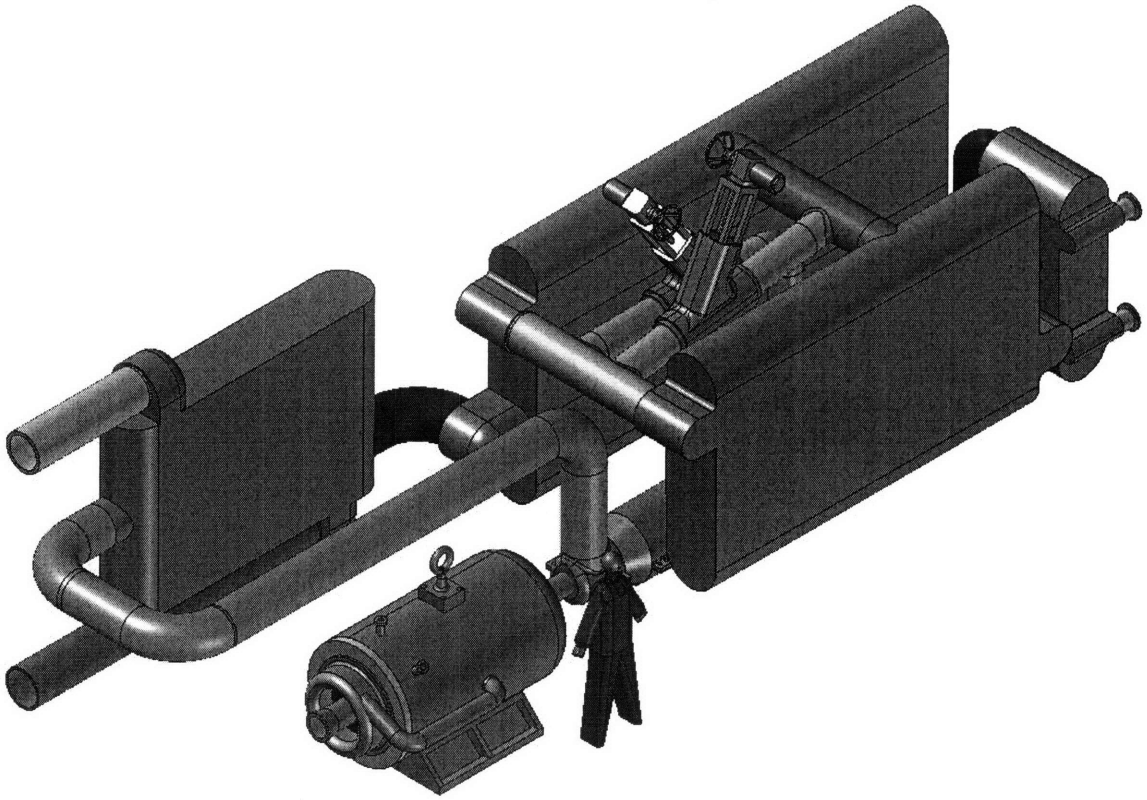

Figure 2.27 20 MWe PCS with IHX and permanent magnet generator (isometric view)

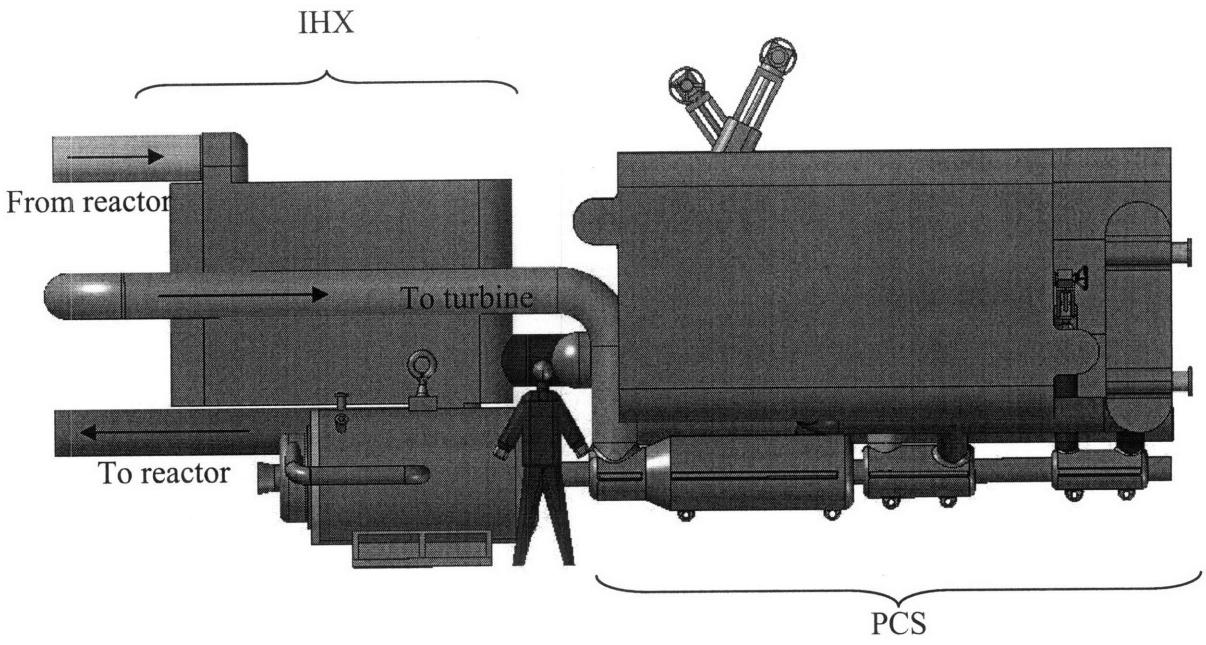

Figure 2.28 20 MWe PCS with IHX and permanent magnet generator (side view)

2.9 Extending to high reactor power ratings

There are several possible combinations to reach the peak power goal of 1200 MWe: four 300 MWe PCS loops each with its own set of turbomachinery (Figures 2.29 and 2.30); two 600 MWe loops utilizing two parallel 300 MWe loops on one turbomachinery shaft (two turbines and four compressors) and one 600 MWe generator (Figures 2.32 and 2.35); two stacked 600 MWe loops each feeding into a set of turbomachinery (one turbine and two compressors (Figures 2.35 through 2.39); and two 600 MWe loops with two 300 MWe loops stacked with one set of turbomachinery and one 1200 MWe generator (Figure 2.40).

Several more plant layouts have been considered for the power ratings on the order of 1200 MWe. The most obvious and simple layout utilizes four, single shaft, 300 MWe, PCS loops each connected to the reactor to obtain the desired 1200 MWe rating. The reactors shown in the following figures are for illustrative purposes only and do not reflect the actual design or size of a specific reactor.

The layout utilizing four 300 MWe loops, each with its own turbomachinery train and generator, exhibits the largest footprint for a 1200 MWe plant. However, this cycle also is the easiest for cutting a loop in and out for partial load operation. Each load can simply be isolated from the reactor by closing isolation valves on the liquid sodium lines to completely cut it out of operation. This enables each cycle to operate at the most efficient power level, full power, for 100, 75, 50, and 25% power.

It is also important to mention here that Figures 2.29 and 2.30 correspond to a direct cycle. If they were adapted to an indirect cycle an IHX would separate the PCS from the reactor loop. This will have two main layout consequences: (1) the overall footprint will become slightly larger and (2) the containment will become smaller because only the reactor and the IHX would be within containment while the rest of the PCS will be outside. See figure 2.39 for a rough representation of the adaptation to an indirect cycle layout.

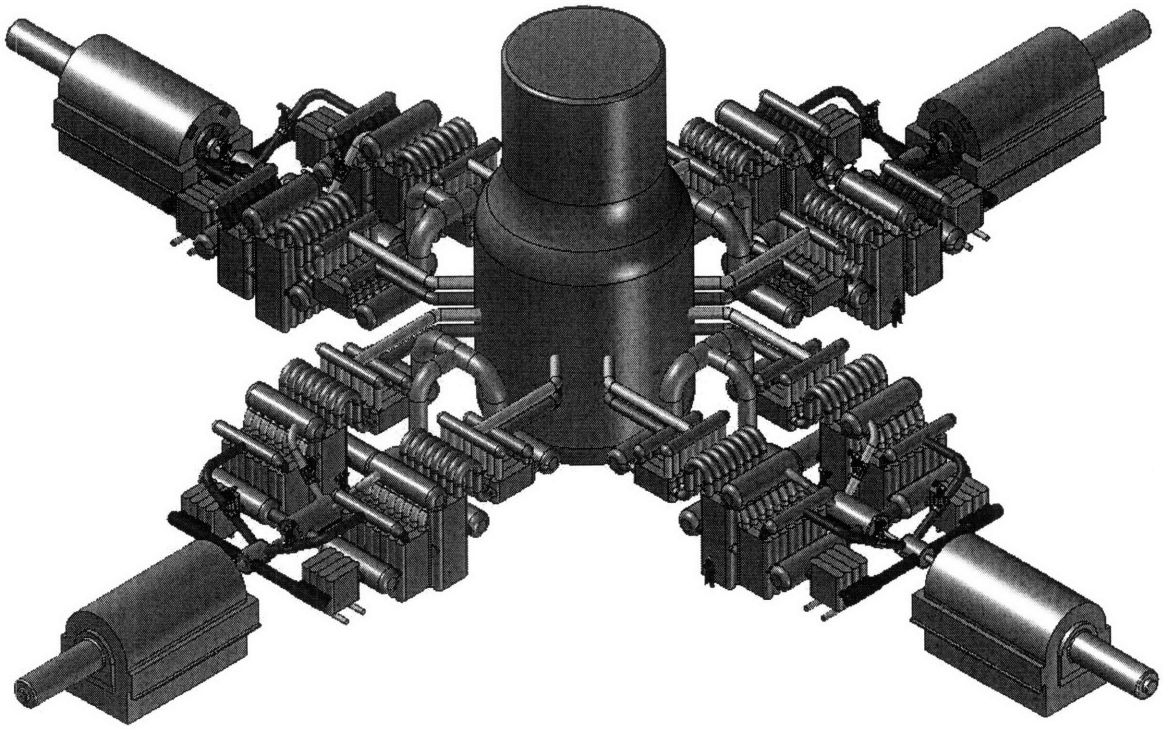

Figure 2.29 Four 300 MWe loops connected to one 1200 MWe reactor
*Primary loop isolation valves not shown

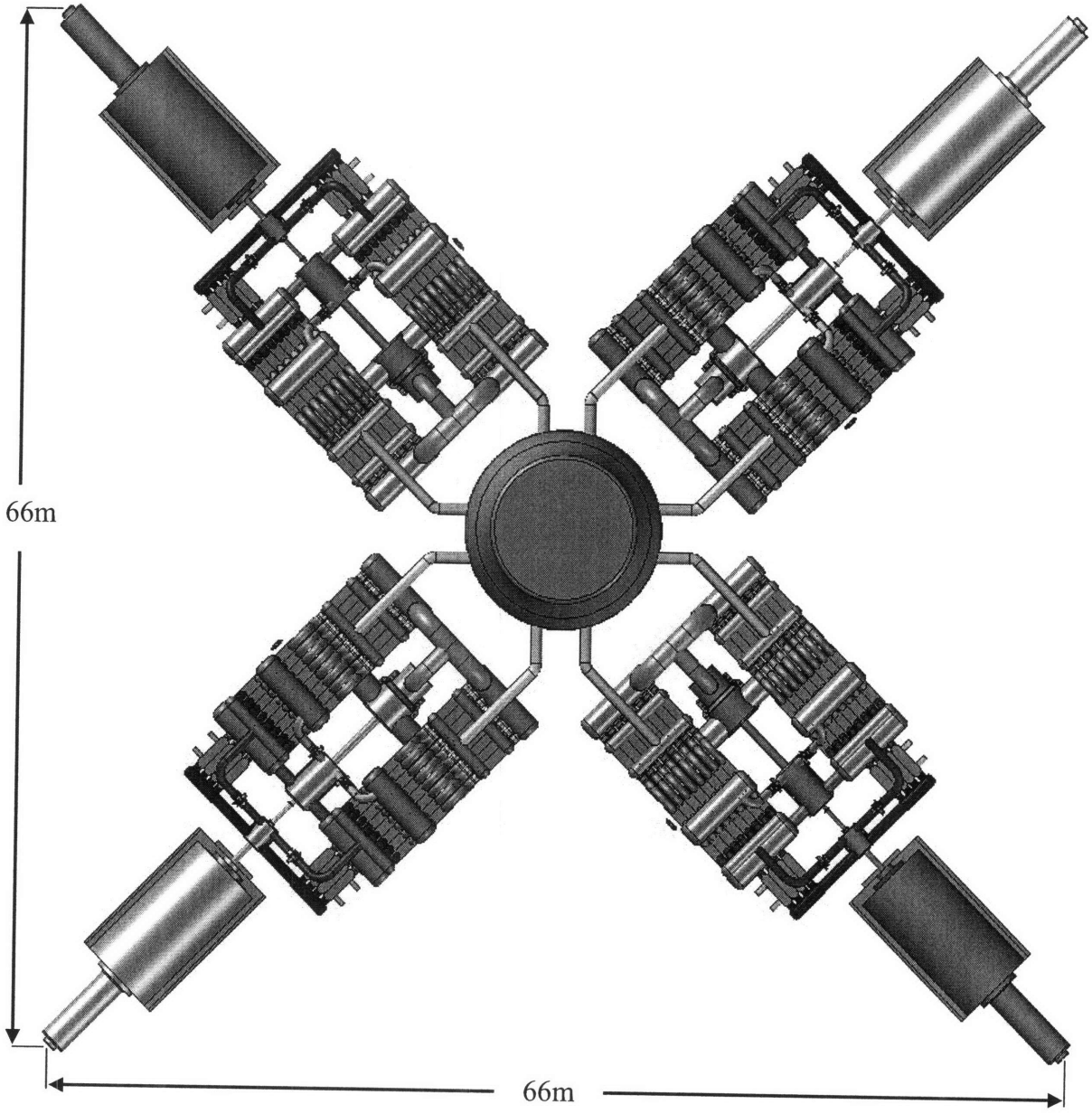

Figure 2.30 four 300 MWe PCS loops connected to one 1200 MWe reactor (top view)
*Primary loop isolation valves not shown
*88m diagonal (tip to tip)

Several options are available to use a two loop system each connected to a 600 MWe generator. The first option (Figures 2.31 and 2.32) discussed employs four 300 MWe PCS loops, with two loops arranged end-to-end while sharing a common shaft. Hence, each shaft will have two turbines and four compressors. The turbines and compressors are arranged in such a way to completely balance the thrust from each machine. This is advantageous because it lowers the demand on a thrust bearing. However, the layout becomes more complicated, with considerable extra piping in addition to its requirement for a very large containment.

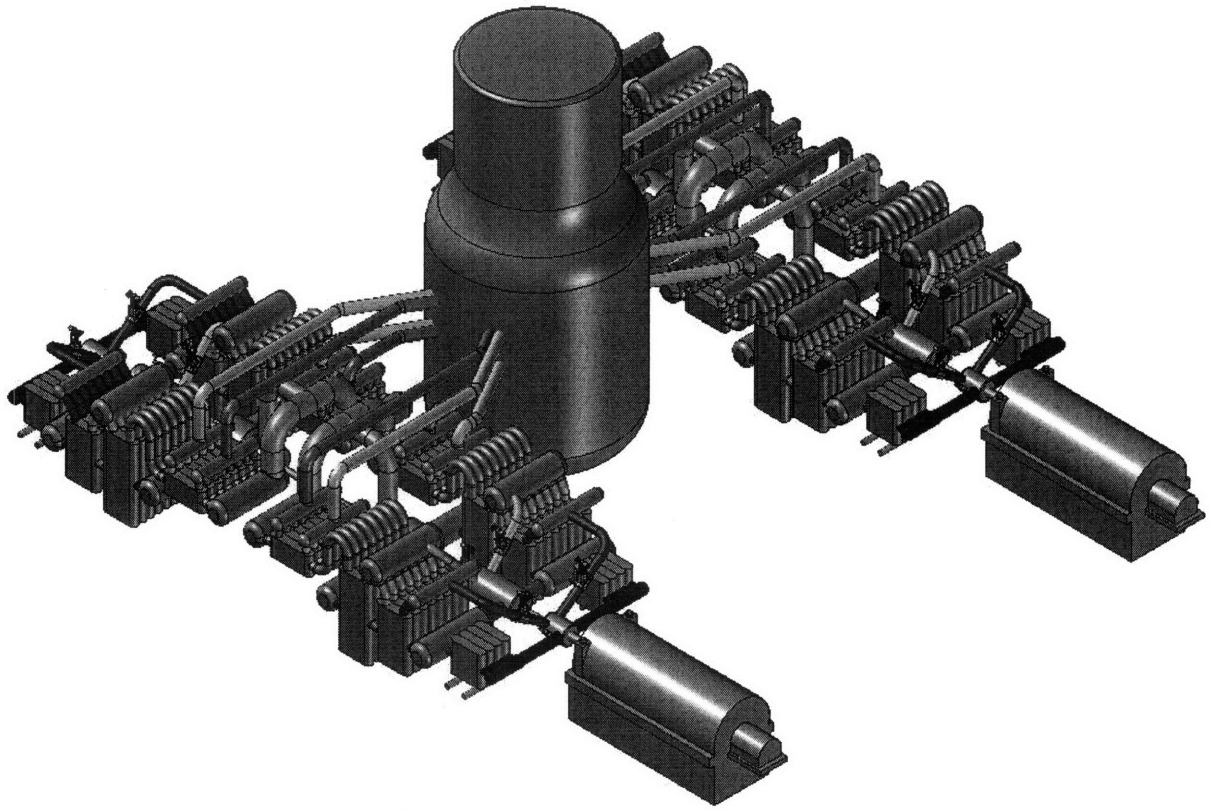

Figure 2.31 2x600 MWe PCS layout isometric view
*Primary loop isolation valves not shown

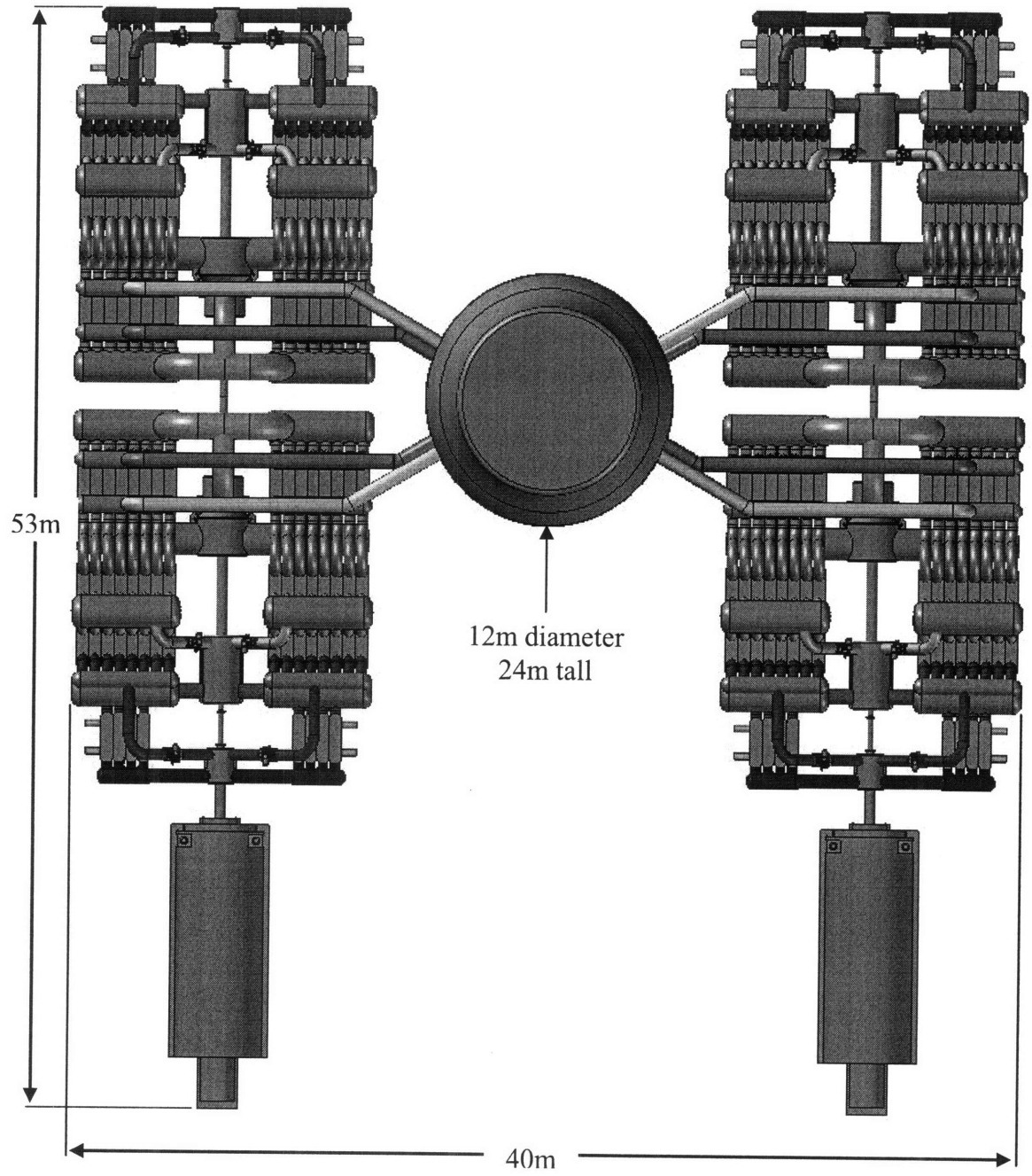

Figure 2.32 2x600 MWe PCS layout top view
*Primary loop isolation vales not shown

The above depicted layout can further be compacted by combining the IHX into two units (it is now shown as four units) serving both 300 MWe PCS loops, thus enabling the use of only one large diameter pipe serving a centralized turbine. The advantage of this layout is the complete balance of axial thrust on the shaft by having equal and opposite facing turbomachinery, possibly only one main turbine, and only two generators, which

will reduce the overall capital cost. At a later point when the IHX is combined into two units, the turbine possibly can be combined into one unit with a central inlet discharging in opposite directions with a diffuser for each loop (Figures 2.33 and 2.34). One additional consideration that needs to be addressed in the future is to determine if it is realistic to attach a 600 MWe generator to the compressor end of the shaft. If these issues are indeed resolved, the complete power cycle will be very compact.

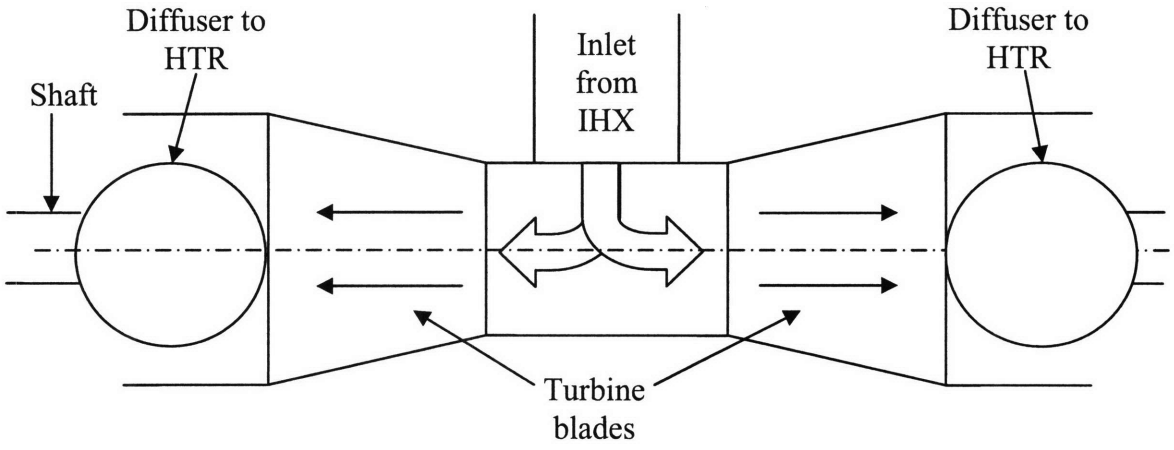

Figure 2.33 600 MWe (net) turbine for two 300 MWe PCS loops on one shaft (side view)

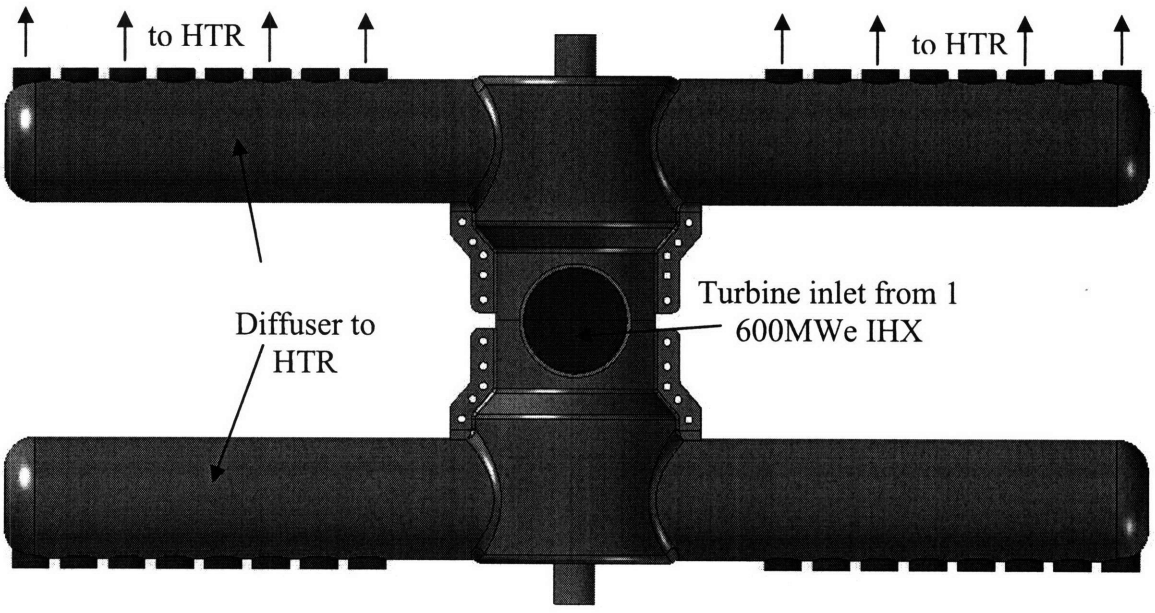

Figure 2.34 600 MWe (net) turbine for two 300 MWe PCS loops on one shaft (top view)

The second option for a 2x600 MWe shaft system expands on the idea to use two 600 MWe turbomachinery trains with the possibility of stacking the two 300 MWe PCS trains, essentially putting each on a separate floor straddling one set of turbomachinery. This arrangement has the advantage of requiring less floor space, which will make the containment more economical. However, the thrust is not balanced through use of counterflow turbomachinery, but it will require only one of each piece of turbomachinery, while the layout shown in Figures 2.31 and 2.32 requires two turbines and four compressors to achieve the 600 MWe. Figures 2.35 through 2.39 show the cycle with the stacked configuration for both the direct and indirect cycles. The direct cycle can fit into a 54 m diameter, and the indirect cycle can fit inside a 34 m diameter, PWR type containment. The indirect cycle containment is considerably smaller because very few components are required to be within the containment and nearly all of the PCS can be located outside. The direct cycle layout would be attached to a S-CO_2 cooled nuclear reactor while the indirect cycle can be attached to many of the proposed GNEP Gen-IV nuclear reactors. The layouts presented in Figures 2.35 through 2.39 appear to be the most promising configurations to reach 1200 MWe with respect to partial load operation, ease of maintenance, and compactness.

The last option is to use a vertical layout with four recuperation loops serving one turbomachinery train; essentially, this is the same as rotating the two-floor design 90° (Figure 2.40). However, the applied forces on the bearings may be intolerable. The most realistic possibility for the vertical arrangement would be for the very small power ratings ($\leq$30 MWe) due to the considerably smaller support and counter-thrust requirements. However, assuming successful development of vertical turbomachinery, this option would be one of the smallest footprint layouts for a distributed PCS. The cartoon layout for this option can be seen in Figure 2.41.

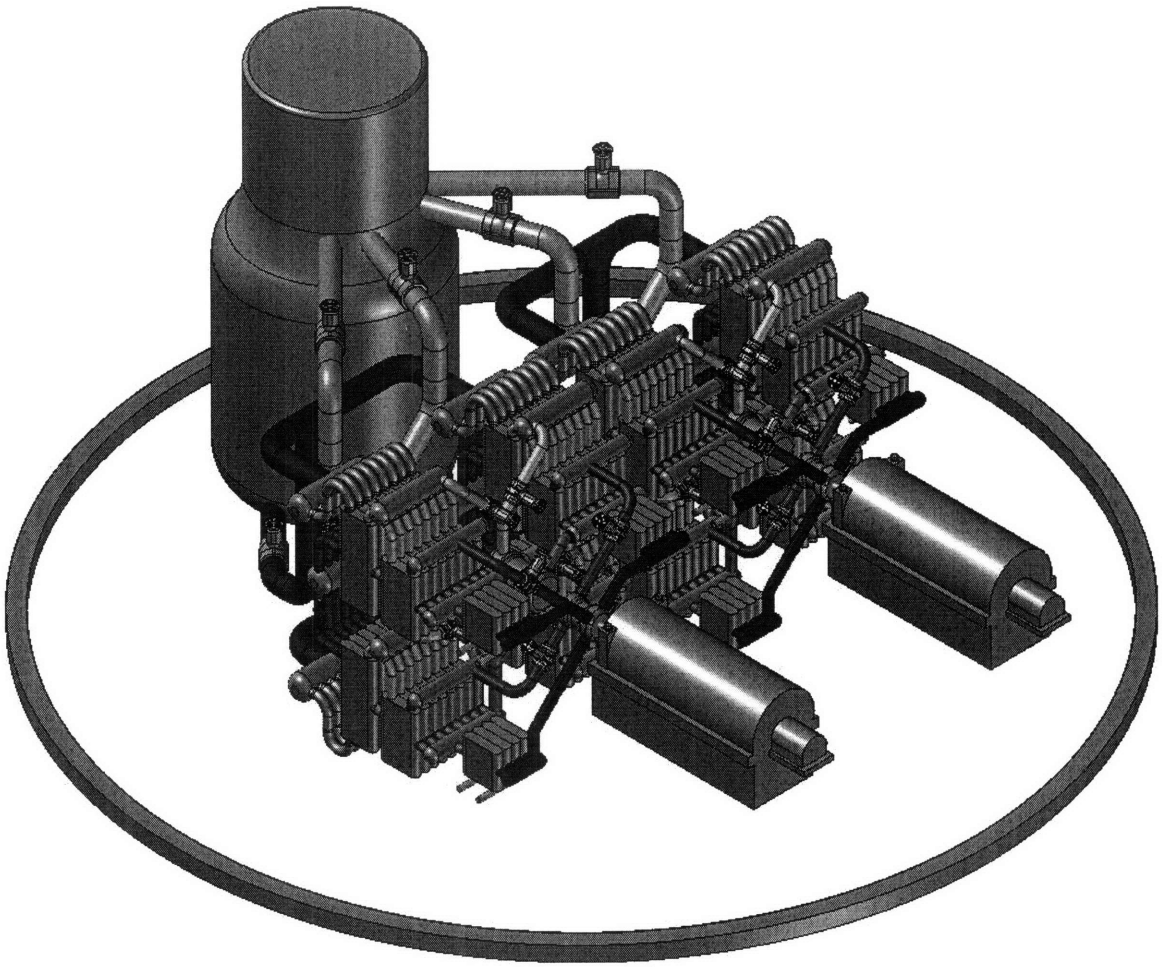

Figure 2.35 1200 MWe direct cycle, 2x600 MWe turbomachinery trains, stacked, isometric view

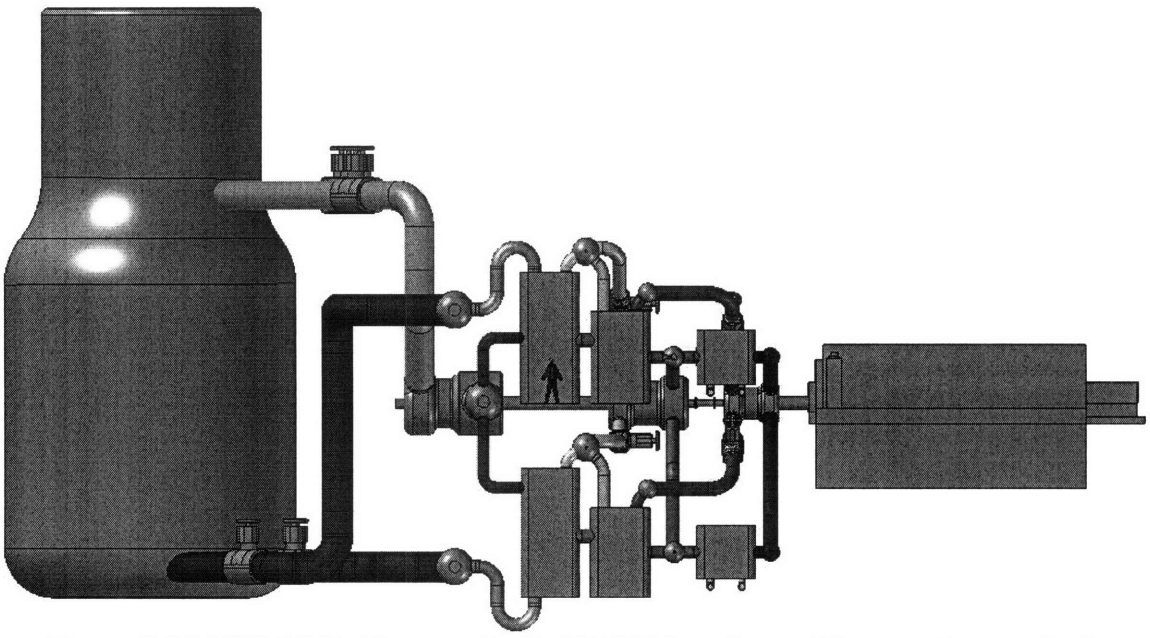

Figure 2.36 1200 MWe direct cycle, 2x600 MWe turbomachinery trains, stacked, side view

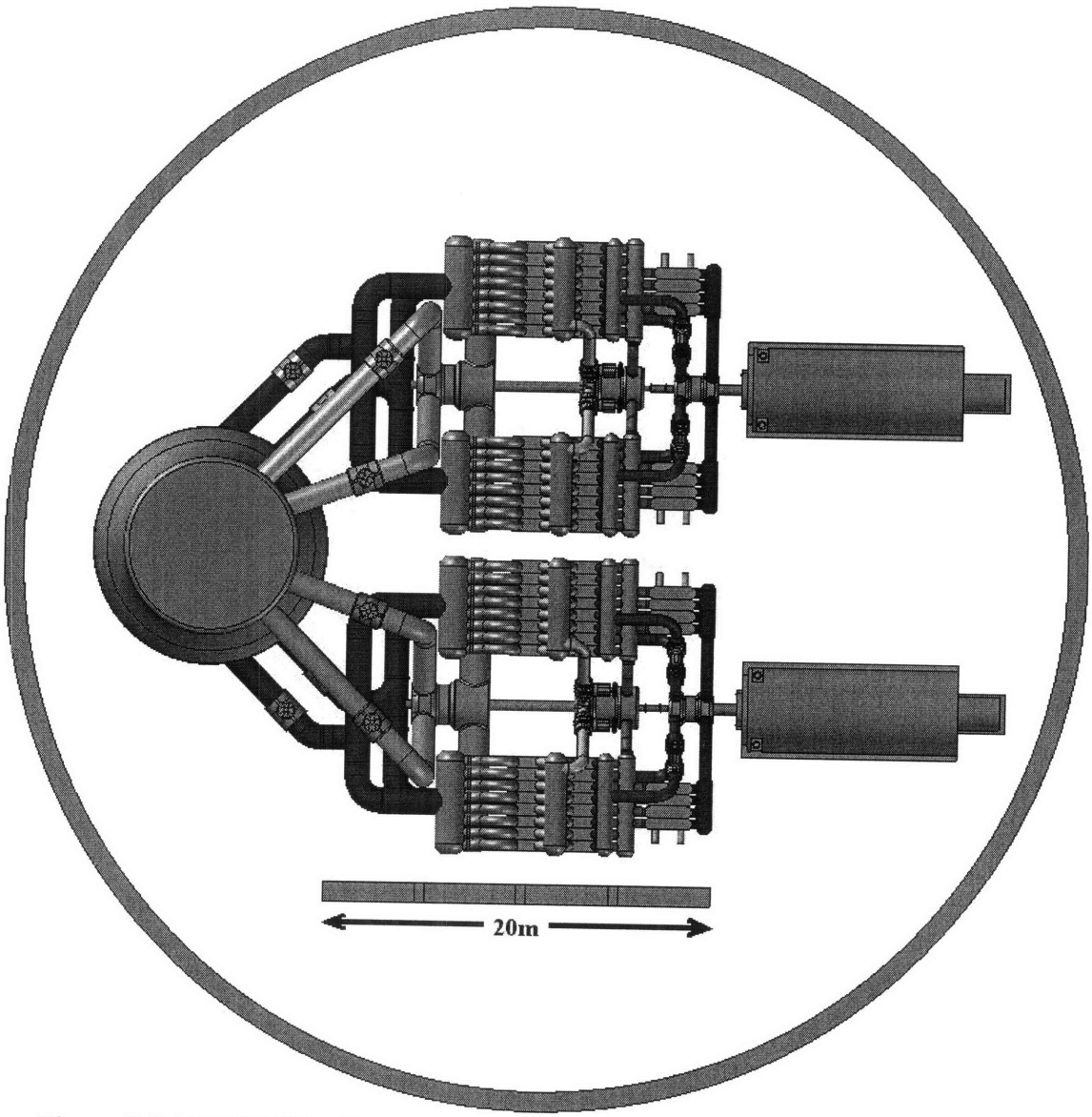

Figure 2.37 1200 MWe direct cycle, 2x600 MWe turbomachinery trains, stacked, top view

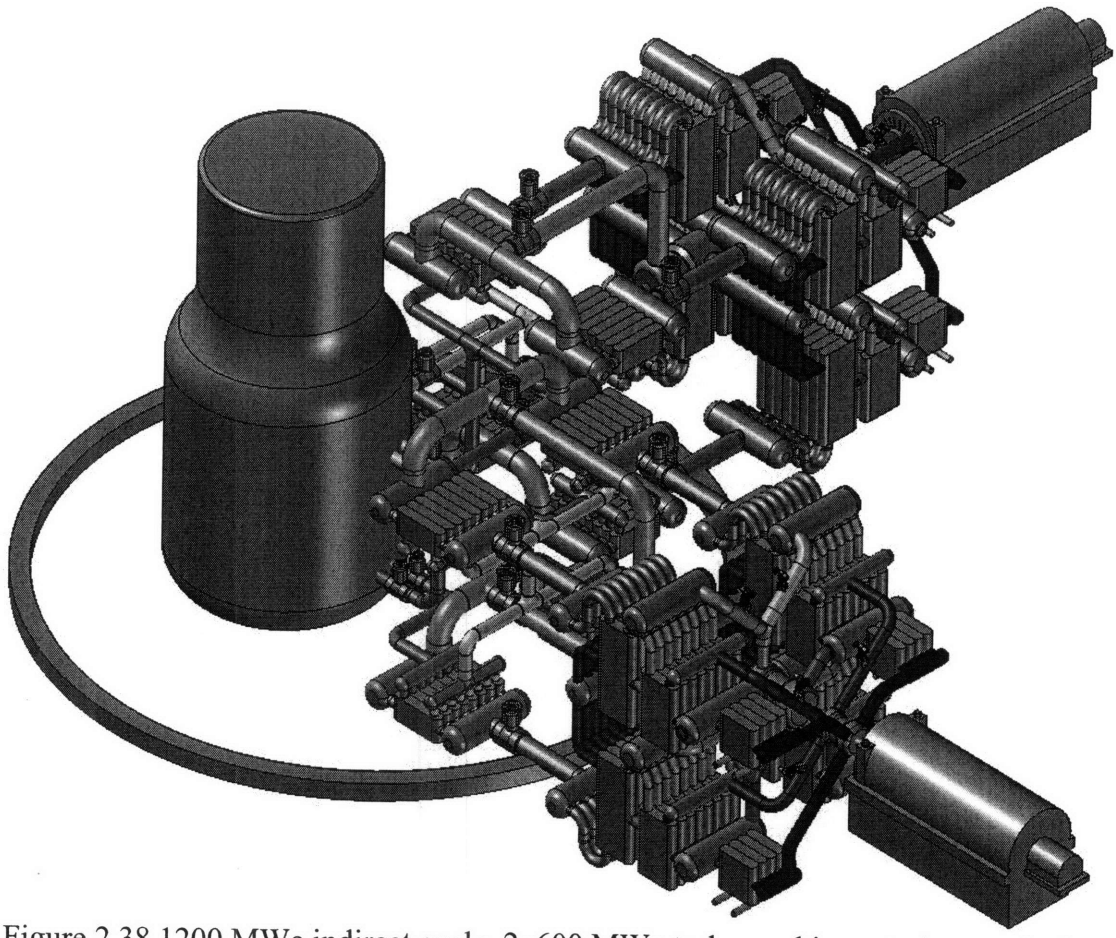

Figure 2.38 1200 MWe indirect cycle, 2x600 MWe turbomachinery trains, stacked, isometric view

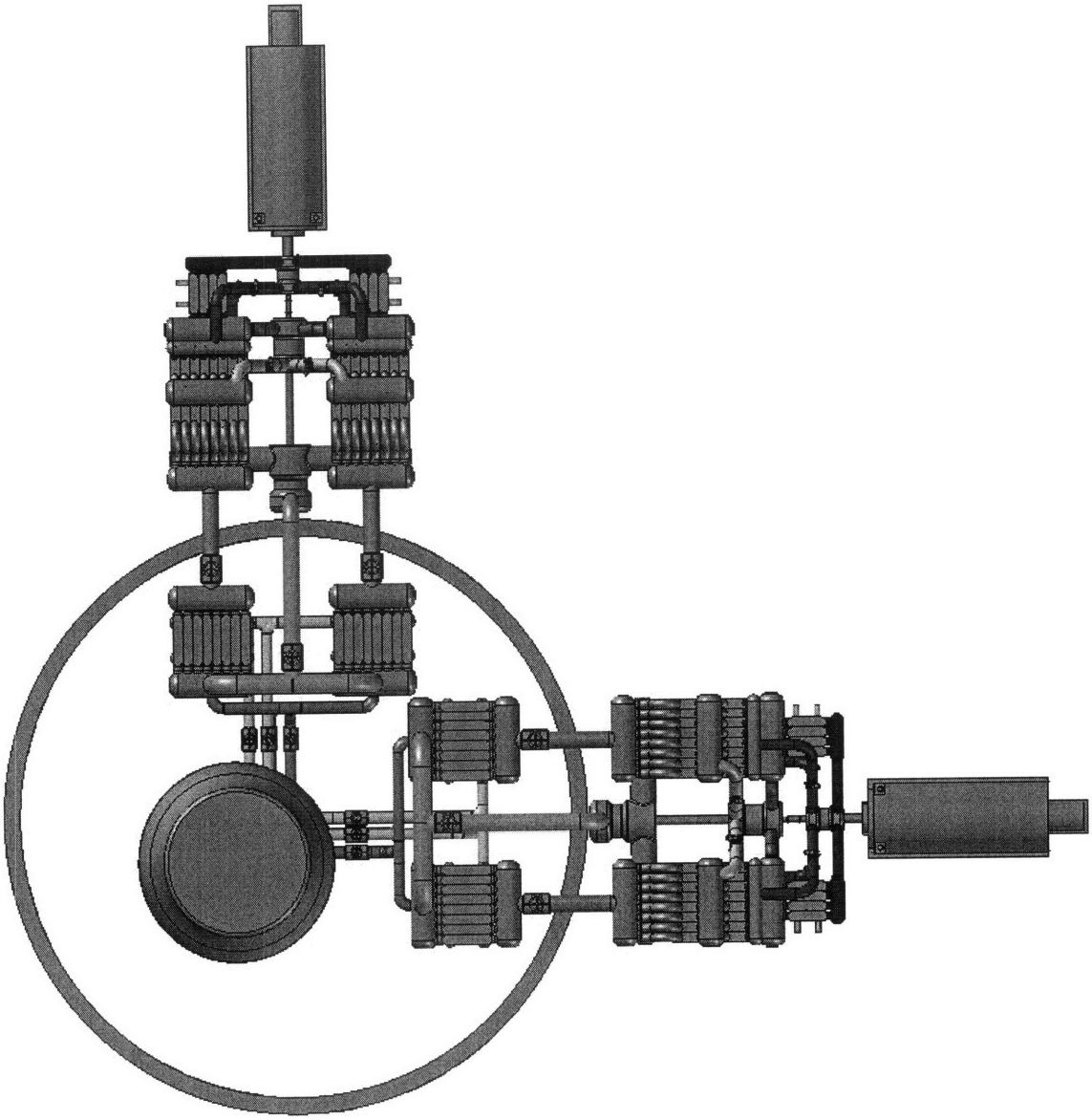

Figure 2.39 1200 MWe indirect cycle, 2x600 MWe turbomachinery trains, stacked, top view

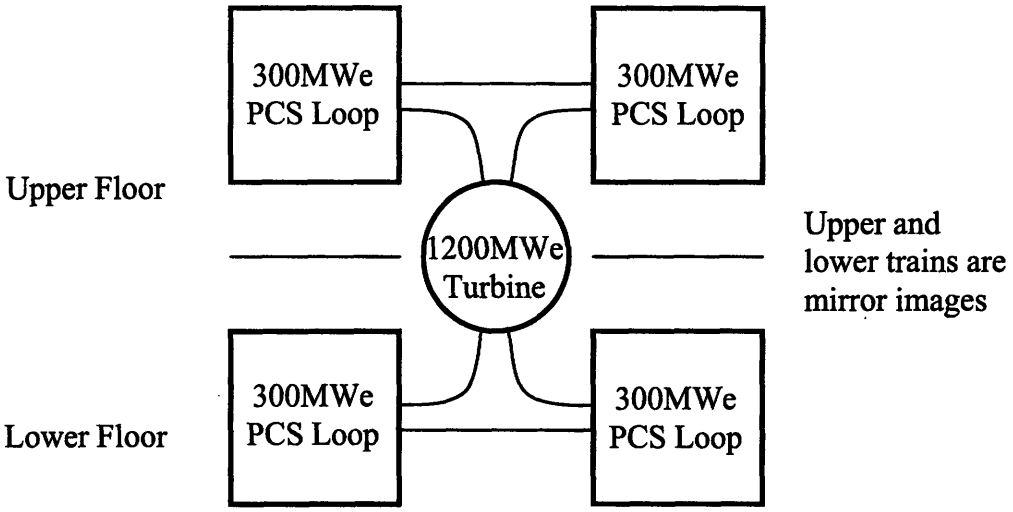

Figure 2.40 Cartoon depiction of an over-under 1200 MWe turbomachinery layout for a horizontal arrangement (end-on view)

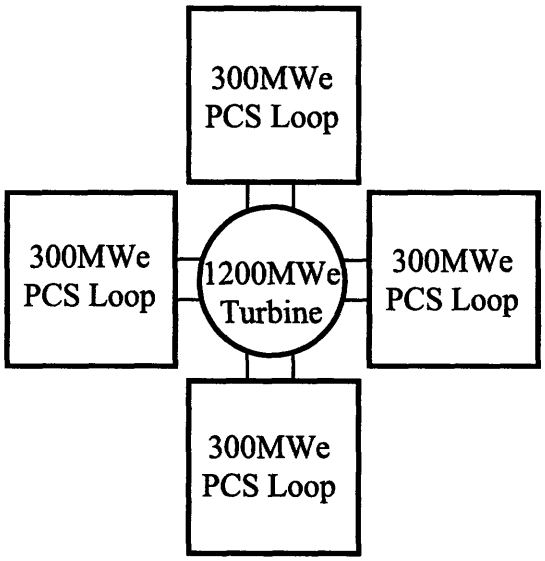

Figure 2.41 Cartoon depiction of a 1200 MWe turbomachinery train layout for a vertical arrangement (top view)

2.10 S-CO_2 PCS Comparison to Rankine Cycle Components

To provide an easily recognizable size comparison, several typical components of a Rankine cycle were produced in SOLID EDGE®. The horizontal steam generator was a unit taken from the Russian designed VVER 440/213 (specifications are in Table 2.8) and the remaining Rankine Cycle components were sized from an early nuclear power plant design text for a 300 MWe pressurized water reactor system [Kuljian, 1968 & www.sujb.cz/docs/anex1.pdf]. The IHX is compared to the steam generators (Figures 2.42 and 2.43); the entire turbomachinery train of the S-CO_2 PCS is compared to the steam chest and low pressure (only) steam turbine (Figure 2.44); the precooler is compared to the main condenser (Figures 2.45 and 2.46); and the HTR and LTR are compared to the feedwater heaters (Figures 2.47 and 2.48). The S-CO_2 PCS has a clear advantage over a typical Rankine cycle with regards to compactness in both component volume and footprint. An actual 300 MWe Rankine cycle layout constructed with all of the feed pumps, steam generators, air ejectors, turbine bleeds, feedwater heaters, etc., would clearly show that the S-CO_2 PCS footprint is considerably smaller.

Table 2.8 Russian VVER 440/213 specifications

Reactor Type		Pressurized water reactor (VVER 440/213)
Nominal thermal output		1375MWth
Generator output		440MWe
Net electrical output		388MWe
Own consumption		52MWe
Number of steam generators		6 (230MWth each)
Steam generator weight		Approx. 165 M.T.
Steam Generator body diameter		3.21m
Steam generator body length		11.80m

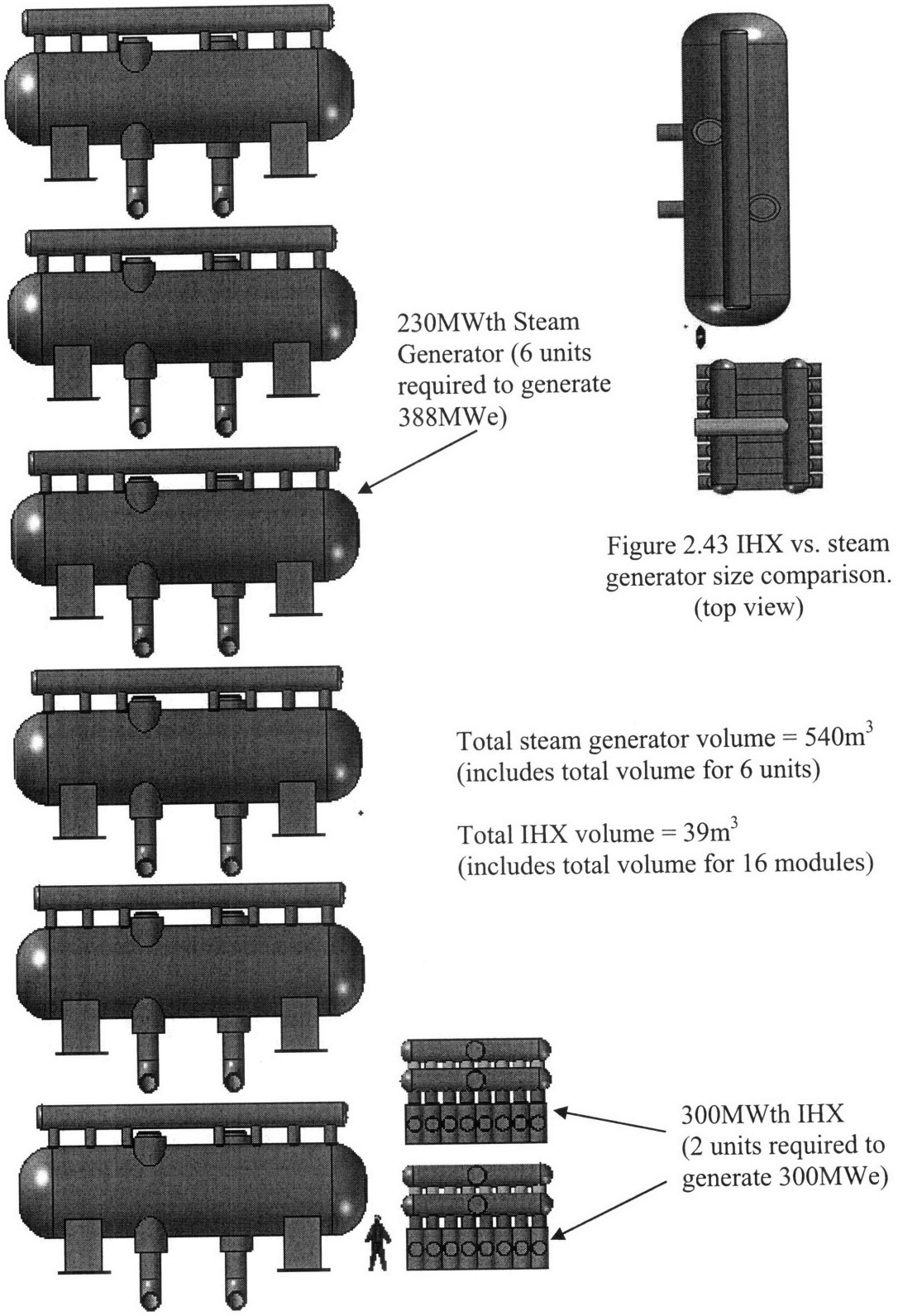

Figure 2.42 IHX vs. steam generator size comparison. (front view)

Figure 2.43 IHX vs. steam generator size comparison. (top view)

The turbomachinery component spacing in Fig. 2.47 is not to scale for the S-CO_2 layout (the turbomachines are shown much closer together than the actual spacing). However, the actual spacing is not important because the focus is on the size comparison between components and not the layout footprint.

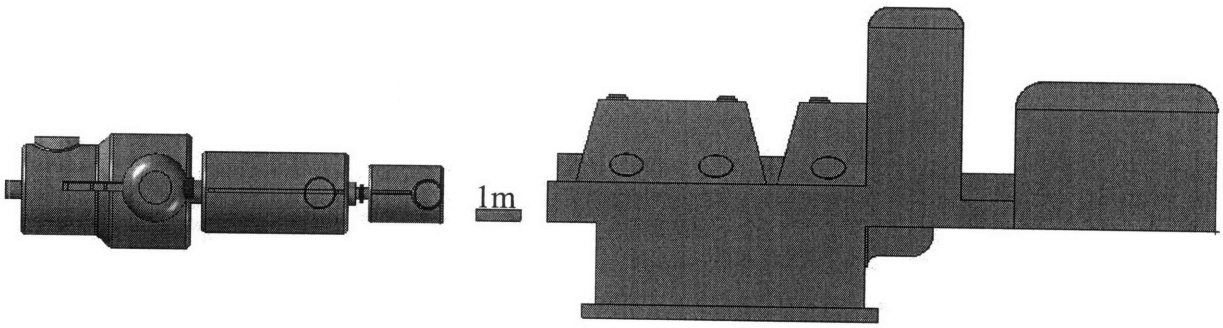

S-CO_2 turbomachinery volume ≈ 48m^3 (includes diffusers)

LP turbine and steam chest volume ≈ 310m^3 (includes steam chest and half of the exhaust path to main condenser)

Figure 2.44 Turbomachinery volume comparison between S-CO_2 PCS turbomachines and the LP turbine plus steam chest from a Rankine cycle for a 300 MWe rating

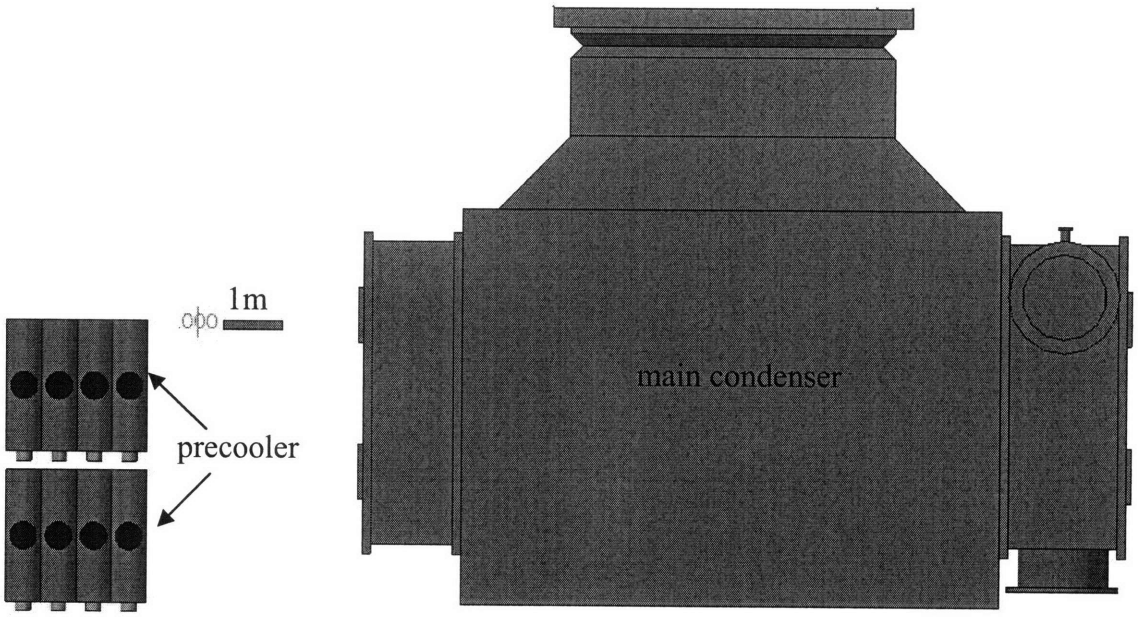

Figure 2.45 Volume comparison of the precooler units from the S-CO_2 PCS with the main condenser from a Rankine cycle for a 300 MWe rating (side view)

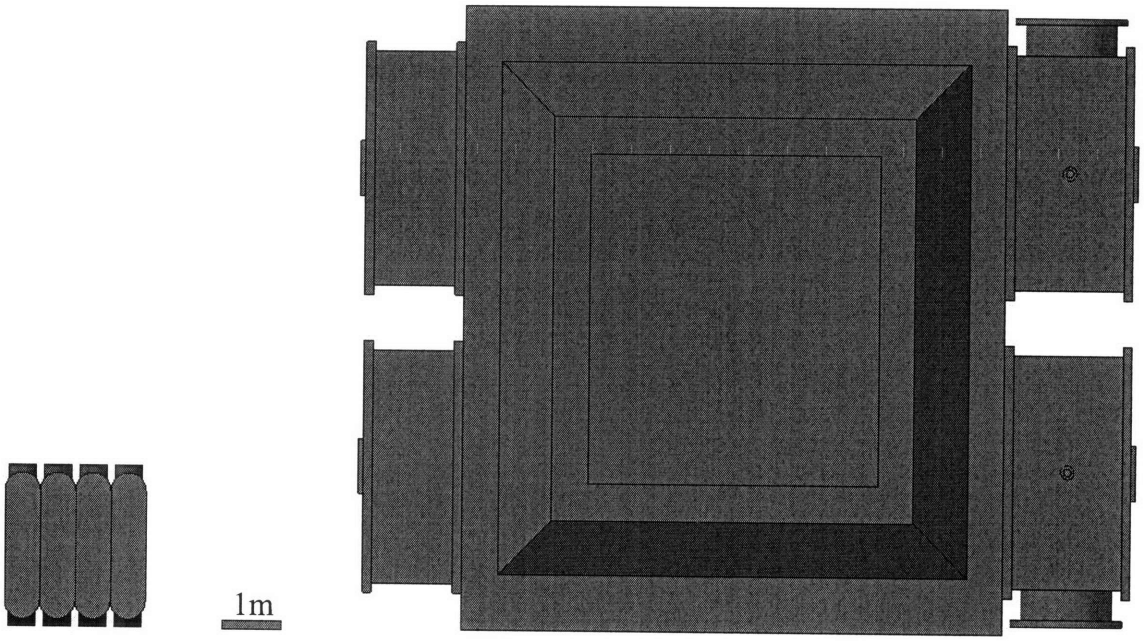

Precooler volume ≈ $24m^3$
(total volume for 8
precooler modules)

Main condenser volume ≈ $910m^3$
(includes half of turbine exhaust path)

Figure 2.46 Volume comparison of the precooler units from the S-CO_2 PCS with the main condenser from a Rankine cycle for a 300 MWe rating (top view)

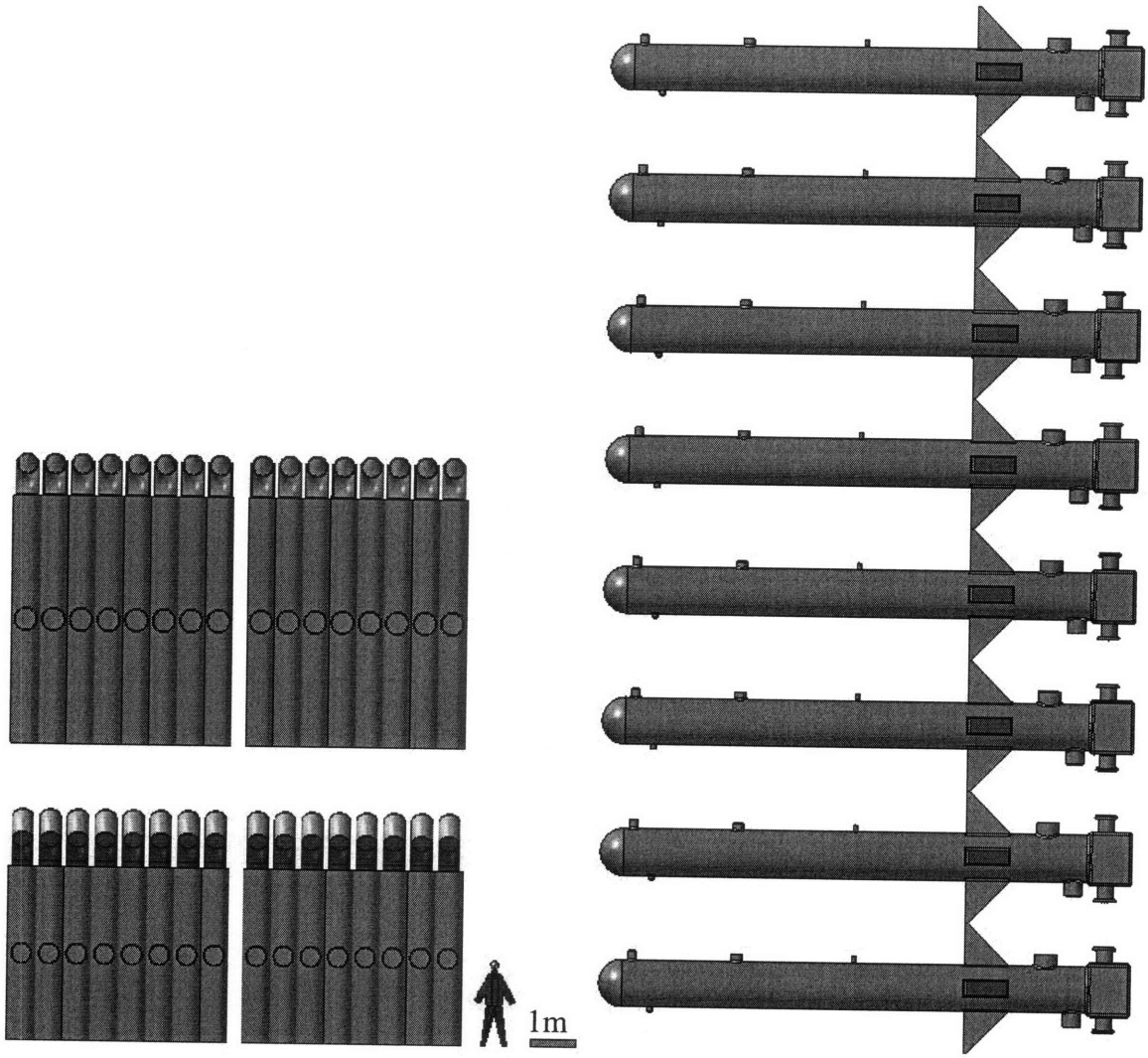

S-CO_2 recuperator volume ≈ 200m^3
(total volume with plena for 32 modules)

Feedwater heater volume ≈ 73m^3
(total volume for 8 heaters)

Figure 2.47 Volume comparison of the recuperators from the S-CO_2 PCS with the feedwater heaters from a Rankine cycle for a 300 MWe rating (front view)

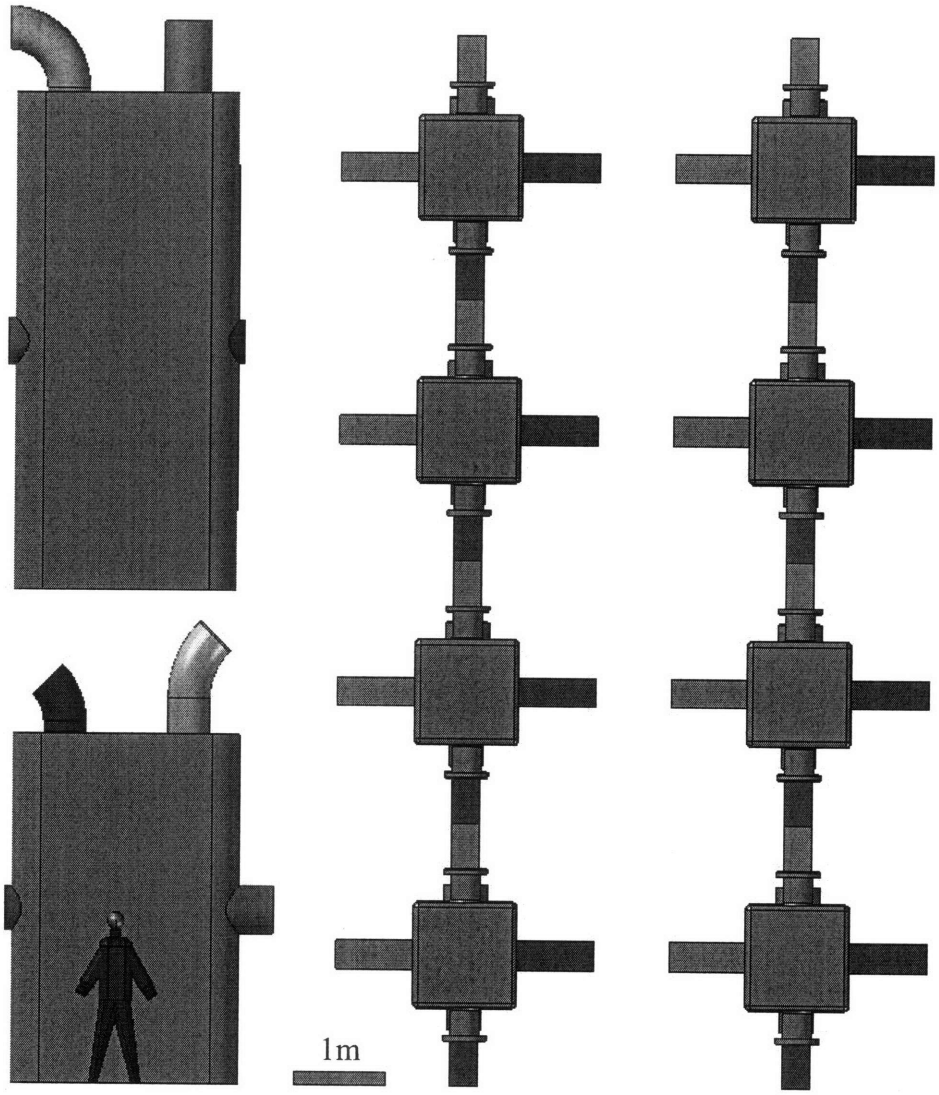

Figure 2.48 Volume comparison of the recuperators from the S-CO_2 PCS with the feedwater heaters from a Rankine cycle for a 300 MWe rating
(side view with components rearranged)

Figures 2.47 and 2.48 are simply provided to show that although the overall recuperator volume is nearly three times greater, it will require a smaller footprint when installed. Typically, the feedwater heaters will be vertical, with the spacing at least twice the distance as depicted here. The number of the required feedwater heaters will vary depending on the rating of the heater and the plant design, but a typical number for a 300 MWe power rating is six or eight heaters.

Figure 2.49 is provided to more simply give a comparison in size between the S-CO_2 recompression cycle and a typical Rankine cycle. Clearly, the S-CO_2 cycle will provide considerable footprint savings! It is anticipated the balance of plant will allow for additional economic savings due to the smaller size.

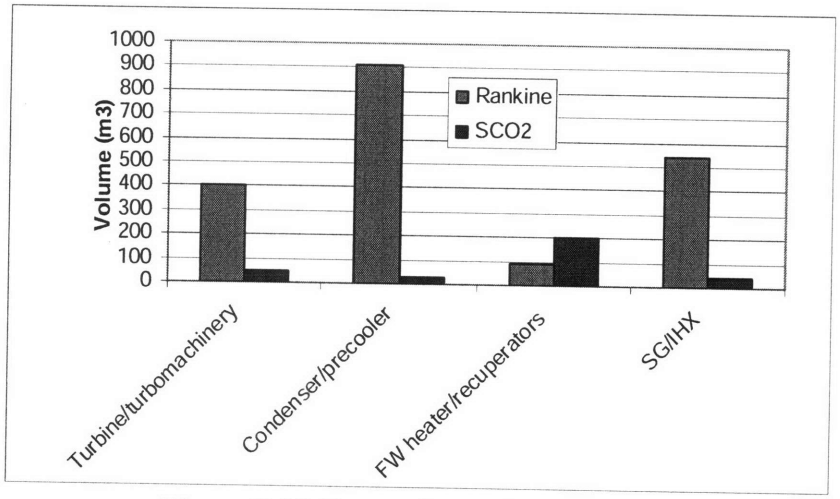

Figure 2.49 Comparison of components

2.11 Chapter Summary and Conclusions

Several S-CO_2 PCS layouts were developed with power ratings ranging from 20-300 MWe for a single unit and up to 1200 MWe for several multi-loop arrangements. Minimizing the footprint and reducing the pressure losses were the main driving forces behind the design. The cycle currently exhibits less than a 1% efficiency reduction due to the pressure losses in the heat exchanger plena and pipes and is a considerable improvement over the previous generation layouts.

For the smaller PCS layouts (≤50 MWe) it is suggested to handle partial loads with variable speed turbomachinery and the appropriate associated power electronics. Also, as the technology progresses, the permanent magnet generator appears to be an ideal match for the PCS and is favorable to using a vertical turbomachinery layout. The larger layouts were designed primarily for multiple loop assemblies which enable individual

loops to be cut in/out to efficiently accommodate the power demand. The stacked 2x600 MWe arrangement appears the most promising layout with regards to minimizing the footprint, while maintaining a dual loop operation which will achieve higher partial load efficiency by being able cut one loop in and out as necessary.

To show the effect of pressure losses in various cycle passages on cycle efficiency, calculations were made for the following cases, which correspond to a 650°C turbine inlet temperature, a 32°C main compressor inlet temperature, and a 20°C cooling water temperature:

- Thermodynamic efficiency = 50.8%
- PCS with only heat exchangers' active core pressure losses (ideal pipes and plena) – cycle net efficiency = 48.7%
- PCS with only heat exchanger pressure losses that include plena (ideal pipes) – cycle net efficiency = 48.4%
- PCS with all pressure losses accounted for - cycle net efficiency = 48.0%

Table 2.9 Summary of layout weights

PCS Rating (MWe)	Approximate Weight (M.T.)
300	1050
150	580
50	152
20	65

This work has identified several areas for future work that may impact the PCS layout and need to be addressed. These are discussed in the future work recommendation section in Chapter 5.

2.12 References for Chapter 2

Atwood & Morrill Co., Inc., "Engineered Valve Products & Solutions", A&M 010304.

Baxi C., "Evaluation of Alternate Power Conversion Unit Designs for the GT-MHR," ICONE-14, Miami, July 2006

Carstens N., Hejzlar P., Driscoll M.J., "Dynamic Response and Safety Implications for Supercritical CO_2 Brayton Cycles Coupled to Gen-IV Reactors", MIT Canes Report, MIT-ANP-TR-114, July 2007.

Dostal V., Driscoll M.J., Hejzlar P., "A Supercritical Carbon Dioxide Cycle for Next Generation Nuclear Reactors", MIT CANES Report MIT-ANP-TR-100, March 2004

Gibbs J.P., Hejzlar P., Driscoll M.J., "Applicability of Supercritical CO_2 Power Conversion Systems to GEN IV Reactors", MIT CANES Report, MIT-GFR-037, September 2006.

Global Nuclear Energy Program (www.gnep.energy.gov)

Gong Y., Carstens N.A., Driscoll M.J., Matthews I.A., "Analysis of Radial Compressor Options for Supercritical CO_2 Power Conversion Cycles", MIT CANES Report MIT-GFR-034, June 2006.

Hejzlar P., Driscoll M.J., Gibbs J., Gong Y., Kao S., "Supercritical CO_2 Brayton Cycle for Medium Power Applications", MIT Report CANES-ANP-PR-117, April 2006.

Kuljian H., Nuclear Power Plant Design, A.S. Barnes and Co., Inc., Cranbury, New Jersey, 1968.

Minatsuki I., "Evaluation for Reasonableness of Power Conversion System Concepts in the Gas Turbine High Temperature Reactor (GTHTR300)", Mitsubishi Heavy Industries, Ltd., Proceedings of ICAPP, May 2007

Nuclear Power Plant Dukovany technical specifications (www.sujb.cz/docs/anex1.pdf)

Shade, N., "Enormous Power In A Small Package", Compressor Tech Two, January-February 2006

SOLID EDGE™ Version 17.00.02.04 © 2005 UGS

Stahle P., Driscoll M.J., Hejzlar P., "Supercritical CO2 Power Conversion System and Layout for 300 MWe Plant", MIT CANES Report MIT-GFR-025R, September 2005.

This page intentionally left blank

3 Recompression Cycle for Medium Power Applications

3.1 Introduction

The objective of this chapter is to evaluate the size and performance of the supercritical CO_2 recompression power cycle for medium power applications. The majority of the attention will be devoted to a reference 20 MWe power rating, but parametric studies will be applied to neighboring power ratings of 5-30 MWe. More detailed power conversion layouts will be discussed. In addition, sensitivity of cycle performance to off design conditions is presented. The sensitivity analyses discussed in this chapter for the recompression cycle, albeit for a considerably lower power rating than in Chapter 2, are directly extendable to the large power ratings.

3.2 Starting Reference Design and Key Constraints

The S-CO_2 cycle developed for 300 MWe Generation IV service [Dostal et al., 2004] has been selected as a starting reference design. The key parameters of the reference cycle are: turbine inlet temperature of 650 °C, compressor outlet pressure of 20 MPa, minimum compressor inlet pressure of 7.7 MPa (pressure ratio 2.6) and minimum compressor inlet temperature of 32°C. These parameters were selected based on cycle optimization with respect to the highest achievable efficiency considering plant capital cost and material limitations [Hejzlar, et. al., 2005]. Specifically, the temperature of 650 °C was chosen considering the compatibility of stainless steels with CO_2, where there is extensive British experience from the operation of 14 CO_2-cooled AGRs (although the effect of pressure on steel corrosion still needs to be determined), and considering significant deterioration of allowable stresses at temperatures above 650 °C. The highest cycle pressure of 20 MPa was selected because it offered a good compromise between cycle efficiency and material stresses and because it is well below current experience with supercritical water plants. Thus, the selected temperature of 650 °C allows the highest plant efficiency that is achievable with current materials. Also the selection of the lowest cycle temperature of 32 °C and pressure of 7.7 MPa was driven by

optimization of the cycle efficiency. Based on this reference design, the sizes of heat exchangers were obtained by linear scaling for the target power range between 5 and 30 MWe with the appropriate turbomachinery efficiencies for the lower power ratings.

Although high efficiency of the S-CO_2 cycle is possible for the 650 °C turbine inlet temperature using available materials, the design of a S-CO_2 cycle at 650°C and 20 MPa is challenging and may result in less reliable operation, as is often the case if the parameters are pushed close to the limits. Thus, a turbine inlet temperature of 550 °C is also investigated because this lower temperature allows the cycle to be paired with more Generation IV nuclear reactor designs, with the liquid sodium cooled reactor being a prime candidate. The higher turbine inlet temperatures can be reached with higher temperature nuclear reactors such as the very high temperature reactor, S-CO_2 cooled reactor (most likely a direct cycle with the PCS), or other higher temperature reactors. Although the cycle at lower turbine temperatures exhibits lower net cycle efficiency, stresses and creep rates of the components and corrosion rates are reduced, resulting in a longer operating lifetime. The compressor outlet pressure of 20 MPa is still being considered for the peak cycle pressure, but it can be increased for lower temperature designs to increase the operating efficiency as a tradeoff for the lower turbine inlet temperature. The power range between 5 and 30 MWe is still covered for the 550 °C turbine inlet case.

Having established the design envelope of key parameters on the high pressure cycle side, constraints on the low pressure cycle side needs to be established. These are primarily constrained by the ambient heat sink temperature. Because CO_2 has a relatively low critical temperature (30.98°C) and the precise cooling water conditions are unknown, it is wise to investigate an envelope of cooling water conditions and their effect on the cycle performance and operation. The lower cooling water temperatures allow a design to take advantage of the higher CO_2 density, thus lower compressor work and higher efficiency. The higher cooling water temperatures will result in slightly reduced net cycle efficiency, but also offer some advantages in the form of easier partial load control. Each of these topics will be discussed in further detail in their respective sections. After

cooling water temperature constraints are determined, the question as to which temperature to optimize the cycle design remains open. Therefore, one design assumes the cooling water temperature to be 20 °C to approximate an average and easily achievable temperature and another design assumes a cooling water temperature of 38 °C, to explore the effect of a heat sink temperature above the critical temperature of CO_2.

The possibility of condensation is an open issue with uncertainties on compressor performance in the two-phase region, and it does not need to be excluded a priori. However, this study is limited to transcritical (above critical point only) cycle operation, except for one case, where condensing cycle performance is evaluated.

3.1.2 General Assumptions

The assumptions of the models used for heat exchanger design and cycle analysis were listed in Chapter 2. Additional key assumptions carried throughout this chapter are:

- Generator efficiency = 98%
- Mechanical (couplings) efficiency = 99%
- Power electronics efficiency = 98%
- No piping losses on the water side of the precooler

However, it is important to note that some calculations were done using cycle efficiency (includes water pumping power) and others for net (electric) cycle efficiency. Net cycle efficiency includes the assumed efficiencies of the generator, mechanical couplings, and power electronics. Simply subtracting 2% from cycle efficiency to obtain net cycle efficiency is a good approximation. Other minor assumptions specific to each section are mentioned where appropriate.

3.3 High Performance Recompression S-CO_2 Cycle

3.2.1 Reference 20 MWe Design

The reference 20 MWe recompression cycle expands on the material covered in Chapter 2 which was primarily focused on the 300 MWe and larger power systems. The plant layout for the 20 MWe recompression cycle is covered in Chapter 2. This chapter primarily focuses on the performance considerations that went into the design and not necessarily the actual plant layout. However, this chapter does expand on what is covered in Chapter 2 for the 20 MWe recompression cycle and will refer to the figures in Chapter 2 pertaining to the plant layout.

Using, iteratively, the S-CO_2 cycle analysis code and Solid Edge software, a 20 MWe power conversion layout was created, as shown in Figures 2.18 through 2.21. Considering difficulties with maintenance, accommodation of thermal expansion and valve placement in an integral design, the distributed layout with easy access to all components was selected as a reference layout, as discussed in Chapter 2. The layout has two control valves for flow split adjustment located at compressor outlets. The final placement of necessary valves has not yet been complete and the pictured layouts represent one possibility for control, although it may not be the optimum. A check valve is placed on the compressor inlet line for startup (connection to startup line not shown). A bypass valve is needed to bypass the turbine in case of transients and for fast control. The check valve causes the most significant pressure loss in the piping because it occurs on the low pressure side of the system which is the motivator to limit valves on the low pressure side of the system as much as possible. The pressure drops through the control valves on the compressor outlets are negligible because the fractional pressure loss at 20 MPa is insignificant. The fractional pressure loss is defined as the local pressure loss divided by the system local pressure. All of the valve and pipe loss data were obtained from [Atwood and Morril] and [Idelchik, 1993], respectively.

Several key considerations for the design layout included whether to make the power conversion layout vertical or horizontal, flow direction through the heat exchangers,

pressure losses within the pipes, and the need to be able to remove the turbomachinery for maintenance. As seen in Figure 2.18, the horizontal layout is ideal due to the smaller axial bearing loading and easier component removal for maintenance. The person in the figure is 6 ft (1.83 m) tall and shows how small the layout is. For the 20 MWe design with the wound rotor generator, the approximate length of the power conversion unit with generator as seen in Figure 2.22 (not including the intermediate heat exchanger) is 10.7 meters, and only 8.3 meters when a permanent magnet generator is used. Placement of the intermediate heat exchanger for the indirect cycle is covered in Chapter 2 in Section 2.9. The length of the wound rotor generator is assumed to be 4.7 meters which is comparable to a 20 MWe Mermaid pod drive propulsion unit plus an exciter. Note that the generator takes about half of the overall PCS volume and if a permanent magnet generator were used the overall length would considerably decrease. A good comparison between the two generators (wound rotor and permanent magnet) can be seen by comparing Figure 2.22. The layout is approximately 2.8 meters wide and 3.2 meters high. The largest components are recuperators. Other arrangements with split recuperators (2 modules each) to reduce the height are also possible, but this layout was preferred because it allows easier access to valves and does not have an issue of non-uniform flow distribution between modules. The layout can also change slightly to accommodate the location of the intermediate heat exchanger or reactor, but the overall layout should be similar because the turbine inlet line and high temperature recuperator return line have several degrees of freedom and do not necessarily represent the best overall plant layout once the cycle layout is later updated, but can easily be changed to accommodate the remaining cycle components. For the indirect cycle the IHX will be within a containment to segregate the rest of the PCS from the radioactive flow while the direct cycle will require the entire PCS to be within a containment. The direct cycle has the challenge of handling the radioactive N-16 formation from the oxygen in CO_2 [Wang, 2005], but the amount formed will be less than the amount created in a typical boiling water reactor.

It is expected that the PCS will employ a turbine bypass and possibly a compressor bypass. The bypass allows high pressure fluid to be discharged to the low pressure side

of the system, thus, the mass flow to the IHX/reactor and turbine as well as reducing the cycle pressure ratio. From a thermal stress point of view the compressor bypass control is more desirable because of the milder fluid temperatures at the specific region in the cycle. If turbine bypass is chosen, the bypass control valve will have to be designed to regulate 650 °C or 550 °C fluid, depending on the turbine inlet temperature chosen for the cycle. Valves to accommodate temperatures this high in combination with high pressure are challenging to design, but commercially available. The physical plant layout is also a parameter for choosing the method of control; however, it is a minor issue. Depending on the desired ease of maintenance and valve placement constraints, one control method may be more desirable than the others. Ultimately, the most important analysis will have to be a dynamic control analysis and will have to be performed at a later time to determine the best form(s) of control [Carstens, et. al., 2007]. Currently, the layout shown in Figures 2.18 through 2.21 employs a bypass control between the high and low temperature recuperators. This is one bypass suggested by Dostal [Dostal, et. al., 2004] and is primarily shown for illustrative purposes only and does not suggest that it will be the only form of bypass control to be used by the PCS.

Because CO_2 has a low specific heat, it requires high flow rates to carry given heat rates, resulting in higher pressure drops. The pipes connecting the cycle components were sized to keep pressure losses to a minimum. Overall, the effect of pressure losses in piping and heat exchangers on cycle efficiency is approximately 1%, but if the pipes are poorly sized the pressure losses can result in an efficiency reduction of more than 10%. The pipe data for the individual sections of the 20 MWe layout are recorded in Table 3.1 with the pressure losses for the heat exchangers recorded in Table 3.2. The pipe sizes correspond to the inner diameter of the pipes. The turbomachinery casing sizes can be increased or decreased depending on the desired pipe size to be attached. However, no significant efficiency gains can be made by increasing the pipe sizes further. It is important to note that the heat exchanger plena are sized according to the pipes. The pipes can be increased to larger sizes, but this will not recover a significant amount of efficiency and will require the overall layout to increase due to the larger required plena.

Statepoints for the 650 °C and 550° turbine inlet temperature reference designs and both of the cooling water temperatures (20 °C and 38 °C) are summarized in Figures 3.1 through 3.4.

Table 3.1 Piping data for 20 MWe S-CO_2 recompression cycle

Pipe Section	**Dia. (m)**	**Length (m)**	**Area (m^2)**	**# of Bends**	**Pressure Drop (kPa)**
IHX to TUR	0.2540	1.0	0.0182	0	13.93
TUR to HTR	0.4064	0.36	0.1297	0	42.35
HTR to LTR	0.3556	1.93	0.0993	0	24.16
LTR to Split T	0.254	1.83	0.0507	1	**112.63**
Split T to Recomp	0.254	0.69	0.0507	0	4.52
Split T to PRE	0.254	2.74	0.0507	0	30.65
PRE to MC	0.1524	3.33	0.0182	2 (90)	46.55
MC to LTR	0.1524	1.17	0.0182	1 (45)	59.18
LTR to merge T	0.3556	0.56	0.0993	0	10.17
Recomp to merge T	0.2540	0.80	0.0507	1 (90)	4.55
Merge T to HTR	0.3556	1.37	0.0993	0	29.05

Total Pressure Loss in piping = 378 kPa

Table 3.2 Pressure losses in heat exchangers' plena

Recuperator	**Pressure Drop (kPa)**
High Temp Recuperator (hot active length)	94.79
High Temp Recuperator (cold active length)	72.57
HP Inlet	9.94
HP Outlet	40.66
LP Inlet	40.47
LP Outlet	13.36
Low Temp Recuperator (hot active length)	82.24
Low Temp Recuperator (cold active length)	17.08
HP Inlet	56.54
HP Outlet	7.03
LP Inlet	9.95
LP Outlet	111.69
Precooler (active length)	44.80
CO2 Inlet	30.42
CO2 Outlet	46.48
Reactor/IHX	500*

Total Recuperators and Precooler Pressure Loss = 678 kPa + 500 kPa Reactor/IHX
*500 kPa was assumed for reactor/IHX. The IHX could be most likely be designed with a smaller pressure loss

As mentioned in Chapter 2; one of the layout differences between the 550 °C and 650 °C turbine inlet temperature designs is that the volume allocation between the three heat exchangers changes, with the precooler experiencing the most noticeable changes, but the overall heat exchanger volume remains constant. The overall heat exchanger volume remaining constant for the lower turbine inlet temperature was a design choice: if the turbine inlet temperature were to be further reduced below 550 °C it would be beneficial to increase the total heat exchanger volumes, but the efficiency gains are negligible down to 550 °C if the heat exchanger volumes are increased. A breakdown of the volume/surface area allocation between the two main turbine inlet temperatures is shown in Table 3.3 and can also be seen in the statepoint diagrams shown in Figures 3.1 through 3.4.

Table 3.3 Total surface area

Turbine inlet temperature	650 °C			550 °C		
	LTR	HTR	PRE	LTR	HTR	PRE
Surface Area (m^2)	1,671	2,250	451	1,631	2,214	552
Area/volume (m^2/m^3)	741	741	705	866	872	689

*32°C main compressor inlet, 20°C cooling water

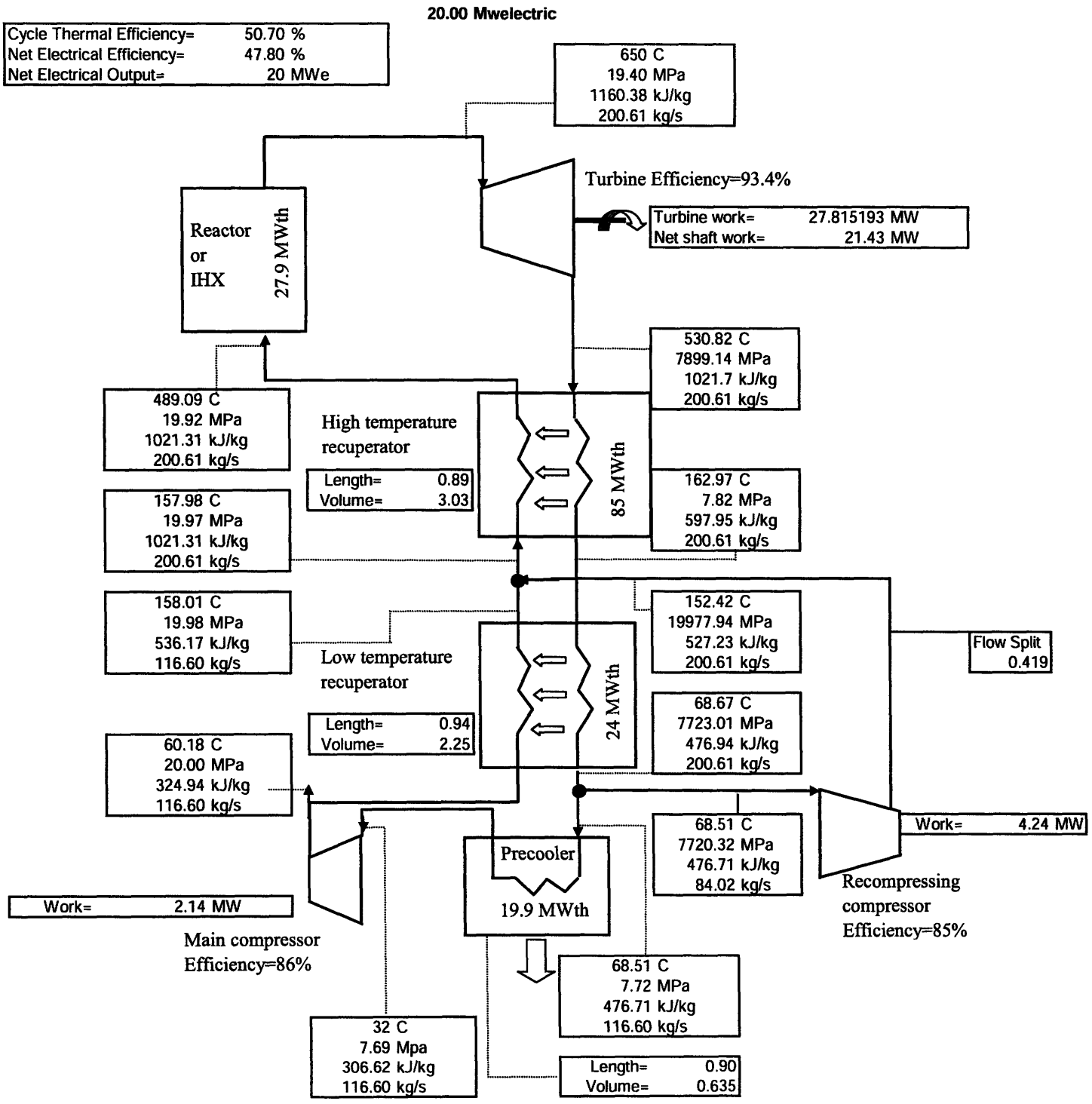

Figure 3.1 State points for a 20 MWe cycle
(650 °C turbine inlet, 32 °C main compressor inlet, 20 °C cooling water)

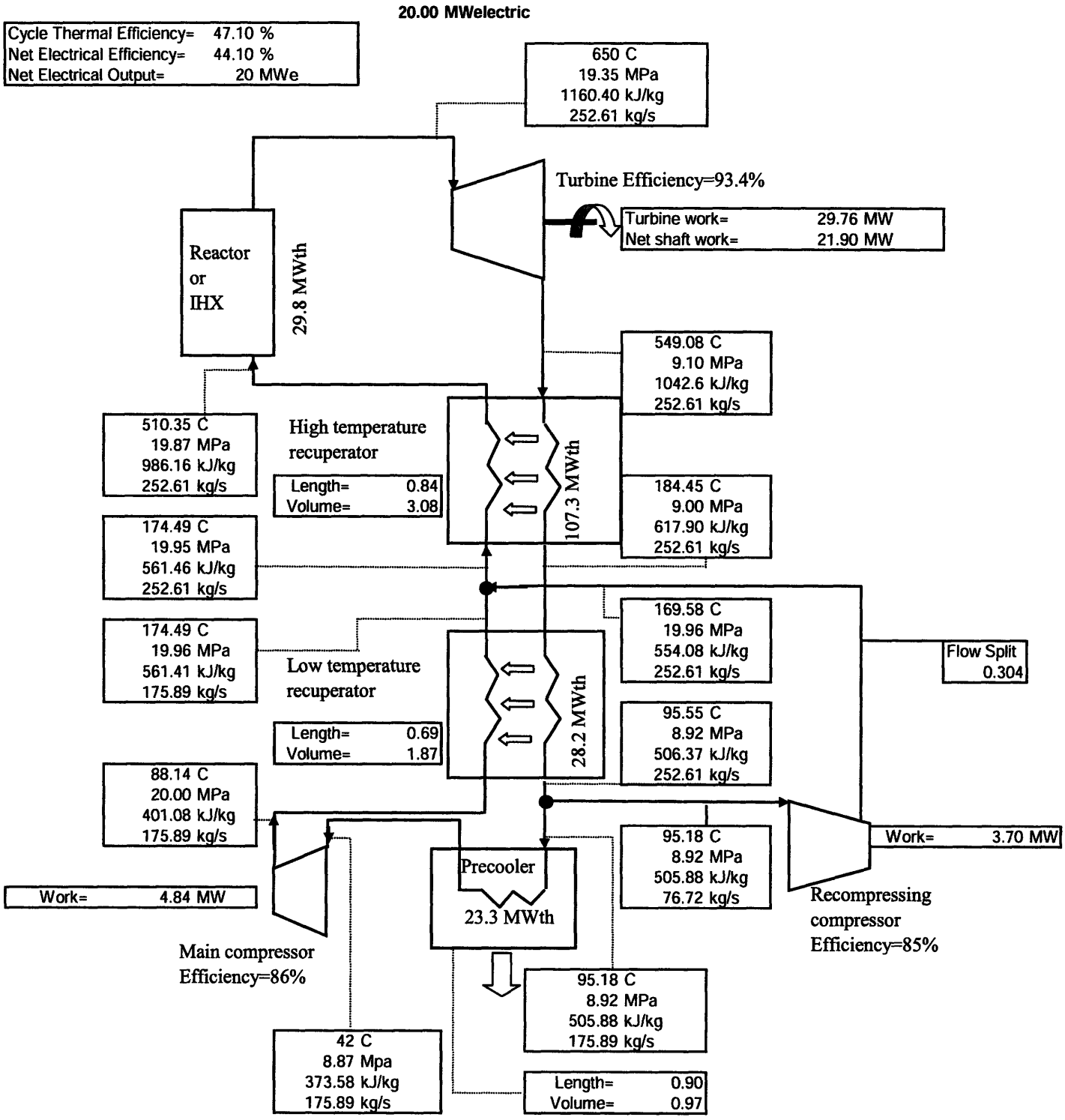

Figure 3.2 Statepoints for a 20 MWe cycle
(650 °C turbine inlet, 42 °C main compressor inlet, 38 °C cooling water)

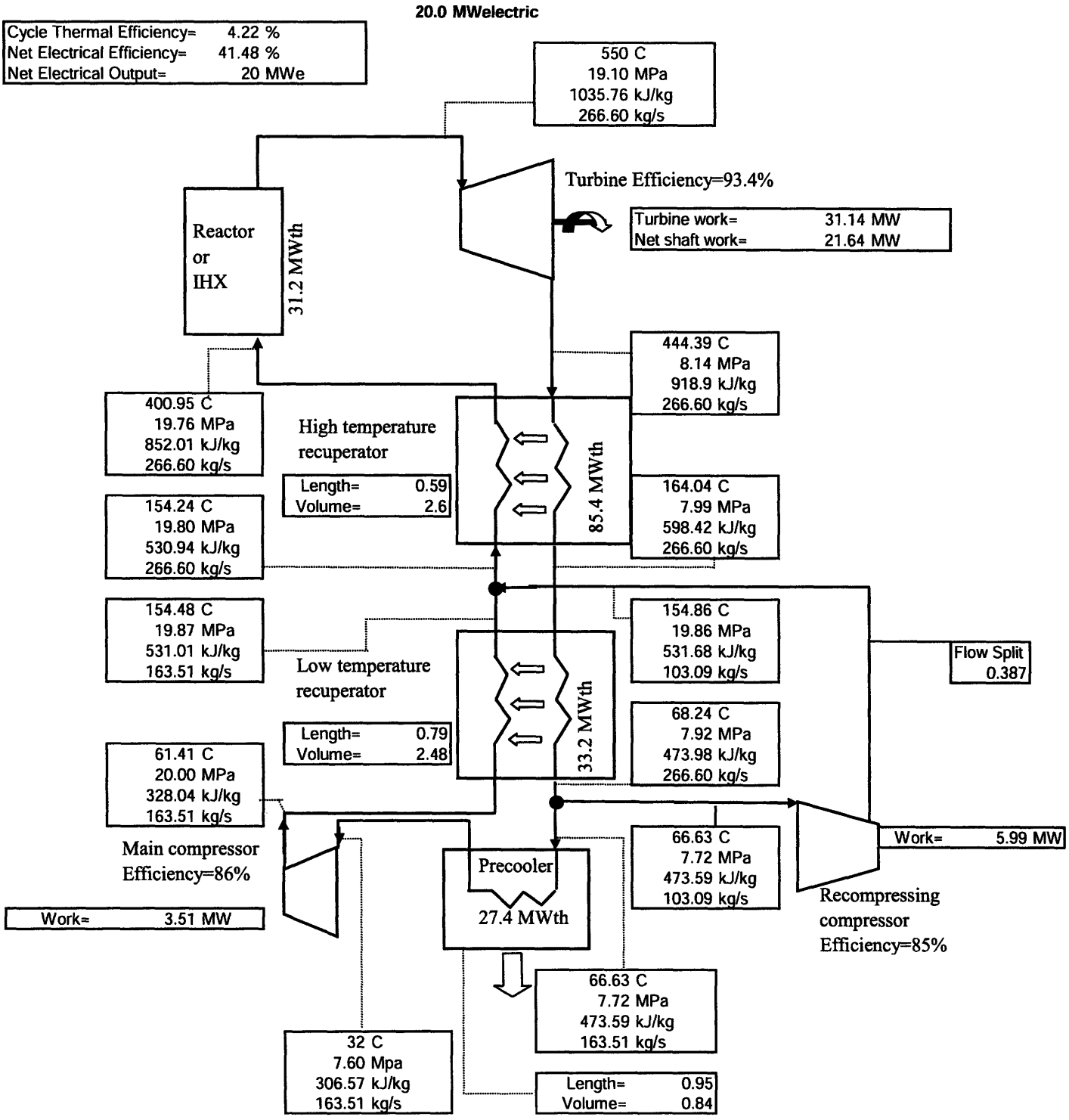

Figure 3.3 Statepoints for a 20 MWe cycle
(550 °C turbine inlet, 32 °C main compressor inlet, 20 °C cooling water)

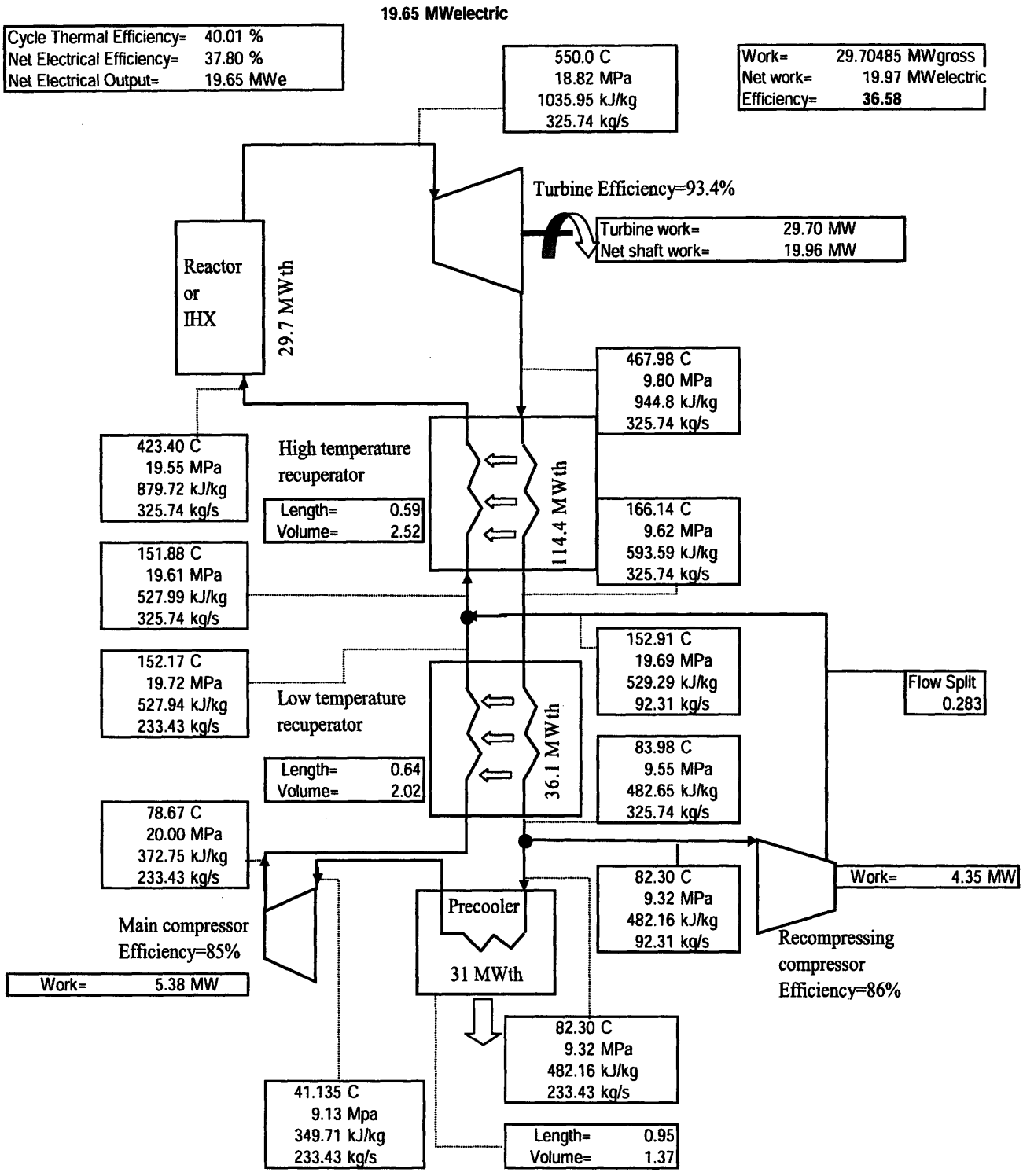

Figure 3.4 Statepoints for a 20 MWe cycle
(550 °C turbine inlet, 42 °C main compressor inlet, 38 °C cooling water)

3.4 Design for Various Power Ratings

The scope of the S-CO_2 analysis included investigating power ratings in the range of 5-30 MWe. Fortunately, the statepoints of each power cycle are nearly identical at each point for the full range of power ratings. However, the cycles do change slightly because the turbomachinery efficiency is slightly lower for lower power ratings and also the performance can vary depending on the pipe sizes chosen for each layout. The larger power ratings are slightly limited by the pipe sizes which can easily be connected to the 0.6m wide heat exchangers, but for the lower power ratings one can exploit their already smaller size and use larger pipes to improve performance and slightly negate the lower turbomachinery efficiencies. This results in a tradeoff between a physical layout footprint and the efficiency. The larger power ratings can also increase the pipe and valve size, but the larger valves and increased bend radii cause the layout to become more spread out. For very large power ratings (300 MWe) the pipes become a problem because such large pipe sizes (in proportion to the sizes used for the 20 MWe distributed layout) are not available unless the design is directed toward a modular approach like the one presented in Chapter 2. Although the pipe data are not shown in the comparison it is important to know that the flow areas were scaled linearly between power ratings. Depending on the results from the actual scaling, several pipe sizes were between two standard pipe sizes, and depending on how close the scaled pipe diameter was to an actual pipe diameter it was either rounded up or down to the closest standard pipe size. Complete pipe data for all power ratings can be found in Appendix A1.

A comparison of the recompression cycle for various power ratings is recorded in Table 3.4 for the cycle optimized for 20 °C. The important points to appreciate from the power rating tables are that the sizes and flow rates are linear and the overall performance is nearly constant across the power ratings. Changes of turbine efficiency with power rating were accounted for using the results of turbine performance estimates. Initially it was expected that the cycle efficiency would be lower for smaller power ratings due to the lower efficiency of the turbine. However, the cycle efficiencies are fairly constant throughout the power ranges because the lower power ratings can achieve similar turbomachinery efficiencies by being optimized at a higher shaft speed. The smaller

pressure drops in the heat exchangers at lower power ratings slightly negate the lower turbine efficiency. Also, the 10-15 MWe power ratings are the most efficient due to the best combination of pressure drop characteristics and turbine efficiency. However, the cycle efficiencies only vary 0.6% between both extremes. Figure 3.5 provides a rough approximation of how the heat exchanger sizes will increase with power rating by comparing a 6 ft. (1.83 m) tall man to the active core of the high temperature recuperator (HTR). It is important to note here that the data presented in Table 3.4 and Figure 3.5 were calculated for the cycle efficiency: to obtain the net cycle efficiency simply subtract about 2% (this corresponds to Table 3.4 and Figures 3.5, 3.6 and 3.8).

Table 3.4 Results for various power ratings

Cycle Data for Various Power Ratings					
Electrical power ($MW_{electric}$)	**5**	**10**	**15**	**20**	**30**
Maximum operating pressure (MPa)	20.0	20.0	20.0	20.0	20.0
Turbine Inlet Temp (°C)	650.0	650.0	650.0	650.0	650.0
Pressure Ratio	2.60	2.60	2.60	2.60	2.60
Reactor/IHX pressure drop (kPa)	500.0	500.0	500.0	500.0	500.0
Cycle Efficiency (%)	**49.34**	**49.64**	**49.59**	**49.16**	**49.04**
Turbine Efficiency (%)	92.2	93.0	93.3	93.5	93.7
Recomp Efficiency (%)	85.0	85.0	85.0	85.0	85.0
Main Comp Efficiency (%)	86.0	86.0	86.0	86.0	86.0
Main Comp Inlet Temp (°C)	32.0	32.0	32.0	32.0	32.0
Cooling water temp (°C)	20.0	20.0	20.0	20.0	20.0
Total Active Vol. of Hx (m^3)	1.25	2.51	3.76	5.01	7.52
Precooler Active Volume (m^3)	0.17	0.30	0.50	.601	0.99
HTR Active Volume (m^3)	0.63	1.27	1.90	2.54	3.80
LTR Active Volume (m^3)	0.50	1.0	1.49	1.88	2.98
Precooler active length (m)	1.0	1.0	1.0	1.0	1.0
HTR active length (m)	0.84	0.84	0.84	0.84	0.84
LTR active length (m)	0.79	0.79	0.79	0.79	0.79

The face area of the heat exchangers scales linearly with power rating, while their length remains constant, independent of power rating (this can easily be seen in Table 3.4 and Figure 3.5). A 6ft tall man is included in Figure 3.5 to provide a reference for the size of each heat exchanger core. For the reference design, the heat exchangers are not broken into modules due to their already small size. This is a significant

advantage in comparison with Generation IV applications, where larger power ratings dictate the use of multiple modules, resulting in a substantial reduction of power density. The possibility to have the recuperator in one module will make it possible to have a cycle with a higher power density and without the concern of non-uniform mass flow distribution among the modules, which could result in a reduction of recuperator effectiveness and thus cycle efficiency.

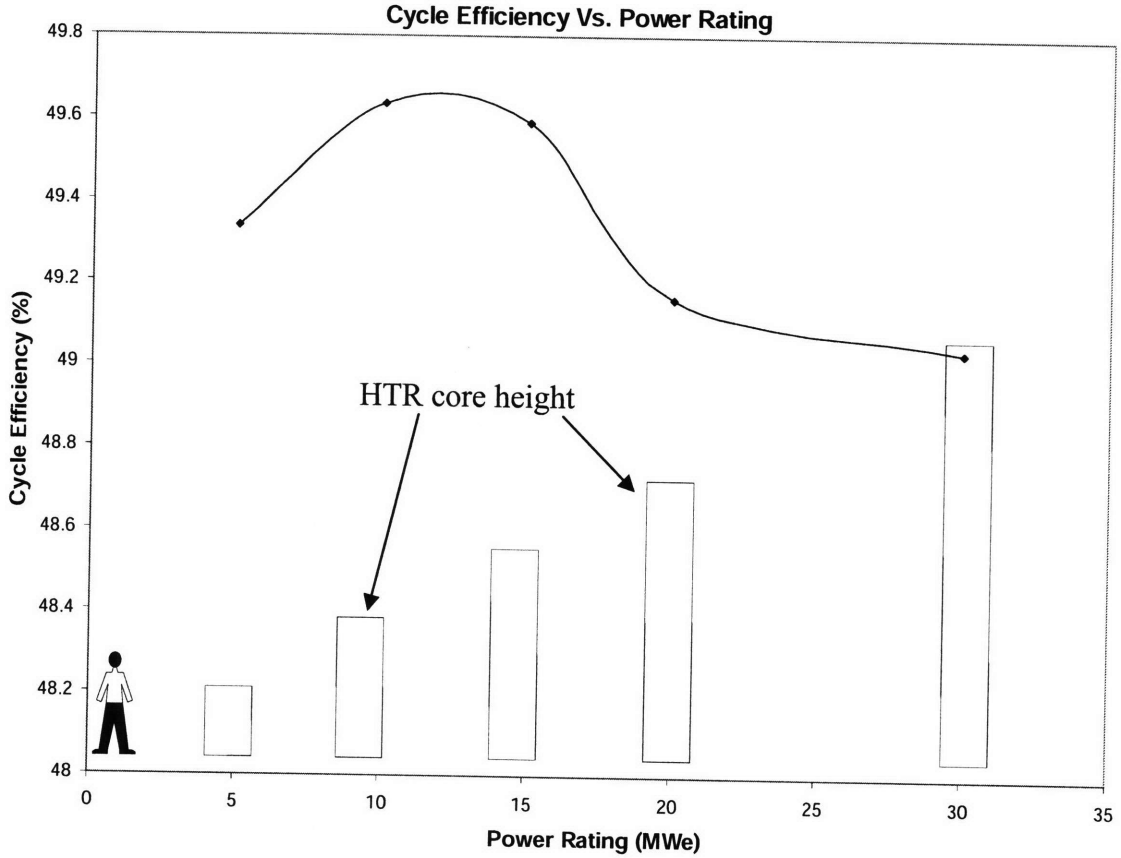

Figure 3.5 Cycle efficiency and HTR core size vs. power rating

3.5 Cycle Performance Sensitivity

Several sensitivity studies were completed to reveal areas for performance improvement, or performance degradation and areas where certain vulnerabilities may occur. All sensitivity studies were performed for a 20 MWe power rating with 20 °C cooling water temperature and a 32 °C main compressor inlet temperature and the reference layout described in the previous section, unless noted otherwise.

3.5.1 Turbine Inlet Temperature

Turbine inlet temperature is a very important cycle parameter because of its large effect on cycle efficiency and also on material selection. As the highest temperature in the cycle, the turbine inlet temperature improves the cycle efficiency but limits the stresses the materials can tolerate. Figure 3.6 shows the effect of the turbine inlet temperature on cycle efficiency for non-normalized electrical output. As expected, the relationship is nearly linear, which is due to the underlying thermodynamic efficiency. A 70% Carnot efficiency plot is also shown in Figure 3.6 to provide a comparison between the Carnot efficiency trend and the S-CO_2 cycle efficiency. If the thermal power is kept constant the recompression cycle exhibits a clean plot of cycle efficiency vs. turbine inlet temperature. However, as the turbine inlet temperature decreases, the thermal power must increase to maintain a constant 20 MWe output. This results in higher mass flow rates and causes the cycle efficiency to drop even more than just the reduction in thermodynamic efficiency, due to lower turbine inlet temperature. The higher mass flow rate substantially increases the piping and heat exchanger pressure losses. Higher thermal loads also require the piping and the total volume of heat exchangers to increase considerably. The plot for normalized electrical output starts off fairly linear but declines rapidly for lower turbine inlet temperatures. This is because the pressure losses really start to take over and deteriorate the cycle performance. Lowering the turbine inlet temperature from 550 °C to 450 °C requires the total heat exchanger volume to increase by 50%. Furthermore, it does not make sense to reduce the turbine inlet temperature below 400°C, because of the excessively large heat exchangers that would be necessary. The 350 °C turbine inlet temperature is not shown on the normalized thermal power plot for varying the turbine inlet temperature because it is extremely difficult to obtain 20 MWe at such a low temperature. Even with twice the total heat exchanger volume as the 550 °C case, the 350 °C cycle only exhibits 14% net cycle efficiency. If the thermal power is further increased, no more electric power is generated and the cycle efficiency only declines due to the huge piping losses. If lower than 400 °C temperatures are desired, modified designs with higher maximum cycle pressure would be possible. It is also very important to note here that Figure 3.6 shows results for cycle efficiency while Figure 3.7 has the results for net cycle efficiency.

Figure 3.6, however, is helpful because it shows the electrical output for fixed input criteria. For a fixed heat exchanger volume of 5.9 m^3 and thermal power of 44 MWth, the cycle will produce about 16 MWe for a 400°C turbine inlet temperature and 18.5 MWe for a 500 °C turbine inlet temperature, etc.

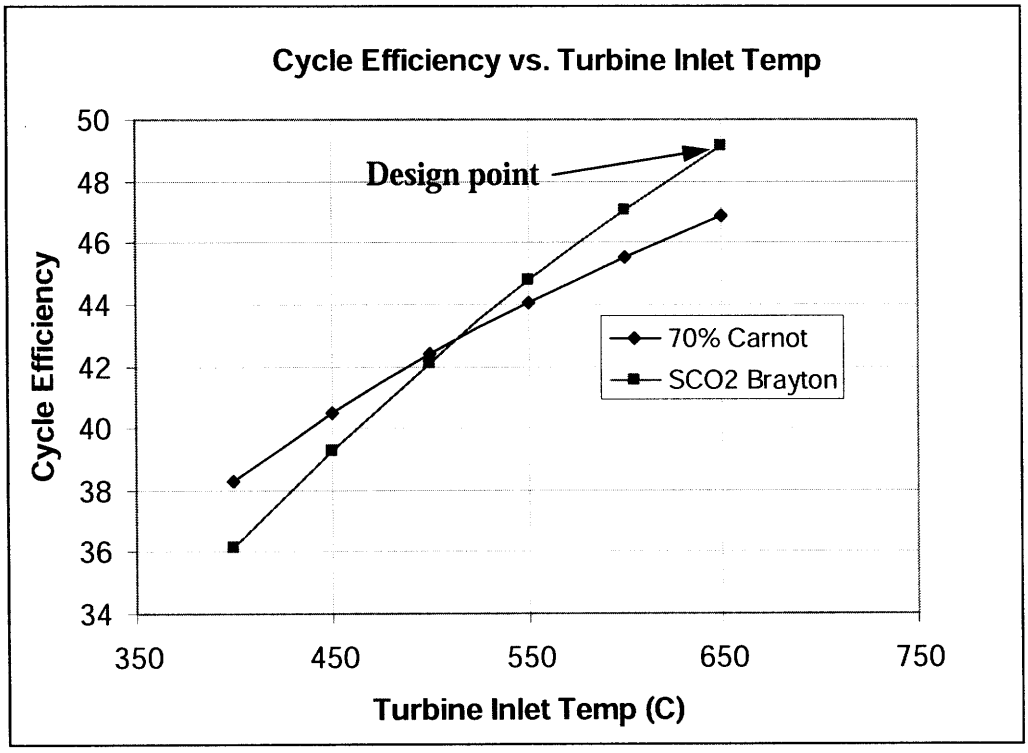

Figure 3.6 Cycle efficiency vs. turbine inlet temperature for non-constant electrical power output

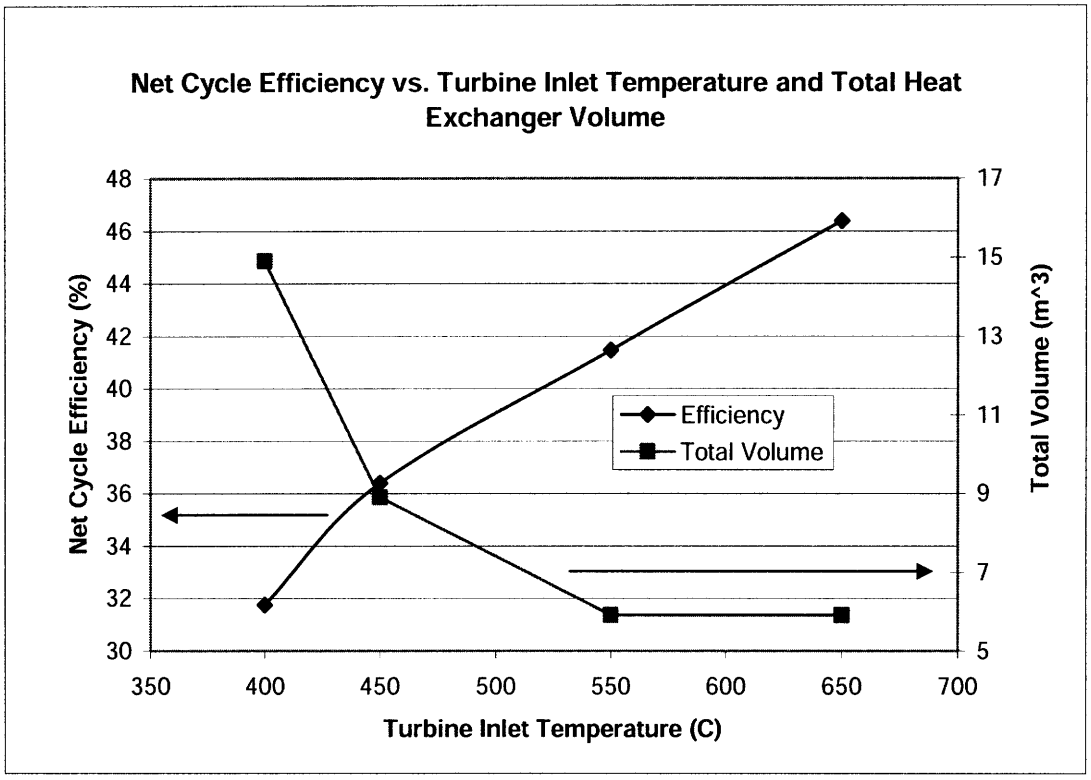

Figure 3.7 Net cycle efficiency and total heat exchanger volume vs. turbine inlet temperature for 20 MWe normalized electrical power

3.5.2 Peak Cycle Pressure

The effect of optimizing the peak cycle pressure was explored and the results are shown in Figure 3.8. The pressure analysis was done for a fully optimized 20 MWe cycle with 20 °C cooling water and a 32 °C main compressor inlet temperature. The data for Figure 3.8 have the same pipe sizes for each pressure and the low cycle pressure is fixed (pressure ratio changes). The current design conditions utilize a 20MPa compressor outlet pressure because it is a nice tradeoff between efficiency and materials limitations. The efficiency significantly drops off below 20 MPa, but about a 2% efficiency gain can be made by increasing the pressure to 23 MPa. Increasing the compressor outlet pressure helps by reducing the system fractional pressures drops and improves the cycle Carnotization. However, the effect of increasing the pressure starts to saturate above 25 MPa because only the reduction of the fractional pressure drops contributes to the efficiency improvement; the saturation is especially dominant in the 550 °C case above

23 MPa. The efficiency for lower turbine inlet temperatures will also drop off quicker because the required thermal power is already greater for the lower temperature, but the added mass flow rate due to the lower pressure makes the pressure losses increase further. Ideally, for low temperature and pressure configurations, the overall volume and pipe sizes should be increased to compensate for the two-fold mass flow rate increase. The reason for changing the effect of pressure on the cycle efficiency can be explained by the recompressing fraction [Dostal et. al, 2004]. It is desired to have a greater amount of mass flow going to the recompressing compressor. Although less work is needed to compress the CO_2 in the main compressor because it is so close to the critical point, sending more mass flow to the precooler causes higher heat extraction from the cycle thus reducing the cycle efficiency by not being at the optimum point of thermodynamic efficiency.

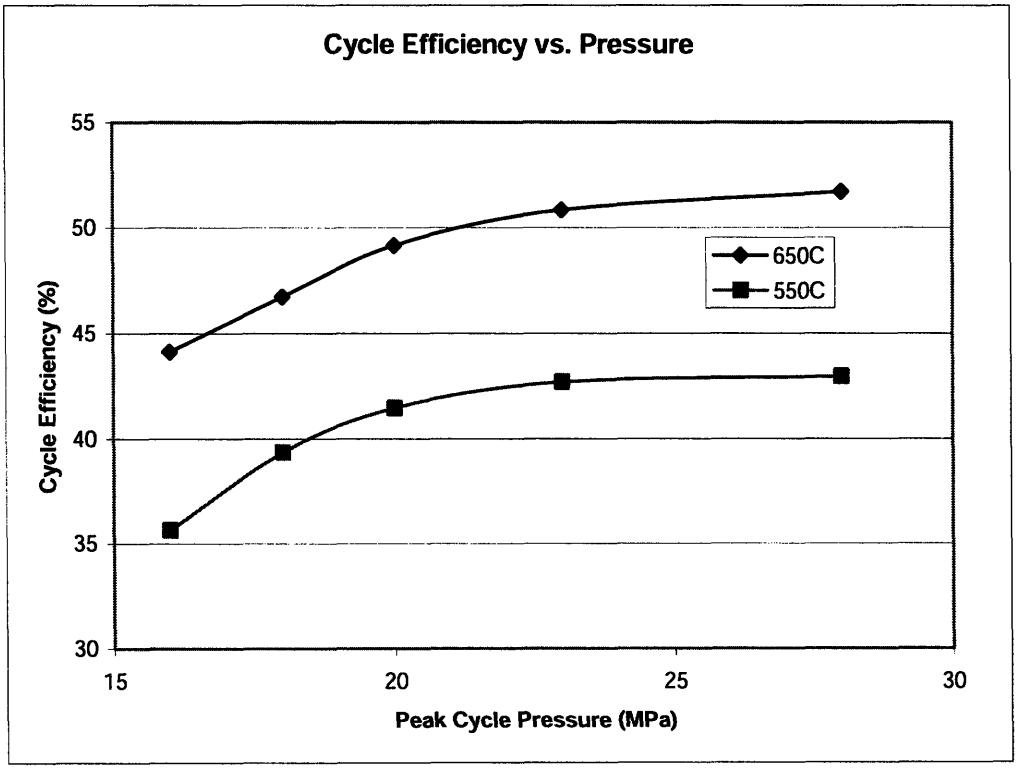

Figure 3.8 Cycle efficiency vs. peak cycle pressure

Because the cycle performance is largely a function of temperature and pressure, a tradeoff of reducing the turbine inlet temperature for better material properties while increasing the highest cycle pressure may be possible and should be investigated. For

example, a turbine inlet temperature of 550 °C still maintains attractive cycle efficiency (~43% at 23 MPa) and allows the materials to tolerate more stress. The possibility of increasing the peak cycle pressure to 23 MPa or higher, while keeping 550 °C as the turbine inlet temperature, should be explored to determine if any attractive gains can be made while maintaining component integrity when coupling the PCS to GNEP Generation IV reactors.

3.5.3 Turbomachinery Efficiency

The sensitivity of the cycle efficiency to turbomachinery efficiency is another important figure of merit, since machinery deteriorates with time. Furthermore, this sensitivity helps one to determine the selection of turbomachinery type in that it is easier to quickly determine the tradeoff of going to a different type of turbomachine with "x%" lower or higher efficiency. Figure 3.9 plots this sensitivity for all turbomachinery components and was generated in such a manner that each original piece of turbomachinery was held at its design condition, and only one was varied at a time to determine the effect that specific machine had on the system. The main compressor, recompressing compressor, and turbine design efficiencies are 85%, 86%, and 93.5%, respectively. Also, the parameters for this analysis are for a specific power rating that degrades with time. Therefore, as the turbomachinery efficiency is decreased, the electrical output also decreases due to the fixed thermal power. One important result to note is that the cycle efficiency will slowly decrease as the turbomachinery efficiency decreases. The analysis included turbomachinery efficiency decreasing to as low as 70%, but the possibility of this occurring is very unlikely. The actual range of interest is for turbomachinery efficiencies above 80% and the lower range was merely to demonstrate that there is no threshold where the cycle efficiency suddenly drops off and causes the cycle to stop working.

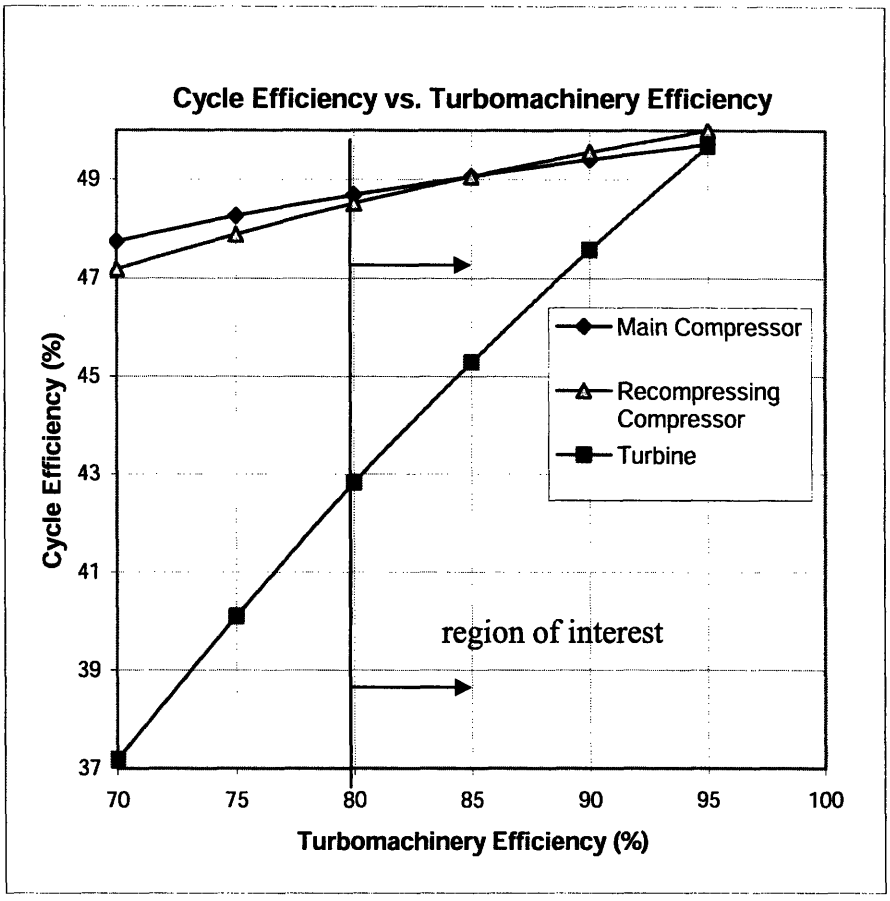

Figure 3.9 Cycle efficiency vs. turbomachinery efficiency

It can be observed that cycle efficiency is insensitive to compressor efficiencies. This is due to the low pumping power (low specific enthalpy rise) near the critical point associated with the high density. Hence, although radial compressors have lower efficiencies than axial machinery they can be used without significant penalty to take advantage of several other favorable characteristics. Cycle efficiency is more sensitive to turbine efficiency because of the larger specific enthalpy change; nevertheless, the penalty is not large. A turbine efficiency reduction of 5% reduces the cycle efficiency by approximately 1.5%. This is beneficial, since it allows the turbine to be built more rugged by increasing the tip clearance and still maintain very attractive cycle efficiency.

3.5.4 Heat Exchanger Channel Plugging

Although the chance of a heat exchanger becoming plugged is unlikely, a sensitivity study was performed to reveal how the cycle would perform if the heat exchangers were to become plugged, as illustrated by Figure 3.10. The analysis assumes equal plugging in each heat exchanger (all by the same percentage of channels), flow remains equally distributed among clean channels, and no heat conduction takes place between plugged channels. The analysis was performed for a fully optimized 38 °C cooling water temperature cycle with no initial plugging.

As expected, the cycle efficiency drops off due to increased plugging. The cycle efficiency reduction is a consequence of the much larger pressure drops through the heat exchangers and reduced heat exchanger effectiveness due to the smaller available heat transfer surface. Although the heat exchanger effectiveness is reduced, it is only a small contributor to the cycle efficiency reduction. As the plugging increases, the speed of the fluid traveling through the heat exchangers increases due to the decreased flow area, which results in higher friction and form losses. However, the increased pressure losses throughout the cycle are the dominant reason for the reduced efficiency. Also, as the plugging becomes more severe, more emphasis is placed on the precooler to reduce the CO_2 to the compressor inlet design temperature, as evident by the steadily increasing required pumping power and mass flow rate on the water side. All of these contribute to the decreasing net cycle efficiency.

One aspect of the cycle ruggedness can be extrapolated from the plot. If the heat exchangers were to become 25% plugged, the cycle only has an approximately 3.5% efficiency reduction. It is very important to note here that the plugging test was done with a fixed thermal power. If the cycle were to become plugged the electrical output of the cycle will be reduced. Therefore, when the initial plant is sized to accommodate the necessary loads, the various areas that can reduce the electrical output need to be accounted for to ensure the plant is appropriately oversized. Furthermore, if plugging were to occur, the heat exchangers could be cleaned by an acid solution or using high pressure air to blow out the channels. Protection against plugging can be further

enhanced by knowing the purity of the CO_2 in the PCS and using adequate strainers or an intermediate cooling loop on the cooling water side to prevent overly large particulates from entering the heat exchanger.

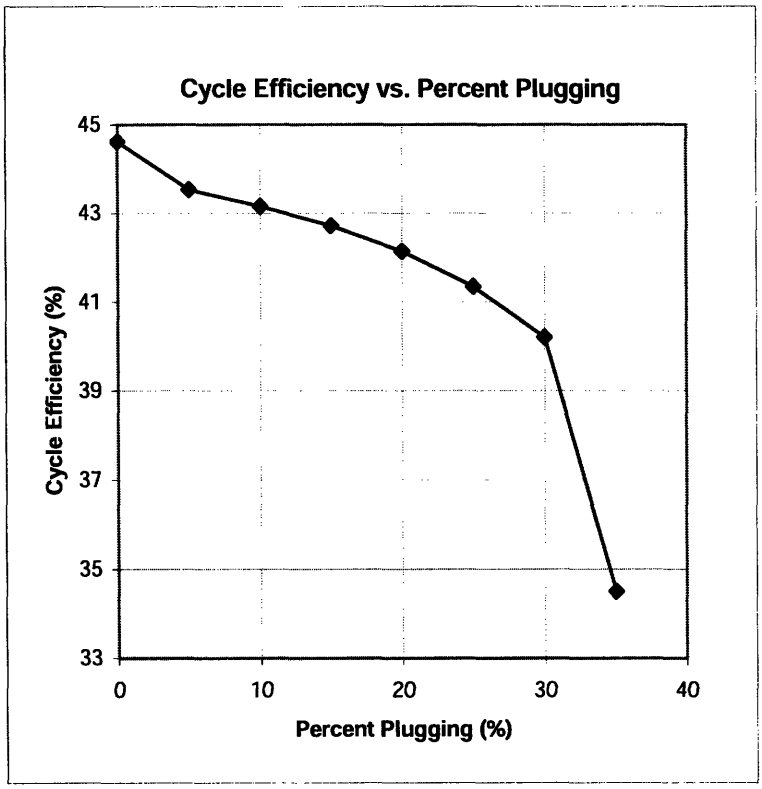

Figure 3.10 cycle efficiency vs. heat exchanger plugging

3.5.5 Heat Exchangers Total Volumes

The efficiency dependence on total volume of the heat exchangers was next investigated to determine if any significant efficiency gains could be achieved by slightly increasing the heat exchangers, or if any substantial reduction in volume could be made for only a minor penalty. The original volume of the heat exchangers was based on the 300 MWth S-CO_2 cycle proposed by Dostal (120 m^3 total volume) and linearly scaled down to the desired power rating. The recuperators were further shrunk when they were adapted to the zigzag channel configuration. It was found that no substantial gains would be made if the precooler also adopted the zigzag configuration [Hejzlar, et. al., 2006]. Figure 3.11

shows the relationship between cycle efficiency and total heat exchanger volume. The design point is at a very optimal location for a nice tradeoff between efficiency and size. Reducing the volume below the current design will cause the efficiency to quickly drop off due to the large increase in pressure drops within the heat exchangers from the higher fluid velocities and mass flow rates, but increasing the total size, an additional 40% volume will only gain slightly higher than 0.5% efficiency. Figure 3.11 is based on the same pipe sizes for each volume. However, the plot is not expected to change much because the pipes at the design condition (100% volume) did not experience appreciable pressure drops. Thus, if the pipes were to later be increased little gains would be made.

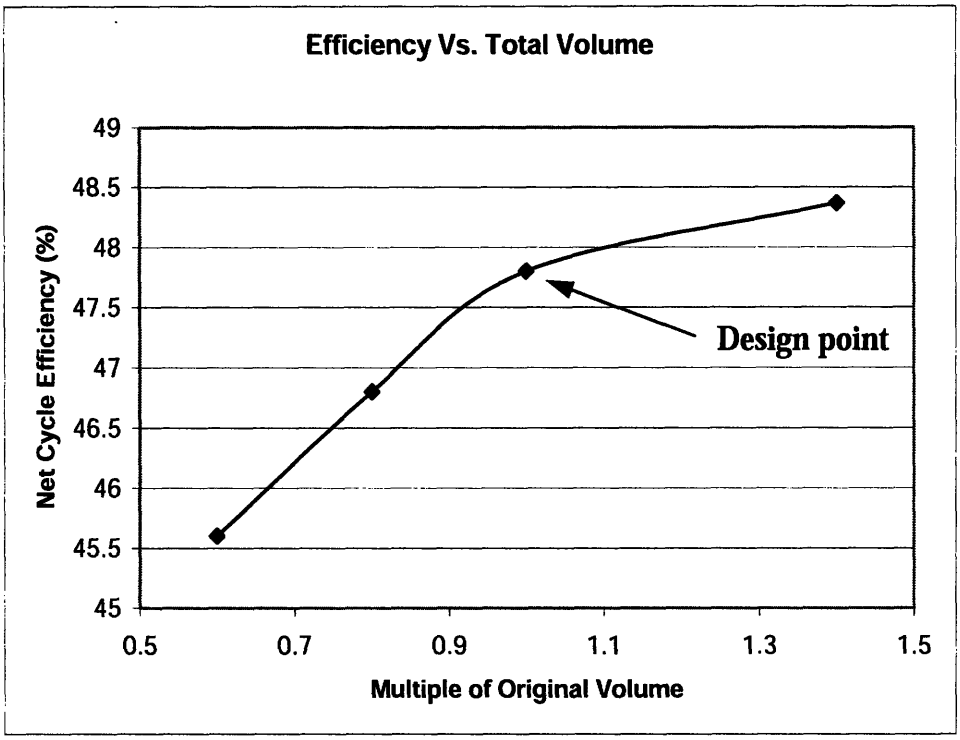

Figure 3.11 Cycle efficiency vs. total heat exchanger volume

Allowing for lower cycle efficiency in the hopes of reducing the overall footprint size, the possibility of trading efficiency for heat exchanger size was investigated and the results can be extrapolated from the above figure. This was done by optimizing each reduced volume cycle with the correct thermal power to maintain 20 MWe for a 32 °C main compressor inlet temperature (20°C cooling water temperature). The total volume of the heat exchangers can be reduced approximately to 60% of the original volume for a 2% efficiency tradeoff. The effect of this volume reduction translates to an overall length

reduction of approximately 2.0 meters based on the layouts presented in Chapter 2. Below 60% volume reduction the cycle will not function without other major changes, such as large pipe size increases. As the total volume is decreased, more and more heat is rejected through the precooler, thus requiring a larger pump. Below 60% of the original volume the pumpwork requirement substantially increases and can easily be higher than 1000 kW. Physically, a pump of this size is not practical. Furthermore, although not investigated for the reduced volume cycles, if the heat exchangers were to become fouled or plugged at the already reduced volumes the cycle may have serious problems and an unacceptably large efficiency decline.

It is important to point out that this analysis was done for a 32 °C main compressor inlet temperature (20 °C cooling water temperature). If it was done for a 42 °C main compressor inlet temperature (38 °C cooling water temperature) the volumes could not be reduced as much due to the higher required mass flow rates to maintain the desired electrical output. This also is an indication that if the peak cycle pressure was lowered, the performance would be even poorer, and the volume could not be reduced as much. Actually, for lower pressures the volumes may actually have to be increased for the cycle to operate at higher cooling water temperatures. Therefore, because not too much space can be saved by trading efficiency for volume and because of the potential unknown vulnerabilities, the volume reduction method should not be considered and other methods should be investigated to shrink the size of the PCS.

3.5.6 Sensitivity to Heat Exchanger Fouling

Even though appreciable fouling is not expected in S-CO_2 cycle heat exchangers because stainless steel and titanium are used as structural materials for the recuperators and precooler, respectively, it cannot be excluded, and potential degradation of the cycle performance from fouling needs to be evaluated. Fouling is a different mechanism than the plugging evaluated earlier, since performance degradation occurs not only because of the reduced channel flow area, but also due to increased heat transfer resistance, both effects being the consequence of the oxide growth.

Using the calculation models for printed circuit heat exchangers that incorporate the effect of oxide layers, sensitivity of the simple S-CO_2 cycle performance was evaluated to oxide buildup in the recuperator and precooler. The reference recompression cycle with turbine inlet temperature of 550°C, the highest pressure of 20 MPa, and the lowest cycle temperature of 32 °C (20 °C cooling water temperature) was used for the sensitivity study. Oxide layer thickness on both the hot and cold sides was varied between 0 and 100 microns, because it is assumed that spalling will occur for thicknesses greater than 100 microns. A value of 25 W/m-K was used for the oxide conductivity in all of the calculations.

Performance degradation (in terms of net electrical efficiency) with fouling of each heat exchanger as well as for all heat exchangers together for the recompression cycle is shown in Figure 3.12. There are four lines: HTR signifies changes of oxide thickness in the high temperature recuperator only (on both sides) while maintaining the precooler and low temperature recuperator clean, LTR models sensitivity to fouling in the low temperature recuperator only, PRE models sensitivity of cycle net efficiency to fouling in the precooler only (on both the CO_2 and water sides) and HTR+LTR+PRE assumes that fouling occurs simultaneously in all heat exchangers.

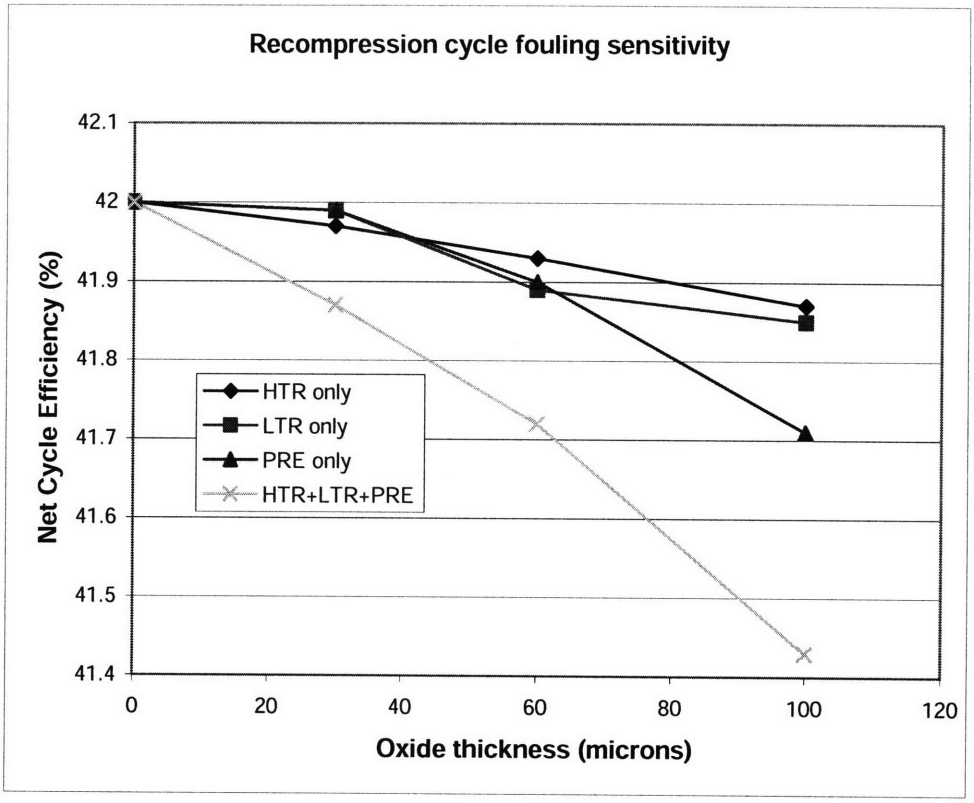

Figure 3.12 Sensitivity to heat exchanger fouling

The high temperature recuperator (HTR) fouling has less of an effect than that of the low temperature recuperator (LTR). Even for a conservatively large oxide thickness of 100 microns in the recuperators, the effect on cycle efficiency is small. This is because the overall heat transfer coefficient is controlled by fluid heat transfer and, if the resistance from the clean heat transfer coefficient is smaller than the oxide resistance, the effect of added oxide on the heat exchanger performance is negligible. The precooler (PRE) exhibits a more pronounced efficiency decrease after a 60 micron oxide layer is accumulated. This is because at about 60 microns, fouling resistance on the water side becomes comparable to that of the water heat transfer coefficient and becomes responsible for a reduced heat transfer rate to water. To overcome this reduction, water flow rate through the precooler has to be increased significantly, resulting in larger pumping power, which is also exacerbated by larger precooler pressure drop due to reduced channel flow area and hydraulic diameter. Moreover, it is important to note that the original volume of the precooler had to be increased from 0.6 m^3 to 0.8 m^3, because a 0.6 m^3 volume requires, for a thick oxide layer, extremely large pumping power and

results in very low efficiency: below 20%. Thus, it is important to oversize the precooler to make allowance for fouling, since performance of the cycle becomes very sensitive to precooler pumping power (on the water side) if the precooler is designed without margins. This is very easy to do without appreciable space penalty since the precooler is a very small heat exchanger and even a 50% increase of its size does not impact the overall footprint appreciably.

Therefore, even though one would expect the recuperator fouling to be more important, it is the precooler fouling that needs to be paid attention to. If corrosion tests confirm that oxide thickness can be kept below 60 microns, the effect of fouling will be "negligible"; for larger oxide thicknesses, a slightly larger precooler could easily overcome the issue of performance degradation from precooler fouling.

3.6 Chapter Summary and Conclusions

This chapter was an extension onto Chapter 2 and focused on the 20 MWe recompression cycle, going more in depth into its layout and operating conditions, and on to a sensitivity analysis to determine its potential weaknesses. A range of power ratings was also explored to determine if the cycle would experience any major penalties for dropping to low ratings. The primary driver for lower efficiencies at the lower power ratings is the typically lower turbomachinery efficiencies at the lower power ratings. If the shaft speed were allowed to be increase substantially for the lower powers then the performance should be able to improve further. Regardless, the design can achieve attractive efficiencies if the correct parameters are chosen: namely, turbine inlet temperature above 500 °C and compressor outlet pressure 20 MPa or above. The cooling water temperature makes a difference, but not using the coolest medium will not make an appreciable contribution to penalizing the performance compared to the turbine inlet temperature and pressure.

Overall, the sensitivity studies suggest that S-CO_2 PCS performance is not very sensitive to degradation and achieves attractive efficiencies over a broad range of conditions for

correctly sized original components. The most important parameter affecting cycle performance is turbine inlet temperature. The recompression S-CO_2 cycle is better suited for higher turbine inlet temperatures and suffers significant efficiency reduction for turbine inlet temperatures below 400 °C due to increased penalties from large pressure drops. This is not surprising and agrees with the earlier findings that the S-CO_2 cycle becomes more attractive than the Rankine cycle in terms of efficiency for temperatures above 500 °C. However, if high efficiency is not the overriding objective the recompression S-CO_2 cycle can be designed for lower turbine inlet temperatures down to 400 °C and still achieve attractive efficiencies. Reducing turbine inlet temperature further is not recommended, even though a design at 350 °C could most likely be developed at pressures higher than 20 MPa.

3.7 References for Chapter 3

Atwood & Morrill Co., Inc., "Engineered Valve Products & Solutions", A&M 010304.

Carstens N., Hejzlar P., Driscoll M.J., "Dynamic Response and Safety Implications for Supercritical CO_2 Brayton Cycles Coupled to Gen-IV Reactors", MIT Canes Report, MIT-ANP-TR-114, July 2007.

Dostal V. M.J. Driscoll and P. Hejzlar, ""A Supercritical Carbon Dioxide Cycle for Next Generation Nuclear Reactors", MIT CANES Report MIT-ANP-TR-100, March 2004.

Hejzlar P., Driscoll M.J., Gibbs J., Gong Y., Kao S., "Supercritical CO_2 Brayton Cycle for Medium Power Applications", MIT Report CANES-ANP-PR-117, April 2006.

Hejzlar P., et. al., "Assessment of Gas Cooled Fast Reactor with Indirect Supercritical CO_2 Cycle", *Nuclear Engineering and Technology*, Vol. 38 No.2, Special Issue on ICAPP, 2005.

Idelchik, I.E., Handbook of Hydraulic Resistance, 3rd ed., CRC Press, p. 752, 1993

Wang Y., "Estimation of N-16 Dose Rate for Direct Cycle CO_2 Gas Cooled Fast Reactors," MIT-GFR-032, Aug. 2005.

4 High Temperature Simple S-CO_2 Cycle for Medium Power Applications

4.1 Introduction

Deemphasizing the achievement of very high efficiency in favor of compactness opens the possibility to use a simple S-CO_2 cycle instead of the recompression S-CO_2 cycle. The primary goals are to achieve the minimum size, maximum simplicity and ruggedness while attaining still attractive net cycle efficiency above 35%. The simple S-CO_2 cycle eliminates the recompressing compressor, the flow split and associated piping and flow split control, and the low temperature recuperator. Thus, the only components needed are a turbine, compressor, precooler, and recuperator. Moreover, the recuperator volume is significantly smaller than the total volume of high temperature and low temperature recuperators, as discussed and shown in Chapter 3. To evaluate the potential of this simple cycle for medium power application it was calculated with the same criteria as the recompression cycle so that a consistent comparison between the two cycles could easily be made. The simple cycle was also compared to the performance of a recompressing cycle with smaller heat exchangers to determine if the recompressing cycle can compete for minimum occupied area by simply reducing the total volume of the recuperators. All analyses of the simple S-CO_2 cycle were performed using the computer model briefly described in Chapter 1.

4.2 Reference 20 MWe Design

The same considerations were given to the simple cycle as to the recompression cycle; however, the main difference is that 550°C turbine inlet temperature was adopted as the high cycle temperature and is used in most of the calculations. This new reference turbine inlet temperature is used because it is less challenging for materials and because it is compatible with most Generation IV reactors. As seen in Table 4.1, the 550°C turbine inlet temperature cycle exhibits approximately 3.5% lower efficiency than the 650°C cycle. Two versions of the simple cycle were developed: (1) long recuperator arrangement where the recuperator consists of one long module (designated simple cycle)

and (2) short parallel arrangement (designated simple parallel cycle), where the recuperator is split into two parallel units. Preliminary 3-D depictions of the simple S-CO_2 cycle in both arrangements were drawn in Solid Edge [SOLID EDGE]. The drawings include the approximate size of a permanent magnet generator [Shade, 2006] and the necessary bypass and control valves for the simple and parallel-simple cycles. The valve and pipe data were obtained from [Atwood and Morrill] and [Idelchik, 1993], respectively. The turbomachinery efficiencies were obtained from [Gong, et. al., 2006]. However, the bypass valves are merely to show the size and possible locations of the control valves. Further studies will have to be performed to determine the actual control method and valve locations. The layouts in vertical arrangements can be seen in Figures 4.1 through 4.6. Component numbering is given in Table 4.2 and the dimensions are recorded in Table 4.5. The results for the simple cycle comparing the single recuperator design to the parallel recuperator design are recorded in Tables 4.3 and 4.4.

It needs to be noted that all the calculations for the simple cycle were done for the net cycle efficiency and include the assumed values for the mechanical efficiency of the couplings, generator efficiency, and the power electronics efficiency. Also, because the design process is an iterative one, several different turbomachinery efficiencies were used at different stages of calculations. However, the values never varied more than 0.2% for the turbine efficiency and 1% for the compressor efficiency and the results for both cases agree within +/- 1% of each other.

Table 4.1 Comparison of simple cycle for 32°C compressor inlet temperature

		550°C	650°C
Electrical power ($MW_{electric}$)		20.0	20.0
Maximum operating pressure (MPa)		20.0	20.0
Turbine Inlet Temp (°C)		550.0	650.0
Pressure Ratio		2.60	2.60
*Reactor/IHX pressure drop (kPa)		500.0	500.0
Net Cycle Efficiency (%)		**36.1**	**39.7**
Turbine Efficiency (%)		91.4	91.2
Compressor Efficiency (%)		90.0	90.0
*Mechanical Efficiency (couplings) (%)		99.0	99.0
*Generator Efficiency (%)		98.0	98.0
*Frequency Converter Efficiency (%)		98.0	98.0
Main Comp Inlet Temp (°C)		32.0	32.0
Cooling Water Temp (°C)		20.0	20.0
Total Vol. of HXs (m^3)		2.60	2.60
Precooler Volume (m^3)		0.87	0.73
Recuperator Volume (m^3)		1.73	1.87
Precooler Active Length (m)		0.60	0.84
Recuperator Active Length (m)		0.74	0.65

*Assumed values

Table 4.2 Simple cycle components

#	**Component**
1	Generator with casing
2	Recuperator
3	Precooler
4	Turbine
5	Compressor
6	Turbine Inlet (from IHX/Reactor)
7	Recuperator Outlet (to IHX/Reactor)
8	Cooling Water Inlet
9	Cooling Water outlet

Table 4.3 Comparison of simple cycle for 32°C main compressor inlet temperature

		Single	Parallel
Electrical power ($MW_{electric}$)		20.0	20.0
Maximum operating pressure (MPa)		20.0	20.0
Turbine Inlet Temp (°C)		550.0	550.0
Pressure Ratio		2.60	2.60
*Reactor/IHX pressure drop (kPa)		500.0	500.0
Net Cycle Efficiency (%)		**36.1**	**36.1**
Turbine Efficiency (%)		91.4	91.4
Compressor Efficiency (%)		90.0	90.0
*Mechanical Efficiency (couplings) (%)		99.0	99.0
*Generator Efficiency (%)		98.0	98.0
*Frequency Converter Efficiency (%)		98.0	98.0
Main Comp Inlet Temp (°C)		32.0	32.0
Cooling Water Temp (°C)		20.0	20.0
Total Vol. of Heat Exchangers (m^3)		2.60	2.60
Precooler Volume (m^3)		0.87	0.87
Recuperator Volume (m^3)		1.73	1.73
Precooler Active Length (m)		0.60	0.60
Recuperator Active Length (m)		0.74	0.74

*Assumed values

The main difference between the simple S-CO_2 designs is that the parallel-simple design uses two parallel recuperators instead of one. The recuperator from the simple cycle was basically cut in half and now the turbine discharges the flow to two parallel recuperators. Using identical pipes for each recuperator, the flow split is assumed to be equal between the two recuperators. If the parallel-simple design is chosen for further review the possible effect of flow maldistribution would have to be analyzed in more detail. The parallel-simple design reduces the overall height of the heat exchangers, but makes the layout a little wider. Including the generator in the height measurements, the parallel-simple cycle is approximately the same height as the simple cycle. Not considering the generator, the height of the parallel-simple cycle is slightly taller than half the height of the simple cycle. The dimensions of each layout can be seen in Tables 4.5 and 4.6. The dimensions do not include the turbine bypass valve or the valve stems. It was expected that the parallel recuperator layout would exhibit slightly higher efficiency than the single recuperator layout due to the smaller pipe losses, but as it turns out the two cycles are nearly identical due to the small pipe loss savings. The cycle efficiency for both the simple and parallel-simple cycles can be further increased by using a turbine with a full

diffuser. A diffuser-less turbine was used to reduce the overall height of the cycle, but the tradeoff for efficiency needs to be carefully considered. Furthermore, the permanent magnet generator is sensitive to temperature; therefore, if a turbine with a full diffuser was used the generator would be further away from the inlet plenum of the recuperator and will be operating in a lower ambient temperature. The specifics of the permanent magnet generator are discussed in Chapter 1.

Because the performance between the simple and parallel-simple cycle is nearly identical, the simple cycle was chosen for the remainder of the study. Cycle state points for the 20°C and 38°C cooling water temperatures are shown in Figures 4.7 and 4.8, respectively.

Table 4.4. Comparison of simple cycle for 42°C main compressor inlet temperature

		Single	Parallel
Electrical power ($MW_{electric}$)		20.0	20.0
Maximum operating pressure (MPa)		20.0	20.0
Turbine Inlet Temp (°C)		550.0	550.0
Pressure Ratio		2.60	2.60
*Reactor/IHX pressure drop (kPa)		500.0	500.0
Net Cycle Efficiency (%)		**33.8**	**33.8**
Turbine Efficiency (%)		91.2	91.2
Compressor Efficiency (%)		89.0	89.0
*Mechanical Efficiency (couplings) (%)		99.0	99.0
*Generator Efficiency (%)		98.0	98.0
*Frequency Converter Efficiency (%)		98.0	98.0
Main Comp Inlet Temp (°C)		42.0	42.0
Cooling water temp (°C)		38.0	38.0
Total Vol. of HX (m^3)		2.60	2.60
Precooler Volume (m^3)		0.93	0.93
Recuperator Volume (m^3)		1.67	1.67
Precooler Active Length (m)		0.95	0.95
Recuperator Active Length (m)		0.64	0.64

*Assumed values

Table 4.5 20 MWe Simple layout dimensions

Height (top of gen.)	Height (w/o gen.)	Width	Length
5.13m	5.0m	1.68m	3.25m

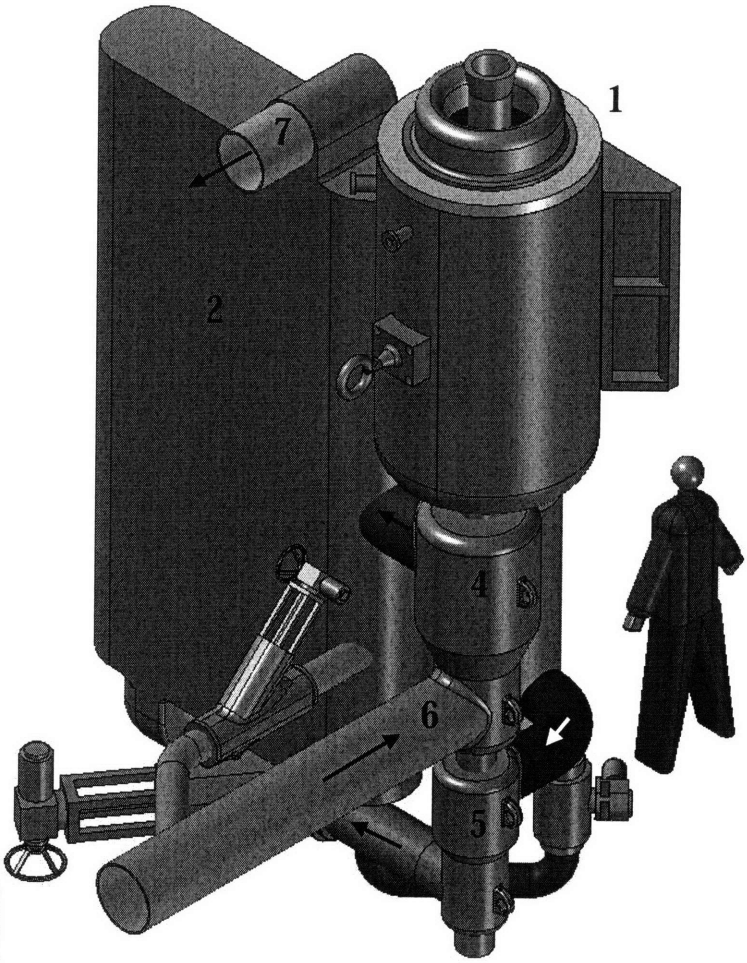

Figure 4.1 Simple S-CO_2 (front isometric)

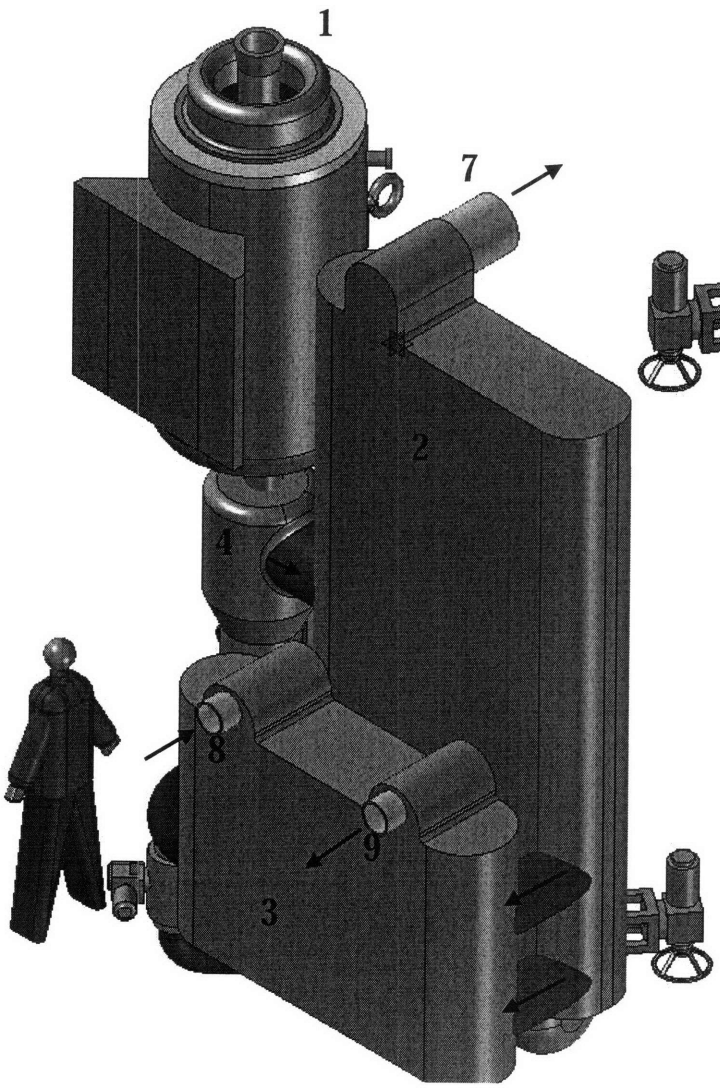

Figure 4.2 Simple S-CO_2 (back isometric)

Table 4.6 20 MWe parallel-simple layout dimensions

Height (top of gen.)	Height (w/o gen.)	Width	Length
5.1m	3.5m	2.1m	3.5m
16.7ft	11.5ft	6.9ft	11.5ft

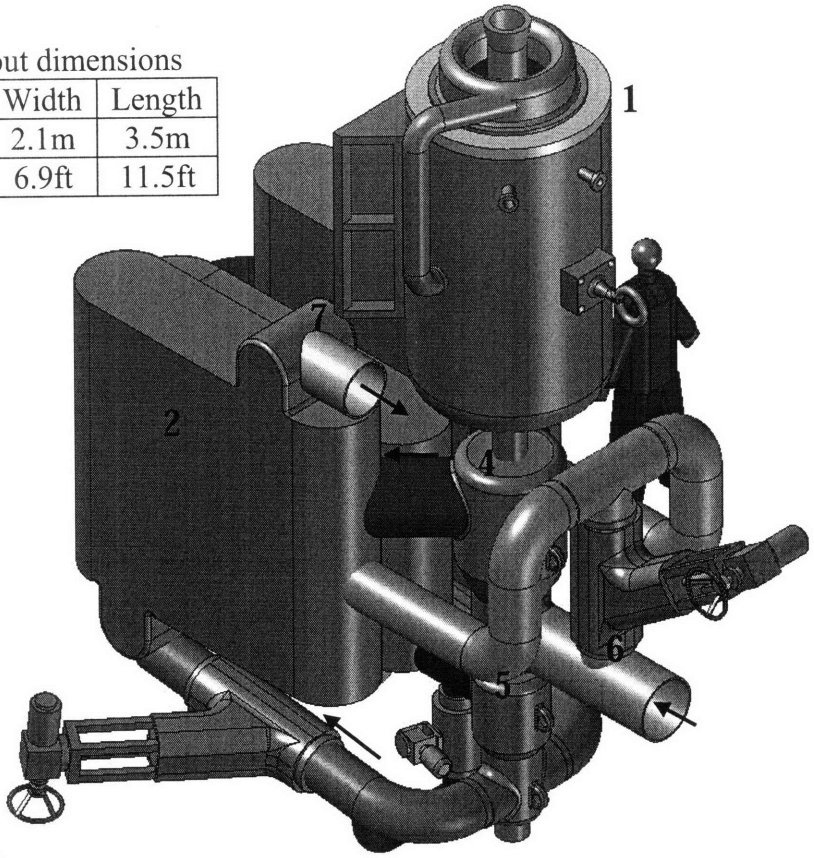

Figure 4.3 Parallel-simple S-CO_2 (front isometric) (turbine bypass)

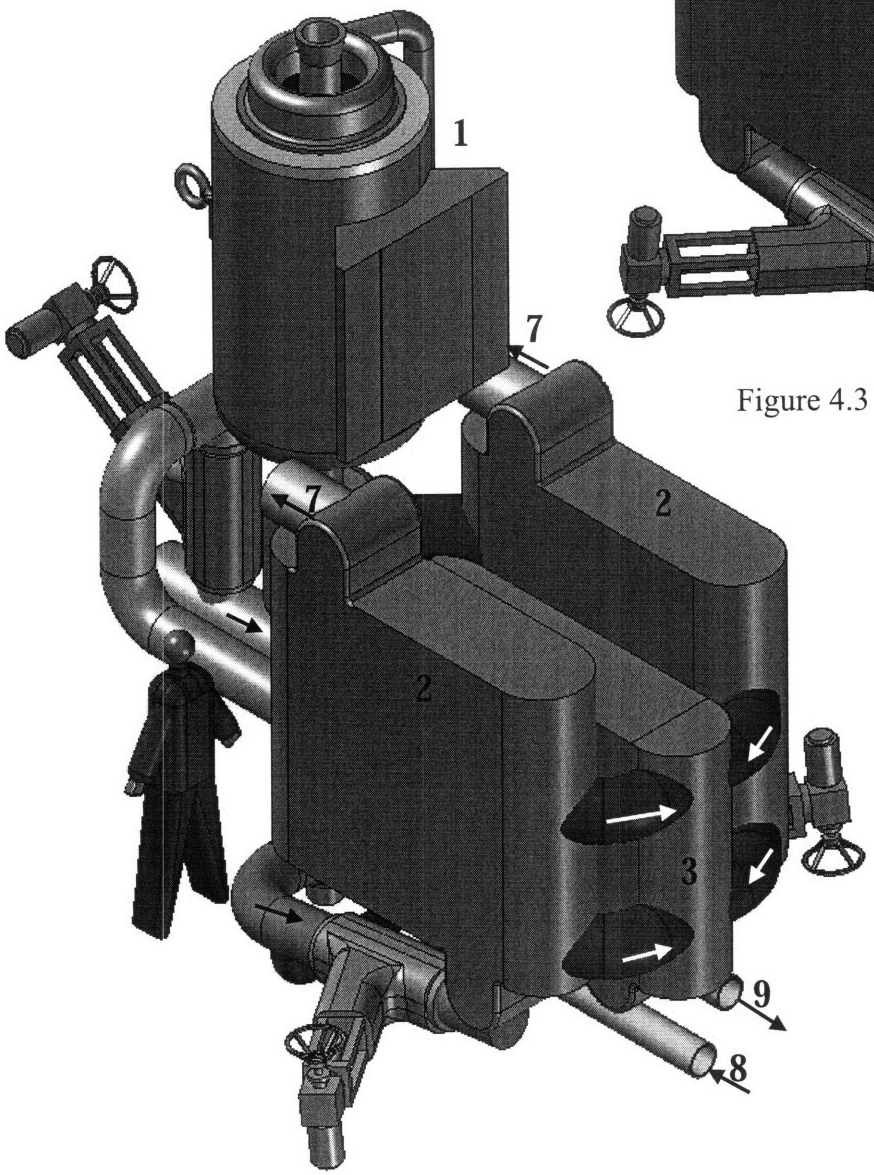

Figure 4.4. Parallel-simple S-CO_2 (back isometric) (turbine bypass)

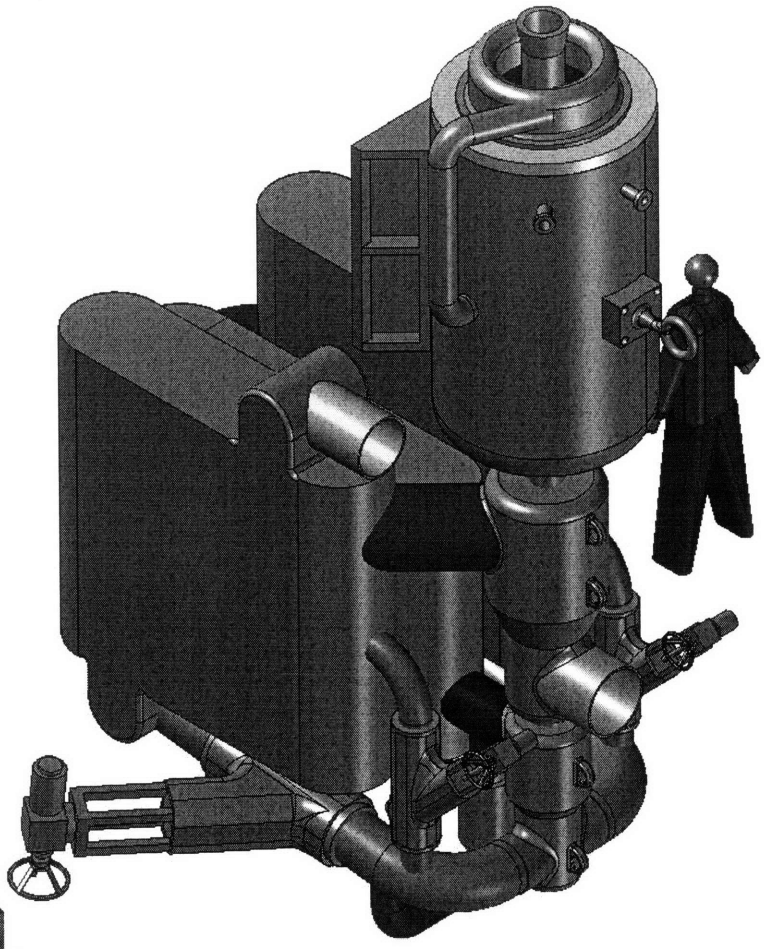

Figure 4.5 Parallel-simple S-CO_2 (front isometric) (compressor bypass)

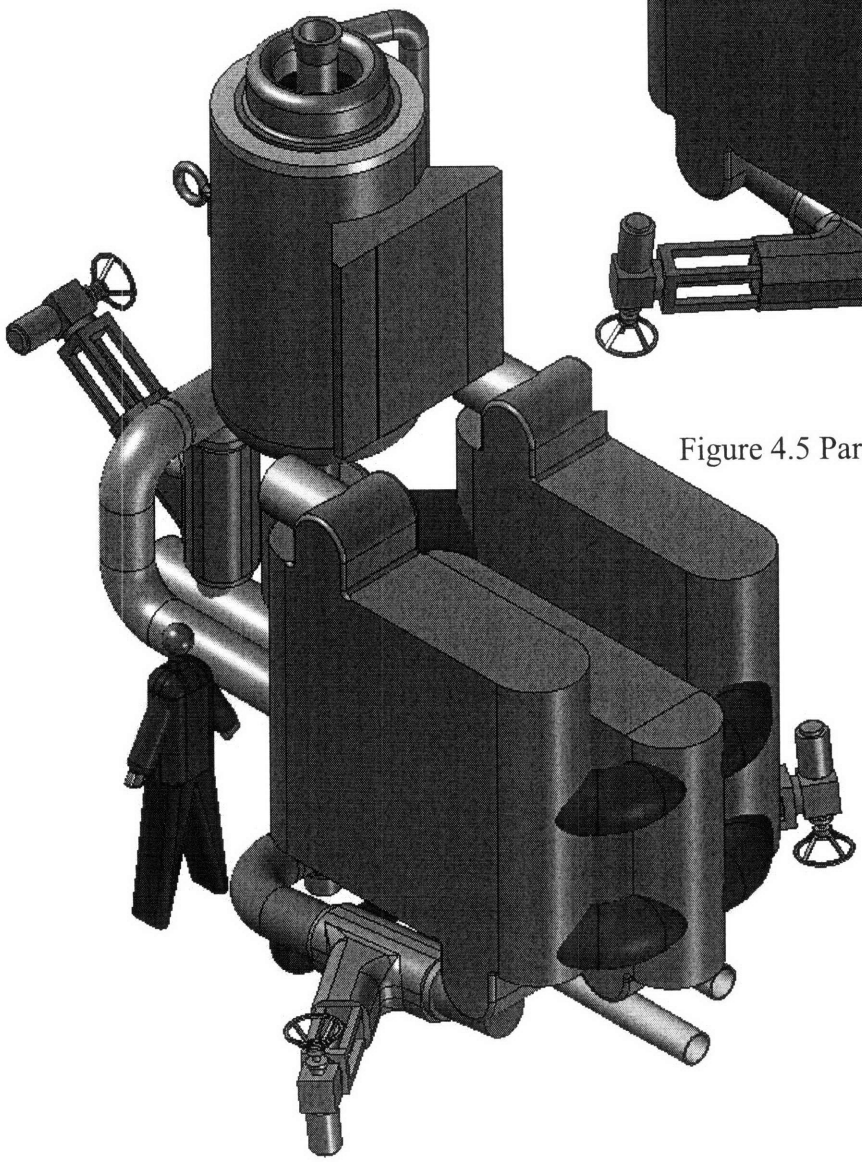

Figure 4.6 Parallel-simple S-CO_2 (back isometric) (compressor bypass)

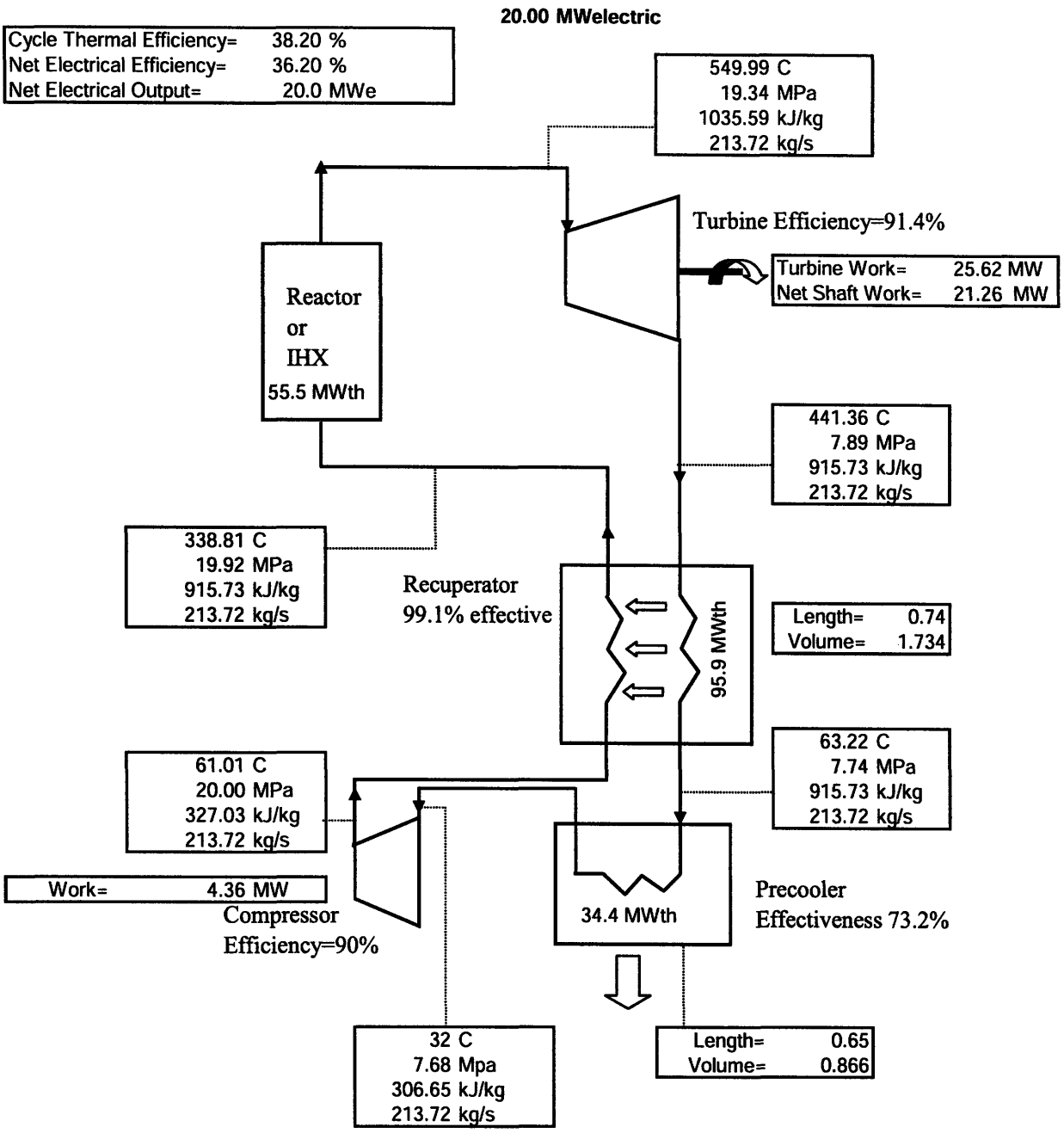

Figure 4.7 Simple cycle statepoints
(550°C turbine inlet, 32°C compressor inlet, 20°C cooling water)

Note: The statepoints are defined in reference to the turbomachinery (i.e. compressor/turbine inlet/outlet). The points that fall between two heat exchangers correspond to the outlet of the heat exchanger upstream relative to the flow. The changes

in statepoints due to the effects of the pipes are small and not observable unless the values were expanded to another decimal place

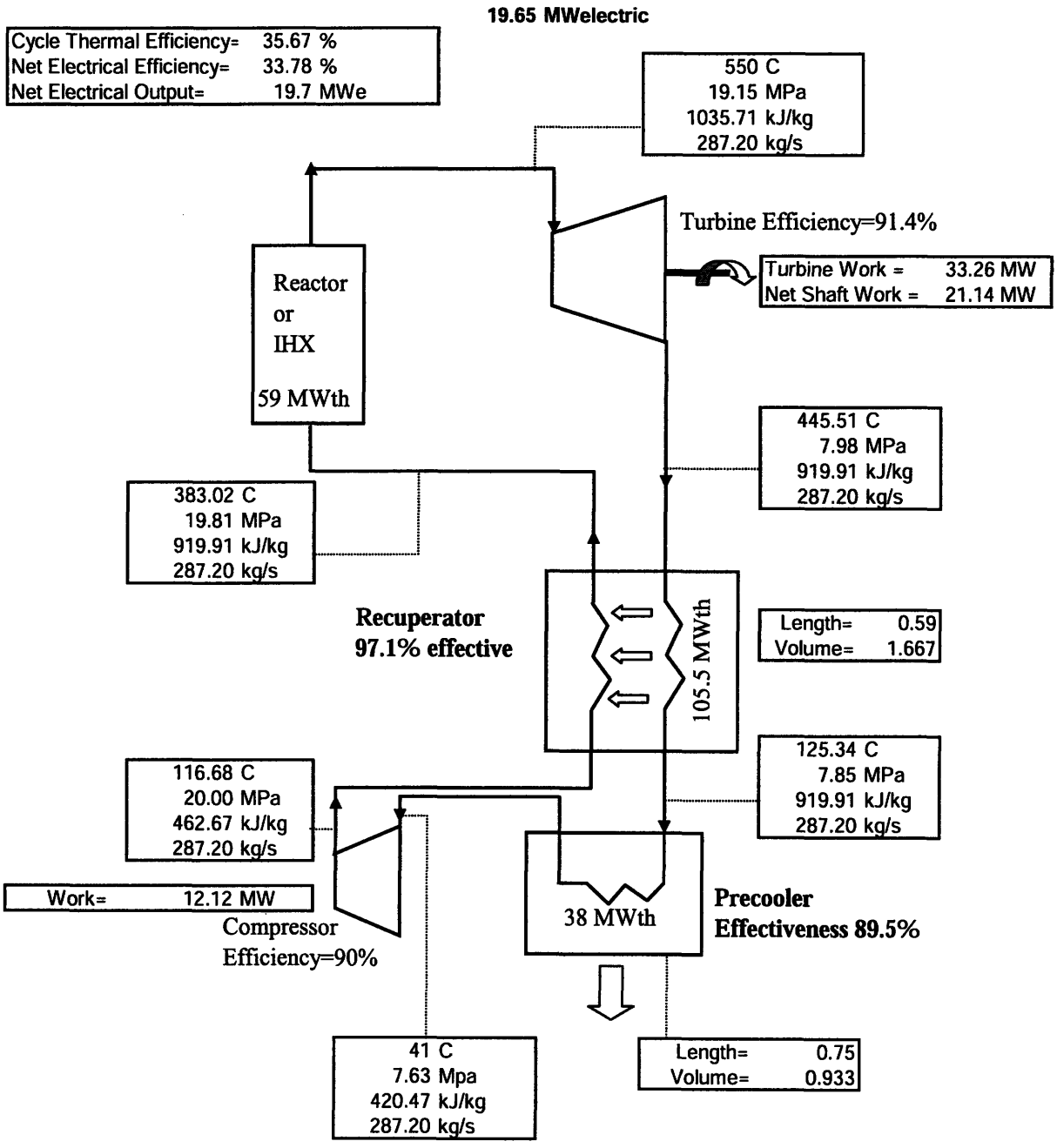

Figure 4.8 Simple cycle statepoints
(550 °C turbine inlet, 38 °C cooling water, 42 °C compressor inlet)

4.3 Design for Various Power Ratings

The simple cycle calculations were also performed for different power ratings ranging from 5-30 MWe. The results are shown in Table 4.7 with the corresponding pipe sizes recorded in Table 4.8. Between the two extremes, the net cycle efficiency only varies by 0.5%. Turbomachinery efficiencies were taken constant across power ratings, based on preliminary assessment of efficiencies in Chapter 4. Regardless of this assumption, the machinery efficiencies will only change slightly for the power ratings of interest, and the current results will be affected only minimally by small turbomachinery efficiency variation and are thus sufficient for all intended purposes. The performance data variation is due to the pipe sizing. The pipes were scaled in the same fashion as in the recompression cycle and rounded to the nearest standard pipe size. Therefore, the data can be skewed by the rounding method. However, the length of each pipe was held constant, equal to that of the 20 MWe system. To get accurate piping lengths each cycle will have to be drawn in an appropriate CAD program, however, the effect of varying pipe lengths for the simple cycle will be negligible because all of the piping lengths are already very small and their contribution to pressure drop is minimal.

Table 4.7. 5-30 MWe power rating chart

Electrical power ($MW_{electric}$)		30	20	15	10	5
Thermal Power ($MW_{thermal}$)		87.0	58.0	44.0	29.5	14.5
Maximum operating pressure (MPa)		20.0	20.0	20.0	20.0	20.0
Turbine Inlet Temp (°C)		550.0	550.0	550.0	550.0	550.0
Pressure Ratio		2.50	2.50	2.50	2.50	2.50
*Reactor/IHX pressure drop (kPa)		500.0	500.0	500.0	500.0	500.0
Net Cycle Efficiency (%)		**33.35**	**33.72**	**33.89**	**34.03**	**34.17**
*Turbine Efficiency (%)		91.2	91.2	91.2	91.2	91.2
*Compressor Efficiency (%)		89.0	89.0	89.0	89.0	89.0
*Mechanical Efficiency (couplings) (%)		99.0	99.0	99.0	99.0	99.0
*Generator Efficiency (%)		98.0	98.0	98.0	98.0	98.0
*Frequency Converter Efficiency (%)		98.0	98.0	98.0	98.0	98.0
Main Comp Inlet Temp (°C)		42.0	42.0	42.0	42.0	42.0
Cooling water temp (°C)		38.0	38.0	38.0	38.0	38.0
Total Vol. of HXs (m^3)		3.90	2.60	1.95	1.30	0.65
Precooler Volume (m^3)		1.40	0.93	0.70	0.47	0.23
Recuperator Volume (m^3)		2.50	1.67	1.25	0.83	0.42
Precooler Active Length (m)		0.95	0.95	0.95	0.95	0.95
Recuperator Active Length (m)		0.64	0.64	0.64	0.64	0.64

*Assumed values

Table 4.8 Pipe size chart for 5-30 MWe power ratings*

Pipe		30MW	20MW	15MW	10MW	5MW
PRE to MC		14	10	9	8	5
MC to REC		14	10	9	8	5
REC to IHX		16	12	12	9	6
IHX to TUR		14	10	9	8	5
TUR to REC		24	16	14	12	8
REC to PRE		20	14	12	10	8

*All dimensions are in inches and correspond to the inner diameter of the pipe

4.4 Cycle Performance Sensitivity

Similarly as for the recompression cycle, sensitivity studies of cycle efficiency to turbomachinery performance, heat exchanger channel plugging and fouling, turbine inlet temperature, and peak cycle pressure were carried out for the simple cycle. All of the simple cycle sensitivity studies were performed for fully optimized 20 MWe cycles for a 550°C turbine inlet temperature, 20 MPa peak cycle pressure, and a 38°C cooling water temperature (42°C compressor inlet temperature). It is very important to note here that for the studies with constant thermal power (turbomachinery efficiency and channel plugging and fouling), when the efficiency declines the electrical output to the grid also will drop.

4.4.1 Turbomachinery Performance

The turbomachinery performance degradation study was performed with design efficiencies of 91.4% for the turbine and 90% for the compressor. The study was done by varying one efficiency and holding the other constant (the compressor was held at 90% and the turbine was held at 91.4%). The results are plotted in Figure 4.9. Similarly to the recompression cycle, the cycle efficiency for the simple cycle is most sensitive to the turbine efficiency. For a 5% turbine efficiency reduction the cycle efficiency is lowered approximately 2% compared to only 1% for a 5% compressor efficiency reduction. Although the turbomachinery efficiencies were plotted down to 70% efficiency, the actual range of interest is from 80-90%. The pertinent data for this analysis is recorded in Table 4.9.

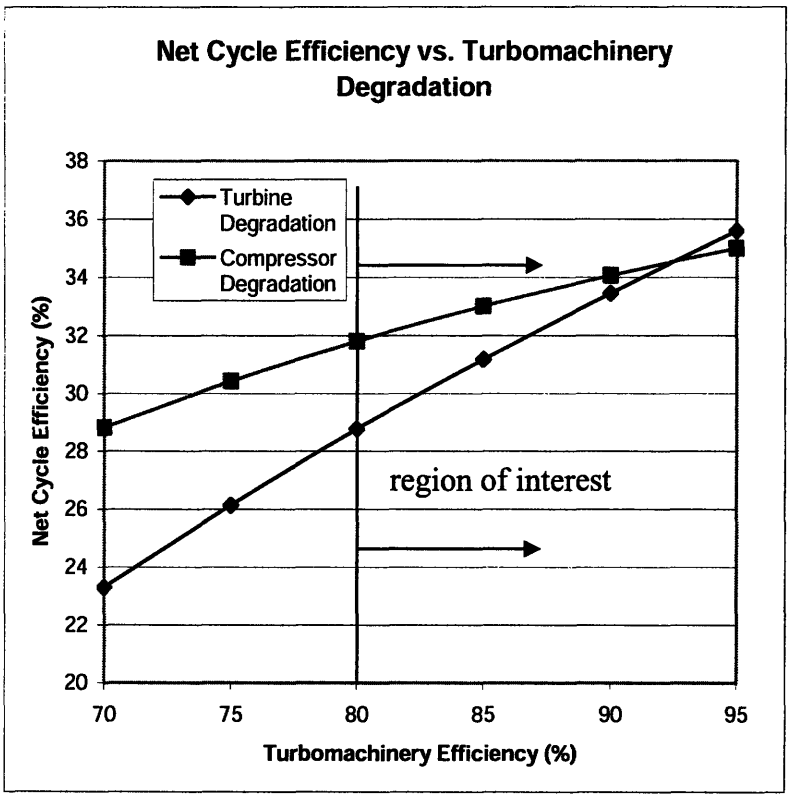

Figure 4.9 Effect of turbomachinery degradation on simple cycle efficiency

4.4.2 Heat Exchanger Channel Plugging

The effect of heat exchanger channel plugging is shown in Figure 4.10. The study simulates the blockage of a number of channels by reducing the available face area for heat transfer. An equal percentage of plugged channels is assumed for both the recuperator and the precooler. As with the recompression cycle, the precooler is more prone to plugging than the recuperator because of the presence of impurities in cooling water. The net cycle efficiency doesn't significantly start to drop off until the heat exchangers are 25% plugged. Thus, the cycle performance is quite resilient to channel blockage, since with 30% of the channels blocked in both the heat exchangers, only about 4% (absolute) net efficiency loss occurs. As the plugging increases the heat exchanger effectiveness decreases due to the smaller heat transfer area, but this effect is less important than the effect of larger pressure drops through the heat exchangers as a result of higher CO_2 velocity. Note that the recuperator effectiveness drops only slightly (nearly linearly) with an increase in channel plugging (by 1.6% for 40% plugging).

The impact of heat exchanger plugging is smaller for the simple cycle than for the recompression cycle. In the recompression cycle, the efficiency was reduced approximately 10% for 35% plugging compared to only 8.5% in the simple cycle. This is because in the simple cycle the majority of the heat is transferred in the first 50% of the active length. A reduction in available volume causes the heat rejection to be spread out more over the entire active length before significantly reducing the cycle performance. The pertinent data for this analysis is recorded in Table 4.9.

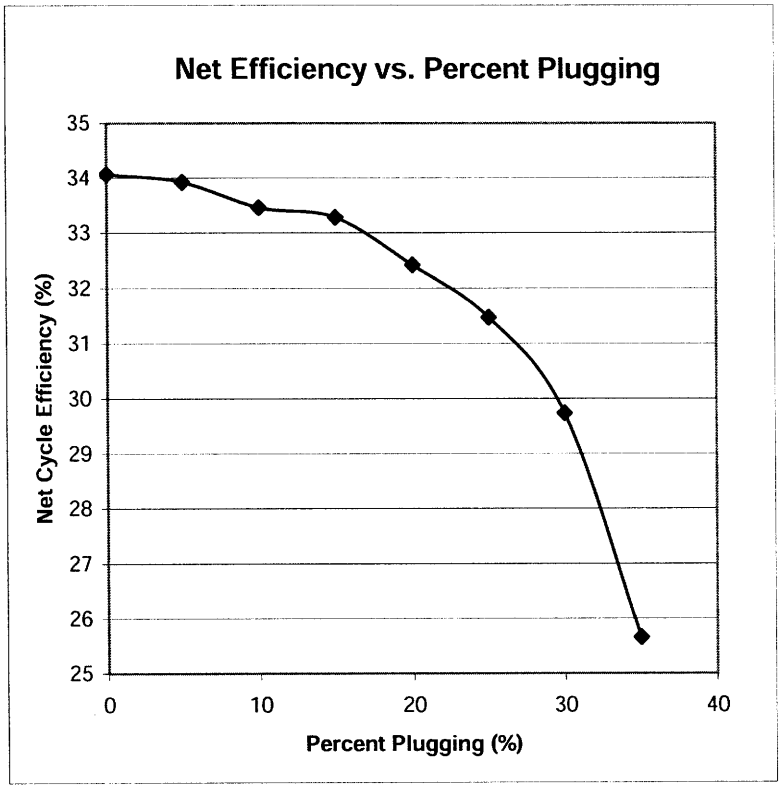

Figure 4.10 Effect of heat exchanger channel plugging on efficiency

Table 4.9 Pertinent data for simple cycle degradation tests

Electrical power ($MW_{electric}$)		20.0/varies
Thermal Power ($MW_{thermal}$)		58.0
Maximum operating pressure (MPa)		20.0
Turbine Inlet Temp (°C)		550.0
Pressure Ratio		2.60
*Reactor/IHX pressure drop (kPa)		500.0
Net Cycle Efficiency (%)		Varies
Turbine Efficiency (%)		91.4/varies
Compressor Efficiency (%)		90.0/varies
*Mechanical Efficiency (couplings) (%)		99.0
*Generator Efficiency (%)		98.0
*Frequency Converter Efficiency (%)		98.0
Main Comp Inlet Temp (°C)		42.0
Cooling water temp (°C)		38.0
Total Vol. of HXs (m^3)		2.60
Precooler Volume (m^3)		0.93
Recuperator Volume (m^3)		1.67
Precooler Active Length (m)		0.95
Recuperator Active Length (m)		0.64

*Assumed values

4.4.3 Heat Exchanger Fouling

Using the calculation models of printed circuit heat exchangers that incorporate the effect of oxide layers, as described in Chapter 2, sensitivity of the simple S-CO_2 cycle performance was evaluated to oxide buildup in the recuperator and precooler. The reference cycle with turbine inlet temperature of 550°C, the highest pressure of 20 MPa, and the lowest cycle temperature of 32°C (20°C cooling water temperature) was used for the sensitivity study. Oxide layer thickness on both the hot and cold sides was varied between 0 and 100 microns and the conductivity was assumed to be 25 W/m-K. Cycle net (electrical) efficiency is plotted on Figure 4.11. There are three lines: REC signifies changes of oxide thickness in the recuperator only (on both sides) while maintaining precooler clean, PRE models sensitivity of cycle net efficiency to fouling in the precooler only (on both the CO_2 and water side) and REC+PRE models fouling in both heat exchangers.

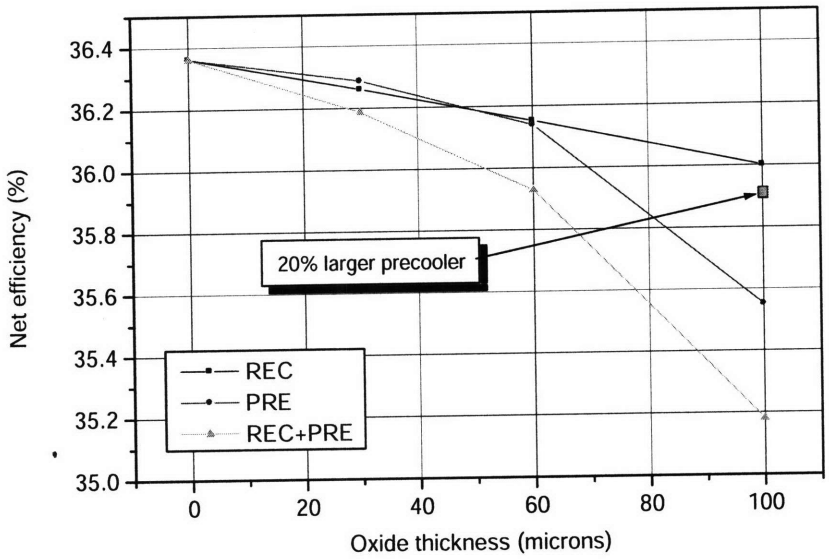

Figure 4.11 Sensitivity to heat exchanger fouling for simple cycle

It can be observed that even a conservatively large oxide thickness of 100 microns in the recuperator has negligible effect on efficiency. This is because the overall heat transfer coefficient is controlled by fluid heat transfer. Since the resistance due to CO_2 fluid to clean wall heat transfer in the recuperator is about an order of magnitude higher than that of the oxide layer, the effect of oxide layer on the overall heat transfer coefficient is negligible and the small reduction of cycle efficiency is primarily due to the oxide layer-induced reduced flow area and hydraulic diameter. Cycle performance degradation from precooler fouling is about the same as from recuperator fouling until an oxide thickness of 60 microns, but becomes more significant for thicker oxide layers. This is because at about 60 microns, fouling resistance on the water side becomes comparable to that of the water heat transfer coefficient, and becomes responsible for a reduced heat transfer rate to water. To overcome this reduction, water flow rate through the precooler has to be increased significantly, resulting in larger pumping power, which is also exacerbated by larger precooler pressure drop due to reduced channel flow area and hydraulic diameter.

Therefore, even though one would expect the recuperator fouling to be more important, it is the precooler fouling that needs to be more closely watched. If corrosion tests confirm that oxide thickness can be kept below 60 microns, the effect of fouling will be negligible, for larger oxide thickness a slightly larger precooler could easily overcome the issue of performance degradation from precooler fouling. For example, increasing precooler volume by 20% can more than recover net efficiency loss from both precooler and recuperator fouling, as shown on Figure 4.11.

Industrial practice is to design heat exchangers with larger heat transfer area to allow for fouling. The percentage of added surface is small if the overall heat transfer coefficient is low regardless of fouling resistance. On the other hand, heat exchangers with high overall heat transfer coefficient need to add appreciable allowance for fouling, because even small fouling resistance can have a significant effect. This can be seen on Figure 4.11 and also agrees with conclusions in [Deng et al., 1990].

4.4.4 Turbine Inlet Temperature

The importance of the turbine inlet temperature for the simple cycle is the same as for the recompression cycle. Because of the interest in cycle performance at lower turbine inlet temperatures, the sensitivity study to this parameter was extended down to values as low as 300°C. Figure 4.12 shows the effect of the turbine inlet temperature on cycle efficiency for a fully optimized cycle at each point, and normalized to net electric power of 20 MWe. As expected, the relationship is nearly linear, but bends down faster at lower temperatures – a consequence of larger mass flow rates and thus higher pressure drops in the ductwork and heat exchangers. The turbomachinery efficiency was assumed to be constant for the range of inlet temperatures. One significant consideration for using a cycle with a lower turbine inlet temperature is the effect of the total volume of the heat exchangers. As the turbine inlet temperature decreases, the necessary heat exchanger volume drastically increases. Figure 4.13 shows how the total heat exchanger volume changes with turbine inlet temperature. The total heat exchanger volume can be slightly reduced if the reduction of the cycle efficiency is also acceptable. The total heat

exchanger volumes must be increased for lower turbine inlet temperatures due to the large increase of the mass flow rate – a consequence of significantly larger thermal power needed to deliver the same electrical power output at low efficiencies. It can be easily seen in Figure 4.14 that the mass flow rate increases considerably for lower turbine inlet temperatures. As the mass flow rate increases, the efficiency will drop due to the larger pressure losses throughout the system. If the total heat exchanger volume is not properly increased the effect of pressure losses throughout the cycle can be greater than a 10% net cycle efficiency reduction. For a simple cycle designed with a maximum pressure of 20 MPa and a turbine inlet temperature of 300°C, the total volume of the heat exchangers is approximately 3.3 times the volume for a simple cycle designed at the same pressure with a 550°C turbine inlet temperature. This will result in a recuperator more than 12m tall requiring either two or three parallel recuperators to reduce the height and minimize the pressure losses. Even if the total volume of the heat exchangers were significantly increased, the net cycle efficiency is slightly less than 15%, and not attractive. However, the pipes connecting the various components in the cycle can also be increased to gain in efficiency, but they will not cause the cycle to improve its performance to an attractive level. The key cycle parameters for this analysis are recorded in Table 4.10.

As indicated earlier, one reason for higher efficiencies at higher turbine inlet temperatures is the mass flow rate. Figure 4.14 depicts the mass flow rate as a function of turbine inlet temperature for a 20 MPa simple cycle. The mass flow rate decreases significantly as the turbine inlet temperature increases. Because the higher turbine inlet temperatures have lower required mass flow rates, the pressure losses will be significantly less, resulting in a cycle with higher efficiency.

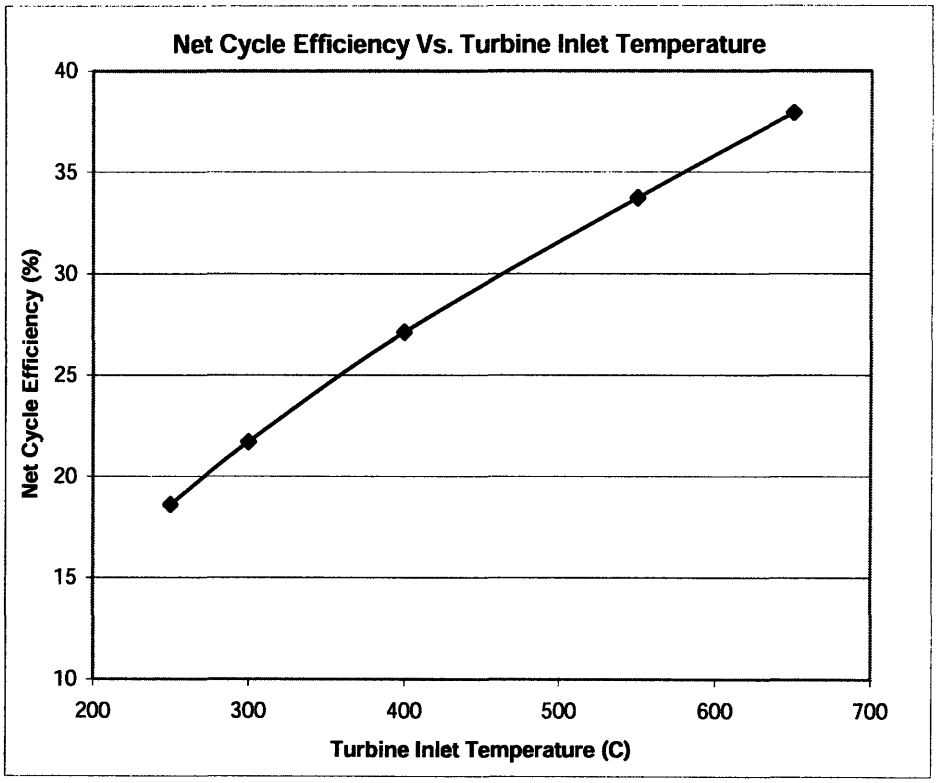

Figure 4.12 Effect of turbine inlet temperature for simple cycle

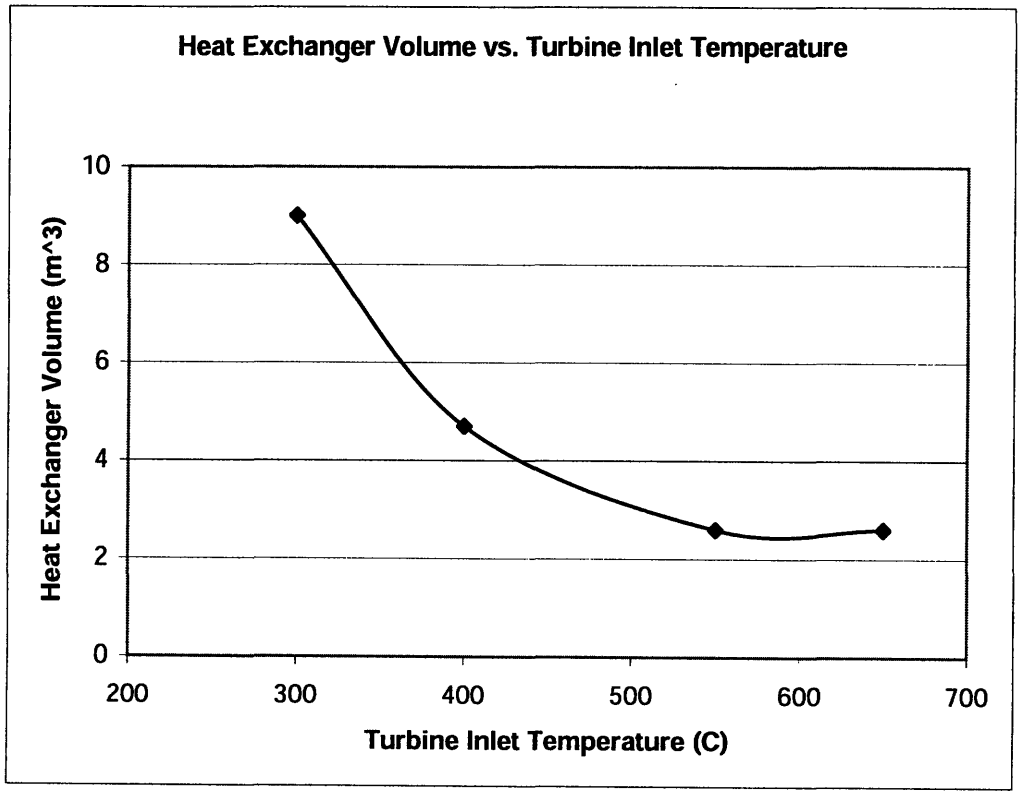

Figure 4.13 Simple cycle total heat exchanger volume sensitivity to turbine inlet temperature

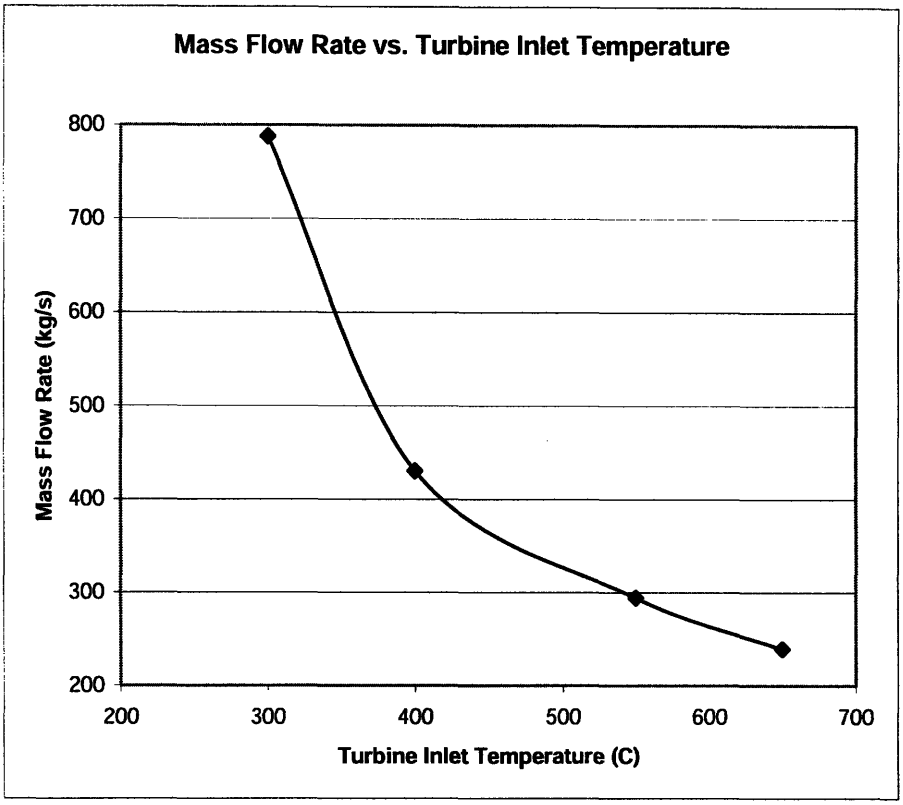

Figure 4.14 Mass flow rate vs. turbine inlet temperature for simple cycle

Table 4.10 Key simple cycle parameters used for simple cycle turbine inlet temperature study

Electrical Power ($MW_{electric}$)		20.0
Thermal Power ($MW_{thermal}$)		varies
Turbine Inlet Temperature (°C)		varies
Turbine Efficiency (%)		91.2
Compressor Efficiency (%)		89.0
Mechanical Efficiency (%)		99.0
Generator Efficiency (%)		98.0
Power Electronics Efficiency (%)		98.0
Cooling Water Temperature (°C)		38.0
Total Volume of HXs (m^3)		varies

It is also of interest to determine how the simple cycle behaves as a function of turbine inlet temperature if the thermal power and the heat exchanger volume are fixed (i.e. for a fixed system, what are the possible electrical outputs?). As seen in Figure 4.15, the net cycle efficiency increases nearly linearly with turbine inlet temperature. The pertinent

data for this analysis is recorded in Table 4.10, except for the thermal power, which is held constant at 58 MW, and the total heat exchanger volume, held constant at 2.6 m^3. Therefore, this cycle can be used for a net electrical output of 15 MWe with a 400°C turbine inlet temperature and 12 MWe with a 300°C turbine inlet temperature, etc.

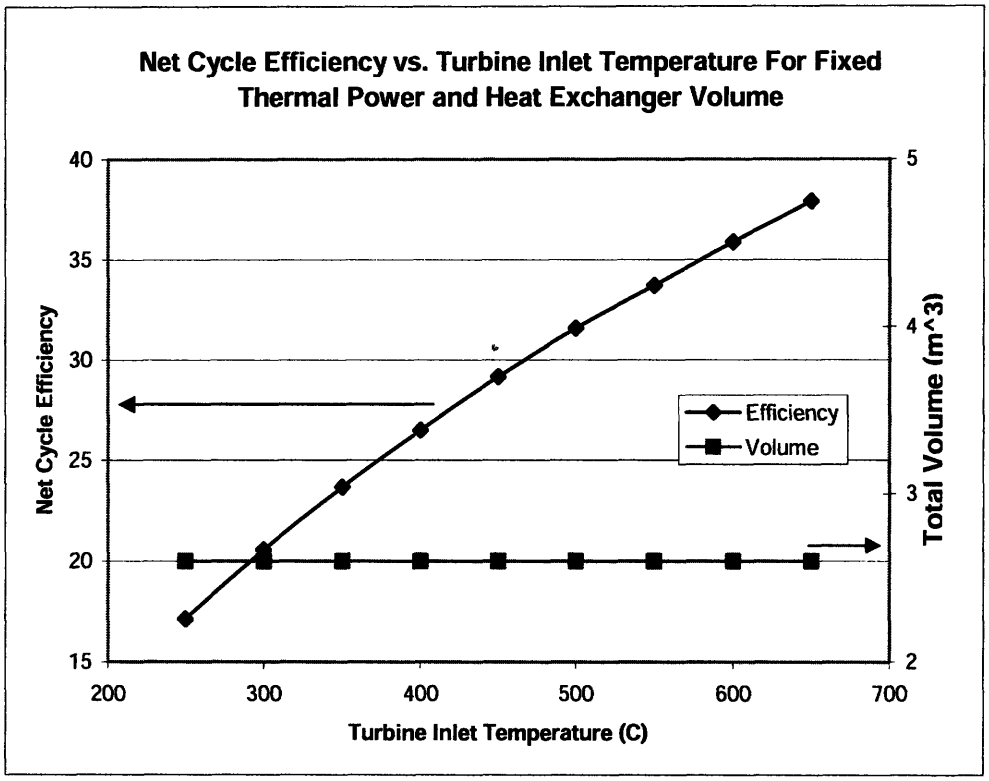

Figure 4.15 Net simple cycle efficiency vs. turbine inlet temperature for fixed thermal power and heat exchanger volume

Although using a simple cycle with a 20 MPa peak pressure and 300°C is unattractive due to the overall physical size and poor efficiency, if the peak cycle pressure was increased to 28 MPa the turbine inlet temperature could be as low as 300°C and maintain nearly 23% net cycle efficiency for a considerably smaller total heat exchanger volume (at 1.8 times the heat exchanger volume utilized for a 550°C turbine inlet temperature compared to 3.3 times). The possibility of a 28 MPa cycle is investigated in the next section.

4.4.5 Peak Cycle Pressure

Because current supercritical steam cycles operate at significantly higher pressures than 20 MPa - up to 34 MPa, it is of interest to evaluate cycle performance at higher pressures, since these are manageable and operational experience (albeit with water) at high pressure has been accumulated. Moreover, higher pressures typically result in more compact machinery. Cycle efficiency for various compressor outlet pressures of the simple cycle is plotted in Figure 4.16a. The pressure ratio for each case corresponds to the ratio of the highest pressure and the compressor inlet pressure of 7.7 MPa, just above the critical point where compressor work is the smallest. All of the turbomachinery efficiencies were held constant. Also, the total volume of the heat exchangers was held constant; only the active length and volume allocation of each heat exchanger changed in the optimization process. The data for this analysis is recorded in Table 4.10. Figure 4.16a was generated for a fully optimized cycle at each point. However, the thermal power level was held constant at 58 MWth, resulting in a non-normalized plot with respect to electrical power output (i.e. the electric power varied with efficiency). The plot will change slightly because of a slightly lower efficiency for pressures below 20 MPa and a slightly higher efficiency above 20 MPa, if normalized to net electrical power output. Figure 4.16b is for a fully optimized 20 MWe for each pressure and various turbine inlet temperatures normalized to 20 MWe power output (the thermal power varies for each temperature and pressure to maintain 20 MWe). The results exhibit the same trend as for the recompression cycle, with the efficiency gains saturating at higher pressures. The reason for the lower efficiencies at lower pressures is the same as for the recompression cycle and Figure 4.16a. When normalization is with respect to electric power output, mass flow rate changes with pressure increase are more pronounced than in case of normalization to thermal power rating and the beneficial effect of reduced mass flow rate at higher pressures remains dominant at high pressures. Hence, no trend reversal is seen on Figure 4.16b versus figure 4.16a.

It can be observed that there is significant efficiency gain between 20 MPa and 23 MPa, which begins to saturate above this value. The highest performance compressor outlet

pressure occurs at 28 MPa (pressure ratio=3.63) and begins to decrease for higher pressures. Three key factors are responsible for this trend.

- The first parameter affecting cycle efficiency is the temperature rise across the IHX/reactor at which the cycle optimizes for a given pressure. As shown in Figure 4.17, S-CO_2 cycles at higher compressor outlet pressures optimize at smaller mass flow rate (due to larger pressure ratio across the turbine, and thus larger enthalpy difference) and hence at a larger temperature rise across the IHX. Consequently, for a fixed turbine inlet temperature, the IHX inlet temperature is reduced, resulting in a lower temperature of heat addition and lower cycle efficiency.
- The second key parameter involves fractional pressure losses around the loop. The smaller mass flow rates for cases with higher compressor outlet pressures lead to reduced pressure losses through the pipes and heat exchangers, resulting in an increase of cycle efficiency.
- Finally, as cycle highest pressure increases, fractional pressure loss is reduced (even for fixed mass flow rate), which leads to higher cycle efficiency. However, it is noted that this effect is of much smaller importance than the first two factors because the lowest cycle pressure is held constant (close to the critical pressure) and it is the low pressure side of the cycle that exhibits the largest fractional pressure losses.

For lower compressor outlet pressures, fractional pressure losses are the prevailing factor, resulting in cycle efficiency increase with pressure, while at pressures above 28 MPa, reduction of average heat addition temperature becomes dominant and is responsible for the saturation of the rate of efficiency increase with pressure and an ultimate efficiency decline. It is also noted that at higher cycle pressures above 28 MPa, the recuperator effectiveness begins to drop noticeably, contributing to efficiency reduction. It is interesting to note that for higher cycle pressures, the previous compressor inlet pressure (≈7.7 MPa), which is very close to the critical pressure, does not necessarily yield the optimum pressure ratio. Rather smaller pressure ratios, with the lowest cycle pressure further above the critical point, may yield higher efficiency in spite of larger compressor work. This is because the negative impact of lower heat addition temperature becomes

more important than the gain from small compressor work. Re-plotting Figure 4.16 at optimum pressure ratios would reverse the efficiency decline at high cycle pressures, and efficiency would remain almost constant. The dip in recuperator effectiveness at 20 MPa is an interesting result of optimization, which identified slightly higher cycle efficiency at a shorter recuperator length, since hot side recuperator pressure drop had a larger effect on efficiency than the recuperator effectiveness (Figure 4.18).

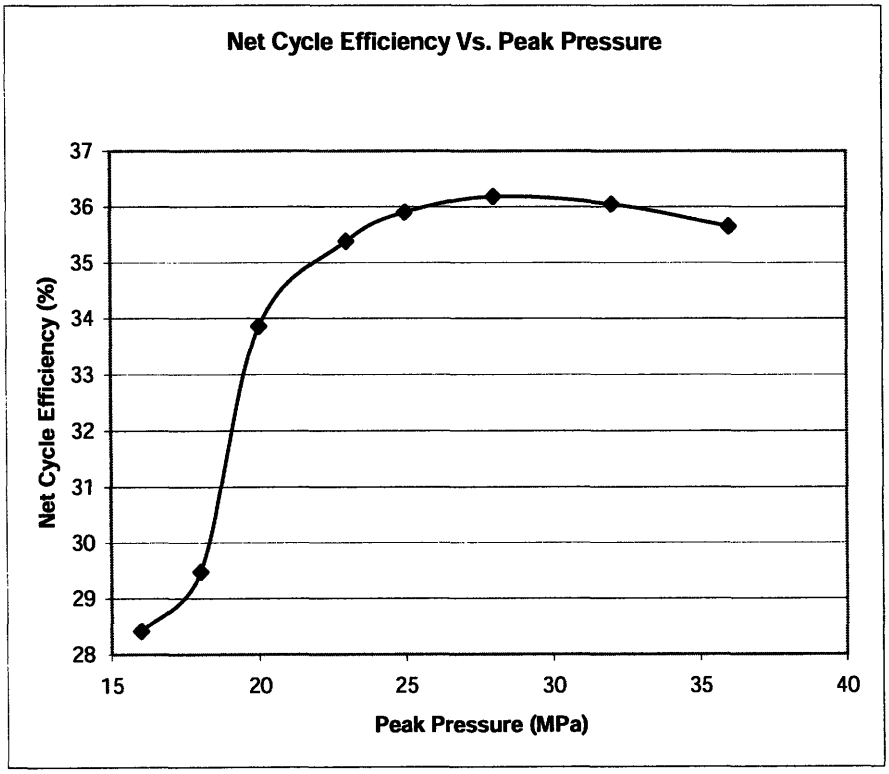

Figure 4.16a Net cycle efficiency vs. cycle pressure variation (simple cycle)

The performance study with respect to cycle pressure suggests that raising the pressure from 20 MPa to 25 MPa, which is still well below the current pressures for supercritical water cycles, increases cycle efficiency by 3%. Since it is typically temperature which is more limiting to materials (both from the corrosion and allowable stress viewpoint), raising the pressure by 5 MPa would allow us to reduce turbine inlet temperature by 50°C while maintaining the same efficiency.

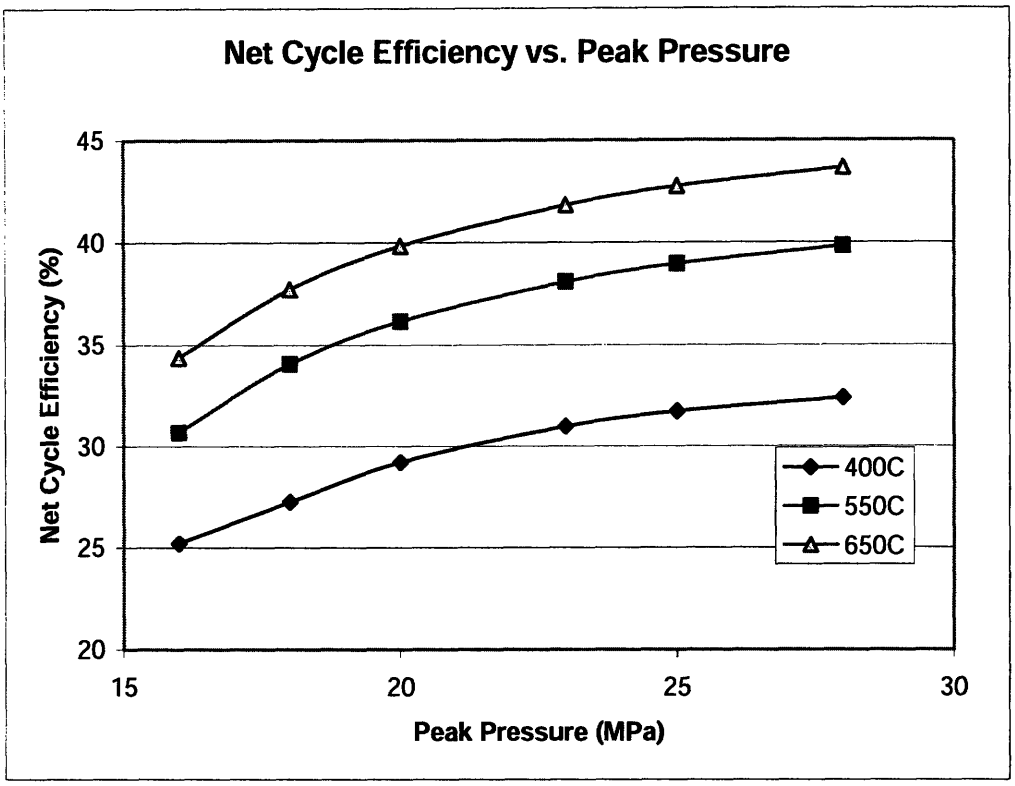

Figure 4.16b Cycle efficiency for various peak cycle pressures and turbine inlet temperatures (simple cycle)

Table 4.11. Pertinent data for simple cycle pressure study

Electrical Power ($MW_{electric}$)	20.0
Thermal Power ($MW_{thermal}$)	58.0
Turbine Inlet Temperature (°C)	550.0
Turbine Efficiency (%)	91.2
Compressor Efficiency (%)	89.0
Mechanical Efficiency (%)	99.0
Generator Efficiency (%)	98.0
Power Electronics Efficiency (%)	98.0
Cooling water Temperature (°C)	38.0
Total Volume of HXs (m^3)	2.60

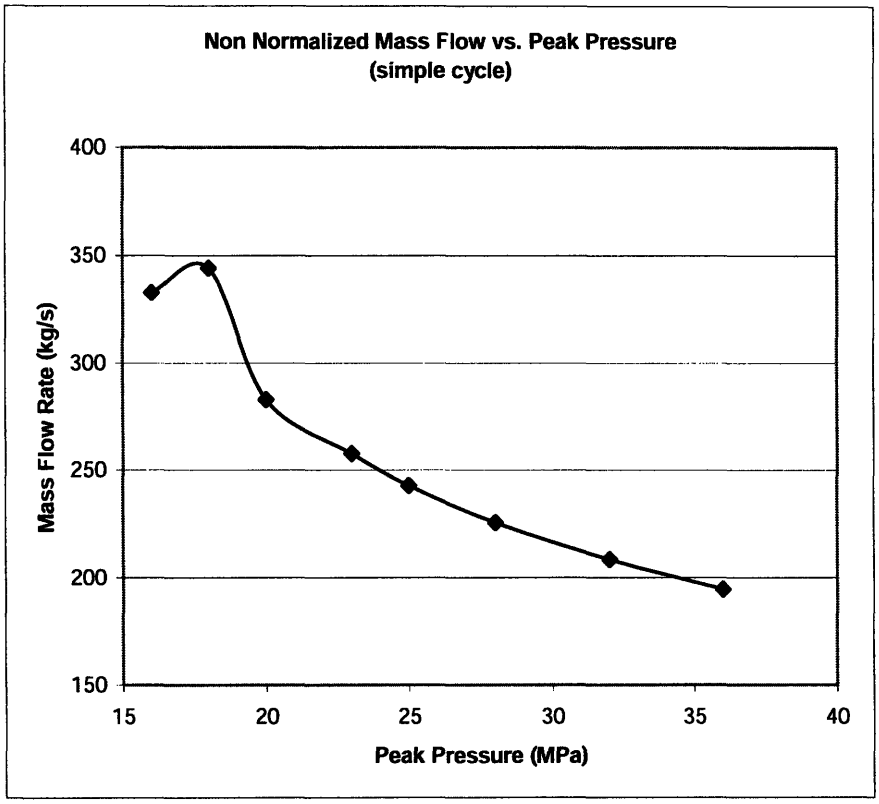

Figure 4.17 Mass flow rate versus the highest cycle pressure (simple cycle)

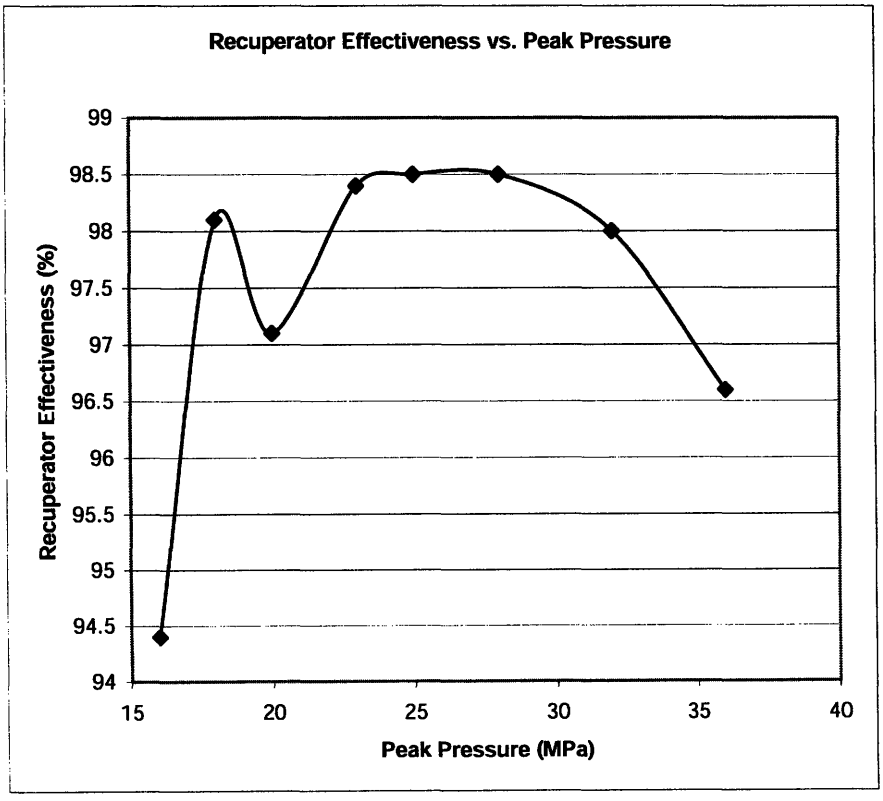

Figure 4.18 Recuperator effectiveness vs. highest cycle pressure (simple cycle)

Another interesting aspect of the high-pressure versions of the S-CO_2 simple cycle is reduced recuperated heat. While the S-CO_2 cycle with 20 MPa highest pressure recuperates 106 MWt, the 28 MPa cycle version needs the recuperator to be rated only at 66 MWth. This effect is even more important in the recompression version, which is highly recuperative. For example, the 20 MWe recompression cycle at turbine inlet temperature of 550°C and the highest cycle pressure of 20 MPa recuperates in the high temperature recuperator 99 MWt compared to only 38 MWt for the same cycle operating at 32 MPa. However, even though the recuperated heat rate is more than 3 times smaller, the size of the high temperature recuperator cannot be reduced by the same ratio because the temperature difference between the hot and cold sides becomes smaller. Nevertheless, about 60% reduction of the HTR volume would be possible. The important point to keep in mind for the design of the overall reactor-power conversion system is the possibility to use the highest S-CO_2 cycle pressure as a design parameter to achieve a desirable temperature rise in the IHX to match that of the primary system. For example, the optimum 150°C temperature rise of the S-CO_2 cycle with the highest pressure of 20 MPa turned out to be a significant constraint for the MIT indirect cycle GFR design, since it required excessive pumping power for primary circulators. Increasing S-CO_2 cycle highest pressure can overcome this concern.

Because of the potential to reduce the total volume of the heat exchangers for a very high pressure cycle, a 28 MPa case was checked to determine if more benefits could be gleaned by further analysis. Maintaining the same thermal power as the 20 MPa, 550°C case, the 28 MPa case was able to reduce the total heat exchanger volume by 33% (down to 2.0m^3) while obtaining a net cycle efficiency of 35.7%. This is 2% higher for the same cooling water conditions (38°C) as the 20 MPa cycle. Another option is to reduce the thermal power and not reduce the heat exchanger volume. The thermal power can be reduced by 4 MW (down to 55 MW_{th}) to produce the same 20 MWe power by maintaining the total heat exchanger volume at 2.6m^3. The reduced thermal power case exhibits a net cycle efficiency of approximately 36.6%. The results can change slightly because the final turbomachinery efficiencies are not available at this time, and are

assumed to be the same as for the 20 MPa cycle. The key cycle parameters are recorded in Table 4.12. Statepoints of the high pressure S-CO_2 cycle with reduced heat exchanger volumes are shown in Figure 4.19.

Table 4.12 Key cycle parameters for a possible 28 MPa, 300°C simple cycle

Electrical Power ($MW_{electric}$)		22.0
Thermal Power ($MW_{thermal}$)		90.0
Turbine Inlet Temperature (°C)		300.0
Turbine Efficiency (%)		91.4
Compressor Efficiency (%)		90.0
Mechanical Efficiency (%)		99.0
Generator Efficiency (%)		98.0
Power Electronics Efficiency (%)		98.0
Cooling Water Temperature (°C)		38.0
Total Volume of HXs (m^3)		4.7

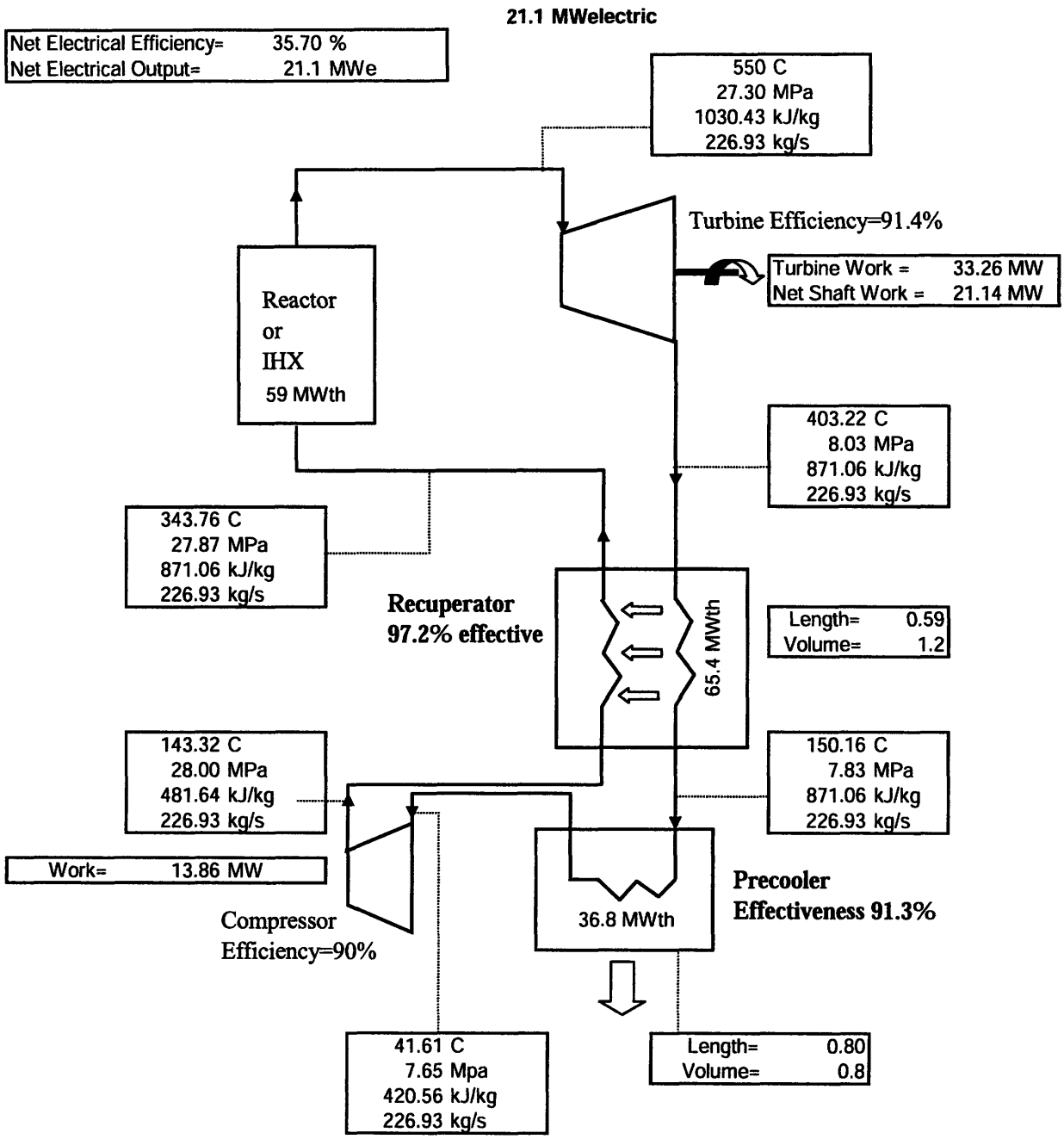

Figure 4.19 State points for a possible 28 MPa, 550°C simple cycle with reduced volumes

4.5 S-CO_2 Cycle Operation Below The Critical Point

Reducing the temperature at which the cycle discharges heat leads to an increase of cycle thermodynamic efficiency. Because the PCS may operate at low cooling temperatures in cold regions, lowering the CO_2 precooler outlet temperature below 32°C should lead to increased cycle efficiency. This section will explore the possibility of simple S-CO_2 cycle operation below critical temperature to reap the benefit of cold cooling water temperature.

There are two possible ways of cycle operation below the critical point. The first possibility is to reduce both temperature and pressure of CO_2 below its critical point and operate in condensing mode. Such a cycle would operate in the same manner as a supercritical CO_2 cycle with one major difference: at the compressor inlet the CO_2 is below the critical point and can either be completely in the liquid phase or a gas/liquid mixture. The compressor will essentially be operating as a pump. The major issue for cycle operation below the dome is the main compressor performance in two phase flow and avoidance of cavitation. It is expected that this may not be such an issue as for steam/water systems because the difference between CO_2 liquid and vapor density below the critical point is small. Nevertheless, significant R&D and experimental tests of compressor operation would have to be performed to confirm the feasibility of compressor operation in two phase flow.

The second approach is to keep the lowest cycle pressure above the critical point and reduce CO_2 precooler temperature to below the critical point and operate on the left side of the dome, just above the saturation line. This way, the cycle operation remains in the transcritical regime and no condensation occurs. This approach is explored in this section.

For the analysis, the compressor inlet temperature was chosen to be 25°C and cooling water temperature was maintained at 20°C to allow for consistent comparison with the reference case. The value of 25°C was selected to maintain sufficient temperature difference for heat transfer to water in the precooler without the need to significantly

increase precooler volume. The reference simple S-CO_2 cycle with turbine inlet temperature of 550°C was used for this study. The prospect of reducing the heat exchanger and pipe sizes was not investigated.

The results are presented in Table 4.13. Case A is the reference case with compressor inlet temperature of 32°C, Case B models a reduced compressor inlet temperature, 25°C, and cooling water temperature of 20°C, and Case C shows the results for 25°C compressor inlet temperature and the same temperature difference between CO_2 and cooling water as the reference case (12°C) for comparison at the same water pumping power.

Table 4.13 Simple condensing cycle comparison for turbine inlet temperatures

Case	**A**	**B**	**C**
Electrical Power ($MW_{electric}$)	20.4	19.8	20.2
Thermal Power ($MW_{thermal}$)	56.0	56.0	56.0
Maximum Operating Pressure (MPa)	20.0	20.0	20.0
Turbine Inlet Temp (°C)	550.0	550.0	550.0
Pressure Ratio (°C)	2.60	2.60	2.60
Reactor/IHX Pressure Drop (kPa)	500.0	500	500.0
Net Cycle Efficiency* (%)	**36.4**	**35.4**	**36.0**
Turbine Efficiency (%)	93.5	93.5	93.5
Compressor Efficiency (%)	86.0	86.0	86.0
Main Comp Inlet Temp (°C)	**32.0**	**25.0**	**25.0**
Cooling water temp (°C)	**20.0**	**20.0**	**13.0**
Total Active Vol. of HX (m^3)	2.54	2.54	2.54
Precooler Active Volume (m^3)	0.8	0.8	0.8
Recuperator Active Volume (m^3)	1.74	1.74	1.74
Recuperator active length (m)	0.74	0.74	0.74
Precooler active length (m)	0.87	0.87	0.87

Although one would expect an increase in cycle efficiency for lower heat rejection temperature, the reversed trend can be observed when comparing Case B with the reference case. There are several reasons for this unexpected trend. First, although the compressor work is reduced due to higher density at 25°C, this reduction is relatively small, since compressor work is already small at 32°C. On the other hand, a smaller temperature difference between CO_2 and cooling water requires increased water flow rate, and thus larger water pumping power, reducing net efficiency. Third, recuperator

effectiveness is reduced and less heat is recuperated, resulting in a slightly larger heat rejection rate in spite of a smaller heat rejection temperature than in the reference case. The net result is reduced cycle net efficiency. If the cooling water temperature is reduced (Case C) to decrease water pumping power to values comparable to those of the reference case, a significant fraction of the lost efficiency can be recovered, but the net efficiency still remains slightly below the reference value – the consequence of reduced recuperator efficiency. Although the recuperator could be re-optimized to recover some efficiency, it is clear that no significant performance gain can be obtained by optimizing the cycle at lower temperatures. On the contrary, the operation of the cycle optimized at such low temperatures would be problematic at higher cooling water temperatures. Hence the condensing cycle was not further pursued.

4.6 Optimized S-CO_2 Design for the Whole Cooling Water Temperature Range

So far, the S-CO_2 simple cycle was optimized for two different cooling water temperatures - 20°C and 38°C, corresponding to compressor inlet temperatures of 32°C and 42°C, respectively. The important issue that needs to be addressed is the feasibility of a compressor that has been designed for operation at one cooling water temperature to operate at a different cooling water temperature. For this purpose, cycle operating points relevant to compressor design have to be determined first. In addition, the impact of various cooling water temperatures on cycle efficiency is of interest.

To evaluate cycle conditions at various cooling water temperatures, the following study has been performed for the 20 MWe simple cycle with turbine inlet temperature of 550°C: (1) the cycle design was optimized at several cooling water temperatures between 20°C and 38°C, (2) the performance of the cycle optimized at a given cooling water temperature was calculated as a function of various cooling water temperatures in a range between 10°C and 38°C. The calculations assumed the same turbomachinery efficiency without taking into account the effect of changed cooling water temperature, and most importantly, of compressor inlet temperature, on turbomachinery performance. These

data primarily serve to evaluate the feasibility of the compressor to accommodate changes of inlet conditions.

The results are summarized in Tables 4.14 through 4.17. The first table of each set is for a cycle optimized at a cooling water temperature, but has a variable compressor inlet temperature because of changing cooling water temperatures. Each variable compressor inlet temperature case has the compressor inlet temperature fixed at 32°C so that lower temperatures remain above the critical point, and it increases when the cooling water approaches and passes the design point. The second table of each set is for a constant compressor inlet temperature for changing cooling water temperatures. Of course, the only true constant compressor inlet temperature is for the 38°C cooling water temperature case (42°C compressor inlet temperature), because the cooling water temperature is never above the design compressor inlet temperature. For the other data sets, the optimal compressor inlet temperature was used when the cooling water temperature was above the design point. Typically, a 4-5°C differential is optimal.

Data used for all calculations are summarized below:
Total heat exchanger volume = 2.6m^3
Turbine Efficiency = 91.4%
Compressor Efficiency = 90.0%
Reactor Pressure Drop = 500 kPa
Mechanical Efficiency = 99.0%
Generator Efficiency = 98.0%
Frequency Converter Efficiency = 98%

Table 4.14 Simple cycle design optimized for 32°C compressor inlet (variable/constant)*

Optimized for a 32°C Compressor Inlet Temperature, 20°C Cooling Water Temperature								
Electric Power Rating ($MW_{electric}$)	20.36	20.34	20.26	18.58	20.12	19.85	19.40	19.17
Thermal Power ($MW_{thermal}$)	56	56	56	56	56	56	56	56
Maximum operating pressure (MPa)	20	20	20	20	20	20	20	20
Minimum operating pressure (MPa)	7.68	7.68	7.68	7.68	7.66	7.64	7.63	7.63
Cycle net efficiency (%)	**36.31**	**36.28**	**36.14**	**33.15**	**35.91**	**35.47**	**34.67**	**34.25**
Cooling Water Temperature (C)	**10**	**15**	**20**	**24**	**28**	**32**	**36**	**38**
Main Comp Inlet Temp (C)	**32**	**32**	**32**	**32**	**34**	**38**	**41**	**43**
Main Comp Inlet Pressure (MPa)	7.68	7.68	7.68	7.68	7.66	7.64	7.63	7.63
Main Comp Outlet Pressure (MPa)	20.0	20.0	20.0	20.0	20.0	20.0	20.0	20.0
Main Comp Outlet Temp (°C)	61.0	61.0	61.0	61.0	91.7	107.3	114.4	118.4
Main Comp Pressure Ratio	2.6	2.6	2.6	2.6	2.61	2.62	2.62	2.62
Turbine inlet temperature (°C)	550.0	550.0	550.0	550.0	550.0	550.0	550.0	550.0
Turbine inlet pressure (MPa)	19.33	19.33	19.33	19.33	19.23	19.15	19.11	19.10
Turbine outlet pressure (MPa)	7.89	7.89	7.89	7.89	8.00	8.07	8.10	8.12
Turbine outlet temperature (°C)	441.5	441.5	441.5	441.5	443.6	445.2	445.9	446.2
Turbine pressure ratio	2.45	2.45	2.45	2.45	2.40	2.37	2.36	2.35
Mass Flow (kg/s)	**215.8**	**215.8**	**215.8**	**215.8**	**250.0**	**269.2**	**277.2**	**281.5**

*The 32°C optimized cycle has only one chart because the 32°C compressor inlet temperature is the lower cycle limit to remain above the critical point.

Table 4.15a Simple cycle design optimized for 35°C compressor inlet (variable)

Optimized for a 35°C Compressor Inlet Temperature, 31°C Cooling Water Temperature (Variable Compressor Inlet)								
Electric Power Rating ($MW_{electric}$)	20.21	20.20	20.16	19.92	20.31	19.96	19.51	19.24
Thermal Power ($MW_{thermal}$)	56	56	56	56	56	56	56	56
Maximum operating pressure (MPa)	20	20	20	20	20	20	20	20
Minimum operating pressure (MPa)	7.68	7.68	7.68	7.68	7.66	7.65	7.64	7.63
Cycle net efficiency (%)	**36.06**	**36.04**	**35.97**	**35.54**	**36.23**	**35.6**	**34.8**	**34.4**
Cooling Water Temperature (C)	**10**	**15**	**20**	**24**	**28**	**32**	**36**	**38**
Main Comp Inlet Temp (C)	**32**	**32**	**32**	**32**	**34**	**36**	**39**	**41**
Main Comp Inlet Pressure (MPa)	7.68	7.68	7.68	7.68	7.66	7.65	7.64	7.63
Main Comp Outlet Pressure (MPa)	20.0	20.0	20.0	20.0	20.0	20.0	20.0	20.0
Main Comp Outlet Temp (°C)	61.0	61.0	61.0	61.0	91.7	101.2	109.8	114.4
Main Comp Pressure Ratio	2.60	2.60	2.60	2.60	2.61	2.61	2.62	2.62
Turbine inlet temperature (°C)	550.0	550.0	550.0	550.0	550.0	550.0	550.0	550.0
Turbine inlet pressure (MPa)	19.34	19.34	19.34	19.34	19.25	19.21	19.17	19.15
Turbine outlet pressure (MPa)	7.88	7.88	7.88	7.88	7.98	8.02	8.06	8.08
Turbine outlet temperature (°C)	441.3	441.3	441.3	441.3	443.3	444.1	444.8	445.3
Turbine pressure ratio	2.45	2.45	2.45	2.45	2.41	2.40	2.38	2.37
Mass Flow (kg/s)	**213.8**	**213.8**	**213.8**	**213.8**	**247.2**	**258.4**	**267.8**	**272.1**

Table 4.15b Simple cycle design optimized for 35°C compressor inlet (constant)

Optimized for a 35°C Compressor Inlet Temperature, 31°C Cooling Water Temperature (Constant Compressor Inlet)									
Electric Power Rating ($MW_{electric}$)		20.23	20.23	20.22	20.22	20.20	19.96	19.51	19.24
Thermal Power ($MW_{thermal}$)		56	56	56	56	56	56	56	56
Maximum operating pressure (MPa)		20	20	20	20	20	20	20	20
Minimum operating pressure (MPa)		7.65	7.65	7.65	7.65	7.65	7.65	7.64	7.63
Cycle net efficiency (%)		**36.08**	**36.08**	**36.07**	**36.06**	**36.02**	**35.6**	**34.8**	**34.4**
Cooling Water Temperature (C)		**10**	**15**	**20**	**24**	**28**	**32**	**36**	**38**
Main Comp Inlet Temp (C)		**35**	**35**	**35**	**35**	**35**	**36**	**39**	**41**
Main Comp Inlet Pressure (MPa)		7.65	7.65	7.65	7.65	7.65	7.65	7.64	7.63
Main Comp Outlet Pressure (MPa)		20.0	20.0	20.0	20.0	20.0	20.0	20.0	20.0
Main Comp Outlet Temp (°C)		97.2	97.2	97.2	97.2	97.2	101.2	109.8	114.4
Main Comp Pressure Ratio		2.61	2.61	2.61	2.61	2.61	2.61	2.62	2.62
Turbine inlet temperature (°C)		550.0	550.0	550.0	550.0	550.0	550.0	550.0	550.0
Turbine inlet pressure (MPa)		19.22	19.22	19.22	19.22	19.22	19.21	19.17	19.15
Turbine outlet pressure (MPa)		8.01	8.01	8.01	8.01	8.01	8.02	8.06	8.08
Turbine outlet temperature (°C)		443.8	443.8	443.8	443.8	443.8	444.1	444.8	445.3
Turbine pressure ratio		2.40	2.40	2.40	2.40	2.40	2.40	2.38	2.37
Mass Flow (kg/s)		**253.9**	**253.9**	**253.9**	**253.9**	**253.8**	**258.4**	**267.8**	**272.1**

Table 4.16a Simple cycle design optimized for 38°C compressor inlet (variable)

Optimized for a 38°C Compressor Inlet Temperature, 34°C Cooling Water Temperature (Variable Inlet Temp)									
Electric Power Rating ($MW_{electric}$)		20.59	20.58	20.53	20.06	20.66	20.25	19.81	19.53
Thermal Power ($MW_{thermal}$)		57	57	57	57	57	57	57	57
Maximum operating pressure (MPa)		20	20	20	20	20	20	20	20
Minimum operating pressure (MPa)		7.68	7.68	7.68	7.68	7.66	7.64	7.63	7.63
Cycle net efficiency (%)		**36.09**	**36.07**	**35.99**	**35.17**	**36.20**	**35.49**	**34.70**	**34.28**
Cooling Water Temperature (C)		**10**	**15**	**20**	**24**	**28**	**32**	**36**	**38**
Main Comp Inlet Temp (C)		**32**	**32**	**32**	**32**	**34**	**36**	**40**	**42**
Main Comp Inlet Pressure (MPa)		7.68	7.68	7.68	7.68	7.66	7.64	7.63	7.63
Main Comp Outlet Pressure (MPa)		20.0	20.0	20.0	20.0	20.0	20.0	20.0	20.0
Main Comp Outlet Temp (°C)		61.0	61.0	61.0	61.0	91.7	104.5	112.2	116.4
Main Comp Pressure Ratio		2.60	2.60	2.60	2.60	2.61	2.62	2.62	2.62
Turbine inlet temperature (°C)		550.0	550.0	550.0	550.0	550.0	550.0	550.0	550.0
Turbine inlet pressure (MPa)		19.34	19.34	19.34	19.34	19.24	19.19	19.16	19.14
Turbine outlet pressure (MPa)		7.88	7.88	7.87	7.87	7.97	8.02	8.05	8.07
Turbine outlet temperature (°C)		441.2	441.2	441.2	441.2	443.2	444.2	444.9	445.2
Turbine pressure ratio		2.45	2.45	2.46	2.46	2.41	2.39	238	2.37
Mass Flow (kg/s)		**217.6**	**217.6**	**217.6**	**217.6**	**251.6**	**266.7**	**275.0**	**278.9**

Table 4.16b Simple cycle design optimized for 38°C compressor inlet (constant)

Optimized for a 38°C Compressor Inlet Temperature, 34°C Cooling Water Temperature (Constant Inlet Temp)									
Electric Power Rating ($MW_{electric}$)		20.19	20.19	20.19	20.18	20.18	20.15	19.81	19.53
Thermal Power ($MW_{thermal}$)		57	57	57	57	57	57	57	57
Maximum operating pressure (MPa)		20	20	20	20	20	20	20	20
Minimum operating pressure (MPa)		7.64	7.64	7.64	7.64	7.64	7.64	7.63	7.63
Cycle net efficiency (%)		**35.39**	**35.38**	**35.38**	**35.37**	**35.36**	**35.31**	**34.71**	**34.28**
Cooling Water Temperature (C)		**10**	**15**	**20**	**24**	**28**	**32**	**36**	**38**
Main Comp Inlet Temp (C)		**38**	**38**	**38**	**38**	**38**	**38**	**40**	**42**
Main Comp Inlet Pressure (MPa)		7.64	7.64	7.64	7.64	7.64	7.64	7.63	7.63
Main Comp Outlet Pressure (MPa)		20.0	20.0	20.0	20.0	20.0	20.0	20.0	20.0
Main Comp Outlet Temp (°C)		107.4	107.3	107.3	107.3	107.3	107.3	112.2	116.4
Main Comp Pressure Ratio		2.62	2.62	2.62	2.62	2.62	2.62	2.62	2.62
Turbine inlet temperature (°C)		550.0	550.0	550.0	550.0	550.0	550.0	550.0	550.0
Turbine inlet pressure (MPa)		19.18	19.18	19.18	19.18	19.18	19.18	19.16	19.14
Turbine outlet pressure (MPa)		8.04	8.04	8.04	8.04	8.04	8.03	8.05	8.07
Turbine outlet temperature (°C)		444.5	444.5	444.5	444.5	444.5	444.5	444.9	445.2
Turbine pressure ratio		2.39	2.39	2.39	2.39	2.39	2.39	2.38	2.37
Mass Flow (kg/s)		**270.0**	**270.0**	**270.0**	**270.0**	**270.0**	**270.0**	**275.0**	**278.9**

Table 4.17a Simple cycle design optimized for 42° compressor inlet (variable)

Optimized for a 42°C Compressor Inlet Temperature, 38°C Cooling Water Temperature (Variable Inlet Temp)									
Electric Power Rating ($MW_{electric}$)		21.24	21.22	21.16	20.27	21.23	20.84	20.35	20.12
Thermal Power ($MW_{thermal}$)		59	59	59	59	59	59	59	60
Maximum operating pressure (MPa)		20	20	20	20	20	20	20	20
Minimum operating pressure (MPa)		7.68	7.68	7.68	7.68	7.65	7.64	7.63	7.63
Cycle net efficiency (%)		**35.97**	**35.95**	**35.62**	**34.33**	**35.95**	**35.28**	**34.50**	**34.07**
Cooling Water Temperature (C)		**10**	**15**	**20**	**24**	**28**	**32**	**36**	**38**
Main Comp Inlet Temp (C)		**32**	**32**	**32**	**32**	**34**	**37**	**40**	**42**
Main Comp Inlet Pressure (MPa)		7.68	7.68	7.68	7.67	7.65	7.64	7.63	7.63
Main Comp Outlet Pressure (MPa)		20.0	20.0	20.0	20.0	20.0	20.0	20.0	20.0
Main Comp Outlet Temp (°C)		61.0	61.0	61.0	61.0	91.7	104.5	112.2	116.4
Main Comp Pressure Ratio		2.6	2.6	2.6	2.61	2.61	2.62	2.62	2.62
Turbine inlet temperature (°C)		550.0	550.0	550.0	550.0	550.0	550.0	550.0	550.0
Turbine inlet pressure (MPa)		19.34	19.34	19.34	19.34	19.25	19.20	19.17	19.16
Turbine outlet pressure (MPa)		7.87	7.87	7.87	7.87	7.96	8.01	8.04	8.05
Turbine outlet temperature (°C)		441.1	441.1	441.1	441.1	443.0	443.9	444.5	444.9
Turbine pressure ratio		2.46	2.46	2.46	2.46	2.42	2.34	2.34	2.38
Mass Flow (kg/s)		**224.2**	**224.2**	**224.2**	**224.2**	**258.9**	**274.0**	**282.3**	**286.6**

Table 4.17b Simple cycle design optimized for constant compressor inlet

Optimized for a 42°C Compressor Inlet Temperature, 38°C Cooling Water Temperature (Constant Inlet Temp)								
Electric Power Rating ($MW_{electric}$)	20.25	20.24	20.24	20.24	20.24	20.23	20.17	20.12
Thermal Power ($MW_{thermal}$)	59	59	59	59	59	59	59	59
Maximum operating pressure (MPa)	20	20	20	20	20	20	20	20
Minimum operating pressure (MPa)	7.63	7.63	7.63	7.63	7.63	7.63	7.63	7.63
Cycle net efficiency (%)	**34.29**	**34.28**	**34.28**	**34.28**	**34.27**	**34.26**	**34.21**	**34.07**
Cooling Water Temperature (C)	**10**	**15**	**20**	**24**	**28**	**32**	**36**	**38**
Main Comp Inlet Temp (C)	**42**	**42**	**42**	**42**	**42**	**42**	**42**	**42**
Main Comp Inlet Pressure (MPa)	7.63	7.63	7.63	7.63	7.63	7.63	7.63	7.63
Main Comp Outlet Pressure (MPa)	20.0	20.0	20.0	20.0	20.0	20.0	20.0	20.0
Main Comp Outlet Temp (°C)	116.4	116.4	116.4	116.4	116.4	116.4	116.4	116.4
Main Comp Pressure Ratio	2.62	2.62	2.62	2.62	2.62	2.62	2.62	2.62
Turbine inlet temperature (°C)	550.0	550.0	550.0	550.0	550.0	550.0	550.0	550.0
Turbine inlet pressure (MPa)	19.16	19.16	19.16	19.16	19.16	19.16	19.15	19.16
Turbine outlet pressure (MPa)	8.06	8.06	8.06	8.06	8.06	8.06	8.06	8.05
Turbine outlet temperature (°C)	445.0	445.0	445.0	445.0	445.0	445.0	445.0	444.9
Turbine pressure ratio	2.38	2.38	2.38	2.38	2.38	2.38	2.38	2.38
Mass Flow (kg/s)	**286.8**	**286.8**	**286.8**	**286.7**	**286.7**	**286.7**	**286.4**	**286.6**

Comparing the two tactics to handle the changing cooling water temperatures: the variable compressor inlet temperature case exhibits higher net cycle efficiency for lower cooling water temperatures, but has a large mass flow rate difference between the two extremes, and the constant compressor inlet temperature case has a more constant mass flow rate across the temperature range. Although the variation of the CO_2 mass flow rate with temperature may not seem significant, there is a significant issue not seen from these tables. Comparing the 24°C and 38°C cooling water temperature cases in Table 4.14, one can observe that flow rate is increased from 215.8 to 281.5 kg/s, or by only 30%. However, CO_2 density at the compressor inlet between the 32°C and 42°C temperatures is reduced from 600 to 225 kg/m^3, or 2.6 times. Therefore, the volumetric flow rate between these two cases is increased 3.4 times! Such a large change of volumetric flow rate will not be possible to accommodate in a compressor of given geometry. Therefore, it is recommended that the cycle be optimized close to the highest cooling water temperature expected, and that compressor inlet temperature be maintained close to constant. Also, optimizing the design further from the critical point reduces rapid density changes and provides more flexibility for control. Note that between 38 °C and 42 °C compressor inlet temperature in Table 4.16b, flow rate increases by 3%, density decreases by 12% and volumetric flow rate by 15%. These changes can most likely be accommodated by the compressor. Further, it is noted that the efficiency of the cycle

optimized at 38°C compressor inlet temperature (32°C water temperature) is 35.3%, which is almost the same as the efficiency for the cycle optimized at 32°C for the same cooling water conditions. If the 38°C cycle were to operate in cooling water at 10°C, the efficiency loss versus the 32°C cycle is only 1%. This is very small penalty considering the serious issues of compressor operation that would have to be addressed for the 32°C cycle.

4.7 T-s Diagram of Simple S-CO_2 Cycle

A T-s diagram of the simple cycle at a turbine inlet temperature of 550°C was generated to elucidate the location of the state points relative to the dome. The diagram is shown on Figure 4.20 and an expanded region near the dome, for better resolution, is shown on Figure 4.21.

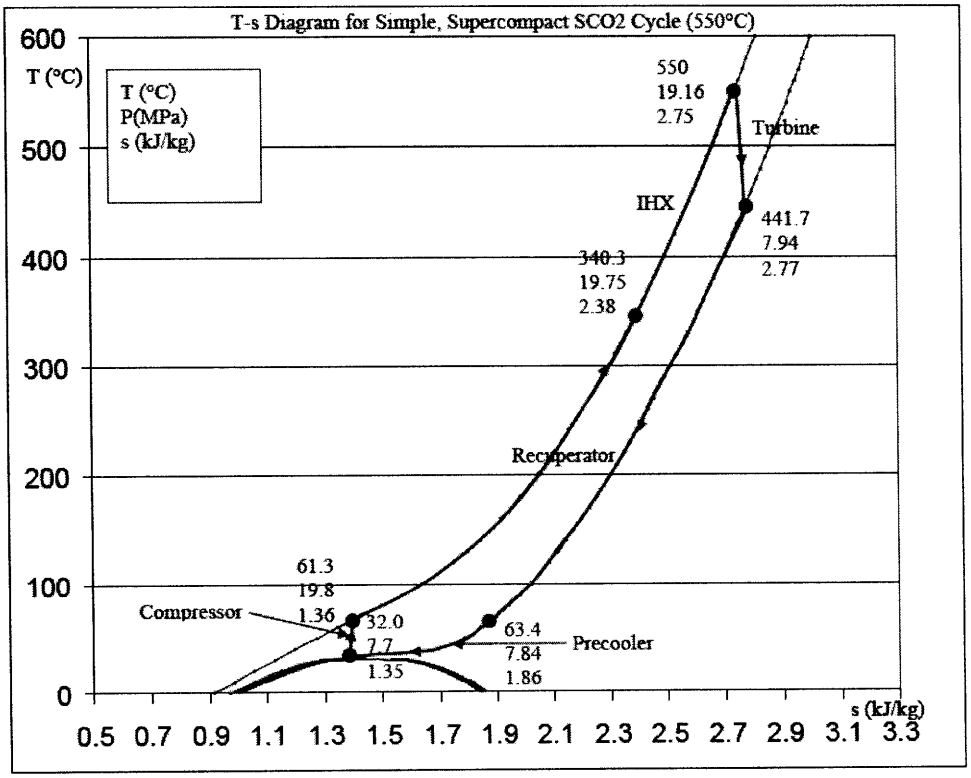

Figure 4.20 T-s Diagram for simple S-CO_2 cycle [Hejzlar, et. al., 2006]

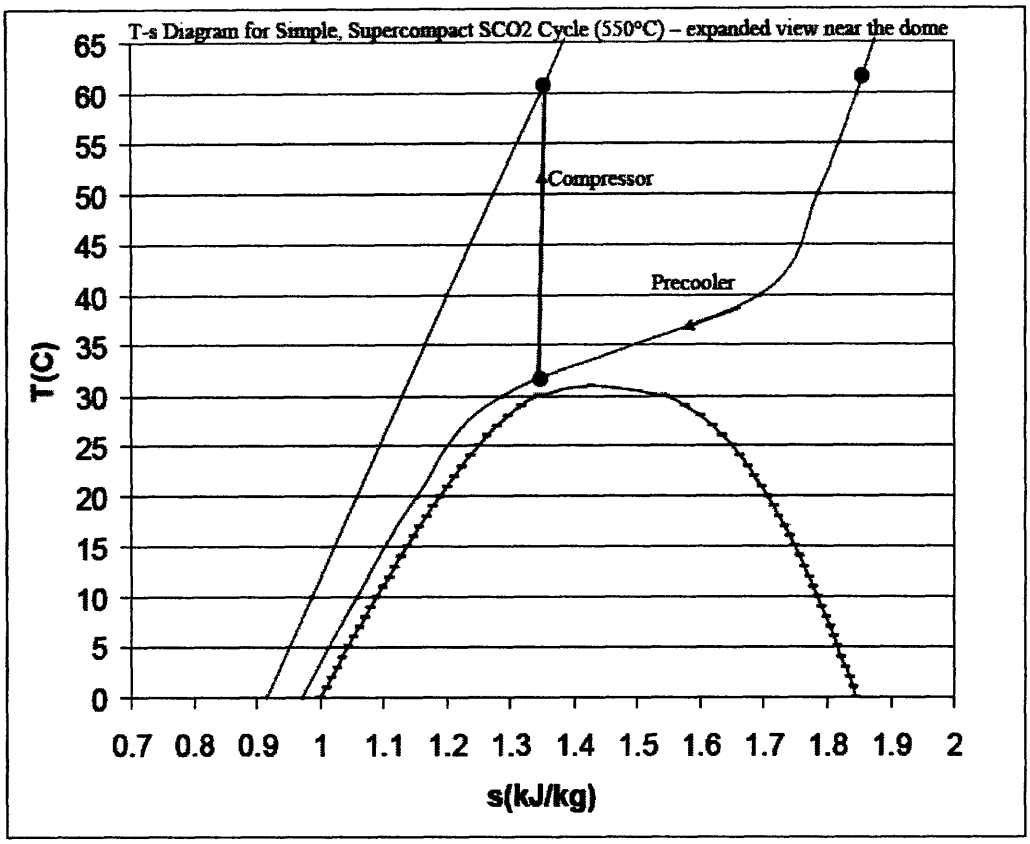

Figure 4.21 T-s Diagram for simple CO_2 cycle – expanded view at dome [Hejzlar, et. al., 2006]

4.8 Chapter Summary and Conclusions

This chapter expanded on the concept of simplifying the recompression cycle to obtain a simple S-CO_2 PCS. The simple cycle exhibits a lower net cycle efficiency, but has the advantage of eliminating the need for one recuperator and one compressor, and leads to a considerably smaller footprint. The same conditions were applied to the simple cycle (650°C, 550°C turbine inlet temperature and 20 MPa compressor outlet pressure), but we also explored the possibility of increasing the compressor outlet pressure to 28 MPa to recuperate some of the thermodynamic losses associated with going away from the recompression cycle.

The simple cycle appears to be ideal for applications with space restrictions if peak cycle efficiency is not the primary objective. The 650°C turbine inlet temperature design is still

able to reach approximately 40% efficiency and the 550°C design is able to reach approximately 36% net cycle efficiency for a 32°C compressor inlet temperature, and 34% and 36%, respectively, for a 42°C compressor inlet temperature. These efficiencies, although not as impressive as the recompression cycle, are competitive with most Rankine cycles, but with a considerably larger power density. Furthermore, if the simple cycle was increased in peak cycle pressure to 28 MPa, it would be able to almost match the performance of the recompression cycle, with approximately 44% efficiency for a 650°C turbine inlet temperature, and 40% with a 550°C turbine inlet temperature. Increasing the peak pressure to 28 MPa is more judicious for the 550°C turbine inlet temperature design, due to material constraints, but recent materials science research and development suggests that a cycle operating at 650°C turbine inlet temperature and 28 MPa may be in the foreseeable future (see section 1.8).

Overall, as with the recompression cycle, the sensitivity studies suggest that the S-CO_2 PCS performance is not very sensitive to degradation, and that the turbine inlet temperature is the most important parameter affecting the cycle. The simple cycle is able to operate at lower turbine inlet temperatures than the recompression cycle, but the efficiency penalty is large.

4.9 References for Chapter 4

Atwood & Morrill Co., Inc., "Engineered Valve Products & Solutions", A&M 010304.

Deng S.J., Veziroglu T.N., Tan, Y.K. and Chen L.Q., Heat Transfer Enhancement and Energy Conservation, Hemisphere Publishing Corporation, New York, 1990.

Gong Y., Carstens N.A., Driscoll M.J., Matthews I.A., "Analysis of Radial Compressor Options for Supercritical CO2 Power Conversion Cycles", MIT CANES Report MIT-GFR-034, June 2006.

Hejzlar P., Driscoll M.J., Gibbs J., Gong Y., Kao S., "Supercritical CO_2 Brayton Cycle for Medium Power Applications", MIT Report CANES-ANP-PR-117, April 2006.

Idelchik, I.E., Handbook of Hydraulic Resistance, 3rd ed., CRC Press, p. 752, 1993

Shade, N., "Enormous Power In A Small Package", Compressor Tech Two, January-February 2006

SOLID EDGE™ Version 17.00.02.04 © 2005 UGS

5 Summary, Conclusions, and Recommendations for Future Work

5.1 Summary and Conclusions

Third generation versions of the recompression and simple-type supercritical CO_2 Brayton power conversion system (PCS) have been developed for use with Generation IV reactor systems. The third generation layouts evolved from the initial integral version similar to the GA GTMHR, to a dispersed component arrangement similar to the ESKOM PBMR, to the final layout described in this work. The prior work at MIT, which was focused on a PCS rated at 300 MWe, was extended to cover the range between 20 and 1200 MWe, to demonstrate applicability to the small, medium, and large reactor power designs under consideration. The recompression cycle is applicable to all power ratings covered in this work, but it is expected that the simple cycle will be employed for smaller power ratings. In the interests of specificity, the reference primary coolant is postulated to be sodium, in view of the recent designation of the sodium cooled fast reactor as the system of choice for the GNEP program. However, no significant differences would be encountered if lead or liquid salt coolants are substituted. Gas phase coolants would require larger IHX surfaces and/or primary-to-CO_2 temperature differences, as well as a significantly higher primary coolant pumping power, with an attendant loss in overall plant thermal efficiency.

One of the principal efforts in carrying out this work was the downselection among the many options available for the S-CO_2 PCS. Two high level choices are (1) indirect versus direct cycle and (2) recompression cycle versus simple cycle. Direct and indirect layouts were presented in this work, but the primary focus is on the indirect cycle. As previously mentioned, it is anticipated that the sodium cooled fast reactor is a prime candidate for a 550°C, indirect, recompression cycle. Furthermore, it is expected that the direct cycle will be coupled to a S-CO_2 cooled nuclear reactor able to achieve a 650°C outlet temperature. Both the recompression and simple S-CO_2 versions are promising and should be retained for further investigation and development. The recompression

versus simple cycle selection may be also driven by space constraints versus achievable efficiency. The simple cycle is appealing because of its high power density, but the recompression cycle is able to achieve higher cycle efficiencies and should be used for large scale power generation. The simple cycle will be preferable in applications with tight space restrictions, while the recompression cycle may be more suitable in applications where space requirements are less demanding and high efficiency is preferable. In either case, the availability of two S-CO_2 cycle alternatives is an asset because it expands the choices available to meet specific needs.

The MIT in-house computer code, CYCLES, which was used for cycle thermodynamic analyses and optimization, was enhanced by adding a model of HEATRIC™ Printed Circuit Heat Exchangers (PCHE). The high and lower temperature recuperators will employ zigzag channels and the precooler will use straight channels. In addition to high power densities of the heat exchanger cores (~30 MW/m^3), other key considerations supporting the choice to use PCHEs include ruggedness and their capability to accommodate a large pressure differential between the high and lower pressure sides (20 MPa against 8 MPa). In addition, SOLID EDGE was used to develop the layouts and determine the flow geometries for the calculations performed with CYCLES.

After CYCLES was further enhanced to model the effect of pressure drops in the piping and distribution plena, the results showed that these pressure drops significantly impact cycle efficiency and need to be included in cycle analyses. In fact, pipe pressure losses can limit power ratings of Brayton cycle units, including the supercritical CO_2 cycle, and large diameter piping is needed to avoid these losses. The high pressure losses were a considerable driver to employ modular and parallel arrangements for large power ratings. This is because the small specific heat of CO_2 requires large mass flow rates, and large power ratings would require either custom fabricated large diameter pipes or many parallel runs with smaller pipes, which are readily available. In addition, the high temperature and pressure in the cycle motivate the employment of parallel piping to more easily accommodate stress. This work showed that well designed PCHE plena and

interconnecting piping for the various power ratings of interest incur an efficiency penalty of only 1%.

The recompression cycle employs two compressors (main and recompression) working in parallel and two recuperators (high and low temperature) and maximizes cycle efficiency while striving for a small plant footprint. The simple cycle has only one compressor and one recuperator. The main focus of the simple S-CO_2 design is cycle compactness and simplicity while achieving still attractive efficiency. The main designs with their corresponding performance are recorded in Tables 5.1 and 5.2 for the recompression and simple cycles, respectively. For the same cycle parameters (turbine inlet temperature of 650°C, highest cycle pressure of 20 MPa, pressure ratio of 2.6, and main compressor inlet temperature of 32°C) net cycle efficiency was calculated to be 39.7%, which is approximately 8% lower than the recompression cycle. The difference in recompression cycle versus simple cycle efficiency is dependent on several factors and the simple cycle is typically 5-8% lower than the recompression cycle. The turbomachinery efficiencies are large contributors to the difference in cycle efficiencies. Table 5.1 also has the performance data for the large (1200 MWe) power rating for both the 550°C and 650°C designs. Table 5.2 has the performance data for the 550°C and 650°C designs, but only for a 20 MWe power rating.

Table 5.1 Recompression cycle performance and primary parameters

Parameter				
Power rating (MWe)	20	20	1200	1200
Turbine inlet temperature (°C)	**650**	**550**	**650**	**550**
Peak cycle pressure (MPa)	20	20	20	20
Compressor inlet temperature (°C)	32	32	32	32
Cooling water temperature (°C)	20	20	20	20
Turbine efficiency (%)	93.4	93.4	95	95
Recompressing compressor efficiency (%)	85	85	85	85
Main compressor efficiency (%)	86	86	87	87
Net cycle efficiency (%)	**47.8**	**41.5**	**48.0**	**42.1**

Table 5.2 Simple cycle performance and primary parameters

Parameter		
Power rating (MWe)	20	20
Turbine inlet temperature (°C)	**650**	**550**
Peak cycle pressure (MPa)	20	20
Compressor inlet temperature (°C)	32	32
Cooling water temperature (°C)	20	20
Turbine efficiency (%)	91.2	91.4
Compressor efficiency (%)	90	90
Net cycle efficiency (%)	**39.7**	**36.1**

The layouts for all of the power ratings employ the dispersed approach, with modular heat exchangers. The number of heat exchanger modules depends on the required power rating: the 20 MWe rating uses only 1 module each for the HTR, LTR, and precooler; and the 1200 MWe ratings use 64 modules each for the HTR and LTR and 32 modules for the precooler. The smaller power ratings do not appear to have significant problems with limits on machinery/component sizes with respect to ductwork/piping constraints, generator sizes, or turbomachinery stresses. However, the principal factors leading to the high power rating layouts were as follows:

1. Turbine blade stress limits one to about 600 MWe per turbine, even at the slow 1800 RPM common to most large electric generators.
2. High pressure/high temperature ductwork and valve diameters were limited to about one meter to stay within current industrial practice.
3. Avoiding an excessive pressure drop penalty on cycle efficiency then restricts heat exchanger train capacity to about 650 MWth (300 MWe)
4. To achieve the required closely-coupled compact arrangement, multiple printed circuit heat exchangers (PCHE), of the type manufactured by Heatric™, are employed in parallel clusters in each train.

Extensive sensitivity studies were performed for both the recompression and simple S-CO_2 cycles to determine areas which could lead to performance improvement, or performance degradation. Cycle efficiency is most sensitive to turbine inlet temperature.

For the recompression cycle, the efficiency reduction is from 47.8% at 650°C to 32% at 400°C. Moreover, reducing the temperature from 550°C to 400°C requires an increase of total volume of heat exchangers by a factor of 3 to maintain reasonable efficiency. Reducing the turbine inlet temperature to below 400°C will make the cycle unattractive due to the lower thermodynamic efficiency and even larger heat exchangers. Furthermore, the cycle efficiency begins to deteriorate more quickly below 400°C because the lower turbine inlet temperatures require higher mass flow rates, which in turn result in higher component pressure losses, deteriorating the performance. The simple cycle exhibits similar performance deterioration at lower temperatures, but can be optimized at temperatures below 400°C. If net cycle efficiency above 20% is desired, the minimum turbine inlet temperature needs to be 300°C. The simple cycle is also similar to the recompression cycle in that the total volume of heat exchangers must also increase with a decreasing temperature, but to a lesser degree (1.8 times the heat exchanger volume used for the 550°C design). Therefore, the conclusion is that S-CO_2 cycles perform much better at higher turbine inlet temperatures.

Cycle maximum pressure is another important parameter affecting cycle efficiency, although to a smaller extent than turbine inlet temperature. Higher pressure gives higher efficiency, but this gain gradually saturates around 28 MPa, especially for the simple cycle, which exhibits efficiency reduction after 28 MPa. There are two key factors affecting this trend: first, as pressure increases, flow rate is reduced, resulting in smaller pressure drops and increased cycle efficiency; second, a larger enthalpy rise across the intermediate heat exchanger at higher pressure leads to reduced average temperature at which heat is added to the cycle, decreasing cycle efficiency. At lower pressures, the first effect is dominant, at higher pressures the second effect begins to prevail. With a turbine inlet temperature of 550°C, the recompression cycle exhibits net efficiency changes between 34% and 42% in the pressure range between 16 and 23 MPa, while the simple cycle varies between 28.5% and 36.1% in the same pressure range.

Sensitivity of power cycle efficiency to compressor efficiency is very small due to small pumping power when compressing near the critical point. Turbine efficiency affects

cycle efficiency to a larger extent, but the impact is not excessive. Even a relatively large reduction in turbine efficiency by 5% (i.e. going from 90% to 85%) would reduce the cycle efficiency by only 2% (i.e. from 47.25% to 45.2%). Increase of turbine tip clearance by a factor of 3 would result in a cycle efficiency decrease by 0.6% [Hejzlar, et. al, 2006]. Hence, the deterioration of turbomachinery performance will have a small impact on overall S-CO_2 cycle performance. This conclusion holds for both the recompression and simple cycles.

Cycle performance is also very resistant to plugging and fouling of heat exchanger channels. For the recompression cycle, plugging 20% of the channels in all PCHEs would reduce the efficiency by approximately 2%. The sensitivity of cycle efficiency to fouling of heat exchangers is also small, with loss of efficiency of 1.5% if all heat transfer surfaces build up a maximum oxide layer of 100 microns. The higher temperature recuperator is the least sensitive, followed by the low temperature recuperator, and the precooler having the largest impact due to the CO_2/H_2O heat transfer. The water heat transfer resistance is small; hence resistance of oxides becomes important at 60 microns thickness and higher, which makes it more difficult for the water to remove energy. The important conclusion from the fouling study is that the precooler needs to be designed with a larger heat transfer surface (oversized by at least 20%) to provide margin for oxide growth and avoid significant performance deterioration. Increasing the precooler size is not a problem since it is a small heat exchanger in comparison with recuperators, and will not affect the PCS overall size appreciably. The simple cycle is even less sensitive to heat exchanger performance degradation, as the cycle does not see significant efficiency reduction until more than 25% of the channels of all PCHEs are blocked. As for the recompression cycle, cycle performance degradation with recuperator fouling is small, and the precooler needs to be overdesigned to provide sufficient margin to fouling on the water side.

Overall, it was found that S-CO_2 PCS performance is not very sensitive to degradation and achieves attractive efficiencies over a broad range of conditions.

5.2 Recommendations for Future Work

In terms of activities which could significantly affect the results summarized in this thesis, the following are worth attention:

Further Configuration Studies

- Although a fairly radical proposition, one could devise a more integral PCS component arrangement by employing a prestressed cast iron vessel (PCIV), hitherto considering mainly for housing the reactor itself [Fishkin, 2004]
- The Japanese have recently published data on an improved PCHE [Ishizuka, et. al., 2005], which could further shrink PCS heat exchanger size.
- Downselecting to fewer reference plant ratings would sharpen the focus on future design efforts.
- Foundations and supports should be designed to identify any potential problems
- Development of more detailed designs and PCS layouts for 600 and 1200 MWe turbomachinery trains to further evaluate the clustered PCS concepts sketched in Chapter 2 would be worthwhile.
- A re-assessment should be made of vertical turbomachinery and bearings as a function of rating.
- Development of a higher rating permanent magnet generator would be quite beneficial

Clarification of Temperature and Stress Constraints

- Carry out further corrosion tests in hot, high pressure CO_2 to set an upper limit on tolerable PCS temperature [Lim, Ballinger, 2006]
- Detailed design of insulation, especially internal
- Support ASME code cases to qualify metals at higher operating temperatures
- Thermal stress analyses, both steady state and transient
- Shaft and pressure stress analysis, to clarify whether to place the turbine closest to the generator or whether compressors can be in between, as depicted in all of the layout figures in this work

Design Auxiliary Systems

- CO_2 coolant storage, charging, and purification
- Evaluate the use of the PCS for shutdown heat removal
- Bearing and seal system design
- Evaluate the necessary maintenance and repair equipment/systems

Expand Control-Related Efforts

- Clarify hardware requirements – e.g. number, nature, and location of valves, and integrate these into the layouts
- Strive for complete automation, minimization of operator action
- Extend the capability for use of variable speed (e.g. permanent magnet) generators to higher plant ratings
- A modest effort is in order on multiple shaft turbomachinery, to have a viable fall-back position should intractable control problems arise for the one-shaft approach

In addition to the above PCS-specific aspects, in view of the recent GNEP initiative, which focuses on the sodium cooled fast reactor, a consensus needs to be reached on whether CO_2 is adequately compatible with sodium, to permit elimination of an intermediate primary-to-PCS loop. This would considerably strengthen the rationale for pursuing the SCO_2 PCS at higher priority. There is a growing amount of test data being reported on this issue [Choi, 2006] [Ishikawa, et. al., 2005].

5.3 References for Chapter 5

Choi J.H., et. al,, "Capsule Test for Investigating the Sodium-Carbon Dioxide Interaction," Proc. of ICAPP '06, Reno, June 2006

Fishkin L.B., "Prestressed Cast Iron Vessel (PCIV) Use for GEN-IV GFR Applications," MIT-GFR-006, April 2004

Hejzlar P., Driscoll M.J., Gibbs J.P., Gong Y., Kao S., "Supercritical CO_2 Brayton Cycle for Medium Power Applications", MIT Report CANES-ANP-PR-117, April 2006.

Ishikawa H., Miyahara S., Yoshizawa Y., "Experimental Study of Sodium-Carbon Dioxide Reaction," Proc. of ICAPP '05, Seoul, May 2005

Ishizuka T., Y. Kato, Y. Muto, K. Nikitin, N.L. Tri, and H. Hashimoto, "Thermal Hydraulic Characteristics of Printed Circuit Heat Exchanger in a Supercritical CO_2 Loop," Proc. of NURETH 11, Avignon, France, Oct. 2-6, 2005

Lim J., Li N., Ballinger R., "Materials Testing in Supercritical CO_2," *Trans. Am. Nucl. Soc.*, Vol. 94, June 2006

Appendix A1 Recompression Cycle Pipe Data

The piping data for the recompression cycle at various power ratings is contained in this appendix. The tables are broken into sections and organized in columns and rows to separate the various pertinent data for the piping calculations. Each section has a title to simply state which part of the cycle the data is for. The following headers with a brief description of their notation are explained below:

IP	Path number
Nsec:	number of sections with various flow areas in path IP
Npipe:	number of parallel passages in the specific section
Dpipe:	hydraulic diameter of the duct/passage in the specific section (m)
Apipe:	cross sectional flow area in the specific section (m^2)
ELpipe:	length of the duct/passage in the specific section (m)
xsi:	total form loss coefficient in the specific section
rough :	surface roughness of the pipe in the specific section
Section:	description of the section passage in the cycle

The 150 MWe piping data was also used to calculate the pressure losses in the 300 MWe layouts. The 300 MWe layout has twice the number of heat exchangers, pipes, and flow channels than the 150 MWe layout. Thus, with the 150 MWe layout having half the thermal power, flow rate, and piping, it is possible to directly calculate the performance of the 300 MWe layout by merely using appropriate turbomachinery efficiencies.

Table A1.1 – 5 MWe piping data

IP	Nsec	Npipe	Dpipe	Apipe	ELpipe	xsi	rough	Section
Precooler to main compressor								
1	4	6	0.1576	0.019500	0.2800	0.04	1.0E-04	!precooler outlet plenum LP
1		208	0.0030	0.000090	0.0050	1.20	1.0E-04	!precooler outlets LP
1		1	0.3500	0.140000	0.1500	0.40	1.0E-04	!precooler side plenum LP
1		1	0.0762	0.00456	3.3300	0.82	1.0E-04	!pipe to main compressor
Main compressor to LTR								
2	3	1	0.0762	0.004560	1.1700	1.716	1.0E-04	!pipe to LTR
2		1	0.3048	0.07297	0.3000	0.40	1.0E-04	!LTR inlet side plenum HP
2		6	0.0748	0.010410	0.3000	0.70	1.0E-04	!LTR inlet dist plena HP
LTR to merge T junction								
3	3	6	0.0748	0.010410	0.3000	0.70	1.0E-04	!LTR outlet dist plena HP
3		1	0.3556	0.099315	0.3000	0.40	1.0E-04	!LTR outlet side plenum HP
3		1	0.2032	0.032430	0.7874	1.32	1.0E-04	!Pipe from LTR to merge T
From merge T junction to HTR								
4	3	1	0.2032	0.032429	1.3700	1.00	1.0E-04	!Pipe from merge T to HTR
4		1	0.3556	0.099315	0.3000	0.40	1.0E-04	!HTR inlet side plenum HP
4		6	0.0748	0.010410	0.6250	0.70	1.0E-04	!HTR inlet dist plena HP
From HTR to IHX (reactor)								
5	3	6	0.0748	0.010410	0.6250	0.70	1.0E-04	!HTR outlet dist plena HP
5		1	0.3556	0.099315	0.3000	0.40	1.0E-04	!HTR outlet side plenum HP
5		1	0.1524	0.018242	1.0000	1.12	1.0E-04	!Pipe from HTR to IHX/RX
From IHX (reactor) to turbine								
6	1	1	0.1524	0.018242	1.0000	0.12	1.0E-04	!Pipe From IHX/RX to turb
From turbine to HTR								
7	4	1	0.2032	0.032430	0.3600	1.12	1.0E-04	!Pipe From turbine to HTR
7		1	0.3500	0.140000	0.6250	0.40	1.0E-04	!HTR inlet side plenum LP
7		2096	0.0030	0.000090	0.0050	1.20	1.0E-04	!HTR inlets LP
7		6	0.2811	0.048750	0.0800	0.40	1.0E-04	!HTR inlet plenum LP
From HTR to LTR								
8	7	6	0.2491	0.048750	0.2800	0.40	1.0E-04	!HTR outlet plenum LP
8		2096	0.0030	0.000090	0.0050	1.20	1.0E-04	!HTR outlets LP
8		1	0.3500	0.140000	0.6250	0.40	1.0E-04	!HTR outlet side plenum LP
8	1	1	0.2032	0.032430	1.9300	1.12	1.0E-04	!Pipe From HTR to LTR
8		1	0.3500	0.140000	0.5000	0.40	1.0E-04	!LTR inlet side plenum LP
8		1665	0.0030	0.000090	0.1000	1.20	1.0E-04	!LTR inlets LP
8		6	0.2228	0.039000	0.2800	0.40	1.0E-04	!LTR inlet plenum LP
From LTR to split T junction								
9	4	6	0.2228	0.039000	0.2800	0.40	1.0E-04	!LTR outlet plenum LP
9		1665	0.0030	0.000090	0.0050	1.20	1.0E-04	!LTR outlets LP
9		1	0.3500	0.140000	0.5000	0.40	1.0E-04	!LTR outlet side plenum LP
9		1	0.1524	0.018242	1.8300	2.12	1.0E-04	!Pipe From LTR to split T
From split T junction to precooler								
10	4	1	0.1524	0.018242	2.7400	1.0	1.0E-04	!Pipe From split T to PRE
10		1	0.3500	0.140000	0.5000	0.40	1.0E-04	!precooler side plenum LP
10		208	0.0030	0.000090	0.0050	1.20	1.0E-04	!precooler inlets LP
10		6	0.1576	0.019500	0.2800	0.04	1.0E-04	!precooler inlet plenum LP
From split T junction to recomp. comp.								
11	1	1	0.1524	0.018242	0.6900	0.50	1.0E-04	!Pipe From split T to RC
From recomp. comp. to merge T junction								
12	1	1	0.1524	0.018242	1.5800	0.796	1.0E-04	!Pipe From RC to merge T

Table A1.2 – 10 MWe piping data

IP	Nsec	Npipe	Dpipe	Apipe	ELpipe	xsi	rough	Section
Precooler to main compressor								
1	4	6	0.1576	0.019500	0.2800	0.04	1.0E-04	!precooler outlet plenum LP
1		415	0.0030	0.000090	0.0050	1.20	1.0E-04	!precooler outlets LP
1		1	0.3500	0.140000	0.3000	0.40	1.0E-04	!precooler side plenum LP
1		1	0.1524	0.018242	3.3300	0.82	1.0E-04	!pipe to main compressor
Main compressor to LTR								
2	3	1	0.1524	0.018242	1.1700	1.716	1.0E-04	!pipe to LTR
2		1	0.3048	0.072966	0.3000	0.40	1.0E-04	!LTR inlet side plenum HP
2		6	0.1151	0.010410	1.0000	0.70	1.0E-04	!LTR inlet distribution plena HP
LTR to merge T junction								
3	3	6	0.1151	0.010410	1.0000	0.70	1.0E-04	!LTR outlet distribution plena HP
3		1	0.3556	0.099315	0.3000	0.40	1.0E-04	!LTR outlet side plenum HP
3		1	0.2540	0.050671	0.7874	1.32	1.0E-04	!Pipe from LTR to merge T
From merge T junction to HTR								
4	3	1	0.2540	0.050671	1.3700	1.00	1.0E-04	!Pipe from merge T to HTR
4		1	0.3556	0.099315	0.3000	0.40	1.0E-04	!HTR inlet side plenum HP
4		6	0.1151	0.010410	1.2500	0.70	1.0E-04	!HTR inlet distribution plena HP
From HTR to IHX (reactor)								
5	3	6	0.2540	0.050671	1.2500	0.70	1.0E-04	!HTR outlet dist plena HP
5		1	0.3556	0.099315	0.3000	0.40	1.0E-04	!HTR outlet side plenum HP
5		1	0.3048	0.073000	1.0000	1.12	1.0E-04	!Pipe from HTR to IHX/RX
From IHX (reactor) to turbine								
6	1	1	0.2540	0.050671	1.0000	0.12	1.0E-04	!Pipe From IHX/RXto turbine
From turbine to HTR								
7	4	1	0.3048	0.072966	0.3600	1.12	1.0E-04	!Pipe From turbine to HTR
7		1	0.3500	0.140000	1.2500	0.40	1.0E-04	!HTR inlet side plenum LP
7		2096	0.0030	0.000090	0.0050	1.20	1.0E-04	!HTR inlets LP
7		6	0.2811	0.048750	0.0800	0.40	1.0E-04	!HTR inlet plenum LP
From HTR to LTR								
8	7	6	0.2491	0.048750	0.2800	0.40	1.0E-04	!HTR outlet plenum LP
8		2096	0.0030	0.000090	0.0050	1.20	1.0E-04	!HTR outlets LP
8		1	0.3500	0.140000	1.2500	0.40	1.0E-04	!HTR outlet side plenum LP
8	1	1	0.2540	0.050671	1.9300	1.12	1.0E-04	!Pipe From HTR to LTR
8		1	0.3500	0.140000	1.0000	0.40	1.0E-04	!LTR inlet side plenum LP
8		1665	0.0030	0.000090	0.1000	1.20	1.0E-04	!LTR inlets LP
8		6	0.2228	0.039000	0.2800	0.40	1.0E-04	!LTR inlet plenum LP
From LTR to split T junction								
9	4	6	0.2228	0.039000	0.2800	0.40	1.0E-04	!LTR outlet plenum LP
9		1665	0.0030	0.000090	0.0050	1.20	1.0E-04	!LTR outlets LP
9		1	0.3500	0.140000	1.0000	0.40	1.0E-04	!LTR outlet side plenum LP
9		1	0.2032	0.032429	1.8300	2.12	1.0E-04	!Pipe From LTR to split T
From split T junction to precooler								
10	4	1	0.2032	0.032429	1.7400	1.0	1.0E-04	!Pipe From split T to precooler
10		1	0.3500	0.140000	0.5000	0.40	1.0E-04	!precooler side plenum LP
10		415	0.0030	0.000090	0.0050	1.20	1.0E-04	!precooler inlets LP
10		6	0.1576	0.019500	0.2800	0.04	1.0E-04	!precooler inlet plenum LP
From split T junction to recomp. comp.								
11	1	1	0.2032	0.032429	0.6900	0.50	1.0E-04	!Pipe From split T to RC
From recomp. comp. to merge T junction								
12	1	1	0.2032	0.032429	2.5800	0.796	1.0E-04	!Pipe RC to merge T junction

Table A1.3 – 15 MWe piping data

IP	Nsec	Npipe	Dpipe	Apipe	ELpipe	xsi	rough	Section
Precooler to main compressor								
1	4	6	0.1576	0.019500	0.2800	0.04	1.0E-04	!precooler outlet plenum LP
1		623	0.0030	0.000090	0.0050	1.20	1.0E-04	!precooler outlets LP
1		1	0.3500	0.140000	0.3000	0.40	1.0E-04	!precooler side plenum LP
1		1	0.1524	0.018242	3.3300	0.82	1.0E-04	!pipe to main compressor
Main compressor to LTR								
2	3	1	0.1524	0.018242	1.1700	1.716	1.0E-04	!pipe to LTR
2		1	0.3048	0.072966	0.3000	0.40	1.0E-04	!LTR inlet side plenum HP
2		6	0.1151	0.010410	1.5000	0.70	1.0E-04	!LTR inlet distribution plena HP
LTR to merge T junction								
3	3	6	0.1151	0.010410	1.5000	0.70	1.0E-04	!LTR outlet dist plena HP
3		1	0.3556	0.099315	0.3000	0.40	1.0E-04	!LTR outlet side plenum HP
3		1	0.3048	0.072966	0.7874	1.32	1.0E-04	!Pipe from LTR to merge T
From merge T junction to HTR								
4	3	1	0.3048	0.072966	1.3700	1.00	1.0E-04	!Pipe from merge T to HTR
4		1	0.3556	0.099315	0.3000	0.40	1.0E-04	!HTR inlet side plenum HP
4		6	0.1151	0.010410	1.8750	0.70	1.0E-04	!HTR inlet distribution plena HP
From HTR to IHX (reactor)								
5	3	6	0.1151	0.010410	1.8750	0.70	1.0E-04	!HTR outlet dist plena HP
5		1	0.3556	0.099315	0.3000	0.40	1.0E-04	!HTR outlet side plenum HP
5		1	0.3048	0.072966	1.0000	1.12	1.0E-04	!Pipe from HTR to IHX (reactor)
From IHX (reactor) to turbine								
6	1	1	0.2540	0.050671	1.0000	0.12	1.0E-04	!Pipe From IHX/RX to turbine
From turbine to HTR								
7	4	1	0.3556	0.099315	0.3600	1.12	1.0E-04	!Pipe From turbine to HTR
7		1	0.3500	0.140000	1.8750	0.40	1.0E-04	!HTR inlet side plenum LP
7		3144	0.0030	0.000090	0.0050	1.20	1.0E-04	!HTR inlets LP
7		6	0.2811	0.048750	0.0800	0.40	1.0E-04	!HTR inlet plenum LP
From HTR to LTR								
8	7	6	0.2491	0.048750	0.2800	0.40	1.0E-04	!HTR outlet plenum LP
8		3144	0.0030	0.000090	0.0050	1.20	1.0E-04	!HTR outlets LP
8		1	0.3500	0.140000	1.8750	0.40	1.0E-04	!HTR outlet side plenum LP
8	1	1	0.3048	0.072966	1.9300	1.12	1.0E-04	!Pipe From HTR to LTR
8		1	0.3500	0.140000	1.5000	0.40	1.0E-04	!LTR inlet side plenum LP
8		2498	0.0030	0.000090	0.1000	1.20	1.0E-04	!LTR inlets LP
8		6	0.2228	0.039000	0.2800	0.40	1.0E-04	!LTR inlet plenum LP
From LTR to split T junction								
9	4	6	0.2228	0.039000	0.2800	0.40	1.0E-04	!LTR outlet plenum LP
9		2498	0.0030	0.000090	0.0050	1.20	1.0E-04	!LTR outlets LP
9		1	0.3500	0.140000	0.5000	0.40	1.0E-04	!LTR outlet side plenum LP
9		1	0.2540	0.050671	1.8300	2.12	1.0E-04	!Pipe From LTR to split T
From split T junction to precooler								
10	4	1	0.2540	0.050671	2.7400	1.0	1.0E-04	!Pipe From split T to precooler
10		1	0.3500	0.140000	0.5000	0.40	1.0E-04	!precooler side plenum LP
10		623	0.0030	0.000090	0.0050	1.20	1.0E-04	!precooler inlets LP
10		6	0.1576	0.019500	0.2800	0.04	1.0E-04	!precooler inlet plenum LP
From split T junction to recomp. comp.								
11	1	1	0.2540	0.050671	0.6900	0.50	1.0E-04	!Pipe From split T RC
From recomp. comp. to merge T junction								
12	1	1	0.2540	0.050671	2.5800	0.796	1.0E-04	!Pipe From RC to merge T

Table A1.4 – 20 MWe piping data

IP	Nsec	Npipe	Dpipe	Apipe	ELpipe		xsi	rough	Section
Precooler to main compressor									
1	4	6	0.1576	0.019500	0.2800	0.04	1.0E-04		!precooler outlet plenum LP
1		830	0.0030	0.000090	0.0050	1.20	1.0E-04		!precooler outlets LP
1		1	0.3500	0.140000	0.3000	0.40	1.0E-04		!precooler side plenum LP
1		1	0.1524	0.018200	3.3300	0.82	1.0E-04		!pipe to main compressor
Main compressor to LTR									
2	3	1	0.1524	0.018200	1.1700	1.716	1.0E-04		!pipe to LTR
2		1	0.3048	0.072966	0.3000	0.40	1.0E-04		!LTR inlet side plenum HP
2		6	0.1151	0.010410	1.5000	0.70	1.0E-04		!LTR inlet distribution plena HP
LTR to merge T junction									
3	3	6	0.1151	0.010410	1.5000	0.70	1.0E-04		!LTR outlet distribution plena HP
3		1	0.3556	0.099315	0.3000	0.40	1.0E-04		!LTR outlet side plenum HP
3		1	0.3556	0.099315	0.7874	1.32	1.0E-04		!Pipe from LTR to merge T
From merge T junction to HTR									
4	3	1	0.3556	0.099315	1.3700	1.00	1.0E-04		!Pipe from merge T to HTR
4		1	0.3556	0.099315	0.3000	0.40	1.0E-04		!HTR inlet side plenum HP
4		6	0.1151	0.010410	1.8750	0.70	1.0E-04		!HTR inlet distribution plena HP
From HTR to IHX (reactor)									
5	3	6	0.1151	0.010410	1.8750	0.70	1.0E-04		!HTR outlet distribution plena HP
5		1	0.3556	0.099315	0.3000	0.40	1.0E-04		!HTR outlet side plenum HP
5		1	0.3048	0.073000	1.0000	1.12	1.0E-04		!Pipe from HTR to IHX (reactor)
From IHX (reactor) to turbine									
6	1	1	0.2540	0.050700	1.0000	0.12	1.0E-04		!Pipe From IHX/RX to turbine
From turbine to HTR									
7	4	1	0.4064	0.129700	0.3600	1.12	1.0E-04		!Pipe From turbine to HTR
7		1	0.3500	0.140000	1.8750	0.40	1.0E-04		!HTR inlet side plenum LP
7		4192	0.0030	0.000090	0.0050	1.20	1.0E-04		!HTR inlets LP
7		6	0.2811	0.048750	0.0800	0.40	1.0E-04		!HTR inlet plenum LP
From HTR to LTR									
8	7	6	0.2491	0.048750	0.2800	0.40	1.0E-04		!HTR outlet plenum LP
8		4192	0.0030	0.000090	0.0050	1.20	1.0E-04		!HTR outlets LP
8		1	0.3500	0.140000	1.8750	0.40	1.0E-04		!HTR outlet side plenum LP
8	1	1	0.3556	0.099315	1.9300	1.12	1.0E-04		!Pipe From HTR to LTR
8		1	0.3500	0.140000	1.5000	0.40	1.0E-04		!LTR inlet side plenum LP
8		3330	0.0030	0.000090	0.1000	1.20	1.0E-04		!LTR inlets LP
8		6	0.2228	0.039000	0.2800	0.40	1.0E-04		!LTR inlet plenum LP
From LTR to split T junction									
9	4	6	0.2228	0.039000	0.2800	0.40	1.0E-04		!LTR outlet plenum LP
9		3330	0.0030	0.000090	0.0050	1.20	1.0E-04		!LTR outlets LP
9		1	0.3500	0.140000	0.5000	0.40	1.0E-04		!LTR outlet side plenum LP
9		1	0.2540	0.050700	1.8300	2.12	1.0E-04		!Pipe From LTR to split T junction
From split T junction to precooler									
10	4	1	0.2540	0.050700	2.7400	1.0	1.0E-04		!Pipe From split T to precooler
10		1	0.3500	0.140000	0.5000	0.40	1.0E-04		!precooler side plenum LP
10		830	0.0030	0.000090	0.0050	1.20	1.0E-04		!precooler inlets LP
10		6	0.1576	0.019500	0.2800	0.04	1.0E-04		!precooler inlet plenum LP
From split T junction to recomp. comp.									
11	1	1	0.2540	0.050700	0.6900	0.50	1.0E-04		!Pipe From split T to RC
From recomp. comp. to merge T junction									
12	1	1	0.2540	0.050700	2.5800	0.796	1.0E-04		!Pipe From RC to merge T

Table A1.5 – 30 MWe piping data

IP	Nsec	Npipe	Dpipe	Apipe	ELpipe	xsi	rough	Section
Precooler to main compressor								
1	4	6	0.1576	0.019500	0.2800	0.04	1.0E-04	!precooler outlet plenum LP
1		1245	0.0030	0.000090	0.0050	1.20	1.0E-04	!precooler outlets LP
1		1	0.3500	0.140000	0.3000	0.40	1.0E-04	!precooler side plenum LP
1		1	0.2032	0.032429	3.3300	0.82	1.0E-04	!pipe to main compressor
Main compressor to LTR								
2	3	1	0.2032	0.032429	1.1700	1.716	1.0E-04	!pipe to LTR
2		1	0.3048	0.072966	0.3000	0.40	1.0E-04	!LTR inlet side plenum HP
2		6	0.1151	0.010410	3.0000	0.70	1.0E-04	!LTR inlet distribution plena HP
LTR to merge T junction								
3	3	6	0.1151	0.010410	3.0000	0.70	1.0E-04	!LTR outlet distribution plena HP
3		1	0.3556	0.099315	0.3000	0.40	1.0E-04	!LTR outlet side plenum HP
3		1	0.4572	0.164174	0.7874	1.32	1.0E-04	!Pipe from LTR to merge T
From merge T junction to HTR								
4	3	1	0.4572	0.164174	1.3700	1.00	1.0E-04	!Pipe from merge T to HTR
4		1	0.3556	0.099315	0.3000	0.40	1.0E-04	!HTR inlet side plenum HP
4		6	0.1151	0.010410	3.7500	0.70	1.0E-04	!HTR inlet distribution plena HP
From HTR to IHX (reactor)								
5	3	6	0.1151	0.010410	3.7500	0.70	1.0E-04	!HTR outlet distrib. plena HP
5		1	0.3556	0.099315	0.3000	0.40	1.0E-04	!HTR outlet side plenum HP
5		1	0.4572	0.164174	1.0000	1.12	1.0E-04	!Pipe from HTR to IHX (reactor)
From IHX (reactor) to turbine								
6	1	1	0.3556	0.099315	1.0000	0.12	1.0E-04	!Pipe From IHX/RX to turbine
From turbine to HTR								
7	4	1	0.4572	0.164174	0.3600	1.12	1.0E-04	!Pipe From turbine to HTR
7		1	0.3500	0.140000	1.8750	0.40	1.0E-04	!HTR inlet side plenum LP
7		6288	0.0030	0.000090	0.0050	1.20	1.0E-04	!HTR inlets LP
7		6	0.2811	0.048750	0.0800	0.40	1.0E-04	!HTR inlet plenum LP
From HTR to LTR								
8	7	6	0.2491	0.048750	0.2800	0.40	1.0E-04	!HTR outlet plenum LP
8		6288	0.0030	0.000090	0.0050	1.20	1.0E-04	!HTR outlets LP
8		1	0.3500	0.140000	2.0000	0.40	1.0E-04	!HTR outlet side plenum LP
8	1	1	0.4572	0.164174	1.9300	1.12	1.0E-04	!Pipe From HTR to LTR
8		1	0.3500	0.140000	1.5000	0.40	1.0E-04	!LTR inlet side plenum LP
8		4995	0.0030	0.000090	0.1000	1.20	1.0E-04	!LTR inlets LP
8		6	0.2228	0.039000	0.2800	0.40	1.0E-04	!LTR inlet plenum LP
From LTR to split T junction								
9	4	6	0.2228	0.039000	0.2800	0.40	1.0E-04	!LTR outlet plenum LP
9		4995	0.0030	0.000090	0.0050	1.20	1.0E-04	!LTR outlets LP
9		1	0.3500	0.140000	0.5000	0.40	1.0E-04	!LTR outlet side plenum LP
9		1	0.3556	0.099315	1.8300	2.12	1.0E-04	!Pipe From LTR to split T
From split T junction to precooler								
10	4	1	0.3556	0.099315	2.7400	1.0	1.0E-04	!Pipe From split T to precooler
10		1	0.3500	0.140000	0.5000	0.40	1.0E-04	!precooler side plenum LP
10		1245	0.0030	0.000090	0.0050	1.20	1.0E-04	!precooler inlets LP
10		6	0.1576	0.019500	0.2800	0.04	1.0E-04	!precooler inlet plenum LP
From split T junction to recomp. comp.								
11	1	1	0.3556	0.099315	0.6900	0.50	1.0E-04	!Pipe From split T to RC
From recomp. comp. to merge T junction								
12	1	1	0.3556	0.099315	2.5800	0.796	1.0E-04	!Pipe From RC to merge T

Table A1.6 – 150 MWe Piping Data

IP	Nsec	Npipe	Dpipe	Apipe	ELpipe	xsi	rough	Section
precooler to main compressor								
1	4	24	0.0354	0.018000	0.2800	0.04	1.0E-04	!precooler outlet plenum LP
1		6225	0.0030	0.000090	0.0050	1.20	1.0E-04	!precooler outlets LP
1		4	0.3500	0.140000	0.6000	0.40	1.0E-04	!precooler side plenum LP
1		1	0.5080	0.202683	4.0000	1.12	1.0E-04	!pipe to main compressor
main compressor to LTR								
2	3	1	0.6350	0.316692	7.5000	2.92	1.0E-04	!pipe to LTR
2		8	0.3048	0.072966	0.3000	0.40	1.0E-04	!LTR inlet side plenum HP
2		48	0.0822	0.010410	1.7800	0.70	1.0E-04	!LTR inlet distribution plena HP
LTR to merge T junction								
3	3	48	0.0822	0.010410	2.0000	0.70	1.0E-04	!LTR outlet distribution plena HP
3		8	0.3556	0.099315	0.3000	0.40	1.0E-04	!LTR outlet side plenum HP
3		8	0.3997	0.125475	1.7874	2.44	1.0E-04	!Pipe from LTR to merge T junction
From merge T junction to HTR								
4	3	8	0.3997	0.125475	0.5500	1.12	1.0E-04	!Pipe from merge T junct to HTR
4		8	0.5080	0.202683	0.3000	0.40	1.0E-04	!HTR inlet side plenum HP
4		48	0.0822	0.010410	2.6500	0.70	1.0E-04	!HTR inlet distribution plena HP
From HTR to IHX (reactor)								
5	3	48	0.0822	0.010410	2.6500	0.70	1.0E-04	!HTR outlet dist. plena HP
5		8	0.3556	0.099315	0.3000	0.40	1.0E-04	!HTR outlet side plenum HP
5		8	0.5080	0.202683	6.2500	2.00	1.0E-04	!Pipe from HTR to IHX (reactor)
From IHX (reactor) to turbine								
6	1	1	1.0000	0.785398	15.000	2.00	1.0E-04	!Pipe From IHX (reactor) to turbine
From turbine to HTR								
7	4	8	0.3997	0.125475	0.2500	1.12	1.0E-04	!Pipe From turbine to HTR
7		8	0.3500	0.140000	2.6500	0.40	1.0E-04	!HTR inlet side plenum LP
7		31440	0.0030	0.000090	0.0050	1.20	1.0E-04	!HTR inlets LP
7		48	0.0359	0.090000	0.2800	0.40	1.0E-04	!HTR inlet plenum LP
From HTR to LTR								
8	7	48	0.0359	0.090000	0.2800	0.40	1.0E-04	!HTR outlet plenum LP
8		31440	0.0030	0.000090	0.0050	1.20	1.0E-04	!HTR outlets LP
8		8	0.3500	0.140000	2.6500	0.40	1.0E-04	!HTR outlet side plenum LP
8	1	8	0.5080	0.202683	0.5000	1.12	1.0E-04	!Pipe From HTR to LTR
8		8	0.3500	0.140000	1.7800	0.40	1.0E-04	!LTR inlet side plenum LP
8		24975	0.0030	0.000090	0.0050	1.20	1.0E-04	!LTR inlets LP
8		48	0.0358	0.072000	0.2800	0.40	1.0E-04	!LTR inlet plenum LP
From LTR to split T junction								
9	4	48	0.0358	0.072000	0.2800	0.40	1.0E-04	!LTR outlet plenum LP
9		24975	0.0030	0.000090	0.0050	1.20	1.0E-04	!LTR outlets LP
9		8	0.3500	0.140000	1.7800	0.40	1.0E-04	!LTR outlet side plenum LP
9		8	0.3997	0.125475	0.5000	1.12	1.0E-04	!Pipe From LTR to split T junction
From split T junction to precooler								
10	4	4	0.3997	0.125475	1.0000	1.12	1.0E-04	!Pipe from split T junct. to PRE
10		4	0.3500	0.140000	0.5000	0.40	1.0E-04	!precooler side plenum LP
10		6225	0.0030	0.000090	0.0050	1.20	1.0E-04	!precooler inlets LP
10		24	0.0354	0.018000	0.2800	0.04	1.0E-04	!precooler inlet plenum LP
From split T junction to recomp. comp.								
11	1	1	0.66040	0.342534	3.5600	0.50	1.0E-04	!Pipe from split T junct to RC
From recomp. comp. to merge T junction								
12	1	1	0.5080	0.202683	4.3000	1.80	1.0E-04	!Pipe from RC to merge T junct.

Appendix A2 Simple Cycle Pipe Data

The piping data for the simple cycle at various power ratings is contained in this appendix. The tables are broken into sections and organized in columns and rows to separate the various pertinent data for the piping calculations. Each section has a title to simply state which part of the cycle the data is for. The following headers with a brief description of their notation are explained below:

IP	Path number
Nsec:	number of sections with various flow areas in path IP
Npipe:	number of parallel passages in the specific section
Dpipe:	hydraulic diameter of the duct/passage in the specific section (m)
Apipe:	cross sectional flow area in the specific section (m^2)
ELpipe:	length of the duct/passage in the specific section (m)
xsi:	total form loss coefficient in the specific section
rough :	surface roughness of the pipe in the specific section
Section:	description of the section passage in the cycle

Table A2.1 – 5 MWe piping data

IP	Nsec	Npipe	Dpipe	Apipe	ELpipe	xsi	rough	Section
Precooler to main compressor								
1	4	6	0.1576	0.019500	0.0700	0.04	1.0E-04	!precooler outlet plenum LP
1		250	0.0030	0.000090	0.0050	0.20	1.0E-04	!precooler outlets LP
1		1	0.3500	0.140000	0.4000	0.40	1.0E-04	!precooler side plenum LP
1		1	0.1270	0.012700	1.0400	0.42	1.0E-04	!pipe to main compressor
Main compressor to REC								
2	3	1	0.1270	0.012700	1.8300	1.716	1.0E-04	!pipe to REC
2		1	0.3048	0.072966	0.3000	0.40	1.0E-04	!REC inlet side plenum HP
2		6	0.1151	0.010410	0.3350	0.70	1.0E-04	!REC inlet distribution plena HP
From REC to IHX (reactor) **								
3	3	6	0.1151	0.010410	0.3350	0.70	1.0E-04	!REC outlet dist plena HP
3		1	0.3556	0.099315	0.0750	0.40	1.0E-04	!REC outlet side plenum HP
3		1	0.1524	0.018200	1.0000	1.12	1.0E-04	!Pipe from REC to IHX (reactor)
From IHX (reactor) to turbine *								
4	1	1	0.1270	0.012700	1.0000	0.12	1.0E-04	!Pipe From IHX/RX to turbine
From turbine to REC								
5	4	1	0.4064	0.1297	0.2540	1.12	1.0E-04	!Pipe From turbine to REC
5		1	0.3500	0.140000	0.2413	0.40	1.0E-04	!REC inlet side plenum LP
5		1048	0.0030	0.000090	0.0050	1.20	1.0E-04	!REC inlets LP
5		6	0.2032	0.032400	0.2800	0.40	1.0E-04	!REC inlet plenum LP
From REC to to precooler								
6	7	6	0.2228	0.039000	0.0700	0.40	1.0E-04	!REC outlet plenum LP
6		833	0.0030	0.000090	0.0050	1.20	1.0E-04	!REC outlets LP
6		1	0.3500	0.140000	0.2413	0.40	1.0E-04	!REC outlet side plenum LP
6		2	0.2032	0.032400	0.6700	1.12	1.0E-04	!Pipe From REC to PRE
6		1	0.3500	0.140000	0.1000	0.40	1.0E-04	!precooler side plenum LP
6		250	0.0030	0.000090	0.0050	1.20	1.0E-04	!precooler inlets LP
6		6	0.1576	0.019500	0.0700	0.04	1.0E-04	!precooler inlet plenum LP

Table A2.2 – 10Mwe piping data

IP	Nsec	Npipe	Dpipe	Apipe	Elpipe	xsi	rough	Section
Precooler to main compressor								
1	4	6	0.1576	0.019500	0.1400	0.04	1.0E-04	!precooler outlet plenum LP
1		500	0.0030	0.000090	0.0050	1.20	1.0E-04	!precooler outlets LP
1		1	0.3500	0.140000	0.2000	0.40	1.0E-04	!precooler side plenum LP
1		1	0.2032	0.032400	1.0400	0.42	1.0E-04	!pipe to main compressor
Main compressor to REC								
2	3	1	0.2032	0.032400	1.8300	1.716	1.0E-04	!pipe to REC
2		1	0.3048	0.072966	0.3000	0.40	1.0E-04	!REC inlet side plenum HP
2		6	0.1151	0.010410	0.6700	0.70	1.0E-04	!REC inlet distribution plena HP
From REC to IHX (reactor) **								
3	3	6	0.1151	0.010410	0.6700	0.70	1.0E-04	!REC outlet distrib. plena HP
3		1	0.3556	0.099315	0.3000	0.40	1.0E-04	!REC outlet side plenum HP
3		1	0.2286	0.041000	1.0000	1.12	1.0E-04	!Pipe from REC to IHX (reactor)
From IHX (reactor) to turbine *								
4	1	1	0.2032	0.032400	1.0000	0.12	1.0E-04	!Pipe From IHX/RX to turbine
From turbine to REC								
5	4	1	0.3048	0.073000	0.2540	1.12	1.0E-04	!Pipe From turbine to REC
5		1	0.3500	0.140000	0.4826	0.40	1.0E-04	!REC inlet side plenum LP
5		2096	0.0030	0.000090	0.0050	1.20	1.0E-04	!REC inlets LP
5		6	0.2032	0.032400	0.1400	0.40	1.0E-04	!REC inlet plenum LP
From REC to to precooler								
6	7	6	0.2228	0.039000	0.1400	0.40	1.0E-04	!REC outlet plenum LP
6		1666	0.0030	0.000090	0.0050	1.20	1.0E-04	!REC outlets LP
6		1	0.3500	0.140000	0.4826	0.40	1.0E-04	!REC outlet side plenum LP
6		2	0.2540	0.050700	0.6700	1.12	1.0E-04	!Pipe From REC to PRE
6		1	0.3500	0.140000	0.2000	0.40	1.0E-04	!precooler side plenum LP
6		500	0.0030	0.000090	0.0050	1.20	1.0E-04	!precooler inlets LP
6		6	0.1576	0.019500	0.1400	0.04	1.0E-04	!precooler inlet plenum LP

Table A2.3 – 15MWe piping data

IP	Nsec	Npipe	Dpipe	Apipe	ELpipe	xsi	rough	Section
Precooler to main compressor								
1	4	6	0.1576	0.019500	0.2100	0.04	1.0E-04	!precooler outlet plenum LP
1		750	0.0030	0.000090	0.0050	1.20	1.0E-04	!precooler outlets LP
1		1	0.3500	0.140000	0.3000	0.40	1.0E-04	!precooler side plenum LP
1		1	0.2286	0.041000	1.0400	0.42	1.0E-04	!pipe to main compressor
Main compressor to REC								
2	3	1	0.2286	0.041000	1.8300	1.716	1.0E-04	!pipe to REC
2		1	0.3048	0.072966	0.3000	0.40	1.0E-04	!REC inlet side plenum HP
2		6	0.1151	0.010410	1.3400	0.70	1.0E-04	!REC inlet distribution plena HP
From REC to IHX (reactor) **								
3	3	6	0.1151	0.010410	1.0000	0.70	1.0E-04	!REC outlet dist plena HP
3		1	0.3556	0.099315	0.3000	0.40	1.0E-04	!REC outlet side plenum HP
3		1	0.3048	0.073000	1.0000	1.12	1.0E-04	!Pipe from REC to IHX (reactor)
From IHX (reactor) to turbine *								
4	1	1	0.2286	0.041000	1.0000	0.12	1.0E-04	!Pipe From IHX/RX to turbine
From turbine to REC								
5	4	1	0.3556	0.099300	0.2540	1.12	1.0E-04	!Pipe From turbine to REC
5		1	0.3500	0.140000	0.7239	0.40	1.0E-04	!REC inlet side plenum LP
5		3144	0.0030	0.000090	0.0050	1.20	1.0E-04	!REC inlets LP
5		6	0.2032	0.032400	0.2100	0.40	1.0E-04	!REC inlet plenum LP
From REC to to precooler								
6	7	6	0.2228	0.039000	0.2100	0.40	1.0E-04	!REC outlet plenum LP
6		2500	0.0030	0.000090	0.0050	1.20	1.0E-04	!REC outlets LP
6		1	0.3500	0.140000	0.7239	0.40	1.0E-04	!REC outlet side plenum LP
6		2	0.3048	0.073000	0.6700	1.12	1.0E-04	!Pipe From REC to PRE
6		1	0.3500	0.140000	0.3000	0.40	1.0E-04	!precooler side plenum LP
6		750	0.0030	0.000090	0.0050	1.20	1.0E-04	!precooler inlets LP
6		6	0.1576	0.019500	0.2100	0.04	1.0E-04	!precooler inlet plenum LP

Table A2.4 – 20MWe piping data

IP	Nsec	Npipe	Dpipe	Apipe	ELpipe	xsi	rough	Section
Precooler to main compressor								
1	4	6	0.1576	0.019500	0.2800	0.04	1.0E-04	!precooler outlet plenum LP
1		1000	0.0030	0.000090	0.0050	1.20	1.0E-04	!precooler outlets LP
1		1	0.3500	0.140000	0.4000	0.40	1.0E-04	!precooler side plenum LP
1		1	0.2540	0.050700	1.0400	0.42	1.0E-04	!pipe to main compressor
Main compressor to REC								
2	3	1	0.2540	0.050700	1.8300	1.716	1.0E-04	!pipe to REC
2		1	0.3048	0.072966	0.3000	0.40	1.0E-04	!REC inlet side plenum HP
2		6	0.1151	0.010410	1.3400	0.70	1.0E-04	!REC inlet distribution plena HP
From REC to IHX (reactor) **								
3	3	6	0.1151	0.010410	1.3400	0.70	1.0E-04	!REC outlet dist plena HP
3		1	0.3556	0.099315	0.3000	0.40	1.0E-04	!REC outlet side plenum HP
3		1	0.3048	0.073000	1.0000	1.12	1.0E-04	!Pipe from REC to IHX (reactor)
From IHX (reactor) to turbine *								
4	1	1	0.2540	0.050700	1.0000	0.12	1.0E-04	!Pipe From IHX/RX to turbine
From turbine to REC								
5	4	1	0.4064	0.129700	0.2540	1.12	1.0E-04	!Pipe From turbine to REC
5		1	0.3500	0.140000	0.9652	0.40	1.0E-04	!REC inlet side plenum LP
5		4192	0.0030	0.000090	0.0050	1.20	1.0E-04	!REC inlets LP
5		6	0.2811	0.048750	0.2800	0.40	1.0E-04	!REC inlet plenum LP
From REC to to precooler								
6	7	6	0.2228	0.039000	0.2800	0.40	1.0E-04	!REC outlet plenum LP
6		3330	0.0030	0.000090	0.0050	1.20	1.0E-04	!REC outlets LP
6		1	0.3500	0.140000	0.9652	0.40	1.0E-04	!REC outlet side plenum LP
6		2	0.3556	0.099300	0.6700	1.12	1.0E-04	!Pipe From REC to PRE
6		1	0.3500	0.140000	0.4000	0.40	1.0E-04	!precooler side plenum LP
6		1000	0.0030	0.000090	0.0050	1.20	1.0E-04	!precooler inlets LP
6		6	0.1576	0.019500	0.2800	0.04	1.0E-04	!precooler inlet plenum LP

Table A2.5 – 30MWe piping data

IP	Nsec	Npipe	Dpipe	Apipe	ELpipe	xsi	rough	Section
Precooler to main compressor								
1	4	6	0.1576	0.019500	0.4200	0.04	1.0E-04	!precooler outlet plenum LP
1		1500	0.0030	0.000090	0.0050	1.20	1.0E-04	!precooler outlets LP
1		1	0.3500	0.140000	0.6000	0.40	1.0E-04	!precooler side plenum LP
1		1	0.3556	0.099300	1.0400	0.42	1.0E-04	!pipe to main compressor
Main compressor to REC								
2	3	1	0.3556	0.099300	1.8300	1.716	1.0E-04	!pipe to REC
2		1	0.3048	0.072966	0.3000	0.40	1.0E-04	!REC inlet side plenum HP
2		6	0.1151	0.010410	1.3400	0.70	1.0E-04	!REC inlet distribution plena HP
From REC to IHX (reactor) **								
3	3	6	0.1151	0.010410	2.0000	0.70	1.0E-04	!REC outlet dist plena HP
3		1	0.3556	0.099315	0.3000	0.40	1.0E-04	!REC outlet side plenum HP
3		1	0.4064	0.129700	1.0000	1.12	1.0E-04	!Pipe from REC to IHX (reactor)
From IHX (reactor) to turbine *								
4	1	1	0.3556	0.099300	1.0000	0.12	1.0E-04	!Pipe From IHX/RX to turbine
From turbine to REC								
5	4	1	0.6096	0.291900	0.2540	1.12	1.0E-04	!Pipe From turbine to REC
5		1	0.3500	0.140000	1.4478	0.40	1.0E-04	!REC inlet side plenum LP
5		6288	0.0030	0.000090	0.0050	1.20	1.0E-04	!REC inlets LP
5		6	0.2032	0.032400	0.4200	0.40	1.0E-04	!REC inlet plenum LP
From REC to to precooler								
6	7	6	0.2228	0.039000	0.4200	0.40	1.0E-04	!REC outlet plenum LP
6		5000	0.0030	0.000090	0.0050	1.20	1.0E-04	!REC outlets LP
6		1	0.3500	0.140000	1.4478	0.40	1.0E-04	!REC outlet side plenum LP
6		2	0.5080	0.202700	0.6700	1.12	1.0E-04	!Pipe From REC to PRE
6		1	0.3500	0.140000	0.6000	0.40	1.0E-04	!precooler side plenum LP
6		1500	0.0030	0.000090	0.0050	1.20	1.0E-04	!precooler inlets LP
6		6	0.1576	0.019500	0.4200	0.04	1.0E-04	!precooler inlet plenum LP

Appendix A3 Sample Input Files: Recompression Cycle

A set of sample input data for the CYCLES code is included in this appendix. This data corresponds to a 150 MWe recompression cycle with a 650°C turbine inlet temperature, 32°C compressor inlet temperature, and 20°C cooling water temperature. For other power ratings and parameters a new set of input data is created. The 150 MWe data set was used for the performance calculations for the 300 MWe layouts. Using the 150 MWe data is accurate to predict the performance of the 300 MWe layout because the 300 MWe layout has twice the number of heat exchangers, pipes, and flow channels than the 150 MWe layout. Thus, with the 150 MWe layout having half the thermal power, flow rate, and piping, it is possible to directly calculate the performance of the 300 MWe layout by merely using appropriate turbomachinery efficiencies. Nearly every piece of data changes for each parameter; however, the heat exchanger plate thicknesses, channel diameters, plate conduction, and number of axial cells remain constant. Table A4.1 is the full set of data for these particular parameters.

Table A3.1 150 MWe Recompression cycle inputs

```
Main Cycle Input Data
0        !Table creation trigger, if 0 old tables are used, if more than 0 new tables are created
1        !Case trigger, if 0 calculates a single operating point from specified conditions, if 1 optimizes the
         heat exchanger volume
20000.0 !Compressor outlet pressure (kPa)
313.0    !Cycle thermal power in (MWth)
2.60     !Pressure ratio of the main compressor (maximum cycle pressure ratio)
650.0    !Turbine inlet temperature (C)
32.0     !Compressor inlet temperature (C)
0.8507   !Main compressor efficiency in dimensionless form
0.898    !Recompression compressor efficiency in dimensionless form
0.950    !Turbine efficiency in dimensionless form
0.99     !mechanical efficiency (Couplings)
0.98     !generator efficiency
0.98     !frequency converter efficiency (including switchyard losses)
20.0     !Cooling water inlet temperature (C)
500.0    !Reactor pressure drop (kPa)
1        !Number of turbines, 1 for no reheating, 2 for 1 reheat, 3 for 2 reheats
1.0d-2   !Precision of pressure drop calculations; reduce if the two calculated cycle efficiencies are not
         sufficiently equal


HTR data
zig1h1c ! HX type (str for straight channels, 1h1c for 1 hot/1cold plate)
0.002    !dh hot channel diameter (m)
```

0.002 !dc cold channel diameter (m)
0.0015 !th hot plate thickness (m)
0.0015 !tc cold plate thickness (m)
1.0 !hs height of the heat exchanger (m)
1.2658 !ws width of the heat exchanger (m)
0.79 !total length of the heat exchanger (m)
21.99317 !recmod high temperature recuperator volume (m3)
25.0 !condsht plate conductivity (W/mK)
40.0 !steps number of axial cells for heat exchanger modeling
0.005 !epsrvo precision of calculation
50.112 !initial step adjustment for volume optimization
1.3 !stepdiv adjuster of initial step for volume optimization

LTR data
zig1h1c ! HX type (str for straight channels, 1h1c for 1 hot/1cold plate)
0.002 !dh hot channel diameter (m)
0.002 !dc cold channel diameter (m)
0.0015 !th hot plate thickness (m)
0.0015 !tc cold plate thickness (m)
1.0 !hs height of the heat exchanger (m)
1.0683 !ws width of the heat exchanger (m)
0.94 !total length of the heat exchanger (m)
17.59453 !recmod low temperature recuperator volume (m3)
25.0 !condsht plate conductivity (W/mK)
40.0 !steps number of axial cells for heat exchanger modeling
0.005d0 !epsrvo precision of calculation
50.112 !initial step adjustment for volume optimization
1.3d0 !stepdiv adjuster of initial step for volume optimization

PRE data
str1h1c ! HX type (str for straight channels, 1h1c for 1 hot/1cold plate)
0.002 !dh hot channel diameter (m)
0.002 !dc cold channel diameter (m)
0.0015 !th hot plate thickness (m)
0.0015 !tc cold plate thickness (m)
1.0 !hs height of the heat exchanger (m)
1.1111 !ws width of the heat exchanger (m)
0.9 !total length of the heat exchanger (m)
4.761 !recmod pre-cooler volume (m3)
25.0 !condsht plate conductivity (W/mK)-titanium
40.0 !steps number of axial cells for heat exchanger modeling
0.0005d0 !epsprec precision of calculation

Pipe data (12 sets)

IP	Nsec	Npipe	Dpipe	Apipe	ELpipe	xsi	rough	Section
precooler to main compressor								
1	4	24	0.0354	0.018000	0.2800	0.04	1.0E-04	!precooler outlet plenum LP
1		6225	0.0030	0.000090	0.0050	1.20	1.0E-04	!precooler outlets LP
1		4	0.3500	0.140000	0.6000	0.40	1.0E-04	!precooler side plenum LP
1		1	0.5080	0.202683	4.0000	1.12	1.0E-04	!pipe to main compressor
main compressor to LTR								
2	3	1	0.6350	0.316692	7.5000	2.92	1.0E-04	!pipe to LTR
2		8	0.3048	0.072966	0.3000	0.40	1.0E-04	!LTR inlet side plenum HP
2		48	0.0822	0.010410	1.7800	0.70	1.0E-04	!LTR inlet distribution plena HP
LTR to merge T junction								

```
3  3     48      0.0822  0.010410      2.0000  0.70    1.0E-04   !LTR outlet distribution plena HP
3        8       0.3556  0.099315      0.3000  0.40    1.0E-04   !LTR outlet side plenum HP
3        8       0.3997  0.125475      1.7874  2.44    1.0E-04   !Pipe from LTR to merge T
junction
From merge T junction to HTR
4  3     8       0.3997  0.125475      0.5500  1.12    1.0E-04   !Pipe from merge T junct to HTR
4        8       0.5080  0.202683      0.3000  0.40    1.0E-04   !HTR inlet side plenum HP
4        48      0.0822  0.010410      2.6500  0.70    1.0E-04   !HTR inlet distribution plena HP
From HTR to IHX (reactor)
5  3     48      0.0822  0.010410      2.6500  0.70    1.0E-04   !HTR outlet dist. plena HP
5        8       0.3556  0.099315      0.3000  0.40    1.0E-04   !HTR outlet side plenum HP
5        8       0.5080  0.202683      6.2500  2.00    1.0E-04   !Pipe from HTR to IHX (reactor)
From IHX (reactor) to turbine
6  1     1       1.0000  0.785398      15.000  2.00    1.0E-04   !Pipe From IHX (reactor) to
turbine
From  turbine to HTR
7  4     8       0.3997  0.125475      0.2500  1.12    1.0E-04   !Pipe From  turbine to HTR
7        8       0.3500  0.140000      2.6500  0.40    1.0E-04   !HTR inlet side plenum LP
7        31440   0.0030  0.000090      0.0050  1.20    1.0E-04   !HTR inlets LP
7        48      0.0359  0.090000      0.2800  0.40    1.0E-04   !HTR inlet plenum LP
From  HTR to LTR
8  7     48      0.0359  0.090000      0.2800  0.40    1.0E-04   !HTR outlet plenum LP
8        31440   0.0030  0.000090      0.0050  1.20    1.0E-04   !HTR outlets LP
8        8       0.3500  0.140000      2.6500  0.40    1.0E-04   !HTR outlet side plenum LP
8  1     8       0.5080  0.202683      0.5000  1.12    1.0E-04   !Pipe From  HTR to LTR
8        8       0.3500  0.140000      1.7800  0.40    1.0E-04   !LTR inlet side plenum LP
8        24975   0.0030  0.000090      0.0050  1.20    1.0E-04   !LTR inlets LP
8        48      0.0358  0.072000      0.2800  0.40    1.0E-04   !LTR inlet plenum LP
From  LTR to split T junction
9  4     48      0.0358  0.072000      0.2800  0.40    1.0E-04   !LTR outlet plenum LP
9        24975   0.0030  0.000090      0.0050  1.20    1.0E-04   !LTR outlets LP
9        8       0.3500  0.140000      1.7800  0.40    1.0E-04   !LTR outlet side plenum LP
9        8       0.3997  0.125475      0.5000  1.12    1.0E-04   !Pipe From  LTR to split T
junction
From  split T junction to precooler
10 4     4       0.3997  0.125475      1.0000  1.12    1.0E-04   !Pipe from split T junct. to PRE
10       4       0.3500  0.140000      0.5000  0.40    1.0E-04   !precooler side plenum LP
10       6225    0.0030  0.000090      0.0050  1.20    1.0E-04   !precooler inlets LP
10       24      0.0354  0.018000      0.2800  0.04    1.0E-04   !precooler inlet plenum LP
From  split T junction to recomp. comp.
11 1     1       0.66040 0.342534      3.5600  0.50    1.0E-04   !Pipe from split T junct to RC
From  recomp. comp. to merge T junction
12 1     1       0.5080  0.202683      4.3000  1.80    1.0E-04   !Pipe from RC to merge T junct.

Data for optimization purposes
44.3487 !Total volume of all cycle heat exchangers (m3)
.501    !Step for optimization of heat exchanger volume split between precooler and recuperators (m3)
0.05    !Step for optimization of precooler length (m)
0.05    !Step for optimization of recuperator length (m)
0.1     !Step for optimization of the ratio of high temperature recuperator volume/low temperature
        recuperator volume
4.761   !guess of precooler volume (m3)
1.25    !guess of the ratio of high temperature recuperator volume/low temperature recuperator volume
0.89    !guess of high temperature recuperator length (m)
0.94    !guess of low temperature recuperator length (m)
0.90    !guess of precooler length (m)
```

Appendix A4 Sample Input Files: Simple Cycle

A set of sample input data for the CYCLES code is included in this appendix. This data corresponds to a 20 MWe simple cycle with a 550°C turbine inlet temperature, 32°C compressor inlet temperature, and 20°C cooling water temperature. For other power ratings and parameters a new set of input data is created. Nearly every piece of data changes for each parameter; however, the heat exchanger plate thicknesses, channel diameters, plate conduction, and number of axial cells remain constant. Table A4.1 is the full set of data for these particular parameters.

Table A4.1 20 MWe Simple cycle inputs

Main Cycle Input Data

```
0       !Table creation trigger, if 0 old tables are used, if more than 0 new tables are created
0       !Case trigger, if 0 calculates a single operating point from specified conditions, if 1 optimizes the
        heat exchanger volume
20000.0 !Compressor outlet pressure (kPa)
60.0    !Cycle thermal power in (MWth)
2.60    !Pressure ratio of the main compressor (maximum cycle pressure ratio)
550.0   !Turbine inlet temperature (C)
32.0    !Compressor inlet temperature (C)
0.89    !Main compressor efficiency in dimensionless form
0.912   !Turbine efficiency in dimensionless form
0.99    !mechanical efficiency (couplings)
0.98    !generator efficiency
0.98    !frequency converter efficiency
20.0    !Cooling water inlet temperature (C)
500.0   !Reactor pressure drop (kPa)
1       !Number of turbines, 1 for no reheating, 2 for 1 reheat, 3 for 2 reheats
1.0d-2  !Precision of pressure drop calculations; reduce if the two calculated cycle efficiencies are not
        sufficiently equal
```

REC data

```
zig1h1c ! HX type (str for straight channels, 1h1c for 1 hot/1cold plate)
0.002   !dh hot channel diameter (m)
0.002   !dc cold channel diameter (m)
0.0015  !th hot plate thickness (m)
0.0015  !tc cold plate thickness (m)
1.0     !hs height of the heat exchanger (m)
1.695   !ws width of the heat exchanger (m)
0.59    !total length of the heat exchanger (m)
1.667   !recmod high temperature recuperator volume (m3)
25.0    !condsht plate conductivity (W/mK)
40.0    !steps number of axial cells for heat exchanger modeling
0.005   !epsrvo precision of calculation
6.6816  !step initial step adjustment for volume optimization
1.3     !stepdiv adjuster of initial step for volume optimization
```

PRE data

```
str1h1c  ! HX type (str for straight channels, 1h1c for 1 hot/1cold plate)
0.002    !dh hot channel diameter (m)
0.002    !dc cold channel diameter (m)
0.0015   !th hot plate thickness (m)
0.0015   !tc cold plate thickness (m)
1.0      !hs height of the heat exchanger (m)
1.176    !ws width of the heat exchanger (m)
0.85     !totall length of the heat exchanger (m)
0.933    !recmod pre-cooler volume (m3)
25.0     !condsht plate conductivity (W/mK)-titanium
40.0     !steps number of axial cells for heat exchanger modeling
0.0005d0 !epsprec precision of calculations
```

Pipe data (6 sets) - for 20MWe Layout

IP	Nsec	Npipe	Dpipe	Apipe	ELpipe	xsi	rough	Section
precooler to main compressor								
1	4	6	0.1576	0.019500	0.2800	0.04	1.0E-04	!precooler outlet plenum LP
1		1000	0.0030	0.000090	0.0050	1.20	1.0E-04	!precooler outlets LP
1		1	0.3500	0.140000	0.4000	0.40	1.0E-04	!precooler side plenum LP
1		1	0.2540	0.050700	1.0400	0.42	1.0E-04	!pipe to main compressor
main compressor to REC								
2	3	1	0.2540	0.050700	1.8300	1.716	1.0E-04	!pipe to REC
2		1	0.3048	0.072966	0.3000	0.40	1.0E-04	!REC inlet side plenum HP
2		6	0.1151	0.010410	1.3400	0.70	1.0E-04	!REC inlet distribution plena HP
From REC to IHX (reactor) **								
3	3	6	0.1151	0.010410	1.3400	0.70	1.0E-04	!REC outlet dist. plena HP
3		1	0.3556	0.099315	0.3000	0.40	1.0E-04	!REC outlet side plenum HP
3		1	0.3048	0.0730	1.0000	1.12	1.0E-04	!Pipe from REC to IHX (reactor)
From IHX (reactor) to turbine *								
4	1	1	0.254	0.0507	1.0000	0.12	1.0E-04	!Pipe from IHX/RX to turbine
From turbine to REC								
5	4	1	0.4064	0.1297	0.2540	1.12	1.0E-04	!Pipe From turbine to REC
5		1	0.3500	0.140000	0.9652	0.40	1.0E-04	!REC inlet side plenum LP
5		4192	0.0030	0.000090	0.0050	1.20	1.0E-04	!REC inlets LP
5		6	0.2811	0.048750	0.2800	0.40	1.0E-04	!REC inlet plenum LP
From REC to precooler								
6	7	6	0.2228	0.039000	0.2800	0.40	1.0E-04	!REC outlet plenum LP
6		3330	0.0030	0.000090	0.0050	1.20	1.0E-04	!REC outlets LP
6		1	0.3500	0.140000	0.9652	0.40	1.0E-04	!REC outlet side plenum LP
6		2	0.3556	0.0993	0.6700	1.12	1.0E-04	!Pipe from REC to split T junct.
6		1	0.3500	0.140000	0.4000	0.40	1.0E-04	!precooler side plenum LP
6		1000	0.0030	0.000090	0.0050	1.20	1.0E-04	!precooler inlets LP
6		6	0.1576	0.019500	0.2800	0.04	1.0E-04	!precooler inlet plenum LP

Data for optimization purposes

```
2.6      !Total volume of all cycle heat exchangers (m3)
.0668    !Step for optimization of heat exchanger volume split between precooler and recuperators (m3)
0.05     !Step for optimization of precooler length (m)
0.05     !Step for optimization of recuperator length (m)
1.0      !guess of precooler volume (m3)
0.84     !guess of high temperature recuperator length (m)
1.0      !guess of precooler length (m)
```